Upregulation of Neprilysin as a Potential Therapeutic Approach in Alzheimer's Disease

---

Dissertation

zur

Erlangung der naturwissenschaftlichen Doktorwürde

(Dr. sc. nat.)

vorgelegt der

Mathematisch-naturwissenschaftlichen Fakultät

der

Universität Zürich

Von

Raphaël POIRIER

aus Frankreich

Promotionskomitee

Prof. Dr. Walter Schaffner

Dr. M. Hasan Mohajeri

Prof. Dr. David P. Wolfer

Zürich 2006

To curiosity and discovery

To Prof. Ross Johnson

SUMMARY

Alzheimer's disease (AD) is the major cause of dementia and cognitive impairments among older people and affects more than 30% of the population above 85 years of age. It is an age dependent neurodegenerative disease histopathologically characterized by the deposition of extracellular β-amyloid (Aβ) plaques and the formation of intracellular neurofibrillary tangles composed of the hyperphosphorylated protein tau. Converging evidence links abnormally high brain concentrations of Aβ, due to a shift in the balance between Aβ production and degradation, to the pathology of AD and to cognitive deficits in transgenic mouse models.

It was previously found in our lab that injection of synthetic fibrillar $A\beta_{1-42}$ into mouse brains caused sustained increases in brain levels of neprilysin protein and led to dramatic reduction of brain Aβ level, as well as prevention of amyloid plaque formation and associated cytopathology. Because of an increase of neprilysin mRNA observed 20 weeks after injection, we investigated the potential regulation of neprilysin expression by $A\beta_{1-42}$ *in vitro* using a luciferase assay driven by one of the three neprilysin promoters and incubation of 293T and SH-SY5Y cells with aggregated $A\beta_{1-42}$, aggregated $A\beta_{42-1}$ or PBS. $A\beta_{1-42}$ incubation did not affect neprilysin promoter activity *in vitro*. However, all trans retinoic acid (RA) which is used to differentiate SH-SY5Y cells, was shown to increase the activity of all three neprilysin promoters during SH-SY5Y differentiation. A similar effect was also found in 293T cells and led to an increase of neprilysin protein levels. Diffusible factors associated with microglia activation did not affect activity of neprilysin promoters *in vitro* and were not responsible for the upregulation of neprilysin observed *in vivo* after $A\beta_{1-42}$ injection. Analysis of a new group of mice, 20 weeks after similar brain injection of aggregated $A\beta_{1-42}$, $A\beta_{42-1}$ or PBS confirmed the $A\beta_{1-42}$-related upregulation of neprilysin protein level but did not show any increase of total neprilysin mRNA level and promoter specific mRNA levels when compared to $A\beta_{42-1}$ injected mice, suggesting that increased protein stability may also be involved in the $A\beta_{1-42}$-related upregulation of neprilysin *in vivo*.

Searching for other Aβ-degrading pathways, we also found that brain injection of aggregated $A\beta_{1-42}$ led to the activation of the plasminogen system. The activity of plasmin, another Aβ degrading enzyme, was increased 20 weeks after intracranial injection of $A\beta_{1-42}$ when compared to mice which received injection of $A\beta_{42-1}$ or PBS. Activation of plasmin was found to be associated with an increased activity of urokinase plasminogen activator (uPA),

which did not involve transcription regulation since uPA mRNA level was unaffected. Interestingly, uPA activity strongly correlated with neprilysin protein level after $A\beta_{1-42}$ injection. Therefore, we investigated the possible association between both increases. $A\beta_{1-42}$ efficiently increased the activity of both plasminogen activators, uPA and tissue-type plasminogen activator (tPA) on different cell types including primary neuronal culture. However, this increase of activity was not associated with upregulation of neprilysin. On the contrary, transgenic overexpression of neprilysin in neurons increased activity of both uPA and tPA in the brain and strongly implied that upregulation of neprilysin may act on the plasminogen system via pathways, which still need to be identified.

Neprilysin is the major rate-limiting peptidase involved in the physiological degradation of Aβ in the brain and its role in amyloidosis was further investigated *in vivo*. We found that partial and total reduction of neprilysin level, led to murine Aβ accumulation with plaque formation without alteration of APP level in the brain. It was associated with signs of neurodegeneration in the hippocampus and cognitive deficits in the conditioned taste aversion paradigm. Mice with neprilysin deletion represent the first mouse model with endogenous murine Aβ plaque like pathology without alteration of APP processing and therefore a valuable tool to study specifically the role of endogenous Aβ. Indeed, many transgenic mice overexpressing the mutated human amyloid precursor protein (APP) were produced and recapitulated many aspects of AD pathology including Aβ amyloidosis and cognitive deficits. These models were used to evaluate therapeutic interventions for AD but could not clearly distinguish the effects related to Aβ accumulation from overexpression of APP or its other proteolytic fragments. To investigate the potential therapeutical effect of neprilysin upregulation against amyloidosis, we generated transgenic mice, overexpressing neprilysin in neurons (NEP mice) and bred them with one of these mouse models of amyloidosis overexpressing human AD-causing mutated APP in neurons (J20 mice). Neprilysin overexpression prevented the accumulation of Aβ without altering neither the APP processing nor the levels of substance P, enkephalin and somatostatin, three other major neuronal neprilysin substrates. Behavioral analysis of the NEP mice showed a significant abnormal locomotion with slight decrease of anxiety both of which disappeared with age. Except a lack of contextual fear conditioning, learning and memory performances were not affected by neprilysin overexpression, suggesting that such an upregulation would present few cognitive side effects. The hyperlocomotion, decreased anxiety and memory deficit during the conditioned taste aversion task observed in the J20 mice were not prevented by neprilysin

overexpression suggesting that either the beneficial effects of neprilysin was limited or APP and its other proteolytic fragments which were not modified by neprilysin overexpression are responsible for these behavioral alterations. However, neprilysin overexpression prevented the memory impairment observed in J20 mice during the Morris water maze task, strongly supporting Aβ as the culprit responsible for this cognitive impairment and neprilysin upregulation as a valid Aβ-lowering therapeutic approach for AD.

ZUSAMMENFASSUNG

Die Alzheimer Demenz (AD) ist ein multifaktorielles Syndrom, welches durch eine progressive Atrophie und die Zerstörung von Neuronen charakterisiert ist, was zu kognitiver Schwäche, Demenz und schliesslich zum Tod führt. AD Forschung hat sich bisher hauptsächlich auf die Generierung und Ablagerung von β-Amyloidpeptiden (Aβ) konzentriert, da die abnormal hohe Aβ-Konzentration als primärer Auslöser von AD gilt. Die extrazellulären Aβ Ablagerungen (Plaques) im Gehirn begünstigen die Entstehung von neurofibrillären Läsionen, die synaptische Fehlfunktion und den Verlust von Neuronen im Gehirn der AD Patienten. Mutationen in APP (Amyloid-Precursor Protein), Presenilin (PS) 1- und 2– Genen verursachen die familiäre Form der Krankheit durch Generierung von erhöhten Mengen von Aβ. Diese Effekte werden durch das Alter verstärkt. Je länger desto mehr wird es klar, dass in den meisten Patienten eine abnormale Akkumulation von Aβ im Gehirn durch mangelhaften Abbau dieses Peptids verursacht wird.

Arbeiten aus unserem Labor zeigten, dass die Injektion von fibrillärem $A\beta_{1-42}$ ins Gehirn der Mäuse zu einem erhöhten Gehalt des Aβ-abbauenden Enzyms Neprilysin in Neuronen führte, was eine signifikante Reduktion der Aβ Mengen und Plaque-Pathologie zur Folge hatte. Die Erhöhung des Neprilysins wurde, unter anderem mechanistisch auf eine höhere Transkriptionsaktivität zurückgeführt. Deswegen haben wir versucht, mittels Luciferase-Assay die Aktivierung von Neprilysin Promoteren durch $A\beta_{1-42}$ *in vitro* zu untersuchen. Dabei konnte keine Aktivierung der Neprilysin-Expression durch $A\beta_{1-42}$ oder eine Beteiligung der diffusionsfähigen Faktoren gezeigt werden. Wir haben aber festgestellt, dass Retinsäure, die für neuronale Ausdifferenzierung der Neuroblastomazellen benützt wird, sich aktivierend auf alle 3 Neprilysin-Promoteren auswirkt. In weiteren *in vivo* Experimenten könnten wir höhere Neprilysin mRNA and Protein-Konzentrationen nicht miteinander korrelieren. Diese Ergebnisse weisen darauf hin, dass eine erhöhte Proteinstabilität *in vivo* auch zur Erhöhung des Neprilysin-Gehalts beigetragen haben könnte. Zusätzlich zeigen wir hier, dass die Aβ Injektionen die Aktivierung von Plasmin, eines weiteren Aβ-abbauenden Enzyms, im Gehirn bewirken. Die Plasmin-Aktivierung war von einer höheren Aktivität des urokinase plasminogen activator (uPA) begleitet. uPA Transkription war jedoch unverändert. uPA Aktivität und erhöhter Neprilysin-Gehalt zeigten eine starke Korrelation *in vivo*. Wir untersuchten diesen Zusammenhang *in vitro* und konnten zeigen, dass $A\beta_{1-42}$ die Aktivität

beider Plasminogenaktivatoren uPA und tissue-type plasminogen activator (tPA) *in vitro* erhöht. Auch neuronale Expression von Neprilysin in transgenen Tieren führte zur Aktivitätssteigerung von uPA und tPA in Gehirn.

Neprilysin ist das wichtigste Aβ abbauende Enzym im Gehirn. Unser Ergebnisse zeigen, dass Neprilysin defiziente Mäuse eine Akkumulation und Ablagerung des Aβ Peptids im Gehirn aufweisen, ohne jedoch das Spaltungsmuster (processing) des APP Moleküls zu verändern. Neprilysin-defiziente Mäuse zeigten auch Anzeichen einer Aβ-abhängigen Neurodegeneration und kognitive Defizite. Diese Mäuse stellen das erste Modell mit muriner Aβ-Pathologie dar und ermöglichen die Untersuchung der Rolle des endogenen Aβ in Pathophysiologie von AD. Dies ist besonderes wichtig, weil die bisherigen Modelle auf der Überexpression des humanen APP in transgenen Tieren basieren. Eine Trennung der toxischen Einwirkungen von Aβ im Vergleich zur Beteiligung anderer APP-Spaltprodukte ist deswegen in diesen Modellen nicht eindeutig machbar. Um das therapeutische Potential der Neprilysin-Aktivierung gegen Aβ-Pathologie zu testen, haben wir unsere transgene Tiere mit einem Mausmodell mit erhöhter Aβ Produktion und Ablagerung (J20) gekreuzt. Wir zeigen hier, dass die Doppelmutanten eine massive Reduktion von Aβ im Gehirn aufweisen, während sich die Konzentrationen anderer APP-Spaltprodukten nicht ändern. Auch die Konzentrationen anderer Neprilysin-Substrate (Substance P, Enkephalin, Somatostatin) waren unverändert. Eine marginale Verminderung der Ängstlichkeit kennzeichnete die jungen NEP Tiere, die aber mit fortschreitendern Alter verschwand. Abgesehen davon, dass die NEP Maüse Schwirigkeiten in einem Angst-Konditionierungstest zeigten, hatte die Überexpression von Neprilysin keinen Einfluss auf die Lernfähigkeit und Gedächnisleistung. Dies denkt darauf hin, dass bei Neprilysin uberexpression wenig Beeinflussungen der cognitiven Leistungen zu erwarten wären. Sowohl die verminderte Lokomotion und Ängstlichkeit als auch die Defizite in konditionierter Geschmack-Aversion der J20 Mäuse wurde durch Neprilysin Überexpression nicht behoben. Eine mögliche Erklärung dafür könnte eine ungenügende Neprilysin-Konzentration sein, um diese Effekte rückgängig zu machen. Alternativ ist es möglich, dass APP und seine anderen Spaltprodukte, deren Gehalt nicht durch Neprilysin reduziert wird, für die oben beschriebenen Effekte verantwortlich sind. Im Gegenteil, die Überexpression von Neprilysin verhinderte die Beeinträchtigung der kognitiven Gedächtnisleistung der J20 Tiere, so dass sie von den Wildtyp Tieren nicht unterscheidbar waren.

Unsere Daten belegen in einem *in vivo* system, dass Aβ eine eigentlich toxische Spezies in der AD Pathophysiologie ist, welche die kognitiven Defizite verursacht. Weil Neprilysin-Aktivierung die Prozessierung des APP Moleküls nicht verändert, stellen wir die Hypothese auf, dass eine Hochregulation des Neprilysins die physiologischen Funktionen des APP nicht verändert. Wir schlagen deswegen eine neuronale Aktivierung des Neprilysins als eine wirkungsvolle Möglichkeit zur Aβ-Reduktion und AD-Therapie vor.

I) INTRODUCTION

1) Alzheimer's disease (AD)

1.1 A major health problem

AD is responsible for up to 70% of all dementia cases and represents up to 85% of moderate or severe cognitive impairments among older people [1, 2]. The age of onset can occur as young as 40 years in the cases of early onset or familial AD (FAD) caused by genetic mutations [3] and starts around 65 years for the sporadic or late onset AD cases, which account for more than 95% of all cases [4]. According to the World Health Organization, the National Institute of Ageing, the Alzheimer's Association and epidemiological studies [1, 2], AD affects 1.5% of the elderly from 65 to 69 years of age and doubles every 5 years reaching 24% of the elderly aged 85 or more in the general western population and up to 50% in USA. Furthermore, with the increase of life expectancy in the developing countries, the number of people with AD, which represents 18 million nowdays, is expected to double by 2025. Following initial diagnosis, AD patients live an average of 8 years and survive half as long as those without dementia, making AD the 3rd cause of disease related death in the US with 7.1% of all death in 1995 [5]. The direct annual cost of care for a patient is $30,000 in the USA. AD not only affects patients but also presents a heavy physical and psychological burden to their relatives who take care of them for most of the time while observing the constant, irreversible aggravation of symptoms, until hospitalization becomes inevitable.

1.2 Clinical symptoms and diagnosis

AD is a neurodegenerative disease with a long asymptomatic phase. It is characterized by a progressive loss of memory and starts with occasional episodic memory deficits, referred to mild cognitive impairment, including difficulties as recalling recent events of daily life [6]. With progression of the disease, the patients encounter difficulties in identifying common objects and familiar persons (agnosia), present a decline in physical coordination (apraxia), impairment of language functions (aphasia) and eventually lose their complete reasoning ability, including time and space orientation. AD patients also show dramatic personality

changes such as anxiety, aggressiveness, depression or hallucinations [7]. Over several years patients presenting a global cognitive deficit, are bedridden, completely dependent on caretakers and die of minor respiratory difficulties such as aspiration or pneumonia [8].

A well trained clinician can nowdays diagnose an AD patient with 90% accuracy. This is mostly due to standardized diagnosis criteria for dementia based on the Diagnostic and Statistical Manual of Mental Disorders, possible and probable AD based on the criteria of the National Institute of Neurological and Communicative Disorders and Stroke and Alzheimer's Disease and related Disorders Association [9, 10]. The clinical diagnosis of AD includes memory deficit and at least one of the major impairments previously presented (agnosia, apraxia, aphasia or reasoning). It is currently based on the patient's history, interviews with relatives after exclusion of other dementia diseases such as vascular dementia, frontotemporal dementia, dementia with Lewy bodies and Parkinson's disease. Cognitive tests like the Mini-Mental State exam or the Blessed Dementia Scale are also extensively used to monitor the development of the patient's cognitive abilities and to distinguish it from normal age-related decline. However, in spite of promising improvement in the *in vivo* detection techniques of one of the histopathological hallmarks of AD, known as amyloid plaques [11, 12] and the increased number of markers [13], the diagnosis of AD still leave an error rate of 10% in the best conditions. The certain diagnosis of AD can definitively be made by autopsy and the presence of the two molecular hallmarks of AD: extracellular amyloid plaques and intracellular neurofibrillary tangles (NFT).

1.3 Histopathology

Since their first description in 1907 by Alois Alzheimer, brain atrophy, extracellular amyloid plaques and intracellular NFT are still used today as the defining features for the AD.

1.3.1 Neurodegeneration

Not all brain areas are equally affected by AD pathology and the early clinical symptoms are due to loss of synaptic function and neuronal degeneration in brain regions responsible for learning and memory [14, 15]. This destructive process is characterized by a typical distribution pattern of brain changes that is specific with respect to area [16], lamina and even cell type [17]. The first area of the brain touched by this atrophy is the medial temporal lobe including hippocampus [15, 17] and the entorhinal cortex [14] . Compromised functions of

these areas correlate well with the early symptoms of the disease [16]. Then, the most vulnerable cells are the pyramidal cells in lamina II and III and V of the neocortex [18], while interneurons seem to be spared [19]. The limbic system including the amygdaloid complex is also affected [20] while the striatum and cerebellum may show some degree of plaque formation but do not develop significant neuronal pathology [21]. This atrophy is accompanied by a marked gliosis and clear neuronal dysfunction with neurotransmitter deficits such as the cholinergic neurons in the septum and basal forebrain [22] and several other regions [23, 24].

1.3.2 Neurofibrillary tangles

NFT are intracellular aggregates of the hyperphosphorylated microtubule-associated protein tau found in neurons (Fig. 1B). Tau binds to tubulin monomers and stabilize them [25] during polymerization of tubulin monomers into microtubules. Its activity is mostly controlled by phosphorylation involving multiples phosphatases and kinases [26, 27]. In pathological conditions, abnormal phosphorylation or hyperphosphorylation of tau disturbs its binding ability to microtubules and tau subsequently precipitates in the somatodentritic compartment. Destabilization of the microtubule and obstruction of the axonal transport lead to synaptic dysfunction, impaired energetic metabolism [28], and may contribute to the neuronal death [29, 30]. Following the complete degeneration of the affected neurons, the highly insoluble NFT remain in the brain. NFT are also present in other neurodegenerative diseases such as frontotemporal dementia, Pick's disease, progressive supranuclear palsy or corticobasal degeneration [26, 31].

1.3.3 Neuritic Plaques

Neuritic plaques, also called senile plaques, are extracellular deposits of amyloid-β protein (Aβ) fibrils (Fig. 1B) intimately surrounded by dystrophic axons and dendrites, activated microglia and reactive astrocytes, generally found in the limbic and association cortices [32]. The core is predominantly composed of the fibrillary 40-42 amino acid long β-amyloid peptides [33] and the longer form, more hydrophobic and therefore more prone to aggregation, is the major species present in the core [34, 35]. The microglia are usually adjacent to the central amyloid core and the astrocytes located at the peripheria of the plaque.

The neuritic plaques are usually accompanied by so called diffused plaques which appear prior to them. They are exclusively formed by the aggregation of the most hydrophobic Aβ petide, $A\beta_{42}$ [34, 35] and still lack the associated neuritic and glial cytopathology [36]. They also occur in cognitively normal, elderly healthy individuals [37] and so, are believed to be a presymptomatic feature of AD [38].

The extracellular plaque pathology and the intraneuronal formation of NFT evolve independently and their distribution pattern differs during the disease progression [39, 40]. The relationship between the β-amyloid plaques and NFT pathologies in AD is not yet clearly understood. However, using transgenic mouse models, it was shown that the amyloid pathology and more particularly $A\beta_{42}$ increases NFT formation *in vivo* [41-43].

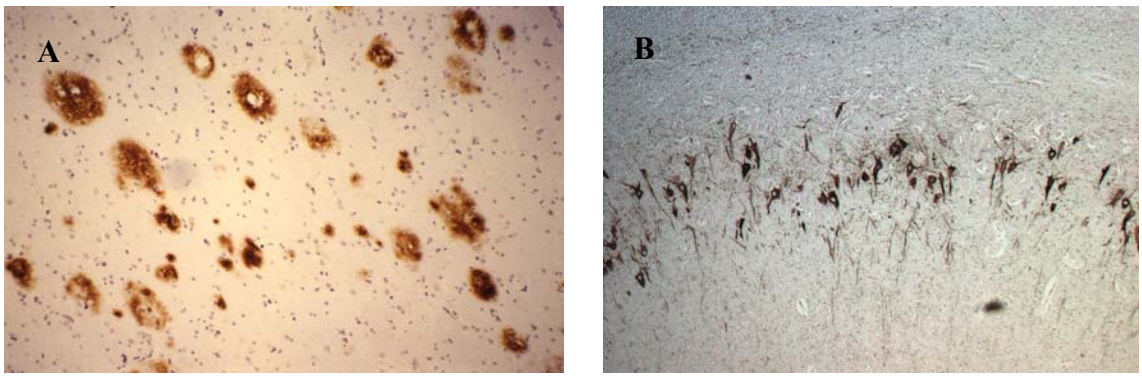

Figure 1. Major histopathological hallmarks of AD. (**A**) Representation of extracellular amyloid plaques formed by β-amyloid aggregation and (**B**) intracellular neurofibrillary tangles formed by hyperphosphorylated tau protein.

1.4 Amyloid precursor protein (APP) and function of its proteolytic fragments

1.4.1 APP and its putative functions

APP is a type I transmembrane protein, with a long extracellular N-terminal fragment, a single transmembrane region and a short intracellular tail [44]. APP presents a high degree of evolutionary conservation [45, 46], is ubiquitously expressed in widespread tissue and cell types including neurons [45, 47] and play an important role in the central nervous system (CNS) (reviewed in [48]). In the adult brain, APP shows widespread expression in the synaptic compartment and in vesicular structures of the cell body, axon and dendrites [49]. Different APP isoforms are derived from a single gene by alternative splicing [50], the most

common being APP695, AP751 and APP770 [45, 50]. The extracellular part of APP presents multiple binding domains for copper [51], zinc [52], heparin [53], collagen [54] and lamilin [55]. APP 751 and 770 also contain a Kunitz type protease inhibitor domain (KPI) which may regulate coagulation factor in the peripheria [56] whereas APP 695, the major isoform found in the brain, lacks the KPI domain [57]. APP can also be N- and O- glycosylated, phosphorylated and sulfated [58, 59]. Two APP gene homologues have also been identified, amyloid precursor like proteins (APLP) 1 and 2 which lack the Aβ region [60]. While APLP2 knockout (KO) mice appear healthy [61], deletion of the APP gene induces decreased locomotion [62], a strong decrease of synaptic protein such as synaptophysin or synapsin, and present a long term potentiation (LTP) impairment associated with memory impairment [61, 63, 64]. Finally, double KO mice for APP and APLP2 are lethal [61, 65] and present reduced synaptic vesicle density and size of the active zone [66]. These data suggest a functional redundancy between APLP2 and APP [61], and an important role for APP in neuronal development, viability and cognitive functions. Indeed, APP is involved in multiple functions, including learning and memory (reviewed in [67]). Disruption or decrease of synaptophysin immunoreactivity, impaired synaptic plasticity with decreased LTP and deficits in cognitive functions were also found in mice expressing wild type APP [68] and mutated APP [69, 70]. APP structurally looks like a potential receptor [44] and is targeted to the plasma membrane [44]. APP has been implicated in signal transduction involved in neuronal migration and positioning [71], cell proliferation, neuroprotection and neurite outgrowth [72-74]. APP was also found in one study to bind to kinesin-1 and to be involved in fast anterograde axonal transport of vesicles [75] but this function was recently challenged by Lazarov *et al*.[76].

1.4.2 APP processing

APP undergoes endoproteolytic cleavage by three secretases named α, β and γ-secretases. APP is initially cleaved by α or β-secretases leading to the non-amyloidogenic and amyloidogenic pathways, respectively (Fig. 2).

Most APP molecules undergo non-amyloidogenic processing [77]. α-secretase cleaves APP between amino acids 687 and 688 of the full length isoform 770 APP, 12 amino acids from the plasma membrane, which correspond to amino acids 16-17 of Aβ, precluding Aβ formation. It induces the release of the large soluble ectodomain of APP (sAPPα) into the extracellular space and produces an 83 amino acid C-terminal fragment (CTFα) which remains in the membrane [77, 78]. The amyloidogenic pathway involves the cleavage of APP

by β-secretase between amino acids 671 and 672, generating a slightly smaller extracellular fragment (sAPPβ) and the membrane bound fragment C99 (CTFβ), starting at amino acid 1 of Aβ. TACE (TNFα converting enzyme, also called ADAM 17) and ADAM (a disintegrin and metalloprotease) 9 and 10 are the major membrane-bound proteases found with α-secretase activity [79-81], but ADAM 10 is believed to be the major one involved in the processing of APP in the brain due to a better overlapping expression [79]. BACE1 (β-site APP cleavage enzyme, also known as Asp2 or memapsin2) and BACE2 have β-secretase activity [82, 83] but evidence that BACE1 was the major β-secretase in brain was confirmed by KO approach [84].

The membrane bound fragments C83 and C99 resulting from α and β-secretase cleavage respectively, can then be further cleaved within the transmembrane region at residue 711 or 713 of the 770 amino acids' isoform of APP by the γ-secretase complex releasing the non-amyloidogenic p3 fragment [85] from the C83 fragment or $A\beta_{1-40}$ and $A\beta_{1-42}$ from the C99 fragment and the APP intracellular domain a cytosolic C-terminal fragment of 57 or 59 amino acids (CTFγ).

The γ-secretase is a multiple protein complex containing presenilin 1 or 2 (PSEN1, 2) as catalytic subunits and different factors such as nicastrin, APH1 and PEN2 [86-88]. However, in spite of being the major enzymes containing the catalytic subunit of the complex, other proteins may also be involved [89].

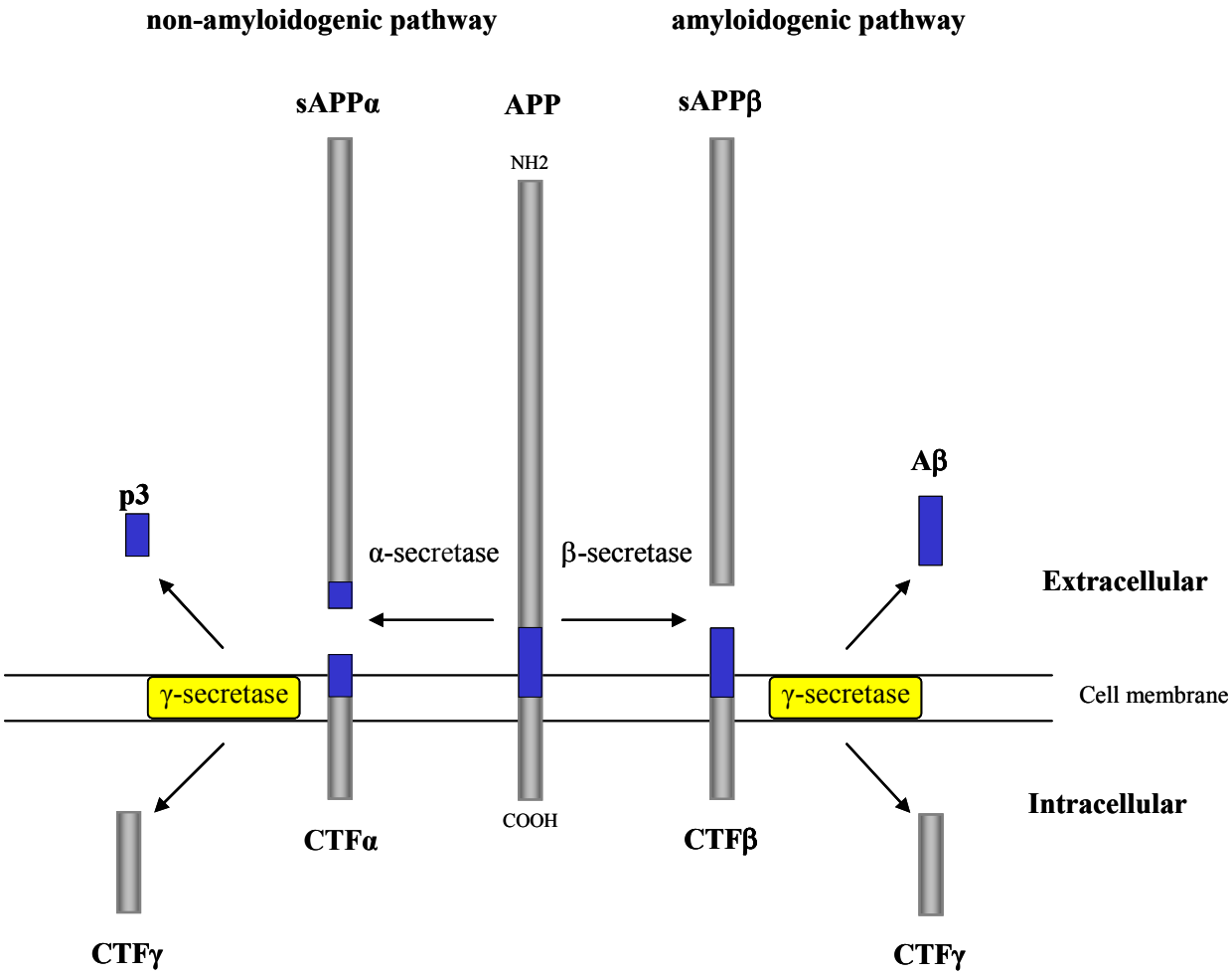

Figure 2. Proteolytic processing of APP. APP can be cleaved by α-secretase in the Aβ domain to producing soluble APPα (sAPPα) and a membrane bound C-terminal fragment (CTFα). Alternatively, APP can also be cleaved by β-secretase producing sAPPβ and CTFβ. Both CTF are further processed by the γ-secretase complex leading to intracellular release of CTFγ and extracellular release of either p3 or Aβ fragment.

1.4.3 Roles of secreted APP in neuronal function

Two forms of secreted APP fragments are produced during the cleavage of APP: sAPPα and sAPPβ (Fig. 2), with sAPPα being the major form produced. sAPP are present in brain tissues and circulate in the cerebrospinal fluid (CSF) [90]. Neuronal activity (induced by excitatory neurotransmitters and membrane depolarization) leads to sAPPα release from cultured neural cells [91], hippocampal slices [92] and hippocampal cells *in vivo* [93], suggesting roles for sAPPα in activity-dependent processes. In fact, both sAPP share similar domains which exerts neurotrophic and neuroprotective effects *in vitro*, such as neurite outgrowth [94, 95] and increase synaptic density [96]. However, sAPPα protected neurons with a 100 fold

greater potency than sAPPβ against death induced by glucose deprivation, excess glutamate and Aβ toxicity *in vitro* [74, 97, 98]. The C-terminal 666-686 region of sAPPα, based on the sequence of the 770 amino acids isoform of APP, contains a heparin binding site that is lacking in sAPPβ and is responsible for the neuroprotective effect of sAPPα via binding to receptors, activation of K+ channels leading to hyperpolarization of the cells and decreased calcium release [97]. Intracerebroventricular (ICV) injection of sAPPα also protected neurons from ischemic injury *in vivo* [99]. On the contrary, mice expressing APP with mutations which preclude the formation of sAPPα displayed severe neuronal degeneration and premature death suggesting that absence of sAPPα is deleterious to the neurons [100].

These growth-promoting properties, together with its structural similarities with cysteine-rich growth factors [101], suggest that sAPP may function as a growth factor *in vivo*. Interestingly, infusion of sAPP into the brain increases synaptic density and improves memory retention [96, 102], its level in the CSF also correlates with performances on memory tasks [103] and the level of sAPP is significantly decreased in the CSF of AD patients [104, 105]. The receptor for sAPP is still unknown but sAPPα was shown to selectively suppress *N*-methyl-D-aspartate (NMDA) receptor current without affecting currents induced by *α*-amino-3-hydroxy-5-methylisoxazole-4-propionate (AMPA) or kainate receptors in hippocampal neurons [106] and it is able to modify the properties required for LTD and LTP on hippocampal slices [107], suggesting that sAPP*α* contributes to various physiological and pathophysiological processes in which NMDA receptors participate.

1.4.4 Roles of amyloid-β in neuronal function

Aβ is a soluble metabolite endogenously produced [47, 108] which has received a lot of attention as a key player in AD. The two major forms are $A\beta_{1-40}$ and $A\beta_{1-42}$. Although $A\beta_{1-42}$ only accounts for 10% of total Aβ, its increased hydrophobicity makes it more prone to aggregation [109, 110] and seems to be the more pathogenic specie involved in AD [111]. The physiological function of Aβ is still unclear. It is proposed to function as a regulator of synaptic transmission and plasticity. Indeed, neuronal activity has been shown to modulate the formation and secretion of Aβ peptides in hippocampal slice neurons that overexpress APP. In turn, Aβ selectively depresses excitatory synaptic transmission via NMDAR onto neurons that overexpress APP, as well as nearby neurons that do not [112]. Aβ also impaired LTP in the same study [113]. Many studies have confirmed the neurotoxic functions of Aβ on various cell types (reviewed in [114]), including primary neuronal [115, 116] and brain slice

cultures [117, 118]. The Aβ toxicity involves multiple mechanisms (reviewed in [119]) such as microglia activation [120], production of reactive oxygen species [121, 122], increased intracellular calcium [123, 124], formation of ion pores [125, 126] and interactions with cell surface receptors [113, 127].

Aβ can be found in various aggregation states, and exists as monomers, dimers, oligomers, while further aggregation yields formation of protofibrils and finally plaques. It is still unclear in which state Aβ is the most toxic *in vivo*. However, transgenic mice showing neuronal dysfunctions, including memory deficits, prior to β-amyloid plaque formation [68, 128, 129] and the lack of correlation between β-amyloid plaque load and cognitive deficits [37, 130-132] suggest that the Aβ fibril intermediates rather than amyloid plaques are the major cause of neuronal dysfunction and cognitive deficits *in vivo*. Recently, ICV injection of different forms of Aβ strongly suggested that oligomers of Aβ were more potent than monomers to block LTP [133] and to induce memory impairment [134].

1.4.5 Roles of CTFα and CTFβ in neuronal function

The functions of C83 and C99 fragments, prior to γ-secretase cleavage and release of Aβ or p3 and AICD, are unclear due to the impossibility to dissociate the effects of these fragments from their cleavage products. However, transgenic models and ICV injections provide evidence of their negative effects on neurons and cognitive functions. Overexpression of different C-terminal fragments of APP such as C100 or C104 in mice induced the formation of Aβ deposits [135], impaired LTP [136], neurodegeneration [137, 138] and cognitive impairments in Morris water maze and Y-maze paradigms [137].

Interestingly, ICV injection of C105 in mice induced a greater cognitive impairment in Morris water maze and Y-maze, cholinergic dysfunction and decrease of mitochondrial pyruvate dehydrogenase levels than $A\beta_{1-42}$ [139], suggesting that γ-secretase inhibitors that decrease Aβ formation but increase CTFs may not be a good therapeutic approach in AD. However, it is unknown if these effects are extracellular or involve reinternalization.

1.4.6 Roles of CTFγ in neuronal function

The CTFγ fragment formed by 59 or 57 amino acids, is released after cleavage by γ-secretase and its generation is independent of Aβ formation [140, 141]. This is a very labile fragment quickly degraded by the insulin degrading enzyme (IDE) [142, 143] or by the proteasome

[144]. However, it has been shown that CTFγ also interact via a YENPTY motif with multiple adaptor proteins (reviewed in [145]), which increase its stability, induce its translocation into the nucleus and allow transcription regulation by CTFγ [146-150]. C59 but not C57 was initially found to repress retinoic acid-responsive gene expression *in vitro* [148, 151] suggesting that genes activated by retinoic acid such as APP [152, 153] or BACE [154] were negatively controlled by the CTFγ. It was, however, recently found in our lab that overexpression of the C50 fragment activated the transcription of APP, BACE, the histone acetyltransferases Tip60, the glycogen synthase kinase 3β GSK3β and the tumor metastasis suppressor KAI1 *in vitro* [146]. Complex formation with CTFγ, translocation into the nucleus and regulation of gene expression was also confirmed for KAI1 *in vivo* [150]. CTFγ is involved in the regulation of phosphoinositide-mediated calcium signalling *in vitro* [155] and exert neurotoxicity on different cell types including differentiated PC12 cells and rat primary cortical neurons by inducing the expression of GSK-3β [156, 157].

APP processing, signalling and functions of CTFγ are difficult to apprehend due to potential competition between the different adaptor proteins [158] for the binding site of CTFγ, leading to either the inhibition of its release by stabilizing or modulating the localization of APP or formation of different transcription complexes activating different pools of genes. Furthermore, CTFγ also competes with other proteins for the adaptor proteins such as Fe65 or Numb. CTFγ was shown to repress transcription mediated by the Notch intracellular domain by binding to Numb *in vitro* [159]. Similarly the low density lipoprotein receptor-related protein (LRP) intracellular domain inhibited the CTFγ-related transcription of KAI1 by binding to Fe65 *in vivo* [160].

1.5 Genetics of AD

The etiology of AD is complex, heterogenous and involves non genetic as well as genetic factors. Based on twin studies, the latter were found to represent 50% to 75% of the risk to develop AD [161-163] confirmed by the fact that after age, family history is the second greatest risk factor for AD [164]. In spite of a similar phenotype, early onset familial AD (EOFAD) with onset age younger than 60 years and late onset AD (LOAD) with onset ages older than 60 can be distinguished among AD cases.

1.5.1 Early onset familial Alzheimer disease

EOFAD accounts for less than 5% of all AD and is attributed to rare but fully penetrant mutations expressed in an autosomal dominant manner [165], in three different genes: APP on chromosome 21 [166], PSEN1 on chromosome 14 [167] and PSEN2 on chromosome 1 [168, 169]. At least 16 mutations in APP, 140 in PSEN1 and 10 in PSEN2 have been determined so far (AD mutation database; http://www.molgen.ua.ac.be/ADmutations). Mutations in the APP gene are estimated to account for less than 5% of FAD, the most frequently mutated gene, PSEN1, accounts for 50% of all EOFAD cases with onset prior to age 50 [170, 171]. While these AD-causing mutations occur in 3 different genes, they all share a common biochemical pathway: they all affect the proteolytic cleavage of APP leading to an increased production of Aβ or a relative overabundance of the $A\beta_{42}$ compared to the $A\beta_{40}$ species, which eventually results in neuronal cell death and dementia. Interestingly, Down syndrome is caused by the triplication of chromosome 21, which includes the genes BACE2 and APP. With plaque formation observed in the brain of Down syndrome patients as young as 8 years old, all individuals develop sufficient neuropathology for a diagnosis of AD by the age of 40 [172].

1.5.2 Late onset Alzheimer disease

In contrast with EOFAD, LOAD represents the majority of all AD cases and is due to polymorphisms with low penetrance but high prevalence. Due to the major role of genetic factors in this form of AD [161, 164], multiple genomic scanning of LOAD patients were performed to determine the genes involved [173, 174].

Until now, only one genetic risk factor for LOAD was confirmed in multiple studies from different ethnic groups and populations [175]: the ε4 allele of the apolipoprotein E (apoE) gene on chromosome 19 [176, 177]. ApoE exists in three major isoforms, ε2, ε3 and ε4. The ε4 allele is only present in 15% of the population and carrying one or two copies of ε4 is neither necessary nor sufficient to cause AD. However, its presence decreases the mean age of onset of 16 years [178] in a dose dependant manner [179, 180], a carrier of one copy and two copies being 3 and 8 times more likely to be affected than controls [178].

ApoE is secreted by glial cells [181, 182] and modulate neuronal plasticity by transporting lipids into neurons through specific receptors, LRP being the major one [183]. ApoE ε2 and apoE ε3 isoforms were found to induce neurite extension in neurons, whereas apoE ε4

inhibited outgrowth [184, 185] via binding to LRP [186]. Similarly apoE ε3 but not ε4 prevented Aβ-induced neurotoxicity by a similar process [187]. ApoE also binds Aβ [176] and play a role in its clearance and deposition. The mechanism by which apoE contributes to AD pathology is unclear but carriers of the ApoE ε4 isoform present a greater number of Aβ plaques when compared to ApoE ε3 carriers [188]. Similarly, overexpression of human apoE ε4 in transgenic mice overexpressing human APP leads to increase Aβ deposition, compared to expressing human ApoE ε3 [189]. *In vitro* studies suggest that apoE ε4 is less efficient than apoE ε3 to inhibit Aβ aggregation [190, 191].

Among the other potential risks factors, alpha-2 macroglobulin (α-2M) and LRP, on chromosome 12 were associated with LOAD [192, 193]. α-2M is a plasma protein, produced in the brain where it binds multiple extracellular ligands including proteases and is internalized by neurons and astrocytes via the LRP receptor. It also binds Aβ with high specificity and prevents its toxicity in neuronal cell culture by internalization via LRP [194, 195]. In AD patients, α-2M is localized in the neuritic but not the diffuse plaques [196]. LRP is a multifunctional scavenger and signaling receptor able to bind many ligands including apoE, APP, α-2M, Aβ and plasminogen (reviewed in [197]). LRP, initially found to mediate the neuronal uptake of astrocyte-derived cholesterol [198], is also involved in removal of protease-protease inhibitor complexes [197]. Increasing evidence also suggest that LRP is involved in the clearance of Aβ and mediates its efflux from the brain to the periphery at the blood brain barrier (reviewed in [199-202]). The Aβ peptide binds avidly to LRP ligands, such as α-2M and apoE, and LRP-mediated clearance of the complex contributes to a reduction in Aβ levels [201, 203].

Among the other candidates potentially associated with LOAD, insulin degrading enzyme [204, 205], neprilysin [206-208] and angiotensin-converting enzyme (ACE) [209, 210] have all been directly involved in the degradation of Aβ. However, these associations could not be always reproduced [211-213], suggesting that the association is not strong and may vary based on the population analyzed.

1.6 Amyloid cascade hypothesis

The amyloid cascade hypothesis was initiated by Glenner *et al.* after identification of the peptide present in the core of the senile plaques from Down syndrome patients and the prediction of an AD gene on chromosome 21 [214]. The hypothesis postulates that the

accumulation of Aβ, due to an imbalance between its generation and clearance, initiates the pathologic cascade in AD leading to inflammation, neurodegeneration, amyloid plaque and NFT.

The main support for the amyloid hypothesis derives from genetic studies. All mutations responsible for EOFAD were found in APP itself and in the presenilins [165]. They all were shown *in vitro* and *in vivo* to directly alter the production of Aβ in a manner that promotes amyloid formation. Most mutations on APP and presenilins selectively increase the production of the more toxic [111] and more amyloidogenic $A\beta_{42}$ peptide [109, 110]. Similarly, the only known risk factor for LOAD, apoE ε4, increases Aβ deposition in the brain of AD and transgenic mouse models [177, 188, 215] and the other genes implicated, such as LRP and α-2M are also involved in Aβ clearance [194, 203]. The major risk factor in AD is aging. All EOFAD present an early age of onset and Down syndrome patients with three copies of the APP gene, develop sufficient neuropathology for a diagnosis of AD by the age of 40 years [172].

The second main support of the amyloid cascade hypothesis comes from biochemical and neuropathological studies. Many studies have confirmed the neurotoxic functions of Aβ on various cell types *in vitro* and *in vivo* (cf. 1.4.4). Transgenic mouse models overexpressing human AD-causing mutated APP develop with aging the major features of AD: first diffuse then fibrillar Aβ plaques, associated with neuronal and microglial damage leading to cognitive deficits (reviewed in [216-218]). Furthermore, brains of Down syndrome patients and apoE ε4 carriers present increased level of Aβ and amyloid plaques formation prior to NFT formation and cognitive deficits [219, 220].

Initial arguments against the amyloid hypothesis included the lack of massive neuronal loss and NFT formation in transgenic mouse models overexpressing the AD causing mutated human APP, exhibiting extensive amyloid deposits [218, 221, 222], the lack of correlation between the degree of dementia and the number of plaques in patients [37, 131, 132] and transgenic mouse models [68, 128, 130] and the different spatiotemporal distribution of Aβ and tau pathologies [39, 40]. In spite of the fact that mouse lifespan may be a limiting factor in determining the degree of pathology and mice may not respond to Aβ accumulation the way humans do, most of these aspects were recently challenged. The lack of neurodegeneration in the transgenic mouse overexpressing mutated APP can also be explained by the neuroprotective effects of APP (cf. 1.4.1) and sAPPα (cf. 1.4.3) overexpression, which are also present in these mice and temper the neurotoxic properties of

Aβ. They were shown *in vivo* to activate the transcription of genes such as transthyretin and the insulin pathways [223], which are involved in the clearance of Aβ and therefore prevent the neurotoxicity of Aβ [224, 225]. Finally, mice overexpressing the C-terminal fragment of APP lacking the sAPPα domain presented signs of neurodegeneration [137, 138].

The second major argument against the amyloid cascade hypothesis concerns the pathophysiological relation between amyloid plaques and NFT formation. It has been shown using transgenic models that the amyloid pathology and more particularly $A\beta_{1-42}$ was responsible for the increase of NFT formation [41-43]. Crossbreeding of mice overexpressing human AD-causing mutated APP and human mutated tau associated with FTDP-17 led to high increase of NFT formation [42]. Similarly, stereotaxic injection of $A\beta_{1-42}$ fibrils into the hippocampus of a tau transgenic mouse caused 5 fold increase in the number of NFT in the amygdala [41]. Even if the relation between the two major hallmarks of AD is not yet fully elucidated, Aβ increases the tau pathology and more specifically the NFT formation.

Finally, a modified amyloid hypothesis was proposed to better take into account the discrepancies between histological lesions and cognitive functions. Indeed, studies on transgenic mice showed that neuronal dysfunctions, including memory deficits, appeared before β-amyloid plaque formation [68, 128, 129], suggesting Aβ fibril intermediates other than amyloid plaques as the major cause of neuronal dysfunction and cognitive abnormalities. Different studies suggested that oligomers of Aβ are more toxic than monomers *in vitro* [226] and more potent in inducing neuronal [133, 227, 228] and cognitive dysfunctions [134] *in vivo*. Oligomers or other preaggregates of Aβ, diffusible and invisible to standard procedures used to visualize amyloid plaques, may be responsible for the discrepancies observed.

With more evidence that increased levels of Aβ initiates the pathologic cascade in AD, therapeutic approach aiming at decreasing its production or increasing its clearance and catabolism are investigated. Among the enzyme involved in Aβ catabolism, neprilysin appears as the major rate limiting factor [229, 230].

2) Neprilysin

2.1 Gene structure and transcription regulation

2.1.1 Gene structure

In humans, the neprilysin gene (*Mme*) is located on chromosome 3q25.1-q25.2 within a candidate locus associated with LOAD cases [231, 232]. The neprilysin gene spans more than 80 kb and is composed of 22 coding exons [233], four 5' untranslated exons and a 3' untranslated region (UTR). The 5' UTR of neprilysin is alternatively spliced, resulting in 5 separate potential mRNA transcripts (Fig. 3).

The presence of three human neprilysin cDNAs each containing different untranslated 5' sequences but a common coding sequence was initially reported [233]. Using a human placental genomic library, these three mRNA species, called type 1, type 2a and type 2b were found to derive from two non-coding exons, exon 1 and 2, the type 2a and 2b mRNA being expressed by alternative splicing of exon 2 [234]. A fourth non-coding exon, exon 1b located between exon 1 and exon 2 was further identified using a human leukocyte genomic library [235]. Finally the existence of a fifth non-coding exon, called exon 3 and located between exon 2 and the first coding exon, was demonstrated by RT-PCR of RNA from human kidney and lung [236].

With 90% identity to the human neprilysin sequence [237], these 5' sequences are highly homologous to rat and rabbit cDNA [238, 239]. For example, mRNAs corresponding to type 1, 2b and 3 have been observed in rat kidney [236, 240]

Expression of neprilysin is transcriptionally regulated via 3 distinct regulatory regions located upstream to exon 1, 2 and 3 of 1200 bp, 550 bp and 3400 bp, respectively [235, 236, 240]. These promoters are characterized by the presence of multiple transcription initiation sites and the absence of classic TATA boxes and consensus initiation elements [241]. Promoter 1 also presents multiple putative binding sites for transcription factors such as Sp1, NF-IL6, NF-κB, PU.1 and ets binding motifs. The promoter 2 contains a GC rich regulatory region with multiple Sp1 binding sites, a retinoblastoma control element and an inverted CCAAT box [235, 241].

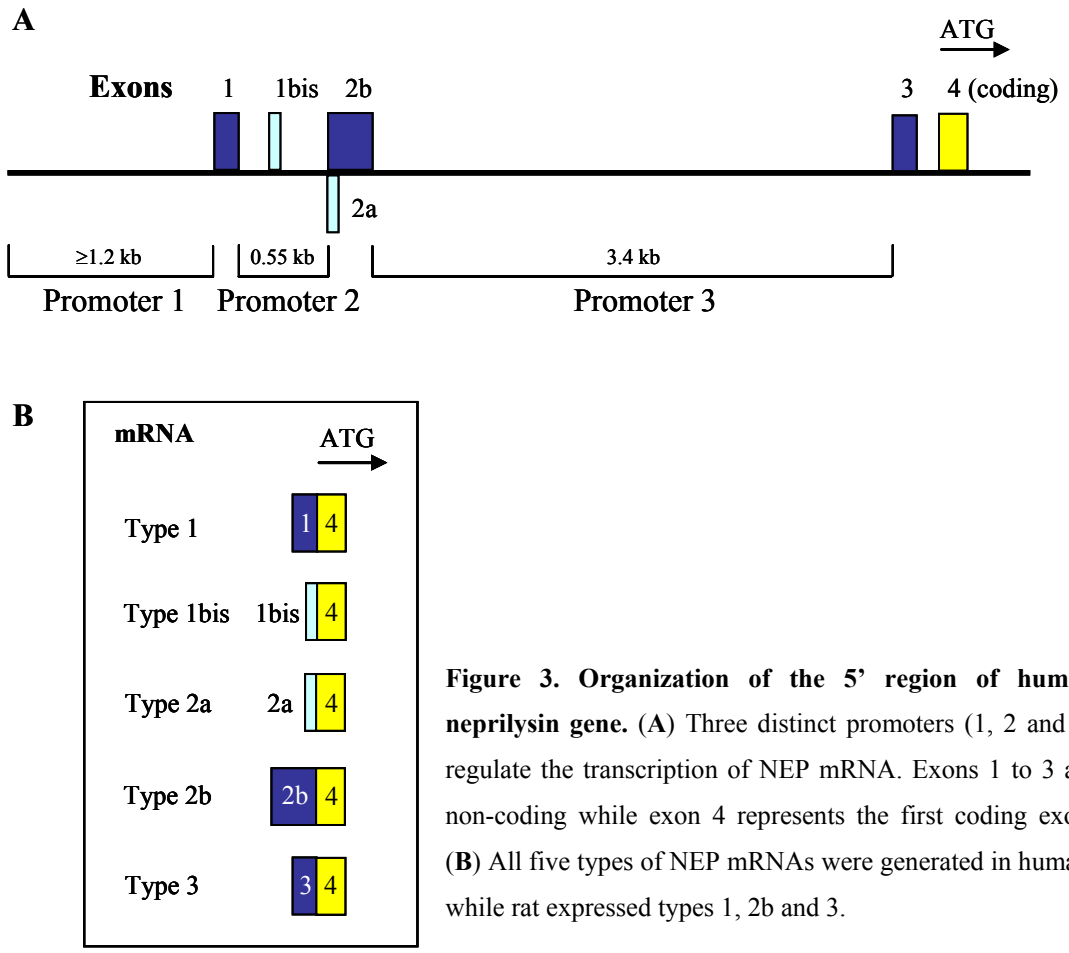

Figure 3. Organization of the 5' region of human neprilysin gene. (**A**) Three distinct promoters (1, 2 and 3) regulate the transcription of NEP mRNA. Exons 1 to 3 are non-coding while exon 4 represents the first coding exon. (**B**) All five types of NEP mRNAs were generated in human, while rat expressed types 1, 2b and 3.

2.1.2 Regulation of neprilysin transcription

Neprilysin gene transcription is regulated in a cell and tissue-specific manner [241] via the three different promoters. Type 1, 2b and 3 transcripts represented in rat brain 67, 18, 15% and in rat kidney 11, 70, 20%, respectively [240]. In rat brain, *in situ* hybridization confirmed a major neuronal expression of the type 1 transcript in neurons and type 3 mRNA expression in oligodendrocytes [240].

Analysis of the promoters confirmed the binding of multiple transcription factors. Using bronchial epithelial, lymphoblastic leukemia, lymphoma and non small cell lung cancer cell lines, CBF/NF-YA transcription factors isoforms were found to bind on promoter 2 and activate neprilysin transcription in a cell specific manner [242]. Using prostate cancer cells, two androgen response element (ARE) were found to activate neprilysin transcription: one in promoter 2 which preferentially binds androgen receptor and one located in the 3' UTR which binds androgen, glucocorticoid and progesterone receptors [243]. It correlates with the enhanced neprilysin expression *in vitro* by steroid hormone treatment such as progesterone

[244] or glucocorticoids [245-247]. Using leukemia cells, a functionally important transcription factor binding site was found in the 5' region of promoter 2 and was shown to be bound by Sp1 [248]. The potential Sp1-binding sites are common in promoters lacking a TATA box since Sp1 is important for the initiation of transcription from TATA less promoters [249] and the protection of CpG islands [250] from methylation [251] (reviewed in [252]). Importantly, the methylation of neprilysin promoters was found in human prostate cancer *in vitro* and *in vivo* leading to inhibition of transcription [253, 254] and the subsequent progression of androgen-independent prostate cancer cells [253, 255].

Neprilysin mRNA and protein level are also regulated by a variety of cytokines: interleukin-1β (IL-1β) and tumor necrosis factor-alpha (TNFα) increased neprilysin mRNA and protein level in human bronchial epithelial cells [245] while interleukin-1α (IL-1α), TNF-α, transforming growth factor (TGF) and interleukin-6 (IL-6) increased neprilysin activity on the surface of intact lung fibroblasts [256] via a mechanism involving cAMP signalling pathway [245, 256].

Upregulation of neprilysin expression and enzymatic activity were also observed during forskolin-induced differentiation of human choriocarcinoma cells [257] via the cAMP signalling pathway [258, 259] and phorbol ester-induced differentiation of choriocarcinoma cells via the protein kinase C signalling pathway [260].

2.2 Protein and structure

Neprilysin (EC 3.4.24.11) also known as neutral endopeptidase 24.11, enkephalinase, common acute lymphoblastic leukemia antigen (CALLA) and CD10 is a 94 kilodaltons (kd) type II integral plasma membrane zinc metalloendopeptidase, classified as a member of the M13 family implicated in inactivation of several biologically active peptides.

Neprilysin consists of a short N-terminal cytoplasmic domain (27 amino acids), a single membrane-spanning segment (23 amino acids) and a large extracellular domain (700 amino acids) containing the active site [261, 262].

It presents 6 N-linked glycosylation sites, 3 of which are glycosylated [263], 12 cysteine residues, all involved in disulfide bridges [262, 263] necessary for the maintenance of the structure and the activity [264]. As a zinc metalloprotease, the catalytic site consists of the canonical HExxH zinc binding motif as well as a conserved consensus sequence ExxA/GD in which the glutamate serves as the third zinc ligand.

Its crystal structure complexed with inhibitors was determined and confirmed the functional motifs involved in catalytic activity and stability [263, 265]. Neprilysin is also a highly conserved protein among the mammalian species. Murine, rat and rabbit neprilysin amino acids sequences present more than 90% identity to the human neprilysin sequence, 95% when compared one at a time, and 100% conservation of critical amino acids and functional motifs [237].

Neprilysin belongs to the M13 subfamily of mammalian neutral endopeptidase, which includes other zinc dependant endopeptidases such as endothelin-converting enzymes ECE-1 [266, 267], ECE-2 [268], the erythrocyte surface antigen KELL [269], the phosphate regulating gene on the X chromosome PEX, the damage induced neuronal endopeptidase DINE [270] also called X-converting enzyme [271] and NEP2 [272] also called soluble secreted endopeptidase (SEP) [273] or neprilysin like peptidase (NEPL1) [274]. The overall homology between neprilysin and these other members is 35, 30, 31, 25, 48 and 65%, respectively. The homology increases when only the 250 C-terminal residues containing the important amino acids necessary for neprilysin activity are taken into account [263, 271, 272]. They all present specific pattern of expression and degrades substrates with different affinity [275, 276].

2.3 Localization

Originally discovered in the brush border membrane of rabbit kidney [277], neprilysin is widely distributed in mammalian tissues including the CNS [278, 279], male genital tract [280], epithelia of intestine and lung [281, 282], fibroblasts [281] and neutrophils [283]. Neprilysin is also present on leukemic cells of pre-B phenotype, which represent 85% of all human acute lymphocytic leukemia (ALL) and therefore is an important cell surface marker in the diagnosis of ALL [284, 285].

Neprilysin is broadly expressed in the brain [286, 287] and neprilysin immunoreactivity was found in the striatum, substantia nigra, choroids plexus and at a lower level in areas including the hippocampus, neocortex, colliculi, amygdala and central gray matter [288-290]. Localization of neprilysin is mainly neuronal [278, 289, 290] but can also be found in glial cells [240, 290]. It presents a synaptic and axonal localization in hippocampal and neocortical neurons with preference for GABAergic and mGluR2/3-positive neurons [288].

2.4 Substrates

Neprilysin preferentially hydrolyzes peptide bonds involving the amino group of hydrophobic residues [277] and cleaves on the N-terminal side of hydrophobic amino acid residues [236]. Thereby, neprilysin is able to cleave a broad range of proteins but preferentially degrades small peptides due to its conformation which restricts access to the active site, therefore, limiting the size of the substrate that can enter and be cleaved [263].

Purified neprilysin was shown to degrade a wide rage of bioactive peptides *in tubo* [291, 292] including substance P (SP) [293], enkephalins [279, 294, 295], atrial natriuretic peptides [296], bombesin-like peptides [297], neurotensin, luliberin and cholecystokinin [294], endothelin [298], angiotensins [299], somatostatin [300-302] and more recently β-amyloid [229, 303].

The number of peptides supposed to be cleaved was, however, smaller than originally anticipated *in vivo* [292] and the physiological function of neprilysin is mostly determined by its cellular localization, the availability of the substrates and of other potential enzymes to competing for the same substrates.

For example, a detailed immunohistochemical mapping of neprilysin in CNS, in comparison with SP and enkephalins, two alleged neuropeptide substrates, has brought to light several discrepancies [278, 290]. This illustrates the importance of colocalization between the enzyme and its substrate and suggests that other peptidases, such as ACE [304], ECE-1 [286, 305] or NEP2 [272, 306] probably remain to be characterized as candidates in the metabolism of SP and enkephalins in the CNS.

2.5 Investigation of neprilysin functions

Three different approaches have been used to investigate neprilysin functions. The most popular is the inhibition of neprilysin activity with specific inhibitors such as phosphoramidon [307, 308] and thiorphan [309]. Such inhibitors allow the analysis of the function of the endogenous neprilysin at a specific time in a specific system. They also represent potential therapeutic tools in conditions where neprilysin inhibition is researched, such as cardiovascular regulation [310, 311], and allow the investigation of potential side effects.

The two other approaches involve overexpression and genetic deletion of neprilysin. The overexpression of neprilysin is a specific tool to determine neprilysin functions including the

degradation of specific substrates *in vitro* and *in vivo*. However, it does not reproduce the specific localization of the endogenous protein nor does it take into account the competition with other enzymes for the same substrate. For example, in spite of neprilysin function, ACE was shown to be the major bradykinin degrading enzyme in cardiac membranes [312] and cathepsin G, the major inactivator of SP in human neutrophils [313].

The targeted deletion of the neprilysin gene (NEP KO or NEP-/-) in mice [314] offers the opportunity to study the effects of a complete and long-term elimination of endogenous neprilysin activity and its effect on substrate levels *in vivo*. The only weakness of this model is the adaptation of the system and presence of potential biochemical compensatory strategies.

2.5.1 The use of inhibitors and their specificity

Neprilysin inhibition was shown to potentiate the SP-mediated neurogenic inflammation in the lung [315], natriuretic factor mediated natriuresis and diuresis in kidney [316], regulation of cellular proliferation in the lung [297] and prostate cancer [255], enkephalin-mediated analgesia [309] and accumulation of Aβ in the CNS [317].

However, with the discovery of new metalloproteases and the better understanding of the systems involved, the specificity of these inhibitors and their action appear questionable. Initially used to confirm the degradation of substrates by neprilysin *in vitro*, neprilysin inhibitors are usually used at final micromolar concentrations. With a constant of inhibition (IC50) of approximatively 2 nM for neprilysin [318, 319] and 295 nM for angiotensin-converting enzyme (ACE) [318], thiorphan at the micromolar concentration most likely inhibited also the widely distributed ACE in several published studies [304]. ACE is known to degrade a wide range of substrate such as bradykinin, SP, enkephalin and angiotensin I [320] and is mainly involved in the cardiovascular system and blood pressure by conversion of angiotensin I into the vasoconstrictor angiotensin II and inactivation of the vasodilator bradykinin [321]. Furthermore, phosphoramidon also inhibits ECE-1, with an IC50 of 1.5 μM compared to 34nM for neprilysin [322, 323]. ECE is another widespread member of the M13 family including endothelial cells [324], smooth muscles [325] and neurons in the brain [286, 305, 326] involved in the degradation of a broad range of substrate including, angiotensin I, SP, neurotensin, bradykinin but is mostly known for its cleavage of big endothelin into the potent vasoconstrictor endothelin-1 (reviewed in [275, 327]) and its role in the regulation of the cardiovascular homeostasis [328]. Similarly, a new endothelin-1 inactivating metalloendopeptidase, mainly localized in the kidney where it mostly degrades the potent

vasoconstrictor endothelin-1 [329], was inhibited by thiorphan and phosphoramidon with an IC50 of 0.28 nM and 0.55 nM, respectively [329, 330]. 10 μM of phosphoramidon or thiorphan similarly inhibited totally neprilysin and DINE [331], a neuron-specific endopeptidase whose expression is highly increased in response to axonal injury in both the CNS and peripheral nervous system [270, 271].

Another member of the M13 family presents a high degree of functional homology with neprilysin: NEP2 [272]. Its two most abundant isoforms lead to the formation of either a membrane-bound or secreted protein, which are mainly present in the brain and the testis, respectively [272]. Due to a 97% homology in the active site, recombinant NEP2 isoforms were shown to cleave the same substrates as neprilysin with similar cleavage site, similar specificity constants and inhibitory patterns [306], suggesting that NEP2 may, in fact, possess some functions previously attributed to neprilysin in the brain. However, they display a rather distinct expression pattern in the brain, suggesting specific functions for each one due to substrates availability and region specificity [286].

Homologues of neprilysin have also been identified in simpler organisms, including prokaryotes [332, 333] and more than 20 neprilysin-like proteins are present in Caenorhabditis elegans and Drosophilia melanogaster [275, 334]. It confirms the important role of these endopeptidases through evolution and suggests that more mammalian homologues of neprilysin could be characterized.

2.5.2 Neprilysin and enkephalin mediated analgesia

Inhibition of brain enkephalin degradation by ICV injection of neprilysin inhibitors resulted in analgesia in various nociceptive tests [307, 335, 336] reversible by opioid receptor inhibitors [337]. These inhibitors enhanced the recovery of enkephalins whose release from rat striatal slices was evoked by potassium [338]. Furthermore, thiorphan protected exogenous enkephalins from degradation in rat brain slices [339], in mouse brain *in vivo* [340] and was associated with an elevation of extracellular enkephalin levels in the CNS [309] or in the peripheria [341].

However, the antinociceptive effects of thiorphan was not always inhibited by an opioid receptor antagonist and did not always correlate with an enkephalin increase [342], suggesting that thiorphan may also induce analgesia in an enkephalin independent manner.

This idea was further suggested by the use of isomers of thiorphan, which were equipotent as neprilysin inhibitors (IC50 = 1 nM) but had significantly different analgesic profiles when

injected ICV [336]. Furthermore, other analogs of thiorphan, less potent inhibitors of neprilysin (IC50 = 0.1μM and IC50 = 100 μM), produced analgesia and potentiated analgesia induced by an enkephalin analog at doses comparable to thiorphan [336]. Similarly, different analogs of a neprilysin inhibitor injected ICV produced analgesia with or without alteration of endogenous enkephalin level in the striatum [343]. These studies suggest that thiorphan produce analgesia through a pharmacological mechanism which is not directly related to inhibition of neprilysin and/or enkephalin degradation.

Genetic elimination of *Mme* also resulted in controversial results. Saria *et al.* found that inactivation of the *Mme* gene in mice, induced analgesia characterized by an increase in the thermonociceptive threshold in the hot plate paradigm [344]. Although neprilysin, previously termed enkephalinase, is a potent enkephalin-degrading enzyme in a test tube paradigm, the phenotype was not associated with modification of enkephalins levels in the cortex, brain stem or striatum. More surprisingly, a reduced enkephalin content in hypothalamus and spinal cord of NEP KO mice further suggests potential biochemical compensatory strategies [344]. Fisher *et al.*, to the contrary, could not reproduce in NEP KO mice the opioid-mediated analgesia observed after pharmaceutical neprilysin inhibition and neprilysin deletion led to hyperalgesia in a model of visceral pain associated with an accumulation of the hyperalgesic peptide bradykinin [345]. Furthermore, quantification of striatal proenkephalin-mRNA levels in NEP KO compared with WT mice did not show any difference [345]. Only a 21% reduction of mu receptor density in crude brain homogenates of NEP KO mice was observed, while delta- and kappa-opioid receptor densities were unchanged [345].

These data suggest that enkephalins levels are not increased in the brain of neprilysin deficient mice and that neprilysin inhibitors-mediated analgesia may involve other substrates.

2.5.3 Anti-inflammatory function of neprilysin

Neurogenic inflammation is regulated by sensory nerves and characterized by extravasation of plasma proteins and infiltration of neutrophils from post-capillary venules and arteriolar vasodilatation. It is well established that SP and bradykinin can interacts with the neurokinin 1 receptor (NK1R) and the bradykinin receptors respectively to initiate neurogenic inflammation. While bradykinin most likely sensitizes nerves to further inflammatory stimuli, SP is the major bioactive mediator of neurogenetic inflammation [346-349].

Administration of neprilysin inhibitors potentiates neurogenic inflammation in the airway by preventing the degradation of SP [315] and overexpression of neprilysin accelerated the degradation of SP by intact epithelial cells and by membrane preparations [350].
Neprilysin deletion in mice markedly increased the basal level of SP in the colon (2.5 fold) [351] and diminished degradation of SP and bradykinin by the intestine membrane [352], suggesting increased bioavailability of substance neurogenic substrates. This is accompanied by an increased protein extravasation in the colon [351] and the intestine [352] without evidence of overt inflammation at the tissue level [351]. Similarly, NEP KO mice also presented widespread basal plasma extravasation in postcapillary venular endothelia [353]. The anti inflammatory function of neprilysin was further investigated in a different model of inflammation. Neprilysin deletion exacerbated induced intestinal inflammation [352, 354] and increased the severity of induced-colitis [351], increased infiltration of inflammatory leukocytes and skin inflammation in a model of allergic contact dermatitis [355]. All these effects were prevented or reversed by exogenous recombinant neprilysin and antagonists of SP (NK1) and bradykinin (B2) receptors, [351-355]. Similarly, delivery of recombinant neprilysin reduced the tackykinins related neurogenic inflammatory response in the respiratory tract [356-358] leading to inhibition of cough induced by exposure to SP [359] and prevented the SP-induced plasma extravasation in the skin [360].
Taken together, these studies confirm the major role of neprilysin in inflammation regulation in different organs.

2.5.4 Neprilysin and cancer proliferation

Lung cancer

Lung cancer is the most common form of cancer in the world, both in terms of incidence (1.35 million new cases or 12.4% of all new cancers detected for the year 2002) and mortality (1.18 million deaths or 17.6% of all cancer-related deaths for the year 2002) [361, 362] with smoking as the leading cause for 86% of men and 49% of women worldwide [362]. Tobacco smoke was shown to decrease the level of neprilysin at the bronchial cell surface [363] and increase the levels of bombesin-like peptides (BLP) in the respiratory tract of smokers [364].
BLP are potently mitogenic in normal bronchial epithelial [365] and fibroblasts cells [366] and stimulate the growth of many small cell carcinomas (sCCa) from the lung [367]. Their importance in lung cancer proliferation was further confirmed with the inhibition of sCCa

colony formation and tumorigenesis in nude mice after anti-BLP antibody treatment [367]. Neprilysin is highly expressed in the different cell types of the lung [281]. It was shown to act as a tumor repressor and prevent the proliferation of sCCa cells by degrading BLP *in vitro* [297, 368]. Furthermore, recombinant neprilysin prevented the growth of lung cancer cells *in vivo* in athymic nude mice by inactivating the peptides involved in lung cancer signal transduction [368].

Prostate cancer

Similarly, neprilysin is expressed in prostatic epithelial cells and was shown to prevent prostate cancer proliferation by degrading the mitogen bombesin and endothelin-1 peptides [369, 370]. Loss of neprilysin is a frequent and early event in human prostate cancer (PC) [254, 371] and its downregulation in metastatic human PC contributes to the development of androgen-independent PC cells [255] by allowing them to use mitogenic peptides such as bombesin and endothelin-1 as an alternate source to androgen in order to stimulate cell proliferation [255, 369, 372]. In PC, two types of cells can be distinguished: the androgen sensitive PC cells present a high level of neprilysin, low level of phosphorylated focal adhesion kinase (FAK) and a slow cell migration rate, and the androgen independent PC cells, which present a low level of neprilysin, high level of phosphorylated FAK and a high cell migration rate [255, 373]. Overexpression of neprilysin in androgen independent PC cells prevented their growth and tumorigenicity *in vitro* and *in vivo* [373-375]. Two mechanisms were involved *in vitro*: neprilysin cleaved and inactivated bombesin and endothelin-1, preventing their activation of the Src kinase and subsequent phosphorylation of FAK [373]. Independently of its enzymatic activity, neprilysin also interacted via the lyn kinase with the p85 subunit of PI3K preventing the phosphorylation of FAK and the subsequent cell migration in androgen independent PC cells [373]. Neprilysin, therefore, may provide a novel approach to the treatment of PC.

Ovarian and breast cancer

Other studies have shown that neprilysin is also involved in neoplastic transformation and tumor progression in other human malignancies, including ovarian and breast carcinomas, by inactivating ET-1 or bombesin [376, 377], which are autocrine growth factors for these tumors [378, 379]. While neprilysin expression is decreased and endothelin-1 level increased in ovarian carcinoma as the grade of the tumor avances [380, 381], overexpression of neprilysin suppressed the progression of ovarian carcinoma *in vitro* and *in vivo* [376]. The role of

neprilysin in breast cancer is less clear since its effect on cancer progression was only shown *in vitro* using inhibitors [377]. Interestingly, the level of neprilysin correlated with the degree of malignancy [382, 383], suggesting that neprilysin may be a useful adjunct in assessing malignancy in mammary fibroepithelial lesions, but also that neprilysin overexpression may not be efficient in all types of cancer.

2.6 Neprilysin and AD

2.6.1 Neprilysin degrades Aβ

Most of AD research has focused on the mechanism by which APP is processed to form Aβ but the steady state concentrations of this actively processed peptide [384] is determined by the dynamic balance between its production and its clearance. In contrast to the FAD cases and mouse models of Aβ amyloidosis where the anabolism of Aβ is genetically increased, the accumulation of Aβ in sporadic AD cases may also be due to a reduced catabolism of Aβ [385]. In the last few years, a variety of Aβ degrading enzymes have been proposed (reviewed in [386]) with neprilysin being the most potent Aβ degrading enzyme identified and the major rate-limiting factor in Aβ degradation *in vivo* (reviewed in [230], [229, 317, 387]). Neprilysin was initially shown to degrade Aβ but not APP *in vitro* [303]. Neprilysin can cleave $A\beta_{1\text{-}40}$ *in vitro* and *in vivo* at 5 different positions (Fig. 4): Glu^{3}-Phe^{4}, Gly^{9}-Tyr^{10}, Phe^{19}-Phe^{20}, Ala^{30}-Ile^{31} and Gly^{33}-Leu^{34} [303] with the initial cleavage being Gly^{9}-Tyr^{10} [317, 331], and is also able to degrade monomers and oligomers of $A\beta_{40}$ and $A\beta_{42}$ *in vitro* [331, 388].

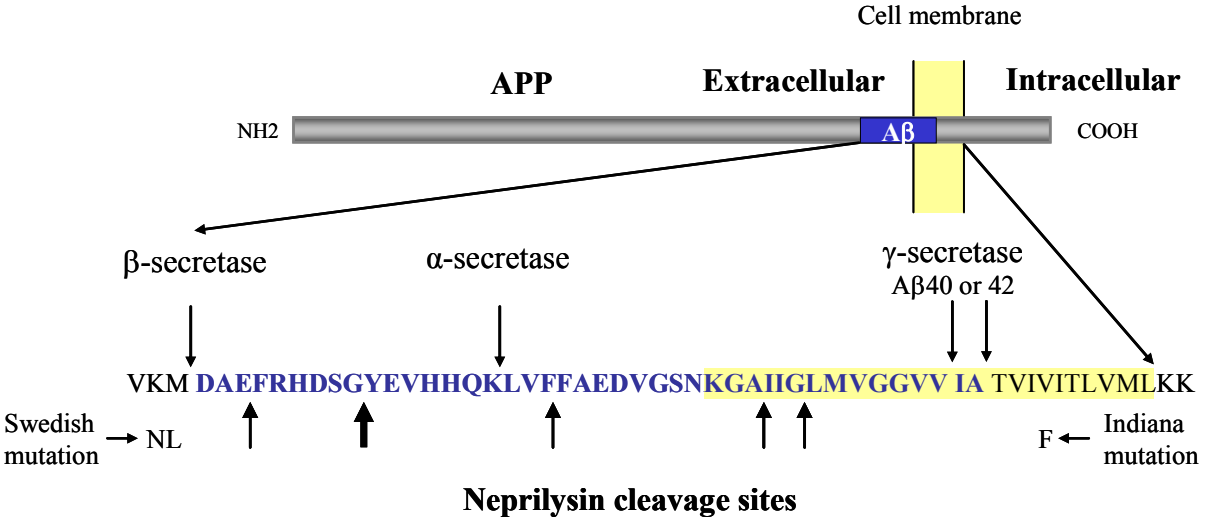

Figure 4. Human APP sequence including Aβ, α,β and γ-secretases and neprilysin cleavage sites. Once secreted, Aβ is cleaved by neprilysin (lower arrows) at position 3-4, 9-10, 19-20, 30-31 and 33-34, 9-10 being the major one. Swedish and Indiana FAD causing mutations, known to increase Aβ production and $A\beta_{42}$ cleavage, respectively, are represented.

2.6.2 Decrease of neprilysin activity associated with Aβ pathology in AD

Intracranial infusion of neprilysin inhibitors led to increased half life of radiolabeled Aβ injected into rat hippocampus, increased levels of endogenous Aβ and formation of diffuse plaques in rats [317]. A similar increase of Aβ levels was reproduced in rabbit [389] and APP transgenic mice brains [317, 390].

Neprilysin deficiency in mice also resulted in defects both in the degradation of exogenously injected Aβ and in the metabolic suppression of the endogenous Aβ in the brain including hippocampus, cortex, striatum and cerebellum. With 1.5 and 2 fold increase of endogenous $A\beta_{40}$ and $A\beta_{42}$ in the heterozygote and homozygote mice, respectively, this effect was dose dependent [229], suggesting that partial downregulation of neprilysin activity may contribute to AD development by promoting Aβ accumulation.

Consistent with this hypothesis, neprilysin expression and protein level inversely correlated with the vulnerability to Aβ deposition in the brain of sporadic AD patients [391, 392]. Expression and protein level of neprilysin were reduced by approximatively 50% in the hippocampus and midtemporal gyrus of AD patients, as compared to age-matched controls, but were unchanged in brain areas with moderate or low plaque burden [392].

Neprilysin was also found decreased in the vasculature of AD brains and inversely correlated with the Aβ levels in the vasculature [393]. Moreover, neprilysin did not efficiently degraded Aβ carrying EOFAD mutations involved in presenile cerebral amyloid angiopathy such as Dutch, Flemish, Italian and Arctic mutations of APP *in vitro* [394]. A genetic study also associated a genetic polymorphism of neprilysin with risk of cerebral amyloid angiopathy [395], further suggesting that neprilysin may be implicated in cerebral amyloid angiopathy.

With age as the major risk factor for AD, it is also interesting that activity and protein level of neprilysin were decreased upon aging in the hippocampal formation of WT mice and humans [396, 397]. Neprilysin downregulation with normal aging may play an important role in the initial accumulation of Aβ and the development of AD. In spite some negative data [212, 398, 399], several recent studies have shown an association of the neprilysin gene, *Mme*, with LOAD [206-208, 400].

2.6.3 Neprilysin as a therapeutic approach for AD

Viral expression of neprilysin in primary neurons led to significant clearance in both the $A\beta_{40}$ and $A\beta_{42}$ levels in the culture media and the cell associated Aβ. [401]. Similarly, hippocampal injection of viral vectors expressing human neprilysin decreased Aβ levels in NEP KO mice and mouse model of Aβ amyloidosis *in vivo* [402, 403]. It also resulted in a 50% decrease in the ipsilateral plaque formation in a plaque-bearing transgenic mouse model of cerebral amyloidosis compared to the contralateral cortex [402], showing that neprilysin overexpression could also induce the degradation of pre-existing plaques. However, this last finding is contradictory with our data showing that biochemical increase of endogenous brain neprilysin levels in aged SwAPP mice with pre-existing plaque pathology did not result in a significant reduction of plaque pathology [404]. Explanations for the observed differences include the cell types that upregulated neprilysin, accessibility to the plaques, inflammation and system adaptation to long term versus short term neprilysin upregulation. Furthermore, transgenic overexpression of neprilysin in a mouse model of Aβ amyloidosis significantly reduced brain Aβ levels, prevented amyloid plaque formation and its associated cytopathology [405].

2.6.4 Aβ injection increases neprilysin and prevent Aβ pathology prior to plaque formation

It was recently found in our laboratory that injection of aggregated $A\beta_{1\text{-}42}$ prior to plaque formation into brains of transgenic mice that expressed the disease-causing Swedish double mutation of APP (SwAPP) as well as into WT littermates caused increases in brain levels of neprilysin mRNA 20 weeks after injection (Fig. 5C) and a sustained increase of protein in a specific manner as early as 3 weeks and at least until 20 weeks after initial injection (Fig. 5A). These increases were associated with dramatically reduced brain concentrations of Aβ as well as with prevention of brain amyloid plaque formation (Fig. 5B) and reduced astrogliosis in the SwAPP mice [406]. Similar treatment of aged SwAPP mice, already containing numerous amyloid plaques, also caused an $A\beta_{1\text{-}42}$ specific sustained increase of neprilysin 20 weeks after injection. Unlike the young mice, however, this treatment could not significantly reduce brain Aβ levels or remove the existing amyloid plaques from brains of aged mice [404]. This difference suggested that neprilysin preferentially degraded Aβ prior to

fibrillization and plaque formation but may also be due to age-dependent biological adaptations to high levels of human Aβ and neprilysin upregulation or the implication of other pathways influencing Aβ degradation.

There is much evidence that neprilysin is able to degrade Aβ. While neprilysin downregulation can play an important role in the development of AD, its upregulation is a promising therapeutic approach.

A

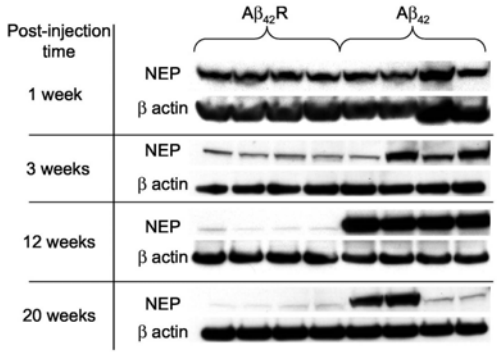

B

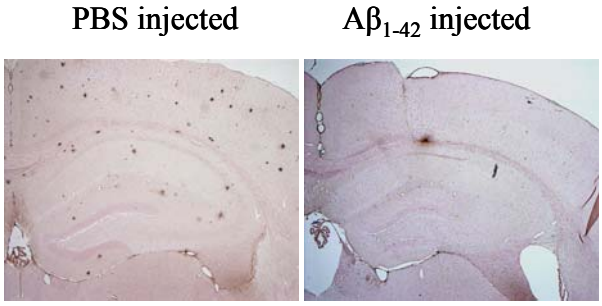

C

	$A\beta_{42-1}$ (±SD)	PBS (±SD)	$A\beta_{1-42}$ (±SD)	BSA (±SD)	uninjected (±SD)
	%	%	%	%	%
1 week	490 (±190)	490 (±180)	420 (±110)	460 (±150)	100 (±160)
20 weeks	57 (±290)	58 (±160)	490 (±120)	110 (±200)	100 (±110)
	ns	ns	*	ns	ns

Figure 5. Intracranial injection of $A\beta_{1-42}$ increased neprilysin levels and prevented amyloid plaque formation in transgenic Swedish APP mice. (**A**) Western blot analysis illustrating the $A\beta_{1-42}$ specific increase of neprilysin level after different post-injection time compared to $A\beta_{42-1}$ ($A\beta_{42}R$) injected mice. (**B**) 20 weeks after injection, mice which received a cranial injection of $A\beta_{1-42}$ showed a significant reduction of 4G8-positive amyloid plaques compared to phosphate buffered saline solution (PBS) injected mice. (**C**) When compared to those of uninjected group (set as 100%), the levels of NEP mRNA were significantly higher one week after the injections in all groups. 20 weeks after the injections, however, mRNA levels of the control-injected mice did not differ from those of the uninjected mice, whereas this value was still high in $A\beta_{1-42}$-injected mice. *: $p \leq 0.05$ for comparison to uninjected group. ns: not significant.

3) The plasminogen system in AD

3.1 The plasminogen system

Plasminogen is an inactive serine protease, mainly synthesized in the liver [407] and secreted in the circulation. To be activated into plasmin, it needs to be cleaved by either the tissue-type plasminogen activator (tPA) or urokinase plasminogen activator (uPA) [408]. The system is further controlled by plasminogen activator inhibitors (PAI) [409] and plasmin inhibitors (α2-plasmin and α2-macroglobulin) [410].

Plasmin acts primarly as a thrombolytic enzyme, involved in degradation of fibrin in the blood [411, 412] and cell migration by degradation of many components of the extracellular matrix (ECM) such as laminin, fibrin and fibronectin [413], either directly or through the activation of matrix-degrading metalloproteases [414]. In the brain, plasminogen and its proteolytic fragment plasmin are abundant in the hippocampus [415] and are involved in neuronal plasticity [416], long term potentiation by degradation of laminin [417], activation of brain derived neurotrophic factor (BDNF) [418], and learning and memory [419, 420].

Plasmin has also been recently implicated in the degradation of Aβ [421, 422].

tPA is secreted as an active enzyme, binds to the extracellular matrix components such as laminin and fibronectin [423, 424] and its activity is highly increased after cleavage by plasmin or binding to cross-β structure such as fibrin or Aβ *in vitro* [425-427]. tPA plays a major role in plasmin generation required for fibrinolysis in the peripheria but is also expressed in neurons [428] of various brain regions of the mouse, including the hippocampus, amygdala, cerebellum and hypothalamus [429], where it participates in synaptic plasticity, LTP [430] and learning [419]. tPA also presents plasmin-independent activity and was shown to increase vascular permeability of the blood brain barrier by binding to LRP receptor [431] and may be directly involved in neurotoxicity [432, 433].

uPA is secreted in its inactive form, pro-uPA [434] and needs to be cleaved by plasmin to be activated. The presence of active uPA in mice lacking plasminogen (Plg KO) mice [435] suggests the presence of other pro-uPA activators. Among them, cathepsins B, C, G and L [436-438] and different members of the kallikrein family [438-441] have been shown to activate pro-uPA. The binding of pro-uPA to a specific cell surface receptor, uPAR (reviewed in [442, 443]), facilitates its activation by plasmin and therefore targeting plasmin generation and further proteolysis to the cell surface. The complex uPA-uPAR is involved in tissue and

synaptic plasticity and brain development in a plasmin dependent and independent manner via the activation of intracellular pathways through uPAR [443-445].

3.2 The plasminogen system and AD

Several studies have suggested an involvement of the plasminogen system in AD. Purified plasmin was initially shown to degrade monomers and fibrils of Aβ [421, 427]. It cleaves $A\beta_{1-40}$ at Arg^{5}-His^{6}, Lys^{16}-Leu^{17} and Lys^{28}-Gly^{29} [421]. Similarly, it was shown that after cleavage of $A\beta_{1-42}$, the formation of β-sheet structures was prevented [446].
The expression of the two plasminogen activators, tPA and uPA were increased in primary neuronal cultures incubated with aggregated Aβ and in APP overexpressing mice [421]. Aβ was also shown to increase tPA activity *in vitro* [426, 427], which in turn led to an increase of plasmin activation [447] and subsequent Aβ degradation [448]. Furthermore, the addition of plasminogen inhibited the Aβ associated neurotoxicity [448]. Similarly, Aβ was shown to increase the expression of uPA and its receptor uPAR and cell surface localization and activity of uPA in human cerebrovascular smooth muscle cells. Plasminogen activation further protected the cells from Aβ toxicity [449]. Both tPA and uPA required plasminogen to modulate Aβ neurotoxicity and deposition *in vitro* [448, 450]. Addition of plasmin or tPA to hippocampal neurons expressing human APP also increased the amount of α cleavage of APP [451] and may represent another potential neuroprotective pathway for AD.

The role of plasmin in Aβ degradation was further investigated using plasminogen and tPA KO mice *in vivo*. In spite the lack of Aβ increase in the brain of plasminogen deficient mice [452], indicating the involvement of others degradation pathways, degradation of Aβ injected into the hippocampus of tPA and plasminogen KO mice was slowed down and more activated microglial cells and neuronal damage were observed when compared to WT controls [422]. This confirms that plasmin helps in the clearance of Aβ *in vivo* and suggests that a reduced activity of this system may contribute to the progression of AD. In fact, level of plasmin was found decreased in the brain of AD patients, especially in the hippocampus [451, 453], indicating that plasmin may be physiologically relevant as a protective factor in AD. The gene encoding uPA, PLAU, is located in an important region on chromosome 10, which has been linked to LOAD and was found associated with it in some studies [454, 455] but not in others [456-458].

II) MATERIAL AND METHODS

1) Engineering, extraction, purification and analysis of DNA

1.1 Plasmid DNA preparation

1.1.1 Preparation and transformation of competent E. coli cells

To transform DNA into Escherichia coli (E. coli), the cell membranes have to be porous. This can be achieved by treating the cells with Ca^{2+}. The addition of DNA leads to the formation of DNA-Ca^{2+} complexes that enter the cells following a short heat-shock.
To generate chemically competent bacteria, cultures of DH5α or XL10 gold cells (Life Technologies) were grown in Luria Bertani (LB) medium at 37°C overnight and harvested when an optical density (OD) at 600 nm of 0.4 was reached. The cells were pelleted on a 5417R centrifuge (Eppendorf) at 4,000 g at 4 °C for 1 min, resuspended in 10 ml of a 0.1 M $CaCl_2$ solution and kept on ice for 1 h. Cells were collected by centrifugation at 4,000 g at 4 °C, resuspended in 0.1 M $CaCl_2$, 0.02 M $MgCl_2$ and 15% glycerol. Aliquots of competent cells were immediately frozen in liquid nitrogen and stored at –80 °C.
To transform cells, diluted plasmid DNA or 5 µl of a ligation reaction were added to 50 µl of thawed competent E. coli and incubated on ice for 20 min. Following a heat shock of 45 s at 42 °C the cells were chilled on ice for 2 min. After addition of 950 µl of preheated LB medium at 37 °C, the cells were incubated on a thermomixer (Ependorf) at 300 rpm for 1 h at 37 °C. Cells were then plated on 37 °C prewarmed LB agarose (Becton Dickinson) plates containing the appropriate antibiotic: ampicillin (Sigma) with a final concentration of 50 µg/ml for selection and were incubated overnight at 37 °C.
LB medium: 10 g/l Bacto tryptone (Becton Dickinson), 5 g/l Bacto yeast extract (Becton Dickinson), 10 g/l NaCl, pH=7.0

1.1.2 Preparation of plasmid DNA

On the following day, colonies that contained the ampicillin resistance marker and therefore could grow on the ampicillin containing plate, were picked and grown in 15 ml Falcon tubes containing 2 ml LB medium and ampicillin (Sigma) 50 µg/ml in a C25 incubator shaker (New Brunswick Scientific) at 250 rpm, 37 °C overnight. Large scale production was then performed using 0.5 ml of the previous mini-culture added to 200 ml LB medium containing 200 µl of 50 mg/ml ampicillin and was incubated in a shaking incubator at 37 °C overnight.
To extract plasmids from E. coli, Qiagen (12125 and 12165) or Sigma (PLN-350 and PLX-50) plasmid purification kits and protocols were used. The principle of these kits is based on selective alkaline denaturation, alkaline lysis of the cells in combination with the anionic detergent sodium dodecyl sulfate (SDS): cell walls are broken and proteins, as well as high molecular weight genomic DNA, is denatured. In contrast, covalently closed circular DNA remains double stranded, stays in solution and can be recovered from the supernatant by binding to an anion-exchange resin. Plasmid DNA was isolated from small scale (2 ml) and large scale (200 ml) bacterial cultures following the manufacturer's protocols. The yield of a plasmid DNA preparation was measured at an OD of 260 nm and its purity accepted when the ratio between the absorption at 260 nm and the absorption at 280 nm was between 1.8 and 2.0.

1.1.3 Phenol/chloroform extraction of DNA

To remove contaminating proteins from nucleic acid preparations, an equal volume of phenol:chloroform:isoamylalcohol (25:24:1) is added to the nucleic acid solution and mixed well on a vortex. The DNA is recovered from the aqueous phase while denatured proteins stay in the organic phase. The tube is centrifuged for 5 min at 20,000 g. The aqueous phase containing the DNA was transferred to a fresh tube and precipitated using NaAc and ethanol.

1.1.4 Ethanol precipitation of DNA

To isolate or concentrate DNA from solution it can be precipitated with ethanol under high-salt condition. The addition of ethanol depletes the hydration shell of the negative charged phosphate groups in the backbone of the DNA. Positively charged ions bind to these groups so that a precipitate can form. DNA was precipitated from solution by adding 1/10 volume of 3 M sodium acetate (pH=5.2) and 2.5 volumes of cold 100% ethanol, incubation at -20 °C for 30 min and centrifugation at 20,000 g for 20 min at 4 °C. After two washes with cold 70% ethanol, the DNA pellet was dried for 5-10 min at room temperature (RT) and resuspended in 10 mM Tris (pH=8.0).

1.2 Cloning

To overexpress neprilysin in a neuronal specific manner, the 2.25 kb NEP-HA cDNA previously inserted in a pBluescript II KS (+/-) at the Sma I site of the multiple cloning site was first removed using the restriction enzymes Hind III and Spe I, separated by agarose gel electrophoresis and further purified (Fig. 6). The psub PDGF WPRE plasmid (gift from Dr. Hansruedi Büeler, University of Zürich) was linearized by the Nhe I restriction enzyme which presents a cohesive end with the Nhe I cleavage site, dephosphorylated and purified on an agarose gel. After ligation of the two cohesive ends, the ends of the new linearized plasmid were blunted. Once more purifed, the linearized plasmid was finally ligated. Presence of intact ITRs and the correct insertion of NEP-HA were confirmed by restriction enzyme and agarose gel analysis.

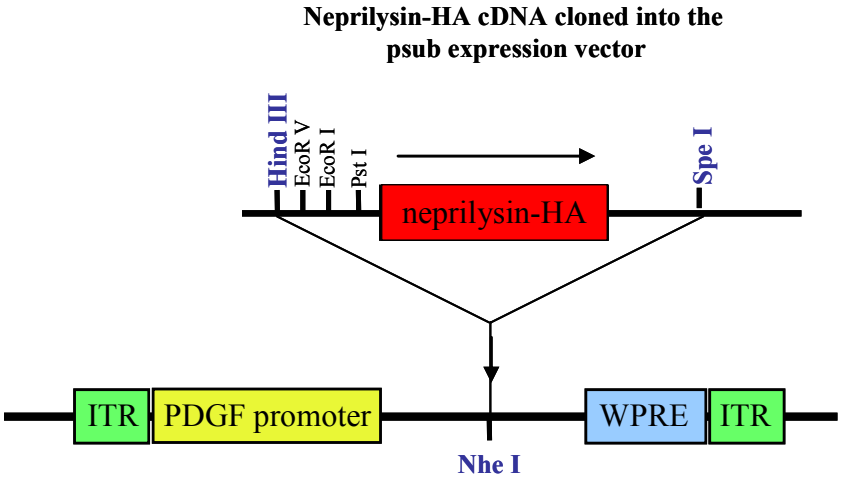

Figure 6. Cloning of neprilysin-HA into the psub expression vector. Schematic representation of the restriction enzymes used (in blue) to remove the neprilysin HA tagged cDNA from the original pBluescript II KS (+/-) and to linearize the psub PDGF WPRE plasmid. After cloning, the restriction sites used were lost.

1.2.1 Restriction enzyme analysis of DNA

For digestion of DNA, type II restriction endonucleases, recognizing and cleaving palindromic sequences of 4 to 8 base pairs (bp) of the DNA, were used. Digestion of 0.2 to 5 µg DNA in a total volume of 20 to 40 µl was performed for 2 h or overnight with 1 U of the restriction enzyme(s), 1X bovine serum albumin (BSA) if required under buffer and temperature conditions as recommended by the manufacturers. 200 ng for analytical purposes and 1 to 5 µg of plasmid DNA for preparative purposes were analyzed by agarose gel electrophoresis. With DNA ladders (New England Biolabs), the length of DNA fragments could be determined.

1.2.2 Agarose gel electrophoresis

To analyze or isolate DNA fragments or PCR products, separation by agarose gel electrophoresis was performed. Due to the negatively charged phosphate groups in the backbone of nucleic acids, DNA migrates towards the positive anode when exposed to an electric field with a migration rate dependly mainly on their size. Depending on the size range of linear DNA to be resolved, 0.4, 0.7 or 2.0% (w/v) agarose (Invitrogen), for a detection of 2,000 to 30,000 bp, 1,000 to 15,000 bp and 100 to 2,500 bp, respectively, was dissolved in Tris-acetate (TAE) buffer by heating the mixture. When cooled down to 50 °C, the gel was complemented with 1 µg/ml ethidium bromide (Sigma) which intercalates between bases of DNA and fluoresces under ultra violet (UV) light. The length of DNA fragments could then be determined by comparison with a DNA ladder marker. When DNA fragments had to be recovered from the gel, 2 mg/ml crystal violet (Sigma,) was preferred over ethidium bromide. It allowed a weaker but direct visual detection without exposition of the DNA to the damaging effects of UV light.
TAE buffer: 40 mM Tris-acetate (pH=7.6), 1 mM EDTA

1.2.3 Recovery of DNA fragments from agarose gels

After having resolved DNA fragments by electrophoresis the band containing the DNA of interest was cut out from the gel using a scalpel and purified using the QIAquick Gel Extraction kit (28706, Qiagen) according to the company's protocol.

1.2.4 Blunting of cohesive ends

Blunting of sticky DNA ends was performed by DNA polymerase I (New England Biolabs). This polymerase fills-in the 5' overhangs and removes the 3' overhangs to form blunt ends. The blunting reaction was performed for 15 min at RT in the EcoPol buffer supplemented with 1 mM DTT, 4 mM dNTP (Sigma) and 1 U of klenow per µg of DNA.)

1.2.5 Dephosphorylation of plasmid DNA

Digested plasmid DNA containing complementary cohesive ends or blunt ends tend to self-ligate producing empty vectors. In order to suppress such self-ligation, shrimp alkaline phosphatase (SAP, Roche) was used to remove terminal 5' phosphate groups from DNA. For

the hydrolysis of 5'-phosphate groups 1 µg DNA fragments and 5 U of SAP were incubated at 37 °C for 1 h in the appropriate buffer according to the manufacturers. Before ligation, vectors were purified with the GenElute PCR clean up kit (NA1020, Sigma) and eluted in 50 µl H_2O.

1.2.6 Ligation

DNA fragments can be ligated to linearized plasmid DNA in an ATP consuming enzymatic process. The E. coli T4 DNA ligase catalyzes the ligation of two DNA strands at the 5' phosphate and the 3' hydroxy groups. Depending on the size of the vector and insert, the amount of vector and insert varied. In general, 0.3 pmol (300 ng) were mixed with 3 pmol of inserts. This mixture was incubated with 400 U of T4 DNA ligase in T4 ligation buffer (New England Biolabs) at 4 °C overnight.

1.3 Genotyping of mice

1.3.1 Preparation of genomic DNA from mouse tails

5 mm of a mouse-tail biopsy was lysed and the DNA extracted using the Gen Elute Mammalian Genomic DNA MiniPrep Kit (G1N-350, Sigma) following manufacturer's protocols. Isolated genomic DNA was stored at 4 °C.
A simplified mammalian DNA isolation was used when genotyping of neprilysin overexpression alone had to be performed: 5 mm of a mouse-tail biopsy was incubated with 22 µl lysis buffer for 1-2 h at 55 °C on a thermomixer (Eppendorf). Following this incubation, 178 µl of double distilled water (ddH_20) was added and Proteinase K denatured at 99 °C for 5 min at 500 rpm in the same thermomixer. The samples were then centrifuged for 5 min at 22,800 g and the supernatant kept at 4 °C.
Lysis-Buffer: 50 mM Tris-HCl (pH=8.0), 1 mM EDTA, 0.1% (w/v) SDS, 20 mM NaCl, 1 mg/ml proteinase K (Roche recombinant PCR kit #3115 844).

1.3.2 Polymerase chain reaction amplification

The polymerase chain reaction (PCR) is a method to amplify DNA sequences of interest [459, 460]. To produce multiple copies of DNA, two specific primers are used that are complementary to one of the two strands and define the sequence to be amplified. Denaturation of the DNA at 95 °C is followed by a decrease in temperature such that the primers can anneal to their complementary sequence on the DNA. Heat stable DNA polymerase catalyses the replication of the DNA by adding deoxynucleotides (dNTP) to the 3'-ends of the primer sequences. By repeating these steps several times the DNA sequence of interest is amplified exponentially.
Transgenic J20 mice overexpressing the Swedish and Indiana mutated human APP under the control of the glial fibrillary acidic protein (GFAP) promoter, were screened with primers PDAPP 1F (5' GGT GAG TTT GTA AGT GAT GCC 3') and PDAPP 2R (5' TCT TCT TCT TCC ACC TCA GC 3'). Briefly, 2 µL (10 to 200 ng) of genomic DNA was added to PCR mix (0.75 U of the Ampli-Taq Gold (Roche), 1X PCR Buffer II (Roche), 2.5 mM $MgCl_2$, 1mM dNTP (Sigma), 20 pmol of each primer in a final volume of 27 µl). Using a GeneAmp PCR system 9700 machine (Applied Biosystem), the reaction was heated to 95 °C for 12 min before a series of 10 single cycles (1 min denaturation at 94 °C, annealing of the primers for 2

min at decreasing temperature starting at 65 °C during the first cycle and finishing at 56 °C during the 10th cycle and 2 min at 72 °C at the end of each cycle) followed by 25 further cycles (1 min denaturation at 94 °C, annealing of the primers at 55 °C and 1.5 min at 72 °C), followed by a final incubation at 72 °C for 10 min, then kept at 4 °C. For sequencing purpose, two different primers were used APP2041 (5' AAC ACA GAA AAC GAA GTT 3') and APP 2520 (5' CCG ATG GGT AGT GAA GCA) to amplify a 480 bp fragment containing the Aβ part of human APP. The same PCR protocol was followed.
Transgenic NEP mice overexpressing neprilysin under the control of the Prion protein promoter (Prp) were screened with oligonucleotides Prp5-(5-3) (5' CAG AAC TGA ACC ATT TCA AC 3') and NEP125-100 (5' CTA TGA TGG TGA GGA GCA GGA CAA G 3'). 1 µl of genomic DNA was mixed with 1 U of the Red Taq polymerase (Sigma), 1X corresponding PCR Buffer, 1 mM dNTP (Sigma), 10 pmol of each primer in a final volume of 20 µl. The reaction was heated to 95 °C for 2 min before a series of 35 cycles (30 s at 94 °C, 30 s at 52 °C, 50 s at 72 °C), then kept at 72 °C for 7min and cooled to 4 °C.
Screening of the NEP KO mice heterozygous and homozygous with depletion of the neprilysin gene [314] was performed using 2 pairs of primers: the oligonucleotides 5' TCA TTC AGC TGG TCA AA 3' and 5' CTT GCG GAA AGC ATT TC 3' were specific for detection of the WT neprilysin allele, whereas 5' TCA TTC AGC TGG TCA AA 3' and 5' ATC AGA AGC TTA TCG AT 3' recognized the targeted depleted neprilysin allele. 1 µl of genomic DNA was mixed with 1 U of the Red Taq polymerase, 1X corresponding PCR Buffer, 1 mM dNTP, 10 pmol of each primer in a final volume of 20 µl. The reaction was heated to 95 °C for 5 min before a series of 35 cycles (30 s at 95 °C, 30 s at 48 °C, 30 s at 72 °C), then kept at 72 °C for 7 min and cooled to 4 °C.
Transgenic SwAPP mice overexpressing mutated hAPP expressing the Swedish double mutations under the control of the Prp promoter were screened with oligonucleotides 5' GTG GAT AAC CCC TCC CCC AGC CTA GAC CA 3' and 5' CTG ACC ACT CGA CCA GGT TCT GGG T 3'. 1 µL of genomic DNA was mixed with 1 U of the Red Taq polymerase, 1X corresponding PCR Buffer, 1 mM dNTP, 10 pmol of each primer in a final volume of 20 µL. The reaction was heated to 95 °C for 2 min followed by 35 cycles (45 s at 95 °C, 1 min at 63 °C, 45 s at 72 °C), then kept at 72 °C for 7min and cooled to 4 °C.

1.4 DNA sequencing

To confirm the presence of the Swedish and the Indiana mutation in the human APP sequence of the J20 mice, the PCR product containing the Aβ sequence of interest was sequenced.
DNA cycle sequencing is based on the dideoxy method developed by Sanger *et al.* [461]. In the cycle sequencing reaction all four deoxynucleotides (A, T, G, C) labeled with different dyes are added to an excess of deoxynucleotides. When one of the dideoxynucleotides is incorporated the elongation of the chain is terminated because these nucleotides lack the 3'-hydroxyl group. The products were gel-electrophoretically separated in a capillar according to their molecular weight. Different wavelengths are used to excite each dye and thus to identify the sequence of the DNA.
Using the Big Dye Terminator v.1.1 Cycle Sequencing kit (4336776, Applied Biosystems), 200 ng PCR product, 3.2 pmol of one of the primer Ab-F (5' CCA GGT TCT GGG TTG ACA AA 3') or Ab-B (5'ACC ACA CCA TGA ATG GA 3'), 4 µl Ready Mix and ddH_2O added up to a volume of 20 µl, were mixed in a reaction tube. The DNA cycle sequencing reaction was carried out using the following program: 96 °C for 1 min followed by 25 cycles (96 °C 10 s, 50 °C 5 s, 60 °C 4 min) and finally kept at 4 °C. The DNA was purified by ethanol precipitation. The DNA pellet was resuspended in 20 µl HPLC-grade water (Aldrich)

and was analyzed with the ABI Prism 310 Genetic Analyzer and ABI Prism 7700 Sequence Detector (Applied Biosystems). Sequence readouts of 200-400 bp by the Sequence detection software 1.9.1 (Applied Biosystems) were transformed to and computationally analyzed with the programs SeqMan II and MegAlign 4.00 (DNASTAR).

1.5 Production of the recombinant adeno-associated virus (rAAV)

RAAV is an attractive approach for gene therapy. It allows a high transfection rate of cells including post mitotic cells such as neurons, stably insert the transgene of interest in the DNA of the cells infected likely promoting long-term expression. RAAV are non-pathogenic and replication-deficit viruses. The delivery of therapeutic transgenes is performed in the absence of viral genes and therefore preclude any potent humoral immune response due to recognition of viral particles.

1.5.1 Production of the rAAV

One day before transfection, 20 to 30 15 cm^2 plates were plated with 1.7 x 10^7 HEK 293T cells/plate in 25 ml Dulbecco's modified Eagle medium (DMEM, Invitrogen) supplemented with 10% Foetal calf serum (FCS) and 50 U/ml penicillin and 50 µg/ml streptomycin (P/S). The next day, 80% confluent 293T cells were transiently cotransfected with rAAV vector plasmid expressing either NEP haemagglutinin-tagged (HA) under the control of the platelet-derived growth factor (PDGF) promoter or the enhanced green fluorescent protein (EGFP) under the control of the PDGF or the cytomegalovirus (CMV) promoter and a helper plasmid pDG which expresses all the virus proteins required for the production of the virus proteins. All rAAV vector plasmid contained a post-transcriptional regulatory element (WPRE) which is known to enhance transgene expression [462, 463]. The medium was first replaced with 25 ml fresh DMEM + 10% FCS without P/S. The calcium phosphate transfection was performed 3 h later. The cells were transfected with a DNA/$CaCl_2$ mix containing 582 µg of the pDG helper plasmid, 285 µg of the rAAV plasmid were mixed in 1.5 ml 2.5 M $CaCl_2$ solution and filled up to 12.5 ml with ddH_20 (protocol for 10 15 cm^2 plates).
12 ml polystyrene snap cap tubes (352057, Bector Dickinson) containing 2.5 ml 2x HeBS buffer (pH=7.12) were prepared. 2.5 ml of DNA/$CaCl_2$ mix was added dropwise to the 2.5 ml 2x HeBS buffer, mixed gently on a vortex genie 2 (Scientific Industries) and incubated 2 min at RT. 2.5 ml of this mixture were distributed dropwise to each of the two plates without delay. Then the plates were gently mixed and incubated at 37 °C with 5% CO_2. The next morning, the medium was replaced with 25 mL DMEM 10% FCS with P/S.
48 h after transfection, the cells were pipetted and centrifuged at 370 g for 5 min at 4 °C.
The supernatant was removed and the cell pellet containing the virus particles frozen at -80 °C.
2x HeBS buffer: 16.4 g NaCl, 11.9 g N-2-hydroxyethylpiperazine-N'-2-ethanesulfonic acid (HEPES), 0.249 g $Na_2HPO_4.2H_2O$, 800 ml ddH_20, pH adjusted to 7.12 with 5 M NaOH, filled up to 1 L).

1.5.2 Purification and concentration of the rAAV

Lysis of the cells
The virus purification was performed according to a protocol published by Auricchio [464]. The cell pellet of 10 15 cm^2 plates were resuspended in 14 ml buffer containing 0.15 M NaCl, 50 mM Tris-HCl pH=8.5 and freeze/thaw 2 times from liquid nitrogen to a 37 °C bath. After

each round, the cells are resuspended with a flamed Pasteur pipette and finally incubated 30 min at 37 °C with 0.1 mg of DNAse I and RNAse A each (Sigma) for each initial 15 cm^2 plate. After 15 min of centrifugation at 1,400 g at 4 °C, the supernatant containing the virus was transferred into a new tube and incubated with 0.5% (final concentration) of deoxycholic acid for 30 min at 37 °C to increase the binding of the virus to the following heparin column.

Heparin column purification
6 ml of a heparin-agarose suspension (H6508, Sigma) was pipetted into a 2.5 cm diameter glass column (C4669, Sigma) equipped with a luer lock (S7396, Sigma). After the agarose suspension had flown through, a filtration membrane (S7271, Sigma) was placed on top of the agarose bedding. The matrix was afterwards equilibrated with 25 ml of PBS. The virus preparation was then sequentially filtered through a 5 µm pore size filter and a 0.8 µm pore size filter (Millex) before it was applied to the column and the lock opened allowing a flow speed of one drop per second. The matrix was then washed twice at the same flow rate with 25 ml of PBS plus 0.1 M NaCl (final NaCl concentration = 0.254 M). The virus was then eluted at the same flow rate with 15 ml of PBS plus 1.3 M NaCl (final concentration 1.454 M NaCl).
PBS: 0.154 M NaCl, 0.0027 M KCl, 0.01 M $Na_2HPO_4.2\ H_20$, 0.0018 M KH_2PO_4 adjusted to pH=7.4

Concentration of the rAAV
The eluate was first concentrated to about 1 ml by centrifugation at 1,800 g at 4 °C with a Millipore Biomax-100K NMWL filter device (UFV2BHK40, Milipore) pretreated overnight at 4 °C with murine serum. To adjust the NaCl concentration to physiological levels, the filter device was refilled with PBS, and the virus concentrated to 400 µl. After removal of the virus containing solution, the membrane of the filter device was washed three times with 100 µl PBS. The purified virus was then aliquoted and stored at -80 °C.

1.5.3 Titration by slot blot hybridization

Southern blotting is a method to detect and quantify specific DNA sequences [465]. Single stranded DNA or denatured double stranded DNA is transferred and tightly bound onto a membrane. Sequences of interest are detected by incubation of a radiolabeled DNA probe hybridizing to the target DNA followed by autoradiography and quantification.

Preparation of the samples and standards
To quantify the concentration of the intact virus particles in our preparations and potential loss, 5 µl of the virus preparation and other solutions used during the purification steps were analyzed by slot blot hybridization. The samples were treated in 200 µl serum free DMEM (Invitrogen) with 5 U DNAse I (Sigma) at 37 °C for 1 h to avoid contamination from DNA released by the destroyed virus particles. 200 µl of 2X proteinase K buffer (20 mM Tris-HCl pH=8.0, 20 mM EDTA, 1% SDS) and 100 µg proteinase K (5 µl of 20 mg/ml stock, Biotechnica) were added and incubated for an extra hour.
The DNA from the originally intact virus was then extracted by phenol/chloroform and purified by ethanol precipitation and ressuspended in 400 µL of 0.4 M NaOH solution containing 10 mM EDTA.
The standards were obtained via a 2 fold serial dilution of the AAV vector plasmid used to generate the rAAV. 40 ng to 0.3125 ng of the plasmid was resuspended in a total of 400 µl of 0.4 M NaOH solution containing 10 mM EDTA.

Before loading, the samples were denatured at 95 °C for 5 min and kept on ice for 1 min.

Fixation of the samples on the membrane
The slot blot apparatus (SL-8125, Scotlab) and a Hybond-N+ membrane (Amersham) were assembled following manufacturer protocol; 400 µl of ddH_2O was added in each well and removed via a vacuum pump minivac P1 (Axon Lab AG). The samples were first loaded in the chosen wells. Afterwards, 400 µL of 0.4 M NaOH, 10 mM EDTA added in the empty wells and the membrane dried up by vacuum pump. The membrane was then incubated 2 min in 2X SSC solution containing 300 mM NaCl, 30 mM NaCitrate at pH=7.0 and the DNA cross linked for 50 s at 120 mJ with the UV Stratalinker 1800 (Stratagene).

Preparation of the radioactive probe
Random labeling of DNA was carried out using the Stratagene Prime-it labelling kit. A part of the target DNA was used as a template for a random synthesis of DNA fragments in the presence of short primers (hexanucleotides) and α32P-radiolabeled dCTP (Hartman Analytic), so that newly synthesized DNA harbours the radioactive nucleotide.
10 ng of target DNA was denatured at 95 °C for 5 min in 45 µl Tris EDTA (TE) buffer containing 10 mM Tris pH=8.0 and 0.1 mM EDTA. The sample was chilled on ice for 5 min and added to the reaction tube, containing hexanucleotides, dATP, dGTP, dTTP and the Klenow fragment of DNA polymerase I (New England Biolabs). After the addition of 5 µl α32P-dCTP with a specific activity of 3,000 Ci/mmol the solution was incubated at 37 °C for 30 min. The QIAGEN Nucleotide Removal kit was used to remove nucleotides that were not incorporated during the reaction and short oligonucleotides (< 100 bp).

Hybridization
The Hybond-N+ membrane was placed in a roller bottle and pre-hybridized in 10 ml prehybridization solution containing 10 µg/ml salmon sperm (Roche) for 2 h at 65 °C. The labelled probe was denatured for 5 min at 95 °C, chilled on ice for 5 min and added to the prehybridization solution. The hybridization was carried out at 65 °C overnight. The hybridization solution was discarded and the blot first washed twice with RT 2X SSC, 1% SDS for 30 min each time at 65 °C then twice with 65 °C preheated 0.2X SSC, 1% SDS for 15 min each time at 65 °C. The membrane was finally washed briefly in 2X SSC and exposed onto a X-ray LS film (Kodak) for 6 to 60 h.
prehybridization solution: 0.2 g BSA, 6.84 ml Na_2HPO_4 1 M, 3.16 ml NaH_2PO_4 1 M, 10 µl EDTA 0.5 M, 3 ml deionized fromamide and 7 ml SDS 20%

2) Isolation, purification and analysis of RNA

Special care was taken to use RNase free conditions. Most glassware were baked, surfaces treated with RnaseAway (Catalsys) and all aqueous solutions were treated with Diethyl pyrocarbonate (DEPC, Sigma) and autoclaved.

2.1 Total RNA extraction from brain tissue

Total RNA was extracted from frontal brain tissue by using a technique adapted from Chomczynski [466]. Mice were sacrificed by decapitation and the brains were removed. The frontal part of the brain was quickly homogenized on ice in 2 ml of TRIzol reagent (Invitrogen) and total RNA was obtained following the TRIzol Protocol (Gibco BRL).

TRizol reagent is a monophasic solution containing phenol and guanidium isothiocyanate that preserves RNA integrity during cell lysis and homogenization, and dissolves cellular components. Addition of chloroform followed by centrifugation separates the solution into an aqueous and an organic phase. RNA remains exclusively in the aqueous phase from where it is recovered by precipitation with isopropyl alcohol, resuspended in DEPC treated water (Ambion) and stored in aliquots at -80 °C.

2.2 Quality assessment of total RNA

The purity, integrity and concentration of total RNA was analyzed with the RNA 6000 nano LabChip kit (Agilent) enabling the detection of RNA ranging from 25-500 ng/µl. 1.5 µl of the extracted samples were analyzed following manufacturer's protocol. The chip supports 16 wells connected to capillaries filled with an acrylamide-like matrix mixed with an RNA dye. All wells were fitted with a mini-electrode upon closing the lid and RNA samples mixed with a fluorescent marker that signals the beginning of an electrophoretic run from a specific well. Transcripts of different size were separated while migrating through the matrix-filled capillaries. 3 wells were used as controls and one for the RNA ladder. This allows accurate quantitation and size measurement of RNA transcripts from the samples. The output is an electropherogram where the relative abundance of the two ribosomal 18S and 28S spikes is used to quantify and evaluate the quality of the RNA samples. The absence of other spikes also confirms the integrity of the RNA population in the sample.

2.3 Quantitative real time PCR

Quantitative real time PCR (qRT-PCR) allows relative quantification of mRNA by measuring the increase in fluorescence caused by the incorporation of a quencher (Taqman from Applied Biosystems/ABI) or the binding of SYBR Green (LightCycler, Roche Diagnostics) to double stranded complementary DNA (cDNA) formed during PCR. The number of PCR cycles required for the accumulation of a specific amount of product (during the exponential phase of the reaction) is a reflection of the relative amount of nucleic acid template present originally in the sample.
First the reverse transcription of 4 µg of RNA was performed using the SuperScript First-Strand Synthesis System for RT-PCR (11904-018, Life Technologies) and random hexamers as primers (Invitrogen) following manufacturer's instructions. The polymerization was performed at 42 °C for 50 min and terminated at 70 °C. The RNA template was subsequently destroyed by the addition of RNAse H (Invitrogen) for 20 min at 37 °C.
For detection during qRT-PCR, the following gene specific HPLC-purified primers (Metabion) were designed to amplify 70-90 bp at the 5' end of the open reading frame (ORF) when possible, using the primer design software Primer Express 1.5 (Applied Biosystems):

Mouse uPA: F 5'-TAT GCA GCC CCA CTA CTA TGG CTC-3'
Mouse uPA: R 5'-GAA GTG TGA GAC TCT CGT GTA GAC-3'

Mouse tPA: F 5'-CTA CAG AGC GAC CTG CAG AGA T-3'
Mouse tPA: R 5'-AAT ACA GGG CCT GCT GAC ACG T-3'

Mouse uPAR: F 5'-ACT ACC GTG CTT CGG GAA TG-3'
Mouse uPAR: R 5'-ACG GTC TCT GTC AGG CTG ATG-3'

Mouse NEP: F 5'-TAA GCA GCC TCA GCC GAA ACT ACA A-3'-3'
Mouse NEP: R 5'-GAC TAC AGC TGC TCC ACT TAT CCA CTC A-3'

Mouse β-actin: F 5'-TGG AAC GGT GAA GGT GAC A-3'
Mouse β-actin: R 5'-GGC AAG GGA CTT CCT GTA A-3'

Mouse NEP exon 1: F 5'-GGA GAT GTG CAA GTG GAG GAG-3'
Mouse NEP exon 1: R 5'-CCT TAG CCG CTC TGC AGC T-3'

Mouse NEP exon2: F 5'-CTG TTT GGT GAC CGA GAG CA-3'
Mouse NEP exon 2: R 5'-TTC CCA GCC CCC AAA TG-3'

Mouse NEP exon 3: F 5'-CAA CTC TTT CTG AGA TCT TCA GTG ATA GA-3'
Mouse NEP exon 3: R 5'-CCA ATC AAC TTT TTT ATT CTT TTG TTT TT-3'

The specificity of the sequence and lack of homology was confirmed by blasting the primer sequences against mouse specific sequences
(http://www.ncbi.nlm.nih.gov/genome/seq/MmBlast.html)

2.3.1 Lightcycler

Light Cycler quantitative real time PCR (LC-PCR) was performed with a RNA SYBR Green kit (Roche Diagnostics) following the manufacturer's instructions. In brief, 1µl of 10 µM primers and 50 ng of template DNA were mixed in a final volume of 20 µL containing 1X LightCycler-DNA Master Sybr Green I. For signal detection, the ABI Prism 7700 Sequence Detector System (Applied Biosystems) was programmed with an initial sterilization step of 2 min at 50 °C, followed by 10 min denaturation and polymerase activation at 95 °C and 40 temperature cycles of 15 s at 95 °C and 1 min at 60 °C. The Sequence Detection Software 1.9.1 (Applied Biosystems) was used for the analysis of raw data and cycle threshold (Ct) values were determined using the standard curve method according to the manufacturer's guidelines (Applied Biosystems). All measurements were performed in triplicate and the relative amount of all RNAs was then calculated by comparing the Ct values of the genes of interest after normalization to the β-actin's Ct values of the samples.

2.3.2 Taqman

qRT-PCR for the exons 1, 2 and 3 of neprilysin was also performed with HPLC-purified primers (Metabion) and TaqMan probes (Biosearch Technologies). The PBGD gene with its specific primers and quencher was used as reference and Ct values were determined. Black Hole Quencher™ TaqMan™ probes were also designed with the Primer Express 1.5 software.
The PCR reaction was carried out using the TaqMan Universal PCR Master Mix (4304437, Applied Biosystems), 333 nM oligonucleotide primers, 200 nM fluorogenic probe and 1 µl (50 ng) of template cDNA or HPLC-H_20 as control in a final volume of 25 µL. For signal detection, the ABI Prism 7700 Sequence Detector System (Applied Biosystems) was programmed with the same program used for the LightCycler analysis. All measurements were performed in triplicate and Ct value of each sample for each exon was normalized with the Ct value for PBGD: The relative amount of RNA was then determined by comparision of the Ct values for each treatment.

Mouse PBGD: F 5'-GCT ATG TCC ACC ACG GGA GA-3'
Mouse PBGD: R 5'-TAC ACG TGG GAG AGG GAC AAG-3'

Probes for the taqman qRT-PCR:
Mouse NEP exon 1: 5'-ACG GAG TGC AGG CGT-3'
Mouse NEP exon 2: 5'-CGC TGC CAA ATT GCA CCG GG-3'
Mouse NEP exon 3: 5'-ATA TGT CTA TTC TTC CTT CAA ATC TCA TGC ACT TGT GTG-3'
Mouse PBGD: 5'-AAG ATT GTT GAT ACT GCA CTC TCT AAG GTA ACG CCA-3'

3) Protein extraction, fractionation and analysis

3.1 Protein extraction from cell cultures

The medium was first removed and the plated cells were washed twice with PBS. The cells were then scraped in 4 °C lysis buffer containing 100 mM Tris, 150 mM NaCl, 1% Triton X-100, pH=7.8 and 1x complete protease inhibitor cocktail (Roche). The cells were removed and homogenated on ice by 12 passages through a 16G and a 26G needle (Becton Dickinson). The samples were then centrifuged at 20,000 g for 10 min on a centrifuge 5417R (Eppendorf) and the supernatant was removed, aliquoted and frozen at -25 °C.

3.2 Protein extraction and fractionation from mouse tissue

The homogenization of mouse tissues was performed in a glass homogenizer kept on ice using an electronic homogenizer (RZR2101, Heidolph) at a speed of 300 rpm.
For assessing transgenic neprilysin expression by immunoblotting, different areas of the brain such as cortex, cerebellum, pons, hippocampus, amygdala and peripherical organs such as kidney, liver and heart tissues were homogenized for 5 min in 25X volume/original weight (v/w) in lysis buffer A containing 100 mM Tris, 150 mM NaCl, 1% Triton X-100 and 1X complete protease inhibitor cocktail (Roche) pH=7.8. Homogenates were centrifuged at 20,000 g for 10 min on a centrifuge 5417 R (Eppendorf) and the supernatant was removed, aliquoted and frozen at -25 °C. Brain of mice treated with intraperitoneal (ip) injection of all trans retinoic acid (RA) were prepared similarly. Amygdala homogeneization was also performed similarly in 12 v/w lysis A with 2% SDS.
To determine neprilysin activity, the frontal brain tissues were not frozen after dissection but immediately homogenized with the lysis buffer A in absence of protease inhibitors.
After completion of the behavioral analysis by the 7 months cohort at 10 months of age for the J20 and NEPxJ20 mice and at 11 months of age for the NEP and WT mice, for combined Western blotting and Aβ enzyme-linked immunosorbent assay (ELISA), frozen frontal brain tissue was homogenized in 25X v/w lysis buffer A. Homogenates were centrifuged at 100,000 g for 45 min at 4 °C in an Optima Ultracentrifuge (Beckman Coulter) in adapted centrifuge tubes (343778, Beckman). Pellets were dissolved in lysis buffer B (lysis buffer A containing 2% SDS) (6 times the original weight) and centrifuged similarly. The SDS insoluble pellet was finally dissolved in 3 times the original weight of 70% formic acid (FA) and neutralized with 1.6 volume of 10 N NaOH.

After completion of the behavioral analysis by the 15 months old mice at the age of 18 months, the brain tissue was first homogenized in 12 v/w with a buffer containing 100 mM Tris, 150 mM NaCl and 1x complete protease inhibitor cocktail (Roche) pH=7.8 and centrifuged. The subsequent pellet was homogenized in 12 volumes /original weight of lysis buffer A and centrifuged as before. The triton insoluble pellet was further homogenized with 8 v/w of lysis buffer B and centriguged. Finally, the SDS insoluble pellet was resuspended in 6 v/w of 70% FA and neutralized.
The brain tissue from mice which received an intracranial treatment ($A\beta_{1-42}$ or $A\beta_{42-1}$) were homogenized in either lysis buffer containing 250 mM sucrose, 10 mM Tris, 1% Triton X-100, 1% SDS, pH=8, and 1X complete proteinase inhibitor mixture for the mice treated prior to amyloid plaque formation [406] or lysis buffer A for the mice treated after amyloid plaque formation [404]. All samples were analyzed by zymography and while samples from the first group were used for the RayBio Mouse Angiogenesis Antibody Array, samples from the second group were used for plasmin activity (SDS inhibited the enzymatic assay).
To investigate plasminogen activators activity, cortex and hippocampus of NEP (n=4) and WT littermates (n=4) were also removed, homogenized in buffer B without protease inhibitors and centrifuged at 20,000 g for 10 min at 4 °C.

3.3 Measurement of protein concentration

Protein concentrations of cell or tissue extracts were measured using the DC protein assay (500-0113, BioRad). Proteins react with an alkaline copper tartrate solution and reduce folin reagent. The reduced folin species have a characteristic blue color with an optimal absorption at 750 nm. Following the instruction manual, protein concentrations were calculated based on the absorptions of a standard curve. The standard curve was recorded with different dilutions of a BSA standard from 0.25 mg/ml to about 2 mg/ml in the corresponding sample buffer.

3.4 Immunoblotting of proteins

Immunoblotting is a method to quantify and determine the size of a protein of interest in a protein extract. Proteins are separated by SDS polyacrylamide gel electrophoresis (SDS-PAGE) and electrophoratically transferred from the gel to a nitrocellulose membrane where they are immobilized and can be detected by specific antibodies.

3.4.1 SDS polyacrylamide gel electrophoresis

By reduction of the disulfide bonds with β-mercaptoethanol, the proteins are dissociated into their polypeptide subunits which are denaturated using the anionic detergent SDS and heat. SDS binds to hydrophobic regions of the polypeptides so that they become negatively charged and migrate to the anode. The amount of SDS bound is proportional to the molecular weight of the protein subunits. This means that the charge density of all polypeptides is the same and they migrate with the same force but different exclusion volumes through the gel, leading to the separation of the polypeptides according to their size (smaller peptides migrating further than bigger ones).
The samples were heated at 95 °C for 5 min in the protein sample buffer, separated on 10-20% Tris-Glycine and 10-20% Tris-Tricine gels (Invitrogen) following the manufacturer's instructions. Equal amounts of protein were loaded to each lane when comparision was

required. Gels were run at 90 V for 2-3 h at RT in the Tris-glycine or tricine running buffer as recommended by the manufacturer.
For the separation of small molecular weight proteins such as Aβ, 10-20% Tris-Tricine gradient gels were used.
2X sample buffer: 450 mM Tris-HCl pH=8.45, 12% (v/v) Glycerol, 4% (w/v) SDS, 7.5‰ Coomassie brillant Blue (Merck) and 2.5‰ Phenol Red
1X tricine running buffer: 100 mM Tris-base, 100 mM Tricine, 0.1% SDS, pH=8.3
1X Tris glycine running buffer: 25 mM Tris-base, 192 mM glycine, 0.1% SDS, pH=8.3
1X NU PAGE running buffer: 50 mM Tris-base, 50 mM Tricine, 0.1% SDS, pH=8.3

3.4.2 Transfer of proteins

Following SDS-PAGE the stacking gel was removed and the running gel equilibrated in transfer buffer for 3 min. Whatman papers and nitro-cellulose membranes (Trans-Blot Transfer medium 0.45 μm, Biorad) are cut to the size of the gel and soaked in transfer buffer. The gel and the membrane are sandwiched between Whatman paper (3030917, Whatman) soaked pieces of sponge and perforated plastic plates. Transfer was carried out in a blotting tank (Novex) for 1h30 at 380 mA at 4 °C with the transfer buffer.
For the detection of β-amyloid, the special nitrocellulose transfer membrane PROTRAN (Bioscience) was used.
Transfer buffer: 3 mM Tris-base, 19.2 mM glycine, 20 % (v/v) methanol 0.02% SDS.

3.4.3 Immunological detection of proteins

After electrophoretical transfer of proteins, the membrane was blocked at RT for at least 1 h in TBST (10X TBST: 0.2 M Tris, 2.5 M NaCl, 1% (v/v) Tween 20) containing 5 % weight/volume (w/v) dry skim milk to prevent unspecific binding of antibodies. The primary antibody was diluted in TBST with 5% milk to an appropriate concentration and the blot was incubated at RT for 2 h or overnight at 4 °C. To remove all traces of unspecifically bound primary antibodies the membrane was washed 5X for 5 min in TBST. Incubation of the blot with the secondary antibody conjugated to horseradish peroxidase in 5% milk TBST was carried out for 2 h at RT. The blot was then washed again 5X for 5 min in TBST. The ECL Western Blotting Detection Reagents (RPN 2106, Amersham Biosciences) or the SuperSignal West Femto Maximum Sensitivity Substrate kit (34095, Pierce) were used following manufacturer protocol and bands visualized by chemiluminescence using X-omat LS films or Light film (Kodak) and the Kodak X-OMAT 2000 Processor.
For the detection of Aβ, the membrane was boiled for 5 min in PBS and cooled down prior to the blocking.
The effective overexpression of neprilysin in the NEP mice was investigated using the rat HA antibody (1867423, Roche, 1/1000) and the mouse neprilysin antibody 56C6 (Novocastra, 1/100) recognizing human and murine neprilysin [406]. The rabbit C-terminal APP antibody (Sigma, 1/5000) and the mouse 6E10 antibody (Signet Laboratories, 1/500) were used to analyze full length APP (flAPP), C-terminal fragments of APP and Aβ levels in NEPxJ20 and J20 mice. The blots were probed for β-actin (Abcam, Cambridge, UK, 1/5000) as a loading control. The secondary antibodies used were the anti-mouse HRP conjugated (NA931, Amersham, 1/5000), the anti-rabbit HRP conjugated (NA934, Amersham, 1/5000) and the anti-rat (NA935, Amersham, 1/5000) antibodies.

3.5 Neprilysin activity assay

Frontal brain tissues from NEP (n=4) and WT (n=4) mice were homogenized in lysis buffer A without protease inhibitors (see 3.2). 34 µg proteins were incubated for 1 h at 37 °C with 100 µM Z-Ala-Ala-Leu-p-nitroanilide (ZAAL-pNA; Bachem) in 50 mM HEPES buffer (pH=7.2). Thereafter, 0.8 mU leucine aminopeptidase (Sigma) was added to the reaction mixtures, incubated for an additional 20 min at 37 °C and OD was measured at 405 nm. To inhibit neprilysin activity, 40 µM thiorphan (Sigma) were added for 5 min at RT before the addition of ZAAL-pNA. To improve the quantification of the test, different concentrations of NEP samples diluted in similarly prepared brain homogenate of a NEP KO mouse [314] that exhibits no neprilysin enzyme activity were also measured.

3.6 Zymography

An overlay gel containing the inactive plasminogen, precusor of the active enzyme plasmin, and milk casein, an opaque substrate of plasmin, allow the detection and quantification of plasminogen activators. When in contact to the opaque gel, the plasminogen activators activate plasminogen into plasmin leading to the degradation of the casein which makes the gel transparent.
The overlay mixture consisted of 0.5 ml of an 8% commercial instant nonfat dry milk solution (the 8% stock solution in PBS was heated at 95 °C for 30 min, centrifuged 10 min at 3,000 g, and the supernatant collected), 0.75 ml of PBS containing 0.9 mM Ca^{2+} and 1 mM Mg^{2+}, 20 µl of a 4 mg/ml solution of purified human plasminogen (gift from Dr. Rime Madani and Prof. JD Vassalli [429, 467]) and 0.7 ml of a 2.5% agarose (50080, Cambrex) solution in ddH_20. Each solution was preheated at 52 °C and mixed in the order specified.
Identical experiments were carried out with overlay mixtures containing 1 mM amiloride (A-7410, Sigma), a specific inhibitor of uPA [468].
For zymography on cryostat tissue sections, 80 µl of the overlay mixture was applied to prewarmed 10 µm thick cryostat tissue sections mounted on poly-L-lysine-coated slides, and spread evenly under 24 x 32 mm glass coverslips. Slides were incubated at 37 °C in humid chambers and zymograms were allowed to develop for 2 to 6 h.
For the enzymatic assay, brain homogenates, cells homogenates and controls (actilyse, medium from cells overexpressing uPA [469], kidney homogenate and urine samples) were subjected to SDS−PAGE under non-reducing conditions. Since aprotinin, one of the standard markers, is a protease inhibitor, and SDS present in the gel can induce degradation of the milk, the marker was cut and the gel was washed first 3X for 10 min in a solution containing 2.5% triton in ddH_2O then 3X for 10 min in a special PBS solution (1 L PBS containing 0.132 g of $CaCl_2$ and 0.2 g of $MgCl_2.6H_2O$). The gel was then added on an underlay gel formed by the mixture which was cooled down to RT for 10 min on a glass plate. Special care was taken in obtaining a homogenous thickness for the overlay.
The zymogram was wraped into saranwrap to avoid dehydratation and was allowed to develop from 1 h to overnight at 37 °C.

3.7 Plasmin activity assay

12 weeks post injection brain homogenates from mice which were intracranially injected with 1 µl of PBS (n=3), a suspension of aggregated synthetic $A\beta_{1-42}$ (n=4) or $A\beta_{42-1}$ (n=6) [406] were tested for plasmin activity.

Plasmin enzymatic activity was assayed using the chromogenic substrate S-2251 (Chromogenix) specific for this protease included in the COAMATIC plasminogen kit (82 2452 63, Chromogenix) following the manufacturer protocol. 150 µg of brain homogenates were placed in a 96 multiwell plate in the presence of 2 mM chromogenic peptide to measure endogenous plasmin activity. Absorbance was measured at 37 °C and 405 nm with a Victor2 1420 multilable counter (Wallace) every 3 min for 45 min. The background activity was determined with 150 µg Plg KO brain homogenate and the linearity of the system investigated via sequential dilution of pure human plasminogen activated by streptokinase in plasminogen KO sample. The absorbance of the plg KO brain homogenate was removed from the analyzed samples and fold increase activity was determined by normalization of the sample absorbance with the absorbance of the PBS injected brain homogenates.

3.8 Enzyme-linked immunosorbent assay (ELISA)

3.8.1 Total murine Aβ ELISA

Frontal brain tissue was weighed and homogenized on ice at a 1/10 (w/v) dilution in 50 mM Tris pH=8.0, 150 mM NaCl, 5 mM EDTA, 1 mM PMSF, 0.8 µg/ml pepstatin and complete protease inhibitor cocktail (Roche) by 10 strokes at 1,000 rpm in a potter homogenizer. Brain homogenates were then centrifuged at 135,000 g for 1 h at 4 °C. The supernatant was collected and used for quantitation of murine Aβ levels by an established sandwich ELISA [470].

Rodent $A\beta_{40}$ and $A\beta_{42}$ standards (American Peptide Company, Sunnyvale, CA, USA) used in the ELISA were dissolved in dimethyl sulfoxide (DMSO) at 1 mg/ml, and further diluted to 5 µg/ml in buffer EC (20 mM sodium phosphate, 2 mM EDTA, 400 mM NaCl, 0.2% BSA (Sigma), 0.05% CHAPS, 0.4% casein, 0.05% NaN3, pH=7.0) and stored at -70°C. Nunc U-bottom high-binding 96 well microtiter plates (Life Technology) were coated with a mouse monoclonal antibody (100 µl at 5 µg/ml) that specifically recognize Aβ amino acid residue 17-24 (4G8, Senetek Research) [471].

Plates were washed 5 times with 200 µl per well of PBS using a Titertek M96 microplate washer (Titertek). 150 µl of the blocking solution consisting of 1 % casein in PBS was then added to each well for 30 min at 37 °C.

Before incubation on coated ELISA plates, brain extracts and standards were thawed and diluted in casein buffer containing 0.1% casein in PBS, 5 mM EDTA, 1 mM PMSF, 0.8 µg/ml pepstatin and complete protease inhibitor cocktail. Samples were diluted up to 1/20 or 1/40 and the standard curve covered the Aβ concentration between 1 to 0.016 ng/ml. ELISA plates were washed with the casein buffer before loading samples, standards, and JRF/rAβ/2-HRP (mouse monoclonal to $A\beta_{1-15}$) labeled antibody (1/2,000 in casein buffer). Incubation was carried out overnight at 25°C. Plates were then washed and assays were developed with tetramethyl benzidine/hydrogen peroxide (TMB/H_2O_2) substrate (Pierce) according to the manufacturer's specifications. The color reaction was stopped with 1 M phosphoric acid and the reaction product was quantified on a Molecular Devices microplate reader at 450 nm.

3.8.2 Human $A\beta_{40}$ and $A\beta_{42}$ ELISA

Brain $A\beta_{40}$ and $A\beta_{42}$ concentrations were quantified using commercially available ELISA kits, purchased from the Genetics Company (Schlieren, Switzerland) and Innogenetics (Ghent, Belgium), respectively. The capture and detection antibodies of the $A\beta_{40}$ kit are reactive to amino acid residues 31-40 and 4-10, respectively and don’t cross-react with $A\beta_{42}$.

Similarly, the capture and detection antibodies of the $A\beta_{42}$ kit are reactive to amino acid residues X-42 and 1-5, respectively and don't cross-react with Aβ40.
The different fractions of the brain homogenates were first acetone precipitated to eliminate the detergents. 4 volumes of -20 °C acetone were added for each volume of sample, mixed and kept at least 2 h at -20 °C. The sample were then centrifuged at 20,000 g for 15 min at 4 °C, the supernatant discarded and the pellet dried by speed vacuum and finally resuspended in the buffer of the ELISA kit for $A\beta_{40}$ on ice in a glass homogenizer using a Heidolph electronic homogenizer at 300 rpm.

3.9 Radioimmunoassay (RIA)

3.9.1 Peptides and chemicals

The synthetic peptide SP was acquired from Sigma Aldrich and Neosystems (Strasbourg, France), respectively. The enkephalin heptapeptide Met-enkephalin-Arg-Phe (MEAP) was obtained from Bachem (Bubendorf, Switzerland). The chromatographic material (SP-Sephadex C-25) was obtained from Pharmacia Biotech AB (Uppsala, Sweden). The iodinated SP used in RIA was prepared from Tyr8-substance P (Arg-Pro-Lys-Pro-Gln-Gln-Phe-Tyr-Gly-Leu-Met-NH_2) was from Sigma Aldrich.

3.9.2 Tissue preparation for radioimmunoassay

The collected mouse brains were weighed and suspended in an Eppendorf tubes containing 1 M acetic acid (1 ml per 100 mg tissue, minimal volume 500 µl) and heated at 95 °C in a water bath for 5 min. The samples were subsequently cooled on ice for 2 min prior to homogenization by ultrasonification. The homogenates were centrifuged at 14,000 g for 10 min at 95 °C and the supernatants were taken for further processing.

3.9.3 Pre-separation procedure using anion exchangers

Prior to RIA, the samples from the previous step were diluted with buffer I containing 0.018 M pyridine and 0.1 M FA, pH=3.1 and purified using ion exchange chromatography. Small plastic columns were packed with 1 ml SP-Sephadex C-25 gel (Pharmacia) and equilibrated with 20 ml of buffer I. Before application onto the columns the samples were diluted by addition of 3 ml buffer I. After additional washing with 10 ml of buffer I, the columns were subsequently washed with 5 ml of 0.1 M pyridine/0.1M FA, pH=4.4 before elution was carried out with 4 ml of 1.6 M pyridine/1.6 M FA, pH=4.4. All buffers contained 0.01% β-mercaptoethanol. The eluates were kept in volumes suitable for the subsequent assay (0.5 ml for MEAP, 1 ml for SP) and evaporated in a Speed Vac vacuum centrifuge (Savant). The dried samples were analyzed by RIA. Before RIA, samples and standards to be assayed for MEAP were oxidized using H_2O_2. Unknown samples were dissolved with 100 µl 1 M acetic acid and added with 10 µl of 30% H_2O_2. Samples were allowed to incubate in a water bath at 37 °C for 30 min and thereafter dried in a Speed Vac centrifuge. A stock solution with MEAP (9.10^{-6} M) to be used for the standard curve was treated in a similar fashion with the exception higher concentration of H_2O_2 was used.

3.9.4 RIA

The RIA for SP and MEAP were based on the charcoal absorption technique and were conducted as described [472-475]. For all RIA, the antibodies were raised in rabbits against

the peptide-thyroglobulin conjugate and the 125-I-labelled synthetic peptides or peptide analogues (see above) were used as tracers. Details (including cross-reactivity and detection limits) for the various RIA are given in the above cited references. Each individual RIA value is given as a mean from triplicate determination.
The RIA for somatostatin was performed using a kit supplied by Euro-Diagnostica (Medeon) and was conducted according to the description given by the manufacturer. The material obtained from the pre-separation on SP-Sephadex mini-columns (0.5 ml of material eluted with 1.6 M pyridine/1.6 M FA, pH=4.4) was dried as above, subsequently redissolved in the assay diluent (included in the kit) and thereafter analyzed by RIA, which was based on a double antibody procedure.

3.10 RayBio Mouse Angiogenesis Antibody Array

To determine the potential role of inflammation in the Aβ-related neprilysin and uPA activity upregulation *in vivo*, 500 µg of brain homogenate from 4 mice which were killed 20 weeks after $A\beta_{1\text{-}42}$ of $A\beta_{42\text{-}1}$ injection (2 mice per group) were analyzed with the RayBio Mouse Angiogenesis Antibody Array1.1 (M0319801, RayBiotech) allowing the detection and quantification of 24 different angiogenesis factors (Fig. 7).
Preparation of the samples, incubation and detection were performed following manufacturer's instructions: membranes were blocked for 1 h and incubated with 500 µg brain homogenate overnight at 4°C and then washed for 30 mn and incubated with a 1 to 250 dilution of biotin-conjugated antibody mix for 2 h. After consecutive washes, a 1/1'000 dilution of streptavidin-conjugated peroxidase was added and incubated for 2 h RT. The membranes were further washed and exposed to peroxidase substrate prior to detection by exposing the membranes to a x-ray film for 1 mn and development.

	A	B	C	D	E	F	G	H
1	POS	POS	POS	POS	Blank	Eotaxin	Fas Ligand	bFGF
2	NEG	NEG	NEG	NEG	Blank	Eotaxin	FasLigand	bFGF
3	G-CSF	GM-CSF	IFNγ	IGF-II	IL-1 α	IL-1 β	IL-12 p40/p70	IL-12 p70
4	G-CSF	GM-CSF	IFNγ	IGF-II	IL-1 α	IL-1 β	IL-12 p40/p70	IL-12 p70
5	IL-13	IL-6	IL-9	Leptin	MCP1	M-CSF	MIG	PF-4
6	IL-13	IL-6	IL-9	Leptin	MCP1	M-CSF	MIG	PF-4
7	TIMP-1	TIMP-2	TNF α	Thrombopoietin	VEGF	Blank	Blank	Blank
8	TIMP-1	TIMP-2	TNF α	Thrombopoietin	VEGF	Blank	POS	POS

Figure 7. Location and name of the factors analyzed by the RayBio Mouse Cytokine Antibody Array. After determination of the background intensity obtained by negative spots (NEG) and blank spots, the quantification of the factors can be performed by comparing their intensity with the one from positive spots (POS). Vascular endothelial growth factor (VEGF) and basic fibroblast growth factor (b-FGF), granulocyte, macrophage and granulocyte-macrophage colony-stimulating factors (G-CSF, M-CSF and GM-CSF, respectively), interferon γ (IFN γ) and monokine induced by IFN- γ (MIG), insulin growth factor II (IGF-II), macrophage chemoattractant protein (MCP1), platelet factor 4 (PF-4), interleukins (IL: IL-1α, IL-1β, IL-12 p40/p70 recognizing both p40 and p70, IL-12 p70, IL-13, IL-6 and IL-9), tumor necrosis factor α (TNFα), , tissue inhibitors of metalloproteinases (TIMP-1 and TIMP-2) are among the factors analyzed.

4) Cell culture

4.1 Culture and storage of cell lines

The following neuronal and non-neuronal mammalian cell lines have been used from the Deutsche Sammlung von Mikroorganismen und Zellkulturen (DSMZ); Human embryonic kidney HEK-293 cells (DSMZ # ACC 305), HEK-293T cells (DSMZ # ACC 305), human neuroblastoma SH-SY5Y cells (DSMZ # ACC 209). Human microglial cells (MIC) were initially produced by Janabi *et al.* [476].
All cell lines were cultivated at 37 °C/ 5% CO_2/ 95% humidity in their specific culture medium. When confluency was reached and dilution required, the cells were washed with PBS, released from the dish by incubation with trypsin/EDTA for 3 min, singled with a flamed Pasteur pipette, centrifuged 5 min at 1,000 g, resuspended in culture medium and plated at ratios of 1/3 to 1/10 depending on the purpose.
For storage, the cells were resuspended in freezing medium and immediately chilled on dry ice and frozen at -80 °C in a Styrofoam box. After one day at -80 °C the aliquots were transferred to liquid nitrogen and kept for long time storage.
To recultivate frozen cells, cell aliquots were thawed quickly in a water bath at 37 °C, and cells were immediately resuspended in cultivation medium and pelleted by centrifugation. After resuspension, cells were plated on dishes at a seeding density corresponding to 50% confluency. SH-SY5Y cells can also be triggered to differentiate to a neuronal-like phenotype [477]. For differentiation, SH-SY5Y cells were seeded on collagen type I (Sigma) coated dishes at a density of 0.3 – 2.0x10^4 cells/cm^2. To induce neuronal differentiation, cells were incubated in medium containing RA for five days, followed by an additional five days in serum free medium supplemented with BDNF (Preprotech).

- culture medium for the HEK-293T cells: DMEM (Invitrogen), 10% (v/v) FCS, 50 U/ml penicillin and 50 µg/ml streptomycin.
- culture medium for the SH-SY5Y cells: DMEM-F12 medium (Invitrogen), 2 mM L-glutamine, 1 mM sodium pyruvate, 10% FCS, 5% HS, 50 U/ml penicillin and 50 µg/ml streptomycin.
- culture medium for the MIC cells: DMEM with Glutamax 1 (Invitrogen), 10% (v/v) heat inactivated FCS, 50 U/ml penicillin and 50 µg/ml streptomycin.
- Differentiation medium I (days 1-5): DMEM-F12, 2 % FCS, 2 mM L-glutamine, 20 µM RA.
- Differentiation medium II (days 5-10): DMEM-F12, 2 mM L-glutamine, 50 ng/ml BDNF.
- Freezing medium: DMEM or DMEM-F12, 20 % (v/v) FCS, 5% HS, 10 % (v/v) DMSO.

4.2 Primary neuronal culture

24 well plates were previously coated with 50 µg/mL poly-D-lysine (P-2636, Sigma) in 0.1 M borate buffer overnight in the cell incubator. The plates were then rinsed with ddH_20 prior to plating.
Primary neuronal cultures were prepared from embryonic C57Bl/6 mice at the developmental stage of 16 to 18 days. Cerebral cortices were dissected from the brains of the embryos in ice-cold Hank's balanced salt solution without Ca^{2+} and Mg^{2+} (HBSS; 10 mM HEPES, 50U/ml penicillin and 50µg/ml streptomycin, pH=7.3) (Gibco) and the hippocampi removed and

freed from meninges in a similar buffer. The hippocampi were incubated at 37 °C for 30 min in pre-heated Hank's medium containing Ca^{2+} and Mg^{2+} to which 0.25% trypsin (Gibco) and 0.05% DNase I (Sigma) were added. The tissues were dissociated to single cells by gentle trituration using flamed Pasteur pipettes. The cell suspension was mixed with Neurobasal medium supplemented with 2% B27 (Gibco), 0.5mM glutamine, 50 U/ml penicillin, and 50 µg/ml streptomycin. The cell suspension was centrifuged at 310 g for 3 min and the resulting pellets were resuspended in the medium described above and plated onto coated 12 or 24-well. The cells were cultured in a CO_2 incubator (5% (v/v), 37 °C) for 10 days before treatment. Half the medium was removed each 2-3 days and replaced with Neurobasal medium supplemented with 2% B27 (Gibco), 0.5 mM glutamine, 50 U/ml penicillin, and 50µg/ml streptomycin. During the 5 days incubation with Aβ, half the medium was changed as usual without further addition of Aβ before cell lysis.
Borate buffer: 1.24 g boric acid, 1.9 g sodium tetraborate in 400 ml ddH_2O pH=8.5, filtered and sterilized.

4.3 Transient transfection and luciferase assay

After transfection of a plasmid expressing luciferase under the control of a promoter of interest, the activation of the promoter correlated with the luciferase activity present in the sample. This system allowed a simple and high sensitive method to quantify reporter activity after a specific treatment.
Transfection of 90% confluent cultures, grown in 24 well plates, was performed with lipofectamine 2000 (Invitrogen), using 1 µg DNA per well and following manufacturer's protocol. Each treatment was performed in three independent wells. Firefly luciferase expressing constructs under the control of one of the three neprilysin promoters or deletions of promoter 1, were transfected alone. Generally 6 h after transfection, the medium was removed and replaced with the adequate culture medium containing the additional substance to be tested. Depending on the cell type and the purpose of the experiment, the cells were harvested from 12 to 72 h after transfection with the passive lysis buffer of the Luciferase assay system (Promega E1500). The luciferase activity was measured according to the manufacturer's protocol using a photoluminometer LB 9507 (Berthold) and normalized by dividing it with the protein concentration of the sample analyzed. When the effect of the differentiating agent, RA, was assessed on SH-SY5Y cells, luciferase activity was not normalized with the protein concentration to avoid overestimating the effect due to higher levels of proteins in the untreated plates. Because of low level of luciferase activity in SH-SY5Y cells, the background activity level determined in non-transfected cells was substracted from all readings.
The Dual Luciferase Reporter Assay System (Promega E1910) used specific buffers which allowed the measurement of firefly and renilla luciferase activities from the same sample without interation between the two luciferases. Firefly luciferase expressing constructs were co-transfected in a molar ratio of 150:1 with pRL-TK renilla luciferase vector (Promega) as the internal control for transfection efficiency. The cells were harvested with the passive lysis buffer of the Dual Luciferase system (Promega) and the luciferase activities were measured according to the manufacturer's protocol.

4.4 Experimental conditions and treatments

4.4.1 Aβ preparation and incubation

$A\beta_{1-42}$ and $A\beta_{42-1}$ were purchased from Bachem, reconstituted in PBS at calculated concentrations of 220 μM were shaken at 1,000 rpm for 24 h at 37 °C in a thermomixer (Eppendorf). Suspensions of $A\beta_{1-42}$ preparations corresponding to 5, 10 and 15 μM soluble peptide were added to each culture for incubations periods ranging from 12 h to 3 days for the cell lines and 5 days for the primary neuronal culture.

4.4.2 All trans retinoic acid (RA) incubation

To test the effect of RA and BDNF on neprilysin promoter activation, SH-SY5Y cells and 293T cells were incubated for 12 h to 5 days in their standard medium containing 10 μM RA (Sigma), or the solvent (DMSO) as control.

4.5 Cell viability

The general cell viability of the cells treated with $A\beta_{1-42}$ and $A\beta_{42-1}$ was analyzed by trypan blue staining of the cells. 0.8 mM of trypan blue in PBS was added to the plates, incubated 5 min at RT and washed. Viable cells exclude trypan blue, while dead cells stain blue due to trypan blue uptake.

5) Transgenic and knockout mice

5.1 Generation of the NEP transgenic mice

Genetically modified mice, overexpressing neprilysin in the CNS neurons, were generated by the following method: a hemagglutinin (HA) tag was fused to the C-terminus of human neprilysin cDNA [331]. This fragment was then inserted into the XhoI site of the MoPrP expression vector [478] to ensure neuronal expression. A standard pronuclear injection of the DNA construct was then undertaken in C57BL/6xDBA/2 embryos. The presence of the transgene was confirmed by PCR analysis of genomic DNA. Several transgenic lines were produced and one line designated NEP was established and kept on 50%x50% C57BL/6xDBA/2 background.

5.2 Other transgenic mice used and breedings

- Mice with targeted depletion of the neprilysin gene were a gift from Dr. Bao Lu [314]. They were crossbred for 10 generations with the C57BL/6 background.
- uPA KO mice lacking uPA protein and activity, mice with a similar background and Plg KO mice lacking an active plasminogen were a gift from Dr. Peter Carmeliet, Center for Transgene Technology and Gene Therapy, Flanders Interuniversity Institute for Biotechnology, Leuven, Belgium.

- J20 mice, expressing the Swedish and Indiana mutated human APP in neurons [70], were donated by Dr. Lennart Mucke, Gladstone Institute, UCSF. They were maintained on a pure C57BL/6 background.
For behavioral and biochemical analysis of the effect of neprilysin overexpression on the Aβ-related pathology, NEP males were mated with J20 females. Their progeny consisting of NEP, J20, WT and NEPxJ20 mice, all littermates with a 75% C57BL/6 25% DAB/2 background were analyzed. All mice were housed under a light cycle of 12 h with dry food pellets and water available ad libitum, when not mentioned differently.
Animal experiments and husbandry were performed in compliance with national guidelines.

5.3 Treatments

5.3.1 Stereotaxic injection of β-amyloid

Synthetic $A\beta_{1-42}$ and reverse Aβ, $A\beta_{42-1}$ were purchased from Bachem, reconstituted in PBS at a final concentration of 350 μM and shaken at 1,000 rpm for 48 h at 37 °C in an Eppendorf thermomixer (Vaudaux-Eppendorf AG) to allow aggregation.
At the age of 1 year, SwAPP mice received a unilateral intracranial injection of 1 μl 350 μM stock concentration fibrillar $A\beta_{1-42}$ (n=5, Aβ high dose group) or 35 μM stock concentration (n=4, Aβ low dose group) in the hippocampus (caudal -1.9 mm, lateral -1.2 mm and ventral -1.9 mm) as described [404, 406]. Control groups consisted of SwAPP littermates which received injections of 1 μL 350 μM stock concentration $A\beta_{42-1}$ (n=6, $A\beta_{42-1}$ high dose group) or did not receive any injection.
Mice were anesthetized with a mixture of 2% xylazine and 10% ketamine (10 μl/g body weight, Streuli-Pharma), placed in a stereotaxic instrument (Stoelting) (Fig. 6), and an incision was made along the midline of the head to expose the skull.
The calvarium was perforated with a drill (Fine Science Tools) at the positions: caudal -1.9 mm, lateral -1.2 mm (Fig. 8).
A 10 μl Hamilton syringe was slowly inserted 2.4 mm into the cortex at (caudal -1.9 mm, lateral -1.2 mm and ventral -1.9 mm) the same coordinates. After 2 min, a total volume of 1.5 μl $A\beta_{1-42}$ or reverse $A\beta_{42-1}$ was injected into the CA1 region of the hippocampus with an injection speed of 0.15 μl/min using a mini pump. The needle was kept in the injection site for another 2 min before slowly being withdrawn. The wound was closed with surgical staples and the mice kept on a heating pad for 3 h.

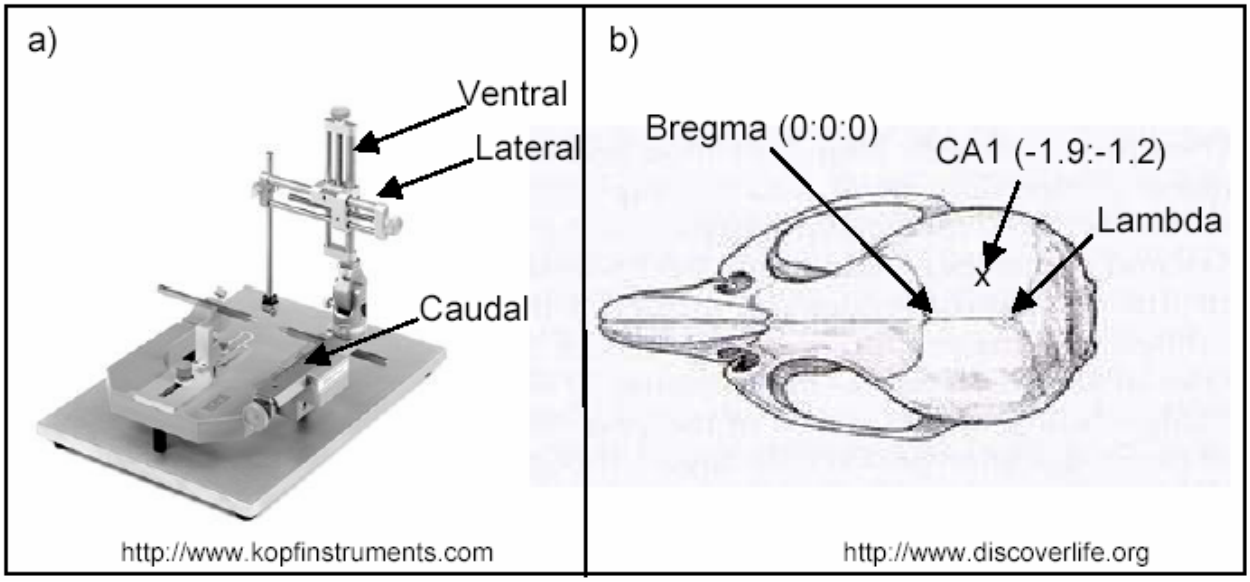

Figure 8. Stereotaxic injection of Aβ

5.3.2 Stereotaxic injection of rAAV

The same protocol was used to inject 2 µl the rAAV preparations in the CA1 region (caudal -1.9 mm, lateral -1.2 mm and ventral -1.9 mm) or the dentate gyrus area (caudal -1.9 mm, lateral -1.2 mm and ventral -2.5 mm) of the hippocampus.

5.3.3 Treatment with RA

A first group of mice was treated chronically during 5 days with 3 µg of RA. A second group was similarly treated with 125 µg RA. Subcutaneous RA tablettes shown to release a constant RA level every day were also implanted during 3 weeks in WT and transgenic mouse models of amyloidosis.

5.4 Tissue preparation

Once under deep anesthesia induced by ip injection of a solution containing 2% xylazine and 10% ketamine (10 µl/g body weight) (Streuli-Pharma) mice are perfused transcardially using a peristaltic pump connected to two reservoirs containing saline and fixative solution, respectively. A cut along the sternum is made in order to expose the end of the sternum, then, with sharp scissors, a cut is made through the skin, diaphragm and laterally on both sides upward across the ribs and parallel to the lungs; the cannula was then inserted through the left ventricle into the ascending aorta. Immediately, the right auricle was punctured to allow the escape of return circulation. Perfusion was performed with PBS during 6 min. Brains were removed, dissected into various areas including frontal brain area sectioned at the bregma line [479], hippocampus, cerebellum and subcortical areas, and frozen immediately on dry ice. Similarly peripherical organs such as kidney, heart and liver were removed and frozen on dry ice.

For dissection of the amygdala, 400 µm frontal brain sections beginning at -0.94 mm and ending at -2.18 posterior to bregma according to a stereological brain atlas [479] were

obtained using a tissue chopper (Bachofer GmbH). Amygdalae were dissected under a light microscope with scalpels and frozen immediately on dry ice and stored at –20 °C.
Following completion of the behavior testing, the brain of the mice was removed following the same procedure. The frontal parts of the brain were sectioned at the bregma level, divided into the sagittal halves and frozen immediately. The dorsal part of the brain was fixed for 24 h in 4% paraformaldehyde (PFA) in PBS at 4 °C. The brains were then dehydrated in an ascending series of ethanol (70%, 96%, 100%; each 3 h, by changing every hour), left overnight in xylol, subsequently immersed in liquid paraffin at 60 °C for 5 h and finally embedded in paraffin.
For cryostat sectioning, after overnight fixation in PFA, brains were cryprotected by incubation overnight in 10%, overday in 20% and overnight in 30% sucrose, then fixed in tissue freezing medium (Jung) and kept at -30 °C.
For paraffin sections, tissue was subsequently dehydrated in an ascending ethanol series of ethanol (70%, 96%, 100%; each 3 h, by changing every hour), left overnight in xylol, subsequently immersed in liquid paraffin at 60 °C for 5 h and finally embedded in paraffin.

5.5 Immunohistochemistry

5.5.1 Immunostaining of paraffin sections

Immunohistochemistry was done on coronal 5 μm thin paraffin sections obtained with a microtome RM2135 (Leica) and brain areas were mapped based on the mouse atlas [479].To allow antibodies to penetrate fixed tissue embedded in paraffin, sections were dewaxed 3X in xylol and rehydrated in a descending series of ethanol (2X in 100%, 1X in 96%, 1X in 70%) and 2X in ddH_2O (5 min each).
To detect an antigen, specific primary antibodies and secondary antibodies (conjugated to fluorescent dyes or biotin) were used. The sections were washed well in PBS (fluorescence) or TBS (DAB) and permeabilized with 0.1% Triton X-100 in TBS (TBST) for 10 min at 37°C. To detect the signal of the HA and neprilysin antibody, further permeabilization with methanol at –20 °C for 5 min or 10 min of microwave at 95 °C in a sodium-citrate buffer 0.01 M, pH=5.8, were tried. Neprilysin staining was observed after 5 mn permeabilisation at 120 °C using a pressure cooker in sodium-citrate buffer 0.01 M, pH=5.8.
Sections were then blocked for 30 min in PBS or TBS containing 10% normal serum and 4% milk. Sections were then incubated with the primary antibody diluted in PBS or TBS containing 5% normal serum and 2% milk overnight at 4 °C. Sections were washed 4 times with PBS or TBS were incubated with the secondary antibody for 2 h at RT, and were washed again. The fluorescence stained sections were mounted directly with Moviol (Hoechst) while vectastain ABC reagent (Vector Laboratories) was added to the DAB labeled sections for 30 min. These sections were washed again and were incubated with peroxidase substrate solution (DAB) (Pierce) for 10 min. The immunostained sections were mounted with antifading medium (Moviol, Clariant) and microscopically analyzed by conventional immunofluorescence.

5.5.2 Immunostaining of cryostat sections

10 μM frozen sections, cut on a cryotome Leica CM 1900 (Leica), were washed twice with PBS and permeabilized with PBS containing 0.1% Triton X-100 for 30 min and blocked for 2 h with 5% goat serum diluted in PBS RT. The primary antibody was diluted in blocking buffer and incubated with the sections overnight in a wet chamber at 4 °C. The brain slides

were then washed 5X with 0.05% Tween-20 in PBS for 10 min. The secondary antibody, conjugated with a fluorescence marker, was diluted in blocking buffer, added to the sections and incubated at room temperature for 2 h in the dark. The sections were then washed three times with PBS for 5 min and embedded in Moviol before immunofluorescent detection under a microscope using the specific filter required.
To detect the signal of the HA and neprilysin antibody, further treatment of the sections including 5 mn incubation in -20 °C methanol, 10 min heat induced antigen retrival at 95 °C in a microwave or 5 mn at 120 °C in a pressure cooker using a sodium-citrate buffer, 0.01 M, pH=5.8 were investigated.

5.5.3 Antibodies

Antibodies used for immunohistochemical detection of HA or neprilysin in NEP mice were the mouse HA (2362, Cell Signalling, 1/200), the goat HA (Ab1266, Abcam, 1/100), the rat HA (1867 423, Roche, 1/100), the mouse neprilysin (CL CD10-270, Novocastra, 1/100) and the rabbit neprilysin (AB5458, Juro, 1/100) antibodies. Only the mouse neprilysin antibody worked for immunohistochemistry. While Aβ staining was investigated with the mouse 4G8 antibody (200-05, Signet, 1/500), astrocytes and microglia activations were stained with the guinea pig GFAP (031223, Advanced Immunochemicals, 1/100) and the Iba I ([480, 481], 1/500) antibodies. Secondary antibodies included the Cy3 anti-mouse (115-165-146, Jackson, 1/200), the Cy3 anti-rat (712-165-153, Jackson, 1/200), the Cy3 anti-rabbit (111-165-144, Jackson, 1/1000), the Cy3 anti-goat (706-165-148, Jackson, 1/100) and the Cy2 anti-guinea pig (706-225-148, Jackson, 1/50).

5.5.4 Electron microscopy

Aged NEP KO and WT littermates (18-20 months, n=3 each) were perfused transcardially with 0.05 M Na-Cacodylat-buffer containing 2 % Glutaraldehyde and postfixed overnight in the same solution. Subsequently the hippocampus was carefully removed and cut into fragments of approximately 1 mm^3. The samples were then postfixed in 0.1 M Na-cacodylate buffer containing 1% OsO_4, dehydrated in an alcohol series and embedded into epon. Semithin sections were stained with Toluidin blue and ultrathin sections (50 nm thick) were contrasted with uranyl acetate and lead citrate.

6) Behavioral analysis

6.1 Animals

Eighteen months old NEP KO, also termed NEP-/- (n=10) as well as NEP heterozygous termed NEP+/- (n=7) and WT littermates (n=8) were subjected to conditioned taste aversion (CTA).
NEP males, kept on a C57BL/6xDBA/2 background (50/50), were mated with J20 female kept on a pure C57BL/6 background. We investigated their progeny at two different ages.
First, 17 WT, 16 NEP, 17 J20 and 13 NEPxJ20 male littermates with similar background (75% C57BL/6x 25% DBA/2) were tested in the CTA at 4.5 months of age (19.5 ± 0.2 weeks). After completion of the CTA, 17 WT, 15 NEP, 17 J20 and 11 NEPxJ20 male mice

were then tested at 7 months of age (30 ± 0.2 weeks) in the open field, the elevated zero maze, the Morris water maze and the puzzle box tests.
At 10 months of age (41 weeks), a bigger group of mice of both genders, including the mice from the 7 months cohort (31 WT, 28 NEP, 31 J20, 26 NEPxJ20) were analyzed in the light-dark test. Finally the J20 and NEPxJ20 males of the first group were biochemicaly analyzed. NEP (n=15) and WT (n=17) littermates were further analyzed in emergence, object exploration, Y maze, rotarod, hot plate and fear conditioning tests.
Another group of mice were tested at 15 months of age, balanced for gender and formed by 16 WT, 15 NEP, 16 J20 and 14 NEPxJ20, were analyzed in the open field, the elevated zero maze, the Morris water maze, emergence and object exploration, hot plate and puzzle box tests. The mice were sequentially analyzed in two sets, which were balanced for the genotype. Data were pooled, as no statistically significant differences were found between sets.
During the experimental period, animals were single-housed in standard mouse cages and kept under an inverted 12 h light/dark cycle. Standard mouse food, water and nesting material were available ad libitum. Thirty min before each test session, the mice were transferred to the behavioral room and dry surfaces of apparatus were thoroughly cleaned with 70% ethanol before releasing the animal. Animal experiments and husbandry were performed in compliance with national guidelines.

6.2 Exploratory behavior and anxiety

6.2.1 Open field test

The round open-field arena had a diameter of 150 cm, a smooth white plastic floor and 35 cm high side walls made of white polypropylene. Illumination was done by indirect diffuse room light (four 40 W bulbs, 12 lux). Each subject was released near the side wall and observed for 10 min. The same procedure was repeated the following day, resulting in a total observation time of 20 min, partitioned into 4 bins of 5 min for time course analysis. Paths were tracked and the arena was divided into an outer zone (within 7 cm of the wall), an inner zone (inner circle with a diameter of 110 cm), and an intermediate zone (Fig. 9A).
Locomotor activity was assessed by measuring the total distance travelled and the total number of zone transitions. Thigmotaxis, defined as moving along the wall, was quantified by measuring the time spent in the outer zone. To determine measures of anxiety and exploratory behavior, the following parameters were assessed: number of visits to the inner zone, average distance to inner zone, and the number of activity state changes. Three activity states were distinguished: progression (periods with a locomotion speed above the progression threshold of 0.085 m/s and a minimal distance moved exceeding 0.05 m), resting (periods lasting at least 2 s with a speed below 0.025 m/s) and lingering (periods meeting neither resting nor progression criteria).

6.2.2 Emergence test

Frames of nonreflective aluminum (37 cm high) were used to partition the earlier described open field into four square 50x50 cm arenas, allowing concurrent observation of 4 animals. Each arena had a 12x8x4 cm plastic home box with an opening of 8x4 cm^2, positioned in a corner at 5 cm from the nearest walls, with the opening facing away from the wall (Fig. 9B). 24 h prior to testing, a thoroughly cleaned home box was placed in the home cage of each test subject. The next day, test subjects and home boxes were introduced into the arenas and observed for 30 min. For time course analysis, this period was partitioned into 3 bins of 10

min. The definitions of the three zones were a home zone of 18x22 cm^2 surrounding the home box and extended to the nearest portions of the sidewall, a 5 cm wide wall zone extending along the rest of the sidewalls and the center of the arena as exploration zone. Motion state, exploration index were calculated as in the open field test.

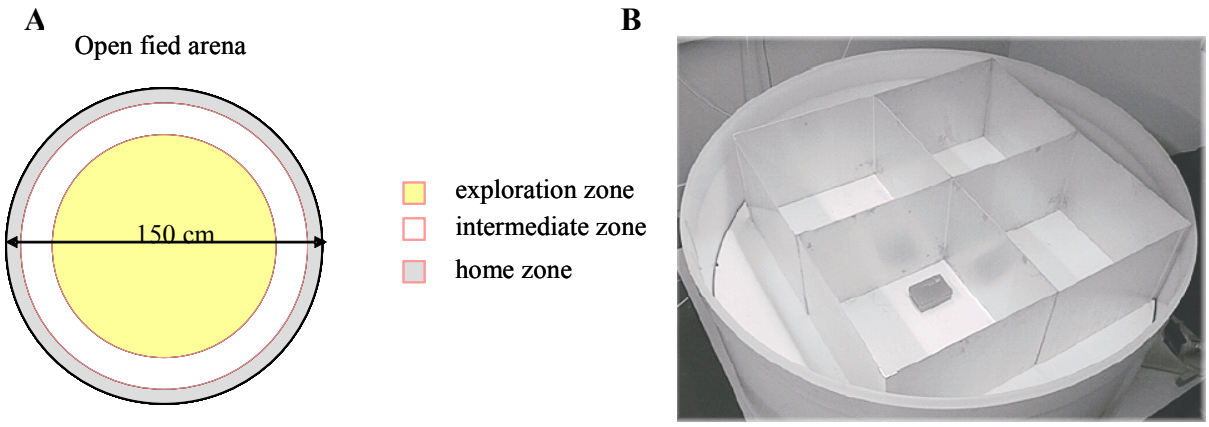

Figure 9. Representation of open field (A) and emergence test (B) arena. Levels of spontaneous locomotor activity, anxiety-like behavior and exploration were assessed by recording the mouse activity state and time spend in the different zones.

6.2.3 Object exploration

Arenas were the same as for the emergence test, but without the home box. The novel object was a 12x4 cm semitransparent 50 ml Falcon tube positioned vertically in the center of the arena. Each subject was observed for 30 min in the empty arena. The novel object was then introduced, and observation continued for another 30 min. For time course analysis, total observation time was partitioned into 6 bins of 10 min. The same measures were calculated as in the emergence test, with three concentric zones defined as follows: a 5 cm wide wall zone, a circular exploration zone of 16 cm diameter around the arena center where the object was introduced, and a transition zone in between. For relevant measures, we extracted object related components by extrapolating object unrelated components from the surrounding transition zone and subtracting them from the raw values measured in the exploration zone. This method brought corrected measures close to zero in absence of the object.

6.2.4 Light-dark (L/D) test

Mice were placed into the 30x20 cm area of a Perspex L–D box that was illuminated with an average of 700 lux. A dark compartment of 15x20 cm was attached opposite to the releasing site with an opening facing the center of the illuminated area (Fig. 10A). Movements were tracked in the illuminated area over a 5-min trial. Anxiety was measured by the latency to enter and the time spent in the dark compartment. Exploration was defined by the number of rearings in the illuminated part, and the percentage of visited tiles/total of 36 tiles (5x3.3 cm) entered with all four paws.

6.2.5 Elevated zero maze

The zero maze consisted of a gray plastic annular runway of 5.5 cm width with an outer diameter of 46 cm located 40 cm above ground level. Two opposing 90 °C sectors were protected by inner and outer walls of gray polyvinyl-chloride (10 or 16 cm high) (Fig. 10B). Animals were released in one of the protected sectors and observed for 10 min. For time course analysis, this time was partitioned into two bins of 5 min. To complement video tracking, head dipping movements were recorded using the keyboard event-recorder function of the tracking system. Motion states were defined as in the other tests with progression thresholds adapted to the more strongly confined movements: speed threshold 4 cm/s, distance threshold 3 cm, deceleration threshold 8 cm/s. Three zones were defined as follows: a transition zone comprising four 30° segments at the ends of the protection walls separated by the two 50° wide protected and the two 70° wide unprotected exploration zones. With these boundaries, the system detected entries to the unprotected sector only when the animal moved into it with all four paws. Head dips that occurred while the animal was registered to the transition zone with all or part of its body between the protection walls were classified as protected dips, all others as unprotected dips.

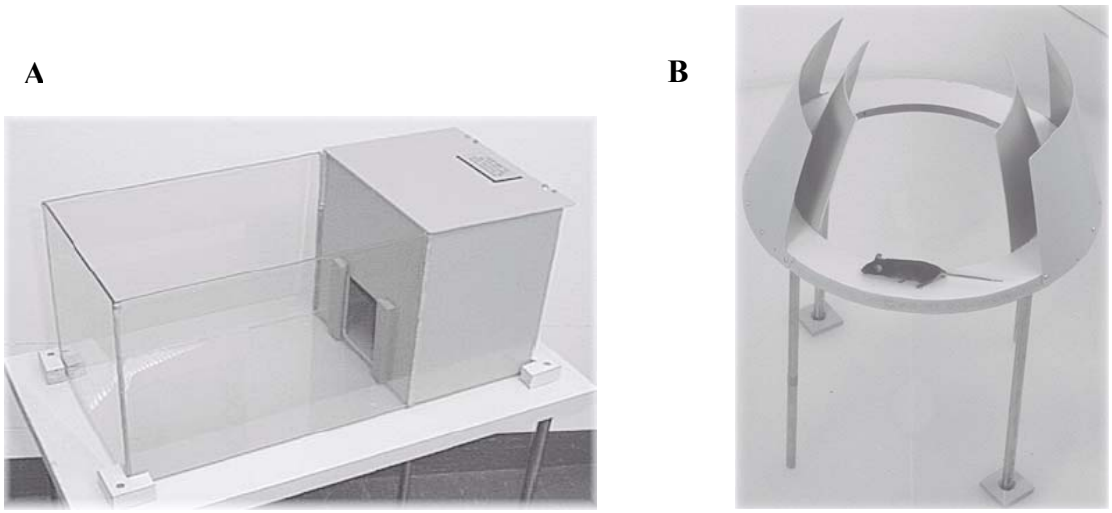

Figure 10. Apparatus of the light-dark (A) and O-maze (B) tests. Based on the natural preference of the mice for dark protected areas, the anxiety state of the mice was determined by the time spent in protected versus unprotected areas.

6.3 Learning and memory behavior

6.3.1 Conditioned taste aversion test

Water-deprived mice were housed in single cages and allowed access to water only two times a day: for 20 min in the morning and for 10 min in the afternoon, with a 4 h interval between sessions on 4 consecutive days. The fluid intake was determined by weighing the tubes before and after the tests. On the conditioning day, water in the morning session was replaced by a 0.5% saccharin (saccharin sodium salt hydrate; Fluka Chemie, Buchs, Switzerland) solution which acted as the conditioned stimulus. Forty min after drinking the saccharin solution, the mice were injected ip with a nausea-inducing solution (0.14 M LiCl solution, 2 % body weight) as the unconditioned stimulus (Fig. 11). The initial consumption of saccharin was defined as the amount of saccharin drank during the conditioning day divided by the mouse weight. 48 h after conditioning, the degree of conditioned aversion was determined in the first

choice test. The mice were simultaneously presented with two bottles and allowed to drink for 20 min. One bottle contained a 0.5% saccharin solution and the other contained water. The aversion coefficient was defined as the amount of saccharin consumption divided by the total fluid intake. To test the degree of CTA extinction, six to seven choice tests, distributed over a period of 30 days, were initially carried out. For the analysis of the NEP deficient mice, forced extinctions were further performed during the 34th and the 42nd day of the test and choice tests on day 35, 43 and 44. Finally, to test for possible changes of an unconditioned, intrinsic aversion, the mice were given a choice to drink either a bitter tasting quinine (Fluka Chemie, Buchs, Switzerland) solution (0.02%) or water.

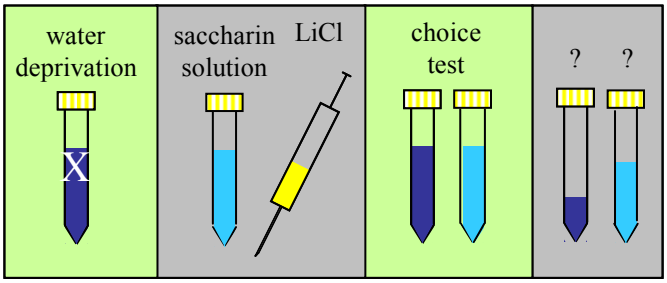

Figure 11. Conditioned taste aversion procedure. On the conditioning day, water-deprived mice were allowed to drink a saccharin solution before injection of LiCl, a nausea-inducing agent. Two days later, the first choice test between saccharin and water solution took place and the percentage of saccharin consumption calculated.

6.3.2 Morris water maze

Spatial learning and memory were assessed in a Morris water maze task [482] adapted for mice. In brief, the testing was done under 12 lux diffuse light in a circular arena made of white polypropylene (diameter 150 cm, wall height 50 cm), filled with water (made opaque by the addition of milk) to a height of 16 cm and maintained at 24–26 °C (Fig. 12). Extra-maze visual cues around the room remained in fixed positions throughout the experiment and a 14 × 14 cm target platform of white wire mesh was placed 0.5 cm below the water surface in the NW, NE, SE or SW quadrant at 35 cm from the wall. Each mouse was first trained for 2 days with 6 trials per day to find a visible platform located at different positions for each trial (12 trials, 120 s for each). Then, the platform was hidden at a constant position for 4 days with 6 trials per day separated by 30 to 60 min intervals and lasting maximally 120 s. This acquisition phase was followed by a probe trial of 60 s where the platform was removed and the spatial retention of the mice was assessed.

Swimming animals were tracked using a Noldus EthoVision 3.0 video-tracking system (www.noldus.com) at 576 × 768 pixel spatial resolution and 4.167 Hz sampling frequency. Raw XY coordinates were transferred to custom-developed public domain software Wintrack [483] (www.dpwolfer.ch/wintrack) for further analysis. The trials were averaged in blocks of two trials and different measures were calculated to assess acquisition and spatial selectivity including escape latency, percentage of time in the goal or opposite quadrant and proximity to the platform.

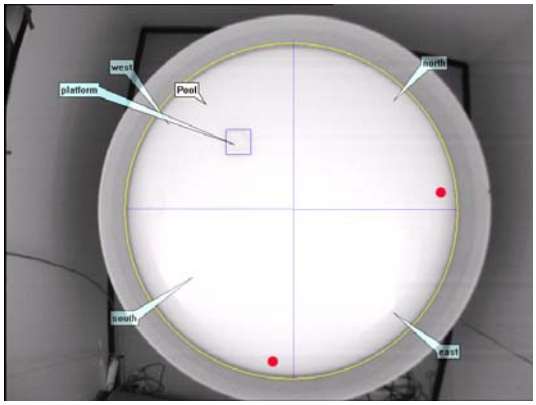

Figure 12: Morris water maze arena. The mice are inserted in the water maze at different positions (red dots) and use external visual clues to find a visible or hidden platform (scare). Latencies of the mice to reach the platform and their ability to remember the platform position allow investigation of the mouse spatial learning and memory.

6.3.3 Puzzle box

This paradigm is adapted from a burrowing task developed in rats [484]. The apparatus is a 73 cm long, 28 cm wide and 27.5 cm high box, divided by a removable barrier into a small dark goal box (14 cm long) containing sawdust and cardboard shapes and a large brightly lit (1,000 lux by two spot lamps) start box (58 cm long). There is a 4 cm wide, 2 cm deep and 15 cm long underpass in the centre of the barrier (Fig. 13). The mice were tested during 3 consecutive days for their ability to enter in the dark protected area through an open door or an underpass (training session), the same entrance blocked by either sawdust (burrowing puzzle) or a T-shaped cardboard plug (plug puzzle). The mice performed 3 trials per day with an intertrial interval of about 1 min. For each trial, the mouse was placed in the start box facing the wall opposite to the goal box and the latencies to enter the protected area was measured with a maximum of 3 min. Mice were allowed about 20 s in the goal box and moved to their home cage. During the first day, the mice were trained to enter the goal box through an open door (trial one) then through an underpass (trial 2 and 3). During the second day, the underpass giving access to the goal box was accessible during the first trial and filled with sawdust during the second and third trial. On day three, the goal box was accessible through the underpass for the first trial and blocked by a 2 g cardboard object during the second and third trial.

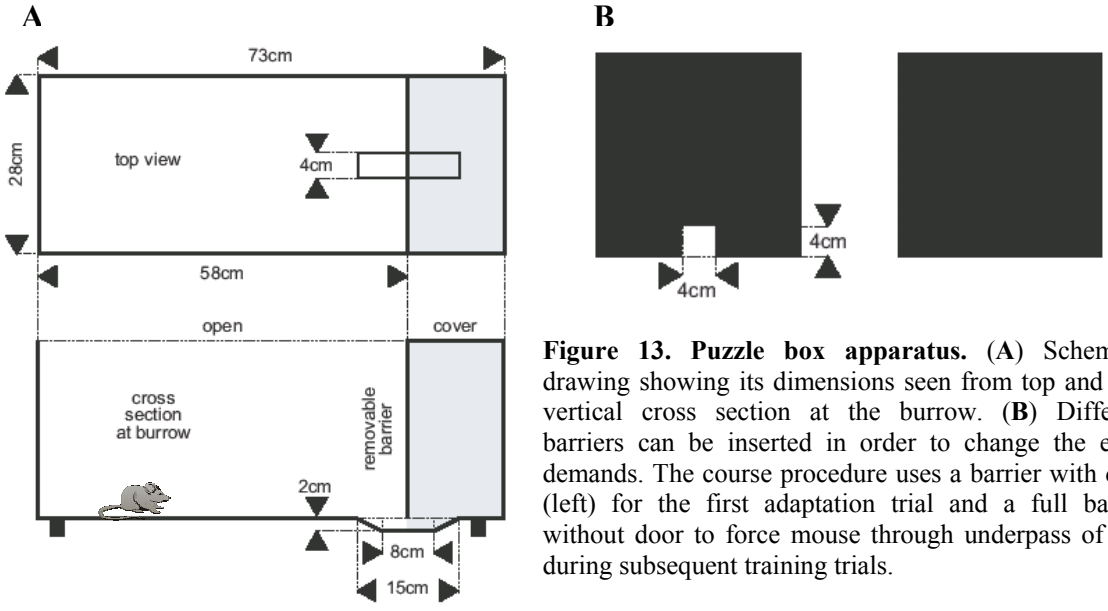

Figure 13. Puzzle box apparatus. (**A**) Schematic drawing showing its dimensions seen from top and in a vertical cross section at the burrow. (**B**) Different barriers can be inserted in order to change the entry demands. The course procedure uses a barrier with door (left) for the first adaptation trial and a full barrier without door to force mouse through underpass of box during subsequent training trials.

6.3.4 Y-maze

To determine spontaneous alternation behavior (measure of spatial working memory), the mice were tested in a Y-maze with 40 cm long, 10 cm wide and 20 cm high arms (Fig. 14). Each mouse received one trial during which it was placed at the end of one of the three arms and allowed to explore the maze for 5 min. Alternations and total numbers of arm entries were recorded. Spontaneous alternation, expressed as percentage, refers to the ratio of arm choices differing from the previous two choices, to the total number of arm entries. Arm entry was considered to be completed when the hind paws of the mouse had been completely placed in the arm.

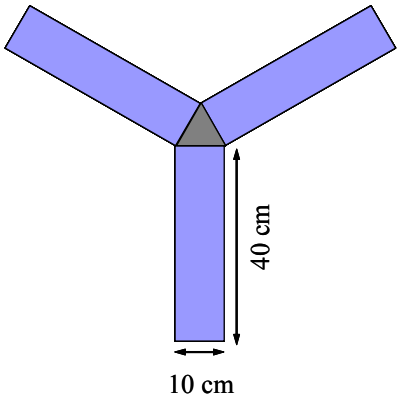

Figure 14. Y-maze paradigm. To test spontaneous alternation behavior, mice were placed at the end of one of the three arms and allowed to explore the maze for 5 min. Alternation was recorded.

6.3.5 Eight arm radial maze

10 WT and 12 NEP mice of the 7 months cohort were tested in this working memory paradigm. The maze, consisting of 8 arms of grey poly-vinyl chloride (7x38 cm) with clear Perspex sidewalls (5 cm high) extended from an octagonal centre platform (diameter 18.5 cm, distance platform centre to end of arm 47 cm), was placed 38 cm above the floor (Fig. 15) in a dimly lit room (four 40W bulbs, 12 lux) rich in extramaze cues. Small cereal pellets (ca. 6 mg) were placed as baits in small metal cups (diameter 3 cm, 1 cm deep) located at the end of the arms, such that the mouse could not see them without completely entering the arm. A reversed box of clear Perspex served to confine the mouse on the centre platform before each test session. The body weight of the mice was gradually reduced to and maintained at 85% of their free-feeding body weight by allowing them to eat a premeasured amount of chow each day. Water was available at libidum. Mice began with two habituation sessions during which they were accustomed to collecting pellets that were distributed all over the maze. For each training trial, all arms were baited with a single pellet. For 10 days each mouse performed one trial per day lasting maximally 10 min or until the animal had collected all pellets. The ability of the mice to remember which pellets they have already removed is quantified by counting the number of pellets they remove during their first 8 choices and the number of reentry errors.

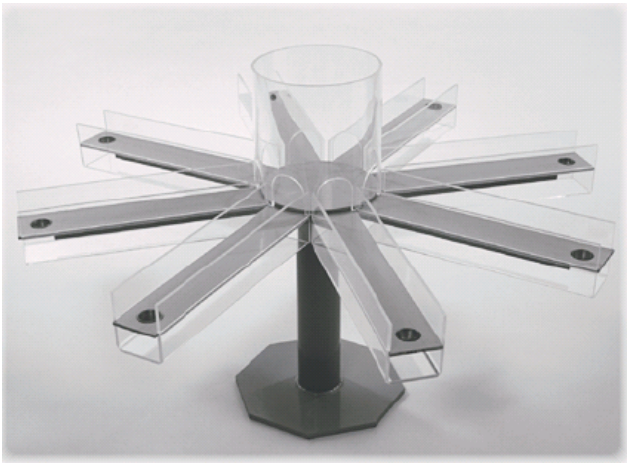

Figure 15. Eight arm radial maze. Each arm is baited with a single food pellet. Mice are inserted in the middle and allowed to visit the arms. The working memory of the mice is determined based on their ability to remember the arms already visited and to remove the food pellets in the most efficient way.

6.3.6 Fear conditioning test

The conditioning chamber consisted of a gray opaque box (16.5x25 cm) with a grid floor through which electric shocks could be delivered (0.15 mA) as the unconditioned stimulus (US). The chamber was placed into a dimly lit sound-attenuating box with a speaker on top delivering a 92 dB/2,000 Hz tone as the conditioned stimulus (CS). To quantify freezing as the conditioned reaction, a grid of photobeams (1x1 cm) detected the inactivity of the mice, which was defined as no photobeam breaks for at least 2 s. During the conditioning session, a 1 min adaptation period in the box was followed by three identical conditioning trials, each trial consisting of 30 s CS presentation, with the US being applied during the last 2 s of the CS, separated by an intertrial interval of 30 s. 24 h after the conditioning session, retrieval tests for context conditioning and, 2 h later, for conditioning to tone were carried out by recording freezing as mentioned above. To evaluate context conditioning, mice were placed for 2 min in the conditioning chamber. To evaluate conditioning to tone, the physical characteristics of the chamber were changed (shape, light, smell, and bedding material). Each mouse was then placed for 2 min into this new chamber, and the CS was presented (Fig. 16).

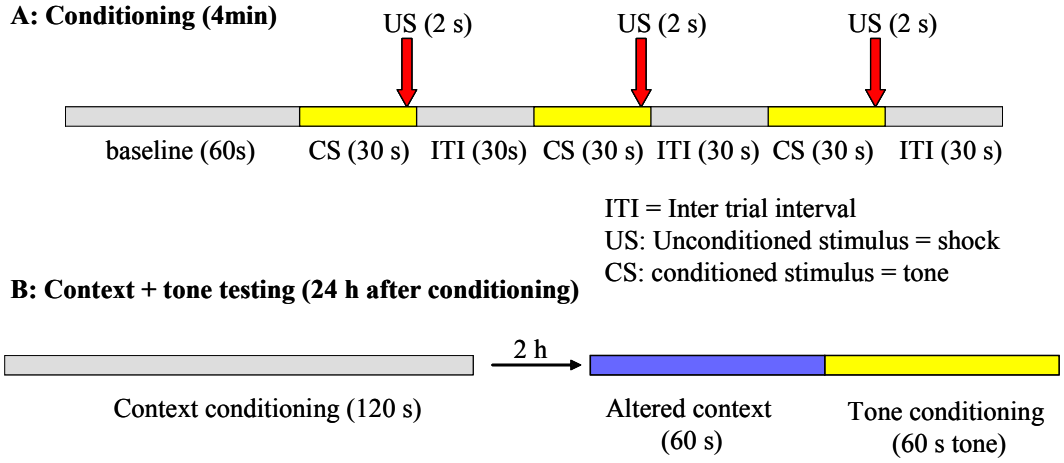

Figure 16. Schematic representation of the fear conditioning protocol. (**A**) During conditioning, a 60 s adaptation period was followed by three conditioning trials consisting of 30 s shock with the tone being applied during the last 2 s, separated by 30 s intertrial intervals of 30 s. Freezing time was used to evaluate the fear conditioning. (**B**) The next day, conditioning to context was assessed by bringing the mouse in the conditioning chamber. Tone conditioning was performed in a totally different and the tone presented.

6.4. Motor and sensory function

6.4.1 Rotarod

The accelerating rotarod 7650 (Ugo-Basile) for mice was used. Five subjects were tested concurrently and placed on the rotating drum at a baseline speed of 4 rpm (Fig. 17). During the 5 min observation period speed increased linearly to 40 rpm. Mice were given 5 trials with an intertrial interval of 30 min. To distinguish dyscoordination and fatigue, mice were also given 5 trials of 5 min with the drum rotating at a constant low speed permitting all mice to maintain their balance.

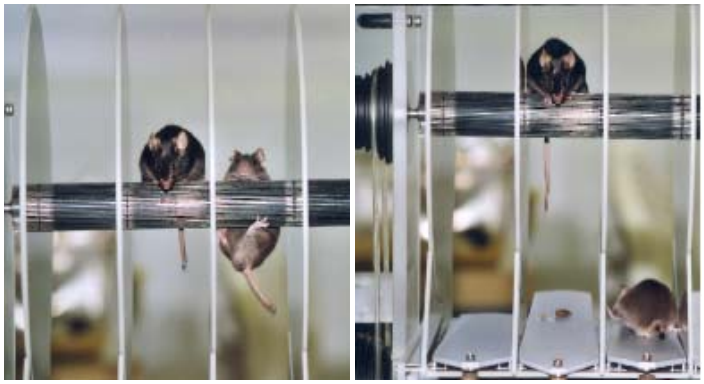

Figure 17. The accelerating rotarod. The mice are placed on a rotating drum at the lowest speed. The rod is then switched to acceleration mode and the time on the rod is recorded for 5 min maximum.

6.4.2 Hotplate

The animals were placed in a transparent cylinder of 20 cm diameter and 30 cm hight, on a hot plate, equilibrated at 52 °C 30 min before testing (Fig. 18). The latency of the first appearance of signs of discomfort (lifting and licking a paw, hopping, or jumping) was recorded and terminated the trial.

Figure 18. Hotplate. The mouse is placed on a 52°C plate and the latency for the first appearance of signs of discomfort is recorded.

6.5 Video tracking

During exploration tests, animals were video-tracked with an electronic imaging system (EthoVision 3.0, Noldus Information Technology) at a frequency of 4.2 Hz and a spatial resolution of 256x256 pixels. For each sample, the system recorded xy positions, object area, and the status of defined event recorder keys on the keyboard. Raw data were then transferred to public domain software Wintrack 2.4 for further analysis, www.dpwolfer.ch/wintrack [483].

7) Statistical analysis

Student's *t*-tests were performed comparing *in vitro* effect of Aβ on luciferase activity triggered by neprilysin promoters.
Other biochemical data were analyzed by non-parametric Mann-Whitney U tests when only comparing two groups or one way ANOVA.

Behavioral data were collected by investigators unaware of the genotype of the mice and between-group comparisons were analyzed using a one way analysis of variance (ANOVA) or a two way ANOVA and repeated measures with time or observation included as a within-subject factor when appropriate. Computations were done using Statview 5.0 (www.statview.com). Significant main effects of genotype were further analyzed post hoc with Games/Howell test for the CTA and Fisher's PLSD for the others. Significance of correlations was determined using Fisher's r to z test. A p-value of <0.05 was considered as being significant and data are presented in all graphs as means ± standard error.

III) RESULTS

1) Consequences of neprilysin deficiency in mice

1.1 AD-like amyloidosis in NEP deficient mice

We determined at an age of 18 months, the brain levels of murine Aβ of mice with targeted deletion of one (NEP+/-) or both NEP alleles (NEP-/-) and compared them to the corresponding levels of the WT littermates. A dose dependent neprilysin enzymatic activity was first confirmed in NEP deficient mice for both or one NEP alleles compared to WT littermates (Fig. 1A). The addition of a neprilysin inhibitor, thiorphan, allowed the determination of specific neprilysin activity. Neprilysin activity was significantly reduced by thiorphan in WT and NEP+/- mice brains ($p=0.004$ and $p=0.007$, respectively) but did not change in NEP-/- mice brains confirming that no active neprilysin was present in the brain of NEP-/- mice (Fig. 1A).

As a consequence of decreased neprilysin activity, quantification of total brain murine Aβ levels showed a significant two fold increase in the NEP+/- and NEP-/- mice when compared to their age-matched WT littermates, with similar levels between NEP-/- and NEP+/- mice (1-way ANOVA genotype $p<0.0004$; NEP-/- versus WT $p<0.0005$, NEP+/- versus WT $p<0.0044$, NEP-/- versus NEP+/- ns) (Fig.1B).

We next analyzed whether high levels of Aβ in the NEP deficient brains may be caused by the presence of higher levels of APP protein. Western blotting with an antibody recognizing murine APP revealed no changes in the amount of full length APP in frontal brains of the NEP deficient mice (Fig. 1C).

To further investigate if increase of murine Aβ levels could lead to plaque formation, one of histological AD hallmark, brain paraffin sections were stained with the anti-murine Aβ antibody 4G8. At 18 months of age, numerous amyloid-like deposits were found in the hippocampus of all NEP mutant mice (Fig. 1E,F, G, arrows) whereas these deposits were found in much lesser numbers only in some of the WT littermates (Fig. 1D). Further investigation by electron microscopy confirmed the presence of electron dense deposits (Fig. 2A, circled) surrounded by a membrane in enlarged nerve fibers of aged NEP-/- mice but not in aged-matched WT littermates.

High resolution electron microscopy revealed the fibrillar structure of these amyloid-like fibrillar deposits. Careful examination of 25 such fibrils revealed an average diameter of 10-12 nm and a length of approximately 100 nm (Fig. 2B, 2C, arrows). Moreover, loosely compacted degenerating myelin sheets (Fig. 2A, D, open arrows) were present in both close vicinity to electron dense deposits (Fig. 2A, circled) and in no obvious proximity to such deposits (Fig. 2D) in hippocampi of the aged NEP-/- mice. Taken together, these data indicate that insufficient NEP expression can lead to biochemical and morphological alterations reminiscent of AD-amyloidosis in mice.

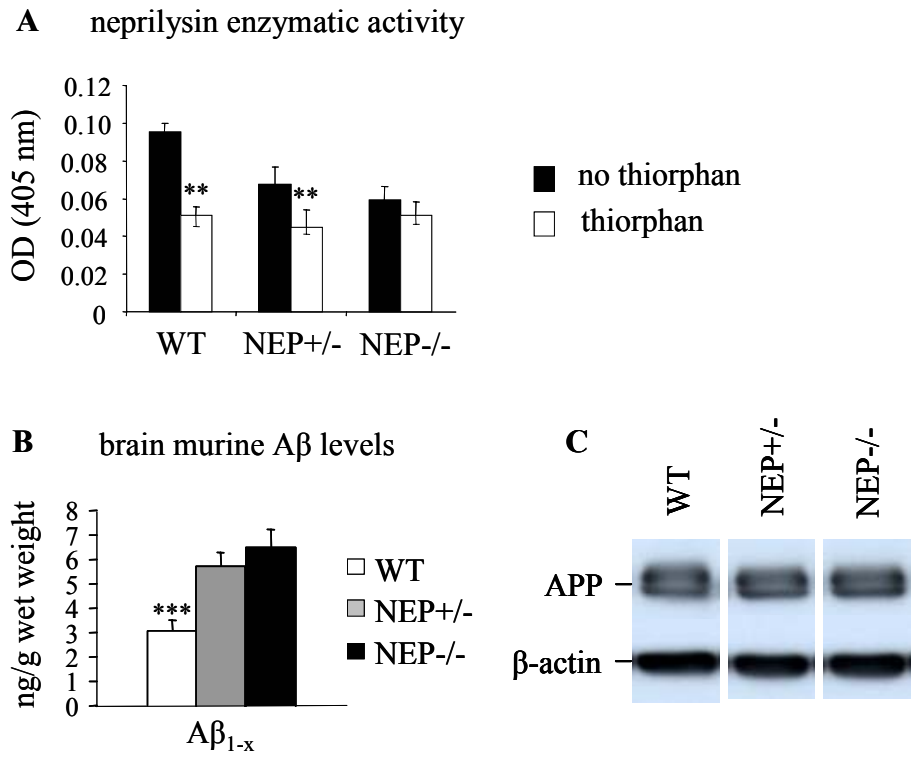

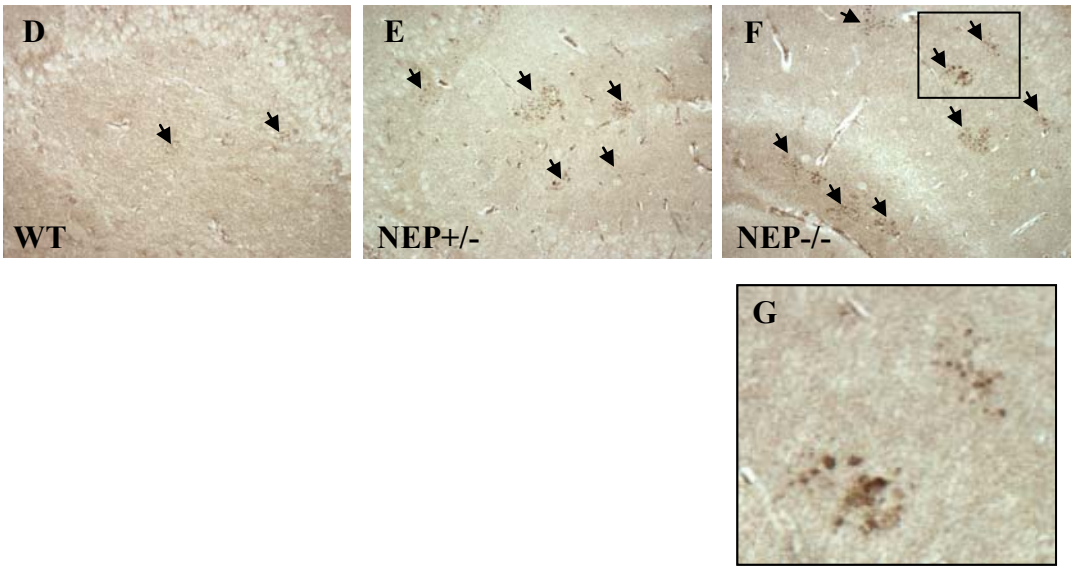

Figure 1. NEP depletion caused AD-like amyloidosis. (**A**) Neprilysin enzymatic assay with or without the specific inhibitor of neprilysin, thiorphan confirmed the absence of neprilysin activity in NEP-/- mice and the dose dependent activity in NEP+/- and WT mice. (**B**) Total brain murine Aβ levels were significantly increased in NEP+/- and NEP-/- compared to their WT littermates. (**C**) Western blot analysis of frontal brain showed no alteration of full length APP protein levels in NEP deficient mice compared to their WT controls. β-actin was used as a loading control. Numerous deposits recognized by the murine Aβ specific antibody 4G8 (arrows) were found in hippocampus of aged NEP+/- (**E**) and NEP-/- mice (**F**) whereas these immunoreactive structures were only occasionally found in the WT mice (**D**).

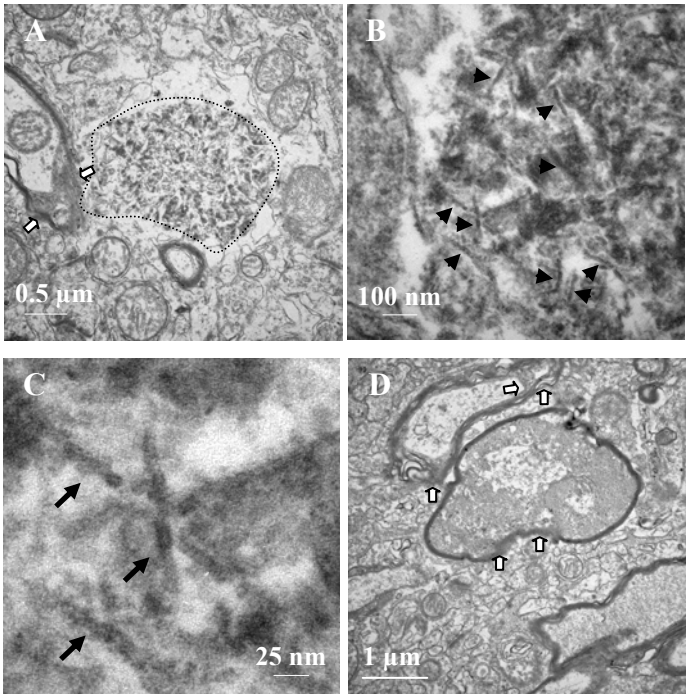

Figure 2. Electron microscopy analysis (**A**) Transmission electron microscopy of brains of aged NEP-/- mice revealed the presence of electron dense deposits (circled by dashed line) within enlarged axons. (**B**, **C**) At higher

magnifications these deposits exhibited a fibril like structure with an average diameter of 10-12 nm and a length of approximately 100 nm (black arrows). (**D**) Un-compacted, degenerating myelin sheets (arrow heads, also in A) were found in hippocampi of NEP-/- mice on electron microscopy level.

1.2 Learning impairment of NEP deficient mice in CTA

The three groups (10 NEP-/-, 7 NEP+/-, 8 WT, age 93.8 ± 0.8 weeks) were analyzed for their associative memory in the conditioned taste aversion test. NEP-/- and NEP+/- mice did not significantly differ from their WT littermates in body weight (Fig. 3B) and amount of water consumed during adaptation ($p=0.80$ and 0.88), respectively. However, NEP-/- mice drank slightly but not significantly more of the saccharin solution during conditioning than WT mice with the data of the NEP+/- mice lying in between ($p=0.078$). Mice of all three genotypes drank similar amount of saccharin during the conditioning day and developed a strong aversion against saccharin after a single conditioning trial. The memory of the aversive taste was measured up to 44 days following the saccharin-LiCl pairing (Fig. 3A). All mice avoided saccharin without extinction across the repeated choice sessions and retained constant aversion to saccharin for at least 29 days. The average saccharin intake during the first choice tests and at day 8 and 9 was significantly higher in both NEP+/- and NEP-/- mice compared to WT littermates (2-way ANOVA: genotype $p<0.0469$, day ns, interaction ns; -/- versus WT $p<0.0457$, +/- versus WT $p<0.0223$; -/- versus +/- ns) indicating that NEP+/- and NEP-/- mice were impaired in taste aversion. A subset of animals (6 NEP-/-, 6 NEP+/-, 3 WT) performed further choice tests after two forced extinction trials with only saccharin available at days 34 and 42 for 2 h. The aversion against saccharin was significantly weaker in NEP-/- and NEP+/- mice than in WT littermates during the following repeated choice tests (genotype $p<0.0231$; post-hoc Games/Howell) with no difference between the NEP+/- and the NEP-/- mice (Fig. 3A). In contrast to the conditioned aversion, all groups showed similar spontaneous quinine aversion ($p=0.937$) (Fig. 3C), suggesting that taste sensitivity was not altered.

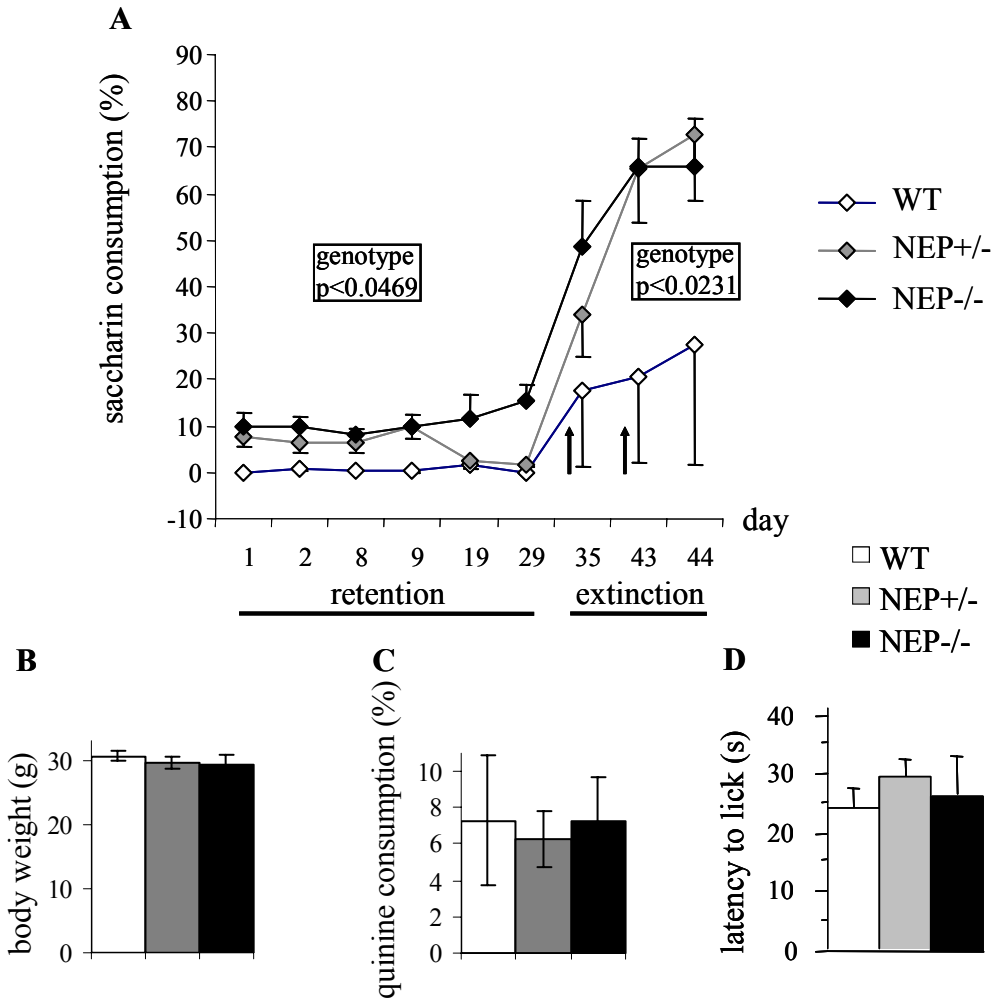

Figure 3. Aged NEP deficient mice showed impaired learning in the CTA. (**A**) Percentage of saccharin consumption is depicted for 9 choice tests over a 44 days period. All animals acquired a strong conditioned taste aversion but NEP+/- and NEP-/- mice drank significantly more saccharin during the first choice test compared to their WT littermates and present a significant learning deficit. Memory was not affected by the genotype prior to forced extinction (arrows) but NEP deficient mice presented a significant decreased aversion against saccharin compared to WT littermates after forced extinction. (**B**) The body weight of the mice was similar between the three groups. (**C**) No genotype effect was observed in avoidance of a bitter tasting quinine solution. (**D**) Hot plate analysis showed similar pain sensistivity for all three groups. Values are ± SEM.

2) Determination of an *in vitro* model to reproduce and investigate the pathway(s) involved in the Aβ-related increase of neprilysin transcription *in vivo*

2.1 Determination of the $A\beta_{1-42}$ incubation time and concentration required

Because of high neprilysin expression in kidney, the role of $A\beta_{1-42}$ in neprilysin transcription was first investigated in human embryonic kidney 293T cells.

After transfection for 5 h with plasmid expressing firefly luciferase under the control of one of the three neprilysin promoters PN1, PN2 and PN3, the transcriptional activity of the three promoters and their regulation by different incubation time with 5 µM aggregated $A\beta_{1-42}$ or PBS were analyzed (Fig. 4). All three promoters were activate and produced luciferase proteins as early as 17 hours after transfection (5 hours of transfection followed by 12 hours incubation with fresh medium containing $A\beta_{1-42}$). Luciferase activity constantly increased during the first 48 h of incubation (Fig. 4) and the increase of luciferase activity under the control of the PN2 promoter still doubled between 48 and 72 h (not shown), suggesting a high stability of luciferase and a slower degradation than production of luciferase. Once normalized with the protein concentration of the lysed cells, PN2 promoter presented the highest level of activation followed by the PN3 and PN1 promoters. A significant 25% increase of luciferase activity under the control of the PN3 promoter was found after 24 h of $A\beta_{1-42}$ incubation (t-test, p=0.0144) and activity of the PN1 promoter was 38% increased after 48 h of $A\beta_{1-42}$ incubation (t-test, p=0.0009). However, 48 h incubation led to overgrowth of the 293T cells and to a potential toxicity of the medium.

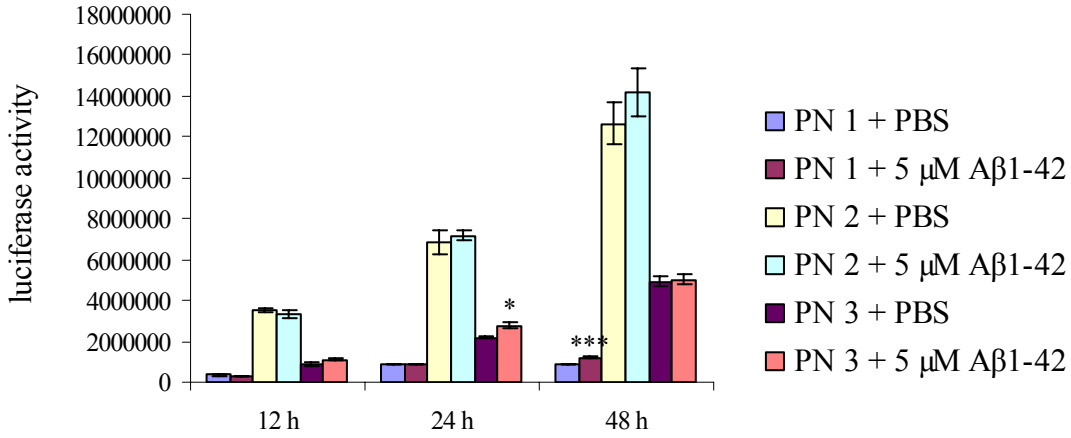

Figure 4. Time point analysis of neprilysin promoters activity after Aβ incubation. 293T cells, transfected with plasmid expressing firefly luciferase under the control of one of the three promoters of neprilysin, PN1, PN2 and PN3, were incubated with 5 µM aggregated $A\beta_{1-42}$ during 12, 24 and 48 h. Luciferase activity was normalized with the protein concentration of the cell lysate. Luciferase activity driven by the promoter PN3 and PN1 was significantly increased after 24 h and 48 h Aβ incubation, respectively. *: $p \leq 0.05$, ***: $p \leq 0.0001$.

To determine the best incubation time and concentration of $A\beta_{1-42}$, a time course analysis was further performed on the promoter PN2 activity with PBS, 5 µM or 15 µM of aggregated $A\beta_{1-42}$ during 12, 24 or 38 h incubation time (Fig. 5A). Incubation during 24 h with 15 µM $A\beta_{1-42}$ induced a significant 50% increase luciferase activity (t-test, p=0.0003), while other time points and concentration did not significantly change the promoter activity ($p \geq 0.1$). Such incubation with 15 µM aggregated $A\beta_{1-42}$ (Fig. 5C) did not modify the trypan blue staining of the cells compared to cells treated with same amount of PBS (Fig. 5B), suggesting the absence of obvious cytotoxicity after 24 h. Incubation with 15 µM $A\beta_{1-42}$ during 24 h appeared to be the best parameters in our model.

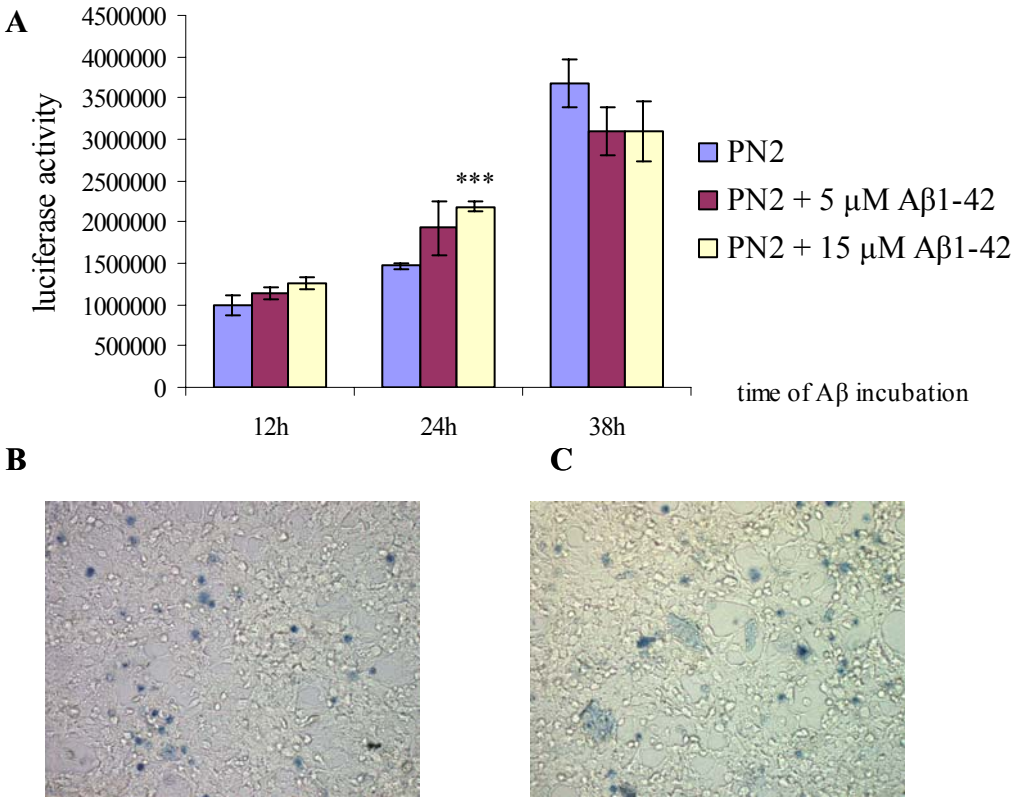

Figure 5. Time point and $A\beta_{1-42}$ concentration determination. (**A**) 24 h of incubation with 15 µM $A\beta_{1-42}$ significantly increased luciferase activity and therefore the activation of the neprilysin promoter PN2. ***: $p \leq 0.0001$. Trypan blue staining of 293T cells transfected with PN2 and incubated with either PBS (**B**) or 15 µM $A\beta_{1-42}$ (**C**) for 24 h did not show signs of cytotoxicity.

2.2 $A\beta_{1-42}$ did not regulate neprilysin expression in HEK 293T cells

The effect of 15 µM $A\beta_{1-42}$ on the activation of PN1, 2 and 3 was investigated in 293T cells. However, the results were not constantly reproducible (Fig. 6). Two experiments testing the effect of 24 h incubation with 15 µM $A\beta_{1-42}$ or PBS on the regulation of neprilysin promoters' activation were done simultaneously using similar material and methods. The first experiment showed a significant increase of the luciferase activity and therefore promoter activation for all three promoters with 55% (p=0.016), 43% (p=0.003) and 60% (p=0.0005) increases for PN1, PN2 and PN3-related activity, respectively (Fig. 6A). This $A\beta_{1-42}$-related increase of neprilysin promoter activation was not reproduced in the second experiment (Fig. 6B).

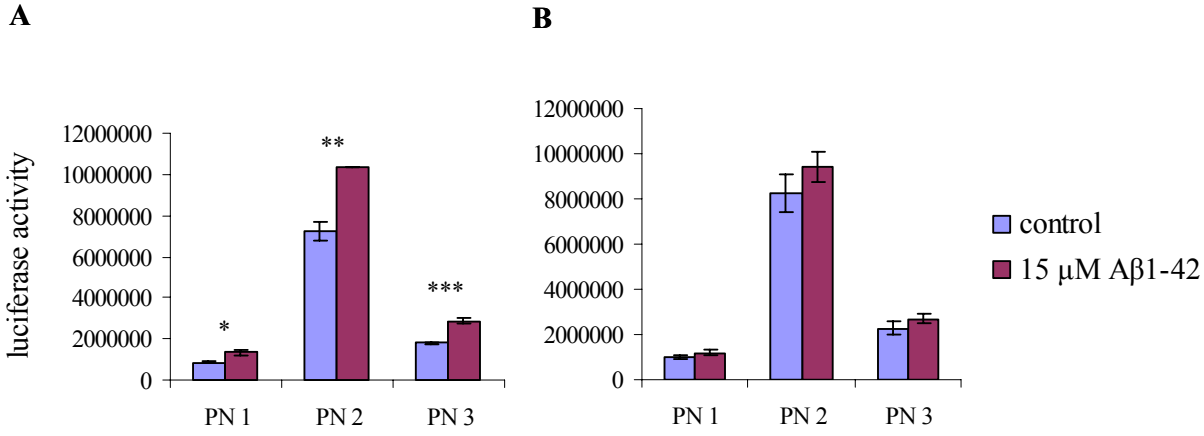

Figure 6. Inconsistency in Aβ-related increase of neprilysin promoter activation. Two experiments were performed at the same time and show a significant (**A**) and a non-significant (**B**) effect of 24 h incubation with 15 µM $A\beta_{1-42}$ on the activity of the three neprilysin promoters, PN1, PN2 and PN3. *: $p \leq 0.05$, **: $p \leq 0.001$, ***: $p \leq 0.0001$.

We further tested the effect of 24 h incubation with 15 µM aggregated $A\beta_{1-42}$, $A\beta_{42-1}$ or PBS as a control on neprilysin promoter activity. Again, Aβ incubation did not significantly increased the activity of any of the promoter (Fig. 7) and even decreased significantly the luciferase activity after incubation with 15 µM $A\beta_{42-1}$ compared to PBS incubation (t-test $p \leq 0.0001$).

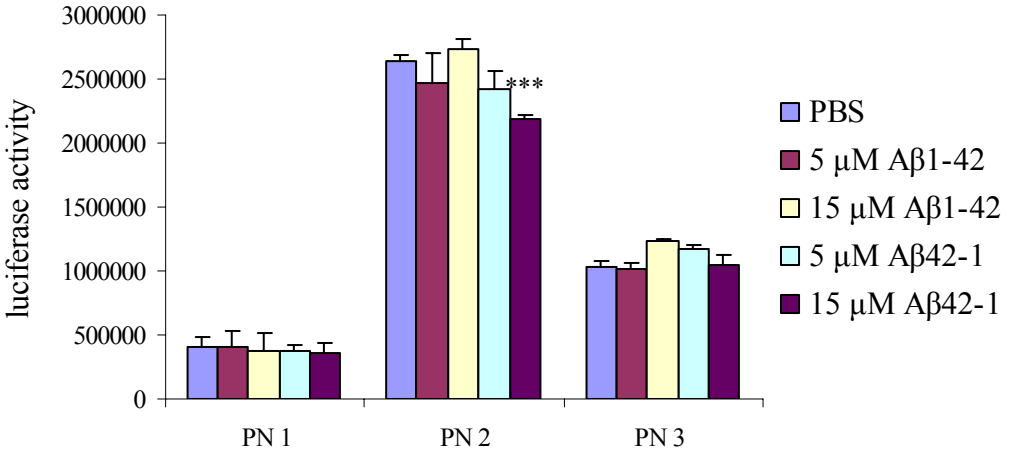

Figure 7. Aβ incubation did not increase the activation of any of the three neprilysin promoters. After transfection with plasmids expressing luciferase under the control of one of the three neprilysin promoters, PN1, PN2 or PN3, 293T cells were incubated during 24 h with PBS, $A\beta_{1\text{-}42}$ or $A\beta_{42\text{-}1}$. 24 h incubation with 5 µM and 15 µM $A\beta_{1\text{-}42}$ did not increase the luciferase activity controlled by any of the three neprilysin promoters. ***: $p \leq 0.0001$.

To eliminate the potential variability due to transfection efficiency, we used the newly-released dual luciferase assay system, which allowed the normalization of the firefly luciferase activity controlled by the neprilysin promoters with the activity produced by another plasmid transfected at the same time which expressed the renilla luciferase. The efficiency of the new kit was tested and showed that the luciferase activity detected was lower than the original luciferase assay kit. However, because of specific buffers used in the dual luciferase assay system, the renilla luciferase activity did not cross-react with the firefly luciferase activity and allowed a more accurate normalization of the results than protein concentration. 24 h incubation with 15 µM $A\beta_{1\text{-}42}$ on 293T cells did not increase neprilysin promoter activation when the new kit was employed (Fig. 8).

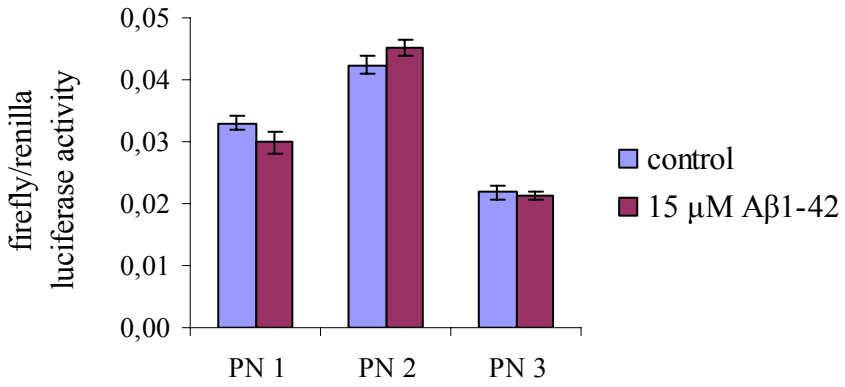

Figure 8. Absence of Aβ effect on neprilysin promoter activation in 293T cells. After 24 h incubation, The new dual luciferase assay system was used to investigate the effect of $A\beta_{1\text{-}42}$ on the activation of the neprilysin promoters PN1, PN2 and PN3, which control the expression of firefly luciferase. Firefly luciferase activity was normalized by renilla luciferase activity and Aβ did not modify the activation of any of the three neprilysin promoter.

2.3 $A\beta_{1\text{-}42}$ did not regulate neprilysin expression in undifferentiated SH-SY5Y cells

Brain injection of $A\beta_{1\text{-}42}$ increased neprilysin protein levels in neurons as determined by immunohistochemistry approach [406], suggesting that the observed increase of transcription may be mainly present in neurons. Therefore, we tested whether Aβ could affect neprilysin expression in SH-SY5Y cells which can be differentiated into neurons.

SH-SY5Y cells transfected with a plasmid expressing firefly luciferase under the control of any of the three neprilysin promoters showed a much lower level of luciferase activity compared to 293T cells. These low levels of luciferase activity were not detectable with the dual luciferase reporter assay system.

24 h incubation with 15 µM $A\beta_{1\text{-}42}$ did not alter the luciferase activity produced by the activation of the three neprilysin promoters (Fig. 9). Undifferentiated SH-SY5Y cells did not reproduce the $A\beta_{1\text{-}42}$-related increase of neprilysin transcription observed *in vivo*.

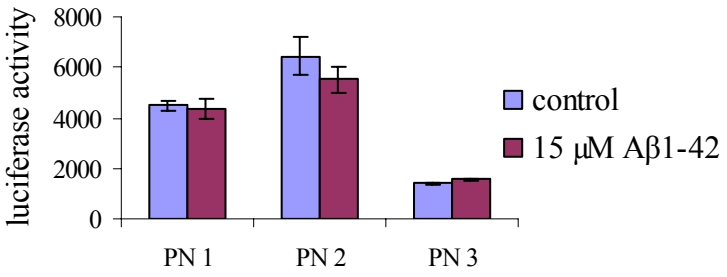

Figure 9. Effect of $A\beta_{1-42}$ on neprilysin promoters' activity in SH-SY5Y cells. After transfection with a plasmid expressing firefly luciferase under the control of one of the three neprilysin promoters, PN1, PN2 and PN3, 24 h incubation with $A\beta_{1-42}$ did not increase neprilysin promoters' activity in undifferentiated SH-SY5Y cells.

2.4 Differentiation of the SH-SY5Y cells induced increase of neprilysin expression

To assess the effect of $A\beta_{1-42}$ on differentiated SH-SY5Y cells, we first analyzed the effect of RA, the first SH-SY5Y differentiating agent, on the activity of the three promoters. Treatment with 10 μM RA for 24 and 72 h significantly increased the luciferase activity, indicating an increased activation of PN1, PN2 and PN3 promoters by RA. We observed a 6.2, 3.5 and 3.7 fold increase after 24 h and 23, 16 and 13 fold increase after 72 h when compared to sister cultures without RA incubation (all $p<0.003$) (Fig. 10). The luciferase activity was normalized by the protein concentration of the cell lysate. The high increase of luciferase activity after RA incubation and the potential related variability between wells caused by differentiation of the SH-SY5Y cells within 5 days suggested that this protocol was not suitable to study the potential small effect of $A\beta_{1-42}$ on the neprilysin promoters' activity.

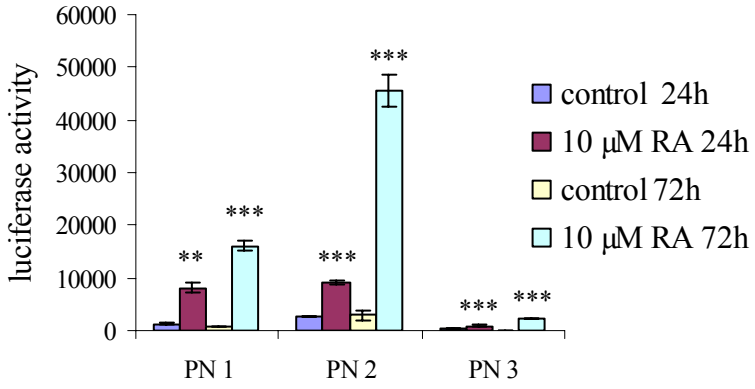

Figure 10. all trans retinoic acid (RA) increased neprilysin promoter activity in SH-SY5Y cells. 24 h and 72 h incubation with the differentiating agent, RA, induced high increases of the firefly luciferase activity controlled by any of the three neprilysin promoters, PN1, PN2 and PN3. **: $p \leq 0.001$, ***: $p \leq 0.0001$.

2.5 No involvement of a microglia diffusible factor in $A\beta_{1-42}$ mediated neprilysin expression *in vitro*

To test the involvement of a potential diffusible factor from the microglia, a human microglia cell line, MIC cells [476], were incubated with 15 μM $A\beta_{1-42}$ or PBS for 48h. The medium containing the factors secreted by the MIC cells was then removed, diluted twice with pre-warmed 293T cells medium. On parallel, 293T cells were grown for 48h and their medium treated similarly. 293T cells transiently transfected with a plasmid containing one of the neprilysin promoter expressing firefly luciferase were then incubated with the 1:1 diluted medium of either the treated MIC cells or the 293T cells. No difference in the luciferase activity was observed between the 293T cells which received the 293T cell medium and medium from the Aβ-treated and untreated MIC cells (Fig. 11).

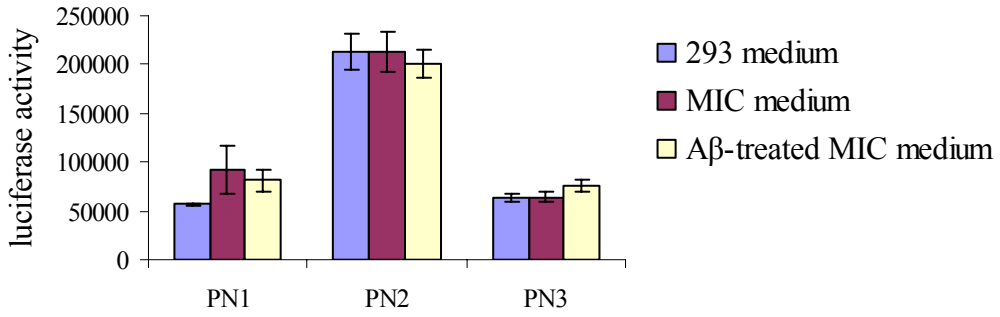

Figure 11. MIC medium from MIC cells treated or not with 15 µM Aβ did not affect neprilysin promoter activation in 293T cells. MIC cells were incubated with PBS or 15 µM $A\beta_{1-42}$ during 48 h and 50% of the medium from 293T cells, which were previously transfected with a plasmid expressing luciferase under the control of one of the three neprilysin promoter PN1, PN2 and PN3, was replaced by MIC conditioned medium. To control for the effect of the MIC medium on neprilysin transcription, the medium from non-treated 293T cells was also tested. The medium did not affect the neprilysin promoter activation.

2.6 $A\beta_{1-42}$ induced increased brain neprilysin protein level

Due to the lack of effect *in vitro*, a group of aged SweAPP mice was either not injected (n=4) or intracranialy injected with 1 µl 350 µM stock concentration fibrillar $A\beta_{1-42}$ (n=5) or $A\beta_{42-1}$ (n=6) to investigate which neprilysin promoter was activated *in vivo*. 20 weeks after injection, brain neprilysin protein and mRNA levels were investigated by Western blot and RT-PCR analysis, respectively. Uninjected and $A\beta_{42-1}$ injected mice exhibited low levels of neprilysin protein in brain homogenates (not shown). In contrast, mice injected with $A\beta_{1-42}$ exhibited a marked elevation of neprilysin levels (Fig. 12A), reproducing our previous data [406].

2.7 No variation of brain neprilysin mRNA 20 weeks after $A\beta_{1-42}$ injection

To determine if the increase of neprilysin levels observed was associated with increased transcription, total mRNA from the same mouse brains was purified, the RNA integrity confirmed and neprilysin mRNA levels quantified with specific primers recognizing total neprilysin mRNA by RT-PCR. With a normalized abundance of 1.0 ± 0.15, 1.8 ± 0.24 and 1.0 ± 0.47 for non-injected, $A\beta_{42-1}$ and $A\beta_{1-42}$ injected groups, the level of total neprilysin mRNA was not significantly changed when comparing the $A\beta_{1-42}$ injected group to the uninjected or the $A\beta_{42-1}$ injected control groups (Fig. 12B).

To further investigate if Aβ injection could specifically act on one of the three major neprilysin promoters, RT-PCR on the samples from injected mice was performed using specific primers for transcripted but non-coding exon 1, 2 and 3. Similarly, with normalized abundance of 1.0 ± 0.48 and 0.61 ± 0.05 for exon 1, 1.0 ± 0.60 and 0.87 ± 0.26 for exon 2 and 1.0 ± 0.27 and 1.89 ± 0.79 for exon 3, levels of $A\beta_{42-1}$ and $A\beta_{1-42}$ neprilysin mRNA were similar (Fig. 12C). Therefore, no variation of neprilysin mRNA levels was observed when comparing the $A\beta_{1-42}$ and $A\beta_{42-1}$ injected group in spite of a clear overexpression of the neprilysin protein level. All primers were tested in absence of DNA for potential artifacts due to dimerization. No background signal was detected. Primers and quencher sequences were also blasted against the entire mouse genome for potential homologies with other murine cDNA sequences. Their specificity was confirmed. The specificity of the sequence and lack of homology was confirmed by blasting the primer sequences against the mouse genome (http://www.ncbi.nlm.nih.gov/genome/seq/MmBlast.html)

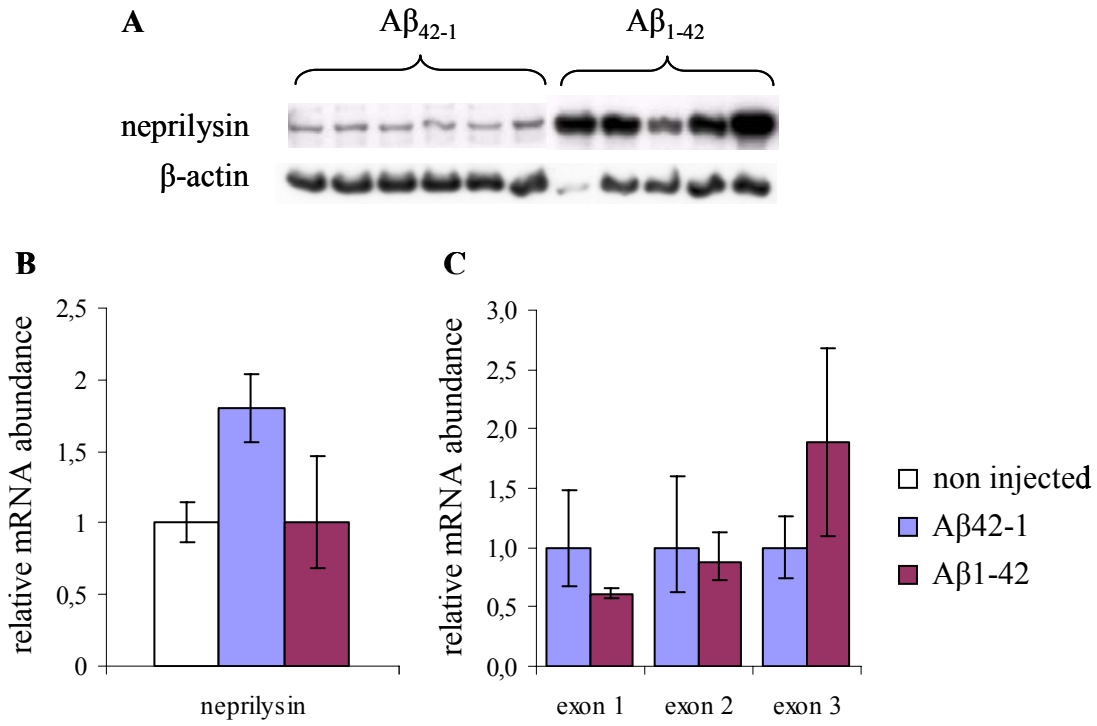

Figure 12. Brain $A\beta_{1-42}$ injection increased neprilysin protein levels without altering mRNA levels in aged SwAPP mice. (**A**) Western blot analysis for neprilysin of the brain homogenates, 20 weeks after intracranial Aβ injection. Neprilysin levels were increased in mice injected with $A\beta_{1-42}$ compared to $A\beta_{42-1}$. (**B**) RNA prepared from frontal mouse brain 20 weeks after $A\beta_{1-42}$ or $A\beta_{42-1}$ injection or non-injected was analyzed by semi-quantitative RT-PCR for expression of neprilysin. The values represent relative mRNA abundance and were normalized to β-actin with the mRNA level in the brain of non-injected mice used as reference. $A\beta_{1-42}$ injection

did not affect neprilysin mRNA level when compared to the two other treatments. (**C**) Use of primers for the three non-coding exons specific for the activity of the three neprilysin promoters confirmed that Aβ injection did not affect neprilysin mRNA levels. All The abundance of the 3 transcripts in the $A\beta_{42-1}$ injected group is used as reference with a relative mRNA abundance of 1. All values were normalized with relative levels of PBGD mRNA and values are ± SEM.

2.8 The specific $A\beta_{1-42}$-related increase of neprilysin level is not associated with difference in levels of important inflammation-related factors

To investigate the potential role of inflammation-related soluble factors involved in the increase of neprilysin mRNA and protein levels observed 20 weeks after injection of $A\beta_{1-42}$ compared to $A\beta_{42-1}$ or PBS, brain homogenate from young WT mice which received an intracranial injection of $A\beta_{1-42}$ (n=2) or $A\beta_{42-1}$ (n=2) and showed an $A\beta_{1-42}$-specific increase of neprilysin mRNA and protein level and increase of uPA activity were analyzed on a mouse array. It allowed comparing the effect of the treatment on 24 angiogenesis factors. Positive control spots confirmed that the arrays worked correctly, in a similar way through the 4 arrays used and allowed normalizing the signal intensity of the spots of interest. Similarly, negative control spots and blank spots confirmed that the signals observed for the factors analyzed were not artifacts due to unspecific binding of the brain homogenates and antibody solution.
Two samples per group do not allow statistical analysis but the brain homogenates from mice which received intracranial injection of $A\beta_{1-42}$ treatment and showed 20 weeks later its associated increase of neprilysin level and uPA activity contained similar levels of the factors analyzed when compared to brain homogenates from mice treated with $A\beta_{42-1}$ (Fig. 13A). In particular signal intensity of IL-1α, IL-1β, IL-6, IFNγ and TNFα, which are all associated with inflammation and were linked to neprilysin *in vitro* [245, 256] were similar. This suggests that the $A\beta_{1-42}$-specific increase of neprilysin mRNA, protein level and increase of uPA activity did not involve were the action of one of these factors.

A

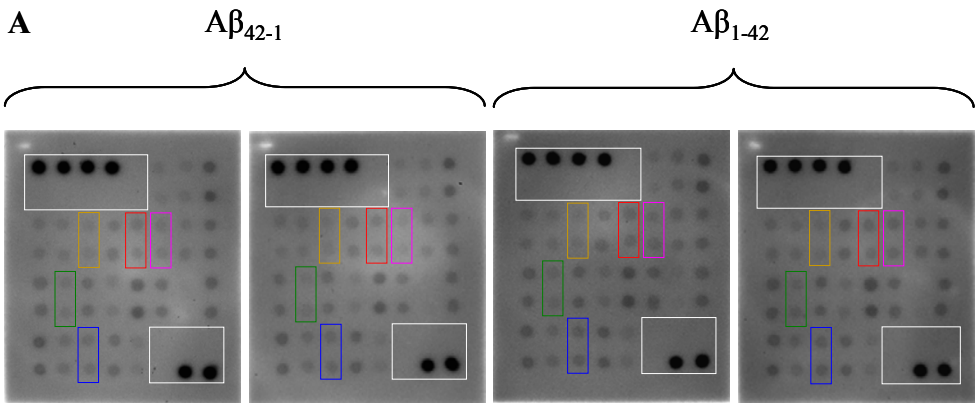

B

	A	B	C	D	E	F	G	H
1	POS	POS	POS	POS	Blank	Eotaxin	Fas Ligand	bFGF
2	NEG	NEG	NEG	NEG	Blank	Eotaxin	Fas Ligand	bFGF
3	G-CSF	GM-CSF	IFNγ	IGF-II	IL-1α	IL-1β	IL-12 p40/p70	IL-12 p70
4	G-CSF	GM-CSF	IFNγ	IGF-II	IL-1α	IL-1β	IL-12 p40/p70	IL-12 p70
5	IL-13	IL-6	IL-9	Leptin	MCP1	M-CSF	MIG	PF-4
6	IL-13	IL-6	IL-9	Leptin	MCP1	M-CSF	MIG	PF-4
7	TIMP-1	TIMP-2	TNFα	Thrombopoietin	VEGF	Blank	Blank	Blank
8	TIMP-1	TIMP-2	TNFα	Thrombopoietin	VEGF	Blank	POS	POS

Figure 13. The $A\beta_{1-42}$-specific increase of neprilysin protein level and increase of uPA activity were not associated with variation of inflammatory pathways. (**A**) Mouse array showing no difference in the signal intensity for the factors analyzed between mice which received $A\beta_{1-42}$ or $A\beta_{42-1}$. White rectangles represented the localization of the positive, negative control and blank spots confirming that the array detection system functioned and the spots observed were not due to background levels. Beige, red, pink, green and blue rectangles represented the localization of the IFNγ, IL-1α, IL-1β, IL-6 and TNFα, respectively. (**B**) Localization and name of the factors analyzed. The colored names are similar to the rectangles used in (A).

3) RA as a potential neprilysin transcription activator *in vitro*

3.1 RA activated neprilysin transcription in 293T cells

The role of RA on neprilysin transcription was further assessed on 293T cells which did not show signs of differentiation or decreased proliferation during RA incubation. When compared to cells incubated with the RA solvent, DMSO, 24 h incubation with 10 µM RA significantly increased the luciferase activity driven by the neprilysin promoters PN1, PN2 and PN3 to 80% ($p<0.0001$), 125 ($p<0.001$) and 155% ($p<0.013$), respectively (Fig. 14).

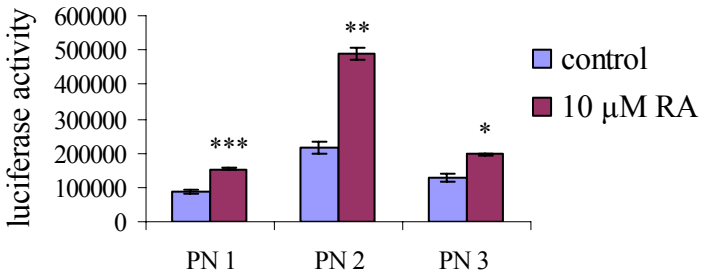

Figure 14. Effect of all trans retinoic acid (RA) on neprilysin promoter activity in 293T cells. 293T cells transiently transfected with a plasmid expressing luciferase under the control of the neprilysin promoter PN1, PN2 or PN3 were incubated with RA during 24 h. RA significantly increased the luciferase activity driven by all three neprilysin promoters when compared to the control RA solvent. *: $p \leq 0.05$, **: $p \leq 0.001$.

3.2 Identification of minimal NEP promoter PN1 responsive to RA

To narrow the promoter fragment involved in the RA-related increase of promoter activity plasmids expressing the firefly luciferase under the control of PN1 or two fragments of 900 and 400 base pairs were cotransfected with the control plasmid expressing renilla luciferase (Fig. 15A). While 24 h incubation with RA still significantly increased the normalized luciferase activity with 40, 24 and 12% increase for PN1, 900 and 400 amino acids promoter fragments, renilla luciferase activities were unchanged (Fig. 15B). This suggested that the observed RA-related increase of firefly luciferase activity was driven by the neprilysin promoter PN1 with the necessary regulatory sequences of the PN1 promoter lying within the first 400 nucleotides upstream of the exon 1. The absence of RA effect on renilla luciferase activity also suggested that RA incubation did not affect renilla luciferase activity, which can be used for normalization.

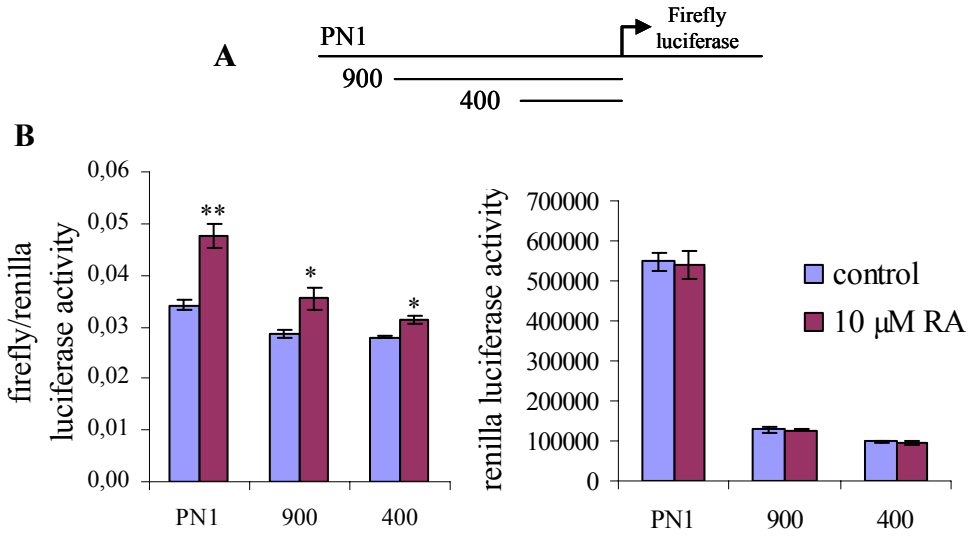

Figure 15. The first upstream 400 base pairs of the PN1 neprilysin promoter are suffisant for the RA-related increase of neprilysin promoter activity. (**A**) Representation of PN1 promoter and its deletion fragments formed by the 900 and 400 upstream base pairs (**B**) 24 h RA incubation of 293T cells significantly increased firefly luciferase activity driven by the neprilysin promoter PN1 or its 900 and 400 base pairs fragments without affecting the renilla activity in transfected 293T cells. *: p≤0.05, **: p≤0.001.

3.3 RA increased neprilysin protein levels in 293T cells

Western blot analysis of 293T cells treated with 10 µM RA or its solvent DMSO for 24 and 48 h showed an increase of neprilysin protein level after retinoic acid treatment (Fig. 16). Because RA incubation could also affect β-actin levels, the samples were normalized with their protein concentration. This data suggest that the RA effect observed on neprilysin transcription level in 293T cells also leads to increased protein levels *in vitro*.

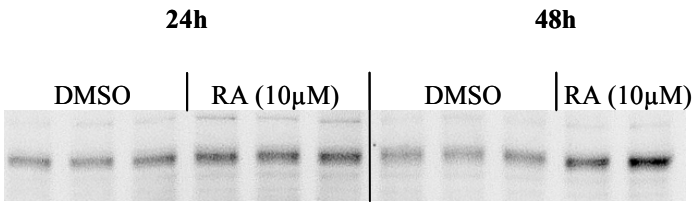

Figure 16. RA increased neprilysin protein level in 293T cells. 293T cells were incubated for 24 and 48 h with 10 µM RA or its solvent, DMSO. Western blot analysis with the antibody 56C6 recognizing human and murine neprilysin showed an increase of neprilysin level after RA incubation.

3.4 RA did not upregulate brain neprilysin level *in vivo*

To investigate the role of RA on neprilysin levels *in vivo*, WT mice were chronically treated with RA or a control treatment. After 5 days treatment with 3 µg RA, 125 µg RA or control treatment, brain neprilysin levels were quantified by Western blot analysis. RA did not alter the level of neprilysin protein after the single (not shown) or the chronic injection treatments (Fig. 17).

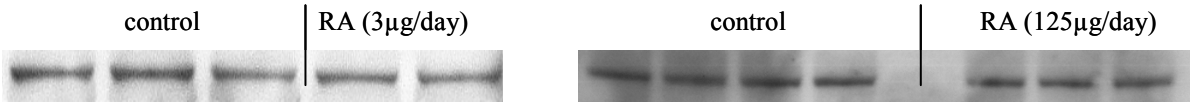

Figure 17. Chronic treatment (5 days) with all trans retinoic acid (RA) did not increase brain neprilysin levels *in vivo*. Western blot analysis for murine neprilysin showed similar neprilysin protein level independent of the treatment.

4) Activation of the plasminogen system by $A\beta_{1-42}$

4.1 Intracranial injection of $A\beta_{1-42}$ increased brain plasmin activity *in vivo*

Intracranial injection of $A\beta_{1-42}$ was found to increase brain neprilysin protein level and activity in mice leading to a decrease of Aβ levels and prevention of amyloid plaque formation [406]. To investigate if other Aβ-degrading pathways could have also been involved, we assessed plasmin activity in the same brain homogenates that have elevated neprilysin levels, 12 weeks post injection [406]. The brain homogenates from mice which were injected with $A\beta_{1-42}$ showed a significant 5 ± 0.7 fold increase plasmin activity when compared to PBS (1.0 ± 0.3) and $A\beta_{42-1}$ (1.0 ± 0.3) injected mice ($p \leq 0.001$ for both) (Fig. 18A).

4.2 $A\beta_{1-42}$–related increased brain plasmin activity *in vivo* is associated with increased uPA activity

Since plasminogen can be activited into plasmin by two specific plasminogen activators, tPA and uPA, their enzymatic activity was investigated in the same brain homogenates from the $A\beta_{1-42}$ and $A\beta_{42-1}$ injected mice. The injection did not affect the level of tPA activity. However, uPA activity was highly increased in brain homogenates of $A\beta_{1-42}$ injected mice compared to $A\beta_{42-1}$ control mice (Fig. 18B). This specific $A\beta_{1-42}$-related increase of uPA activity was further confirmed in two independent groups of mice 20 weeks after similar intracranial injection of PBS, $A\beta_{1-42}$ or $A\beta_{42-1}$ (Fig. 22A, B). This suggests that the increase of plasmin activity is due to an increased activation of uPA and does not involve tPA.

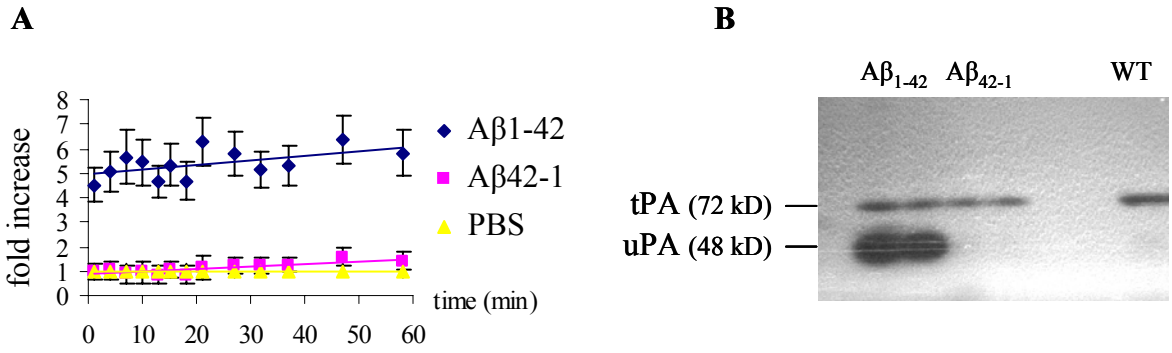

Figure 18. $A\beta_{1-42}$ activated the plasminogen system *in vivo*. (**A**) Plasmin activity was initially measured at intervalles of three min. 12 weeks after intracranial injection of $A\beta_{1-42}$, $A\beta_{42-1}$ or PBS, $A\beta_{1-42}$ significantly increased brain plasmin activity compared to its controls. Linear curves represent the average values over the 1 h period. (**B**) Zymography of the same samples showed that $A\beta_{1-42}$-related increase of plasmin activity was associated with increased uPA but no variation of tPA activity when compared to $A\beta_{1-42}$ injected or a non-injected (WT) mice. Values are average ± SEM.

4.3 Brain localization of uPA activity after $A\beta_{1-42}$ injection

Mice (n=10) received an intracranial injection of $A\beta_{1-42}$ and zymography on slide was performed 12 weeks post injection on cryostat sections. Since the zymography allows the detection of tpA and uPA, the addition into the gel of amiloride, an uPA inhibitor, allowed the localization of tPA and by subtraction localization of uPA activity. The activitites of tPA and uPA were located in the meningeal cell layer (white arrows) surrounding the brain and in the hippocampus. Zymography after the addition of amiloride to the gel layer suggested that uPA activity was highly present in the meningeal epithelium cells but also present in the neurons of the CA1 region of the hippocampus and the dentate gyrus (black arrows) (Fig. 19A, B).

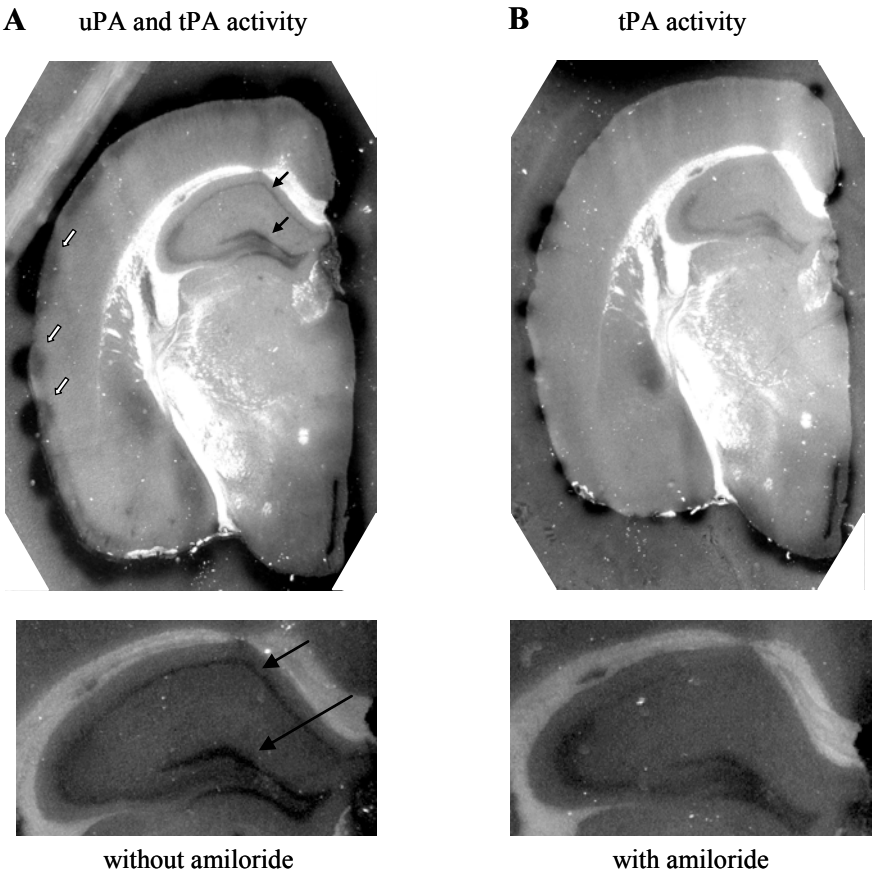

Figure. 19. uPA localization after $A\beta_{1-42}$ injection. 12 weeks after $A\beta_{1-42}$ injection, zymography on brain slide with (**B**) or without an uPA inhibitor (**A**), amiloride, showed uPA activity in the meningeal epithelium located around the brain (white arrows) but also CA1 and dentate gyrus of the hippocampus (black arrows).

4.4 Aβ injection did not change mRNA levels of the plasminogen activators

To determine whether $A\beta_{1-42}$ affected transcription of the plasminogen activators, mRNA levels of uPA, its receptor uPAR and tPA were quantified 20 weeks after $A\beta_{1-42}$ or $A\beta_{42-1}$ intracranial injection by RT-PCR in the brain of mice and normalized to β-actin expression levels. Aβ injection did not affect the mRNA levels of uPA, uPAR or tPA (Fig. 20). Therefore, the $A\beta_{1-42}$-related increase of uPA activity is not due to increased uPA mRNA levels.

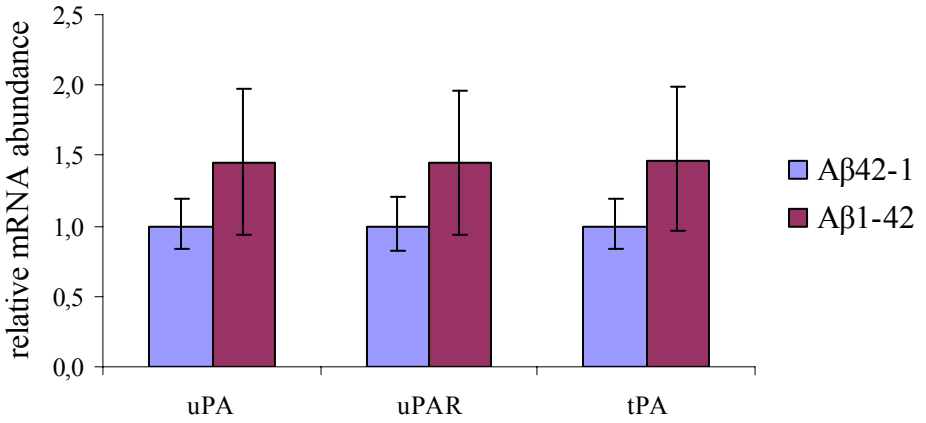

Figure 20. $A\beta_{1-42}$ injection did not affect mRNA levels of uPA, uPA receptor and tPA. 20 weeks after intracranial injection of $A\beta_{1-42}$ or $A\beta_{42-1,}$ the relative abundance of brain mRNA levels for uPA, uPA receptor (uPAR) and tPA were unchanged. Values are ± SEM and were normalized with the reference gene β-actin.

4.5 UPA deficiency did not alter murine Aβ levels

To investigate in $A\beta_{1-42}$ injected mice the potential role of increased uPA activity in the observed decrease of Aβ levels and subsequent prevention of plaque formation, total murine Aβ levels were quantified in the frontal brain area of 9.6 ± 0.25 months old uPA KO mice (n=11) and their aged matched WT littermates (n=11, 9.6 ± 0.8 months old) (Fig. 21). 12.8 ± 2.0 ng/g wet tissue and 13.4 ± 1.2 ng/g wet tissue were found in uPA KO and WT mouse brains, respectively, demonstrating that brain total Aβ levels were not affected by uPA deficiency. This suggests that uPA is not a rate limiting enzyme in Aβ degradation *in vivo*.

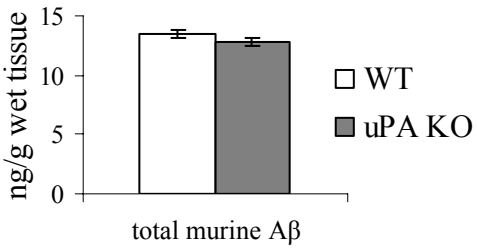

Figure 21. Total murine Aβ quantification. Frontal brains from 12 months old uPA KO mice (n=11) and WT littermates (n=11) showed no difference in the amount of total murine Aβ quantified by ELISA.

4.6 Neprilysin protein levels and uPA activity correlated after Aβ injection *in vivo*

Intracranial $A\beta_{1-42}$ injection increased neprilysin protein levels and uPA activity in a similar manner. 20 weeks after PBS or Aβ injection, brain neprilysin protein level and uPA activity were only increased in the $A\beta_{1-42}$ injected mice. Furthermore, $A\beta_{1-42}$ injected mice exhibiting a low increase of neprilysin level also displayed lower level of uPA activity (Fig. 22A) and samples with high levels of neprilysin exhibited high uPA activity (Fig. 22B). Spearman's correlation analysis between neprilysin protein level and uPA activity in the second group of mice injected with $A\beta_{1-42}$ (n=5) confirmed a significant correlation between both (p=0.037).

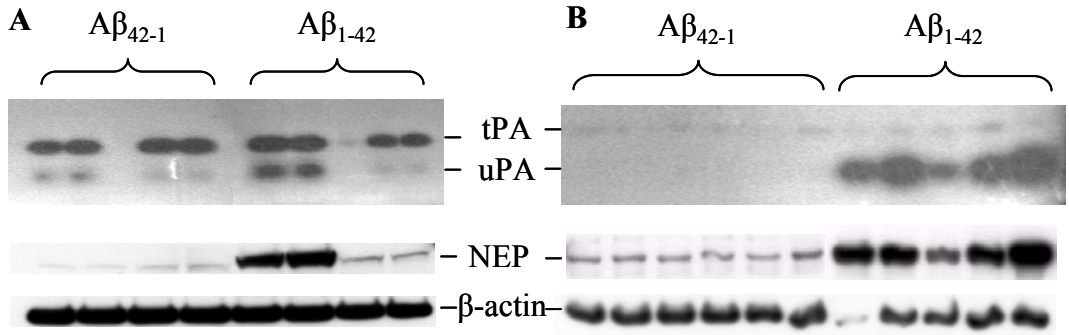

Figure 22. Correlation between neprilysin protein level and uPA activity induced by $A\beta_{1-42}$ *in vivo*. 20 weeks after $A\beta_{1-42}$ or $A\beta_{42-1}$ injection, two independent groups (**A**) and (**B**) showed a similar increase of brain uPA activity on zymography and neprilysin protein level on Western blot. $A\beta_{1-42}$ induced increase of neprilysin protein level significantly correlated with uPA activity (p=0.037).

4.7 No correlation between $A\beta_{1-42}$-related increase of uPA activity and neprilysin level *in vitro*

4.7.1 $A\beta_{1-42}$ activated both plasminogen activators *in vitro*

To study the potential link between $A\beta_{1-42}$-related increase of neprilysin protein level and uPA activity observed *in vivo*, SH-SY5Y and MIC cells were incubated during 2 days with PBS or 10 μM of aggregated $A\beta_{1-42}$ and tPA and uPA activity were further analyzed by zymography. $A\beta_{1-42}$ treatment was associated with an increase of tPA and uPA activity in SH-SY5Y cells (Fig. 23A) and led to an increase of uPA activity in the MIC cells without detection of tPA activity (Fig. 23B).

To investigate the specific role of $A\beta_{1-42}$, SH-SY5Y cells (Fig. 23C) and primary neuronal cultures (Fig. 23D, E) were also incubated with PBS, 10 μM of aggregated $A\beta_{1-42}$ or aggregated $A\beta_{42-1}$ for 2 and 5 days, respectively. $A\beta_{1-42}$ incubation increased uPA and tPA activity in both systems when compared to cultures treated with PBS. However, the uPA and tPA activity of the $A\beta_{42-1}$ treated cells were also increased when compared to PBS treated cultures but was lower than $A\beta_{1-42}$ treated cells. Similarly, an increase of tPA-tPA inhibitor complexes was found in both cell systems and increased levels of uPA-uPA inhibitor appeared after Aβ incubation in primary neuronal culture (Fig. 23E). These results suggest that $A\beta_{1-42}$ can activate the plasminogen system via a general mechanism present in different cell types. However, the effect is not specific to $A\beta_{1-42}$ and may be due in part to the aggregation state of the protein.

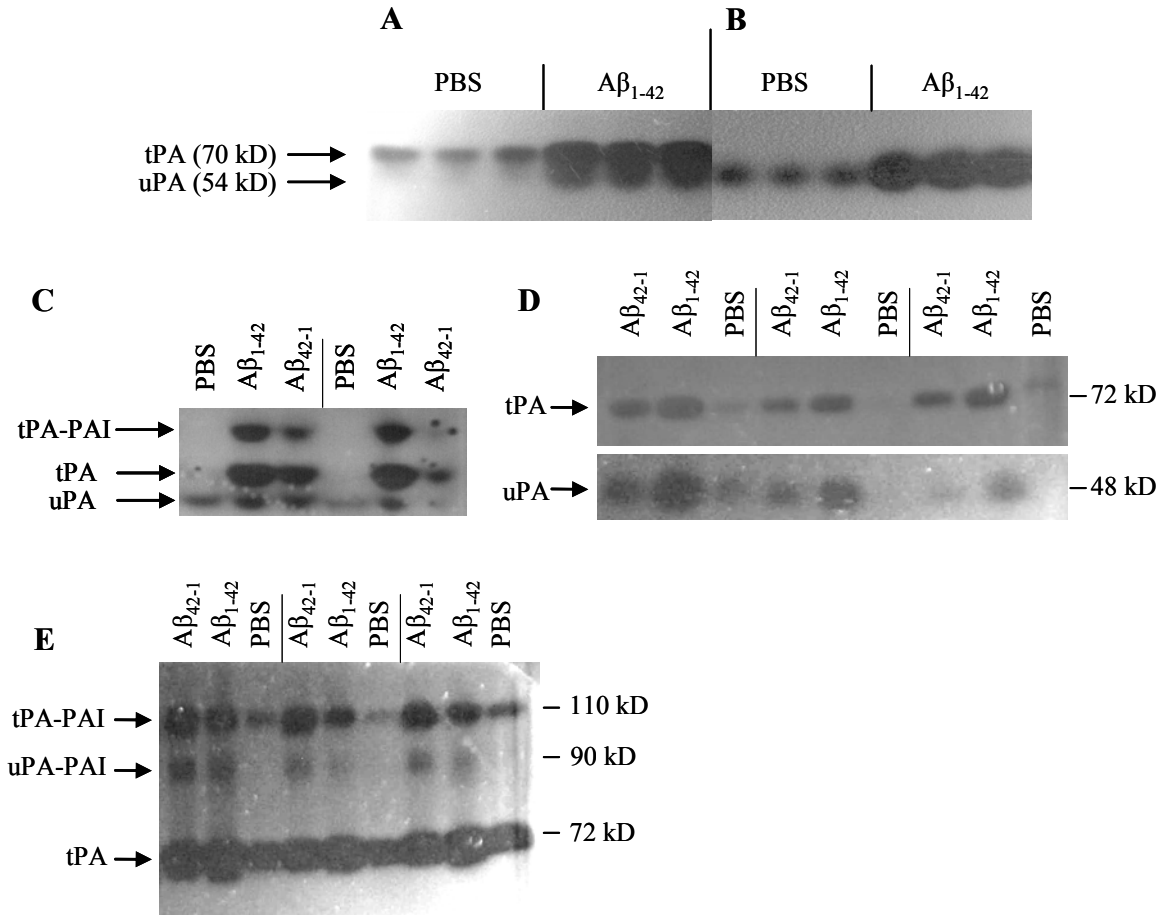

Figure 23. Aβ activated the plasminogen activators *in vitro*. SH-SY5Y cells (**A**, **C**), MIC cells (**B**) and primary neuronal cultures (**D**,**E**) were incubated with 10 μM $A\beta_{1-42}$, $A\beta_{42-1}$ or PBS during 2 for the cell lines and 5 days for the neuronal culture. $A\beta_{1-42}$ incubation increased cell tPA and uPA activity when compared to PBS treated cultures. $A\beta_{42-1}$ also increased uPA and tPA activity compared to PBS treated cells but with a less extend than $A\beta_{1-42}$. tPA and uPA complexed with inhibitors (PAI) were also increased after Aβ treatment (**D**,**E**).

4.7.2 $A\beta_{1-42}$ does not increase neprilysin protein level *in vitro*

Effect of Aβ incubation on neprilysin levels was investigated in MIC cells which exhibited a high increase of uPA activity but no tPA activity after $A\beta_{1-42}$ incubation, being therefore a potential model to the *in vivo* specific $A\beta_{1-42}$-related increase of uPA activity. The effect of Aβ on neprilysin level was also investigated in primary neuronal culture, since the increase neprilysin protein levels in $A\beta_{1-42}$ injected mice was localized in neurons [406].

Western blot analysis showed no alteration of neprilysin levels after $A\beta_{1-42}$ and $A\beta_{42-1}$ treatment compared to PBS treated MIC cells (Fig. 24A) and primary neuronal culture (Fig. 24B). β-actin staining was used as a loading control. Therefore, the observed $A\beta_{1-42}$-related increase of uPA or tPA activity in these two cell models did not lead to increase of neprilysin protein levels. These *in vitro* models did not reproduce the effect observed *in vivo* after intracranial Aβ injection. These data either suggest the absence of a direct link between uPA activity and neprilysin levels in Aβ injected mice or indicate that these *in vitro* systems are not good models for the *in vivo* situation.

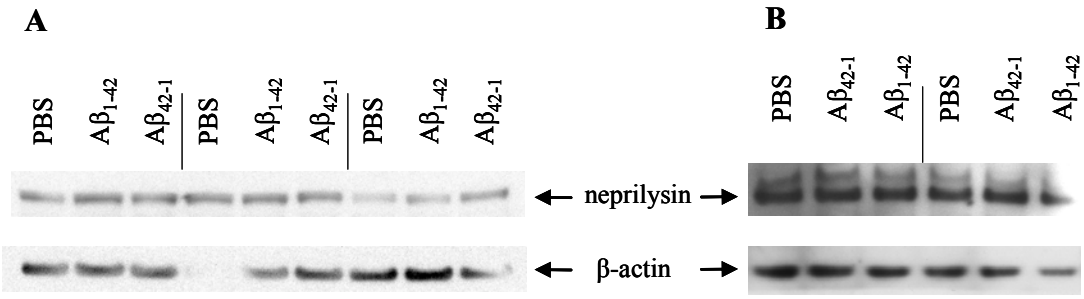

Figure 24. Aβ incubation did not increase neprilysin protein level *in vitro*. Western blot analysis showed no difference in neprilysin levels after 2 days incubation on MIC cells (**A**) and 5 days incubation on primary neurons (**B**) with 10 μM $A\beta_{1-42}$, 10 μM $A\beta_{42-1}$ or PBS.

4.8 Neprilysin overexpression increased plasminogen activators activity *in vivo*

To investigate if the $A\beta_{1-42}$ specific increase of neprilysin protein level and activity could be responsible for the observed increase of uPA activity, we analyzed by zymography the plasminogen activators' activity in the cortex and hippocampus of transgenic mice overexpressing neprilysin in neurons (NEP mice; n=4) compared to WT littermates (n=4). An increase of both tPA and uPA activity was observed in the cortex and hippocampus of the transgenic mice overexpressing neprilysin at the age of 18 months when compared to WT littermates (Fig. 25). While these data suggest a link between neprilysin overexpression and

increase of plasminogen activators activity, the presence of increased tPA activity imply that the pathways involved in the NEP mice may be different than the one involved in the brain of mice 12 weeks after intracranial injection of $A\beta_{1-42}$ where only an increase of uPA activity was observed.

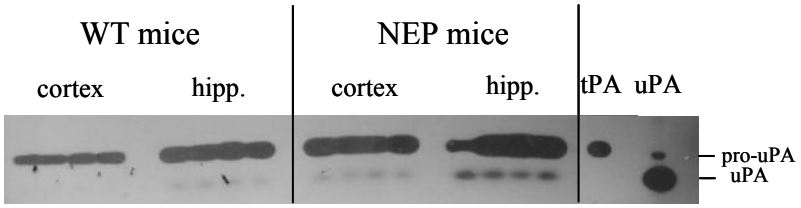

Figure 25. Transgenic neprilysin overexpression increased plasminogen activators activity in the brain. Zymography analysis showed an increase of tPA and uPA activity in the cortex and hippocampus (hipp.) of NEP mice (n=4) compared to WT littermates (n=4). TPA and uPA were also loaded as positive controls.

5) Evaluation of intracranial injection of recombinant adeno-associated virus (rAAV) to overexpress neprilysin *in vivo*

5.1 Intracranial injection of rAAV efficiently transfect neurons

To investigate the efficiency of rAAV to transfect cells in a large area *in vivo*, 2.5 10^8 intact rAAV particles expressing EGFP under the control of the CMV or the PDGF promoter were injected in a volume of 2 µl in the hippocampus and striatum of WT mice.

One week after injection of rAAV expressing EGFP under the control of the CMV promoter, a strong EGFP fluorescence was observed mainly localized in the striatum (green) (Fig. 26A). Staining for activated astrocytes with the GFAP antibody (red) showed a lack of colocalization with EGFP fluorescence suggesting that the transfected cells were mainly neurons. Four weeks after injection of rAAV expressing EGFP under the control of the PDGF promoter, EGFP fluorescence was observed in neurons of the dentate gyrus (Fig. 26B) and the striatum (not shown). Injection of rAAV led to a localized overexpression of EGFP around the injection sites. Therefore, rAAV injection appears to be a good tool for hippocampal overexpression of neprilysin. However, the areas of the brain transduced by these injections were restricted.

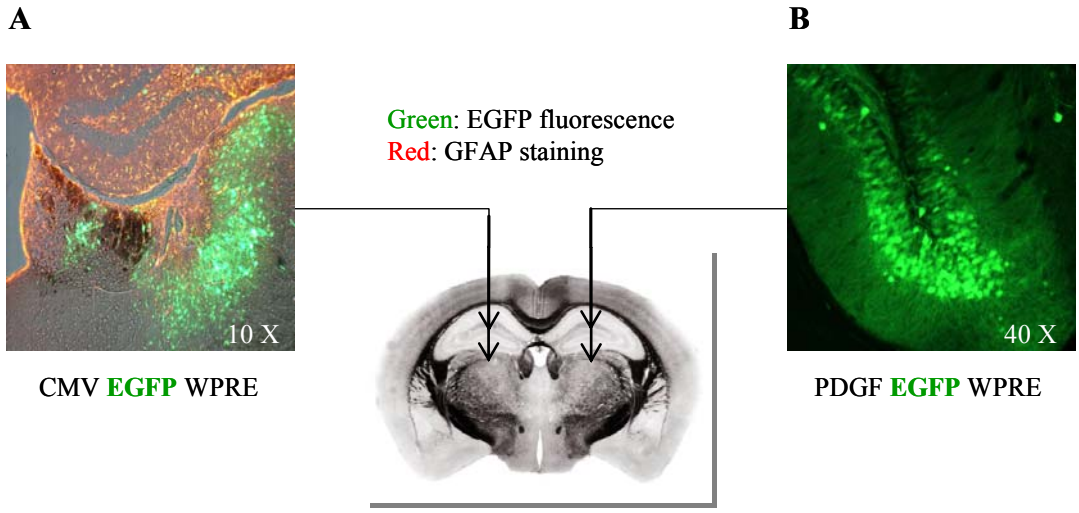

Figure 26. EGFP fluorescence in brain cells transfected via intracranial injection of rAAV. Mice were injected at the hippocampal and striatum levels with rAAV expressing EGFP under the control of the CMV (**A**) or the PDGF promoter (**B**) and analyzed one week and one month after, respectively. The lack of EGFP fluorescence colocalization with a GFAP staining suggested a neuronal transfection by rAAV.

6) Biochemical analysis of NEPxJ20 mice

6.1 Transgenic overexpression of neprilysin in the NEP mice

We have generated 10 transgenic lines of mice expressing human neprilysin in brain neurons under the control of the PrP regulatory sequences. Transmission to their progeny was confirmed by PCR in 8 lines. Localization of the brain neprilysin overexpression was investigated by immunohistochemistry and NEP mice exhibited neuronal staining in different areas of the brain including the thalamus, striatum (not shown) and frontal cortex (Fig. 27A). Due to inconsistency in the neprilysin staining, comparison of neprilysin levels and selection of the best line were achieved by Western blot analysis. All lines tested exhibited significant increases of neprilysin protein levels in the cortex, hippocampus, subcortical area and cerebellum, compared to WT littermates (Fig. 27B), with line 1 and 5 expressing the higher and the lower level of neprilysin, respectively. Line 1, also named NEP, was further analyzed. Neprilysin overexpression resulted in a significant 34 ± 1.5 (mean ± SEM) fold increase of neprilysin activity (Mann–Whitney U test, $p \leq 0.021$) in the frontal brain area of NEP (n=4) mice compared to WT controls (n=4) (Fig. 27C).

NEP males were further mated with J20 females, overexpressing in neurons the AD-causing human mutated APP and their progeny analyzed. Similar high levels of neprilysin protein were found in different areas of the brain, including frontal brain, hippocampus, amygdala and subcortical areas overexpression in NEPxJ20 mice when compared to J20 mice (Fig. 27D).

To determine if the neprilysin overexpression triggered by the PrP promoter led to neprilysin overexpression elsewhere than the brain, neprilysin protein levels were also quantified in the kidney, heart and liver of NEP mice. Western blot analysis for HA and neprilysin (Fig. 27E) confirmed the expression of the construct in these three peripherical organs and showed an increase of neprilysin protein levels in NEP mice compared to WT littermates.

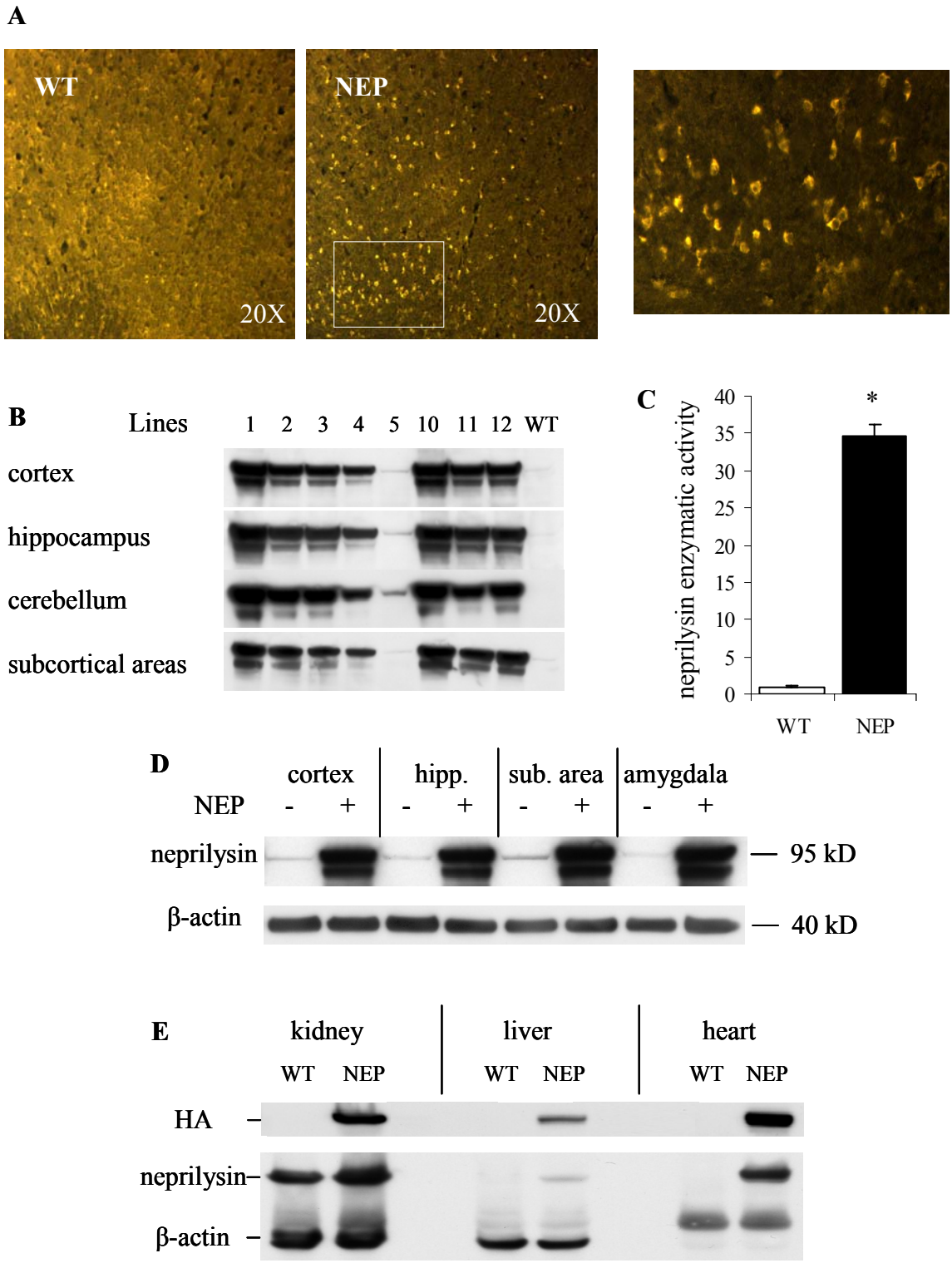

Figure 27. Characterization of the NEP transgenic mice. (**A**) Frontal brain area of NEP and WT mice showing neprilysin staining in mice overexpressing neprilysin. (**B**) Western blot analysis of the neprilysin transgene in different areas of the brain with the 56C6 antibody showed a high elevation of neprilysin protein levels in different neprilysin overexpressing lines. (**C**) Neprilysin activity analyzed in the frontal brain area of NEP mice was 34 ± 1.5 fold higher than in WT littermates (*: p=0.0021; n=4 per group). Values represent the mean ± SEM. (**D**) Similar high neprilysin levels in different brain areas of the NEP transgenic mice (NEP)

compared to WT littermates. The membrane was further probed with β-actin antibody as a loading control. Sub. Area: subcortical area, Hipp: hippocampus. The protein molecular weights are represented in kilodaltons (kD). (**E**) HA and neprilysin staining confirmed the presence and the increased levels of neprilysin protein in peripherical organs of NEP mice compared to WT littermates.

6.2 Neprilysin overexpression decreased Aβ levels without altering the APP processing *in vivo*

To investigate if overexpression of neprilysin would lead to a decrease of Aβ levels without alteration of APP processing, NEP mice were crossbred with J20 mice which express the AD-causing mutated human APP and as a processing product, Aβ. The levels of Aβ, full length APP and its CTF were analyzed in different brain areas of NEPxJ20 and NEP mice. Western blot analysis showed a decrease of Aβ levels in brain areas including cortex (Fig. 28A, C), amygdala (Fig. 28B, C), hippocampus and subcortical areas (Fig. 28C) and no alteration of APP levels or its CTF in NEPxJ20 double transgenic as compared to J20 mice (Fig. 28A, B), emphasizing that removal of Aβ by a neprilysin-dependent mechanism would not interfere with processing and physiological functions of APP.

The effect of neprilysin overexpression on triton-soluble and SDS-soluble Aβ levels was further determined in frontal brains of NEPxJ20 and J20 mice, sequentially extracted with triton and SDS containing buffers. Western blot analysis confirmed the decrease of Aβ levels in NEPxJ20 mice compared to J20 littermates and the lack of APP processing alteration in both fractions (Fig. 29A).

Overexpression of neprilysin resulted in significant 71% and 72% reductions in brain concentrations of triton soluble $A\beta_{42}$ and $A\beta_{40}$, respectively (both $p<0.001$) (Fig. 29B), as determined by specific ELISA systems. Similarly, brain levels of SDS soluble $A\beta_{42}$ and $A\beta_{40}$ were also significantly decreased by 72% and 50%, respectively (both $p<0.001$) (Fig. 29B). After extraction of SDS-soluble Aβ, no FA extractable Aβ was detected by ELISA in the brain tissue of the J20 and NEPxJ20 mice.

To analyze the efficiency of neprilysin to prevent the formation of $A\beta_{42}$ and $A\beta_{40}$ in the two fractions, the ratio $A\beta_{40}/A\beta_{42}$ of the triton and the SDS fractions was calculated for the NEPxJ20 and J20 mice (Fig. 29C). In the triton fraction, NEPxJ20 and J20 mice displayed similar ratios $A\beta_{40}/A\beta_{42}$ with 1.86 ± 0.09 and 1.91 ± 0.06 (mean ± SEM), respectively, illustrating the similar degradation of triton-soluble $A\beta_{40}$ and $A\beta_{42}$ by neprilysin in NEPxJ20 mice. In the SDS fraction, the ratio of $A\beta_{40}/A\beta_{42}$ in J20 mice, with 1.48 ± 0.07 (mean ±

SEM), was significantly lower than in the triton fraction (Mann–Whitney U test, $p \leq 0.002$) suggesting an increased propensity of $A\beta_{42}$ versus $A\beta_{40}$ to be present in this fraction. The NEPxJ20 mice displayed a ratio of 2.72 ± 0.21 (mean ± SEM) in the SDS fraction, which is significantly higher than the J20 mice (Mann–Whitney U test, $p \leq 0.002$). This is due to the decreased efficiency of neprilysin to prevent the formation of SDS-soluble $A\beta_{40}$ versus $A\beta_{42}$.

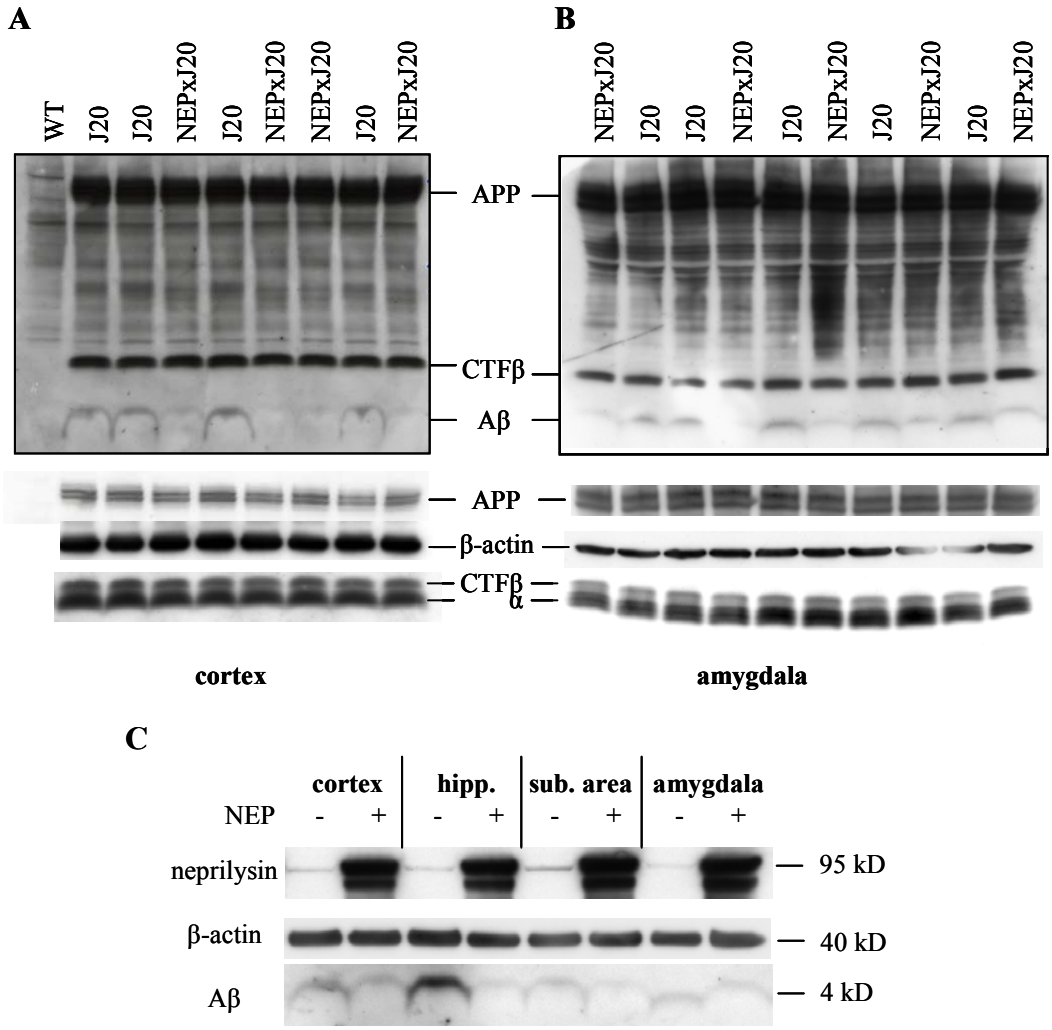

Figure 28. Neuronal neprilysin overexpression decreased brain Aβ levels in the NEPxJ20 mice without affecting the APP processing. Western blot analysis of neprilysin, full length APP (flAPP), APP C-terminal fragments (CTFα and CTFβ) and Aβ in the cortex (**A**), the amygdala (**B**) of NEPxJ20 and J20 mice. While no change of full length APP or its CTF were observed in NEPxJ20 mice compared to J20 mice, Aβ levels were decreased in NEPxJ20 mice compared to J20 mice. β-actin was used as a loading control and the cortex of a WT mouse (WT) shows specificity of the 6E10 antibody recognizing human APP, CTFβ and Aβ. (**C**) Representative Western blot analysis of neprilysin, Aβ and β-actin levels in the cortex, the hippocampus (hipp.), the subcortical area (sub. area) and the amygdala of NEPxJ20 and J20 mice. Overexpression of neprilysin led to reduced levels of Aβ in all areas.The protein molecular weights are represented in kilodaltons (kD).

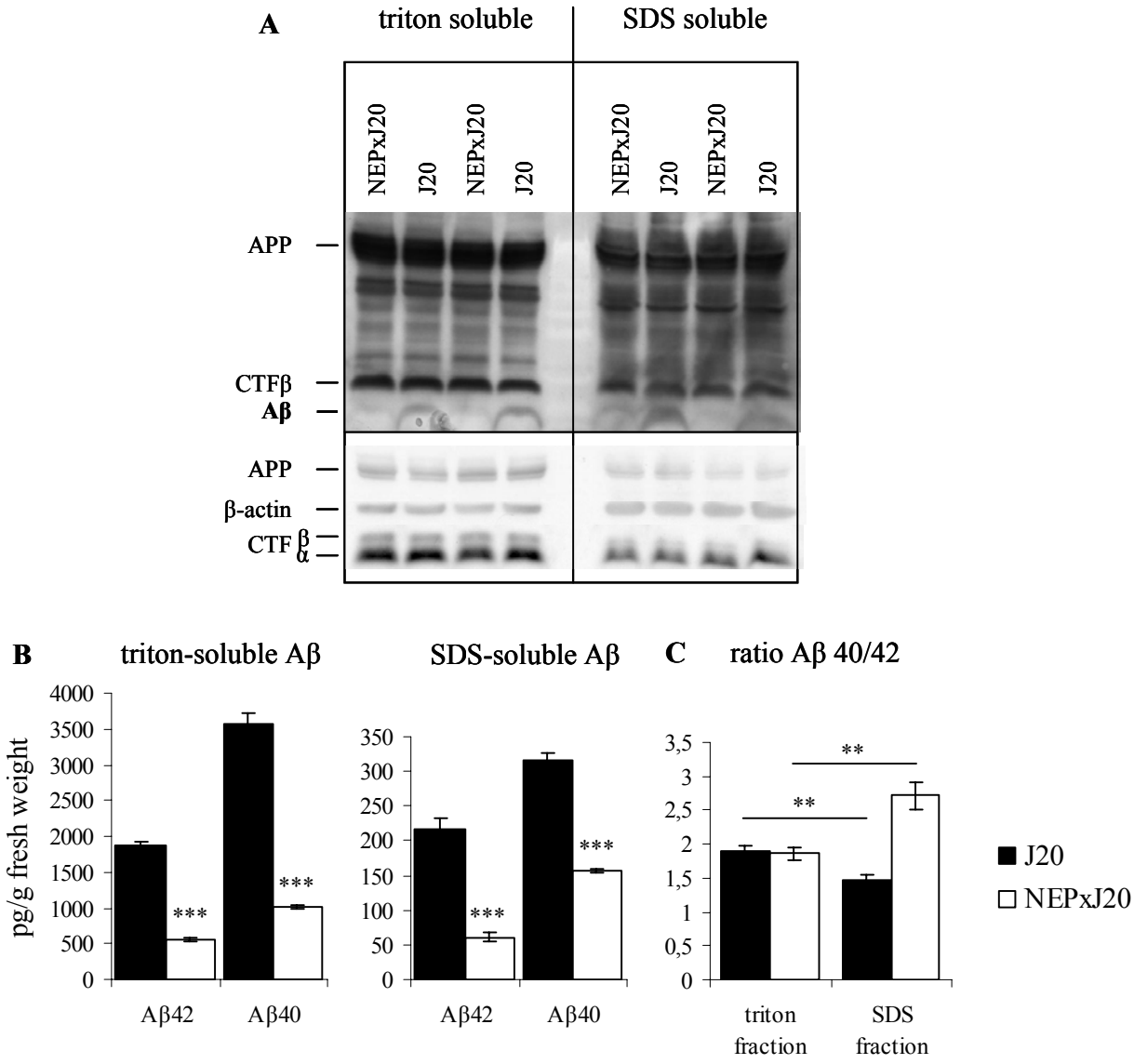

Figure 29. Neuronal neprilysin overexpression decreased brain $A\beta_{40}$ and $A\beta_{42}$ levels in the NEPxJ20 mice without affecting the APP processing. (**A**) Representative Western blot analysis of neprilysin, full length APP (flAPP), APP C-terminal fragments (CTF) and Aβ in the sequentially extracted triton and SDS fractions from the frontal brain of NEPxJ20 mice compared to J20 littermates. No changes of full length APP or its CTF were observed in NEPxJ20 mice compared to J20 mice. In contrast, Aβ levels were reduced in NEPxJ20 mice. (**B**) Triton and SDS soluble $A\beta_{40}$ and $A\beta_{42}$ levels were significantly reduced in 9 months old NEPxJ20 mice when compared to their J20 littermates. (**C**) Ratio of the triton soluble and SDS soluble $A\beta_{40}/_{42}$ in J20 and NEPxJ20 mice showed similar Aβ ratios in the triton fraction but an increased ratio in the SDS fraction of the NEPxJ20 mice compared to the J20 mice. In J20 mice, the ratio also significantly decreased in the SDS fraction compared to the triton fraction. However, the ratio of the SDS fraction was decreased in J20 mice and increased in NEPxJ20 mice compared to their respective triton-soluble Aβ ratios. Values represent the mean ± SEM. (**: $p<0.01$, ***: $p<0.001$).

6.3 Neprilysin overexpression decreased Aβ levels in aged mouse brains

Effects of neprilysin overexpression on Aβ levels and APP processing were confirmed in the 15 months cohort following behavioral analysis. After sequential extraction of tris soluble Aβ, triton soluble Aβ, SDS soluble Aβ and FA soluble Aβ, Western blot analysis confirmed the decrease of Aβ levels in tris, triton and SDS fraction of the NEPxJ20 mice compared to their control J20 littermates (Fig. 30A). No FA soluble Aβ was detected.

Semi quantification by Western blot suggested that most of the Aβ was present in the SDS and the tris fraction rather than in the triton fraction (Fig. 30B).

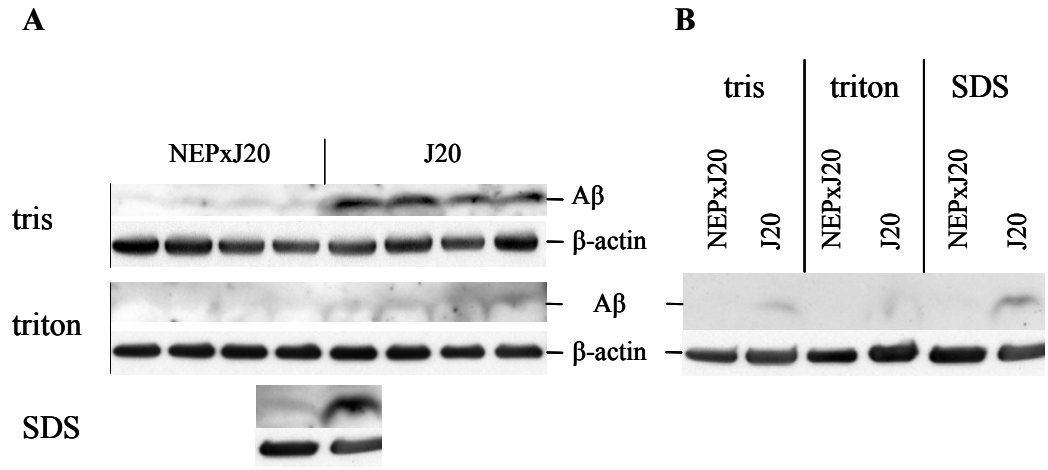

Figure 30. Neprilysin prevented Aβ formation in 18 months old NEPxJ20 mice. (**A**) Western blot analysis of Aβ levels in sequentially extracted tris, triton and SDS soluble Aβ from frontal brain of NEPxJ20 and J20 mice. (**B**) Western blot comparison of the Aβ levels in the three fractions.

6.4 Absence of amyloid pathology in the J20 mice

Following the behavioral studies, brains were analyzed by an immunohistological approach. No amyloid plaques were found in the J20 or the NEPxJ20 mice at 11 and 18 months of age. These data are in agreement with the absence of FA soluble Aβ species by ELISA or Western blot approaches (not shown). Similarly, the number of activated astrocytes (Fig. 31A) and microglia (Fig. 31B) did not differ between all four groups analyzed at the age of 11 months.

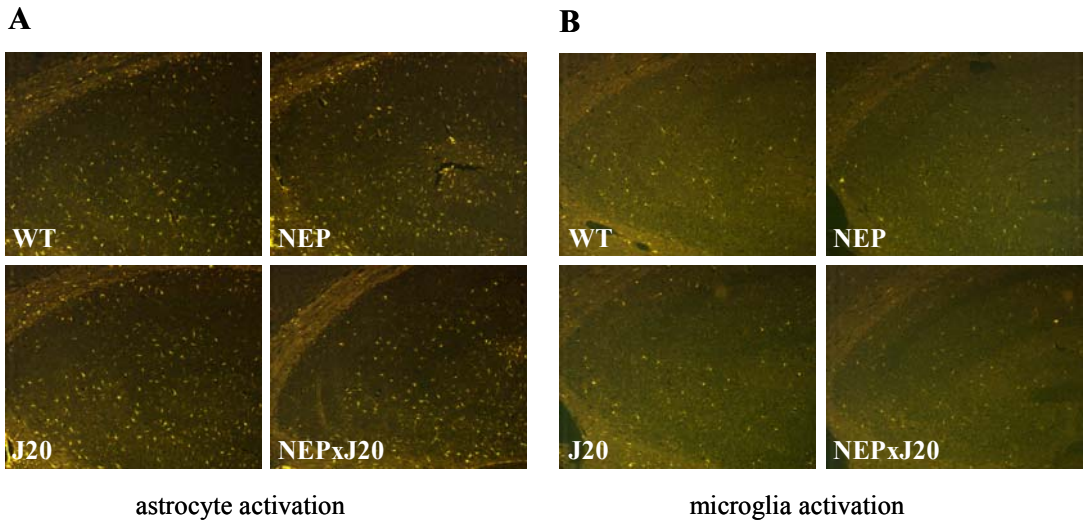

Figure 31. No difference in gliosis in 11 months old NEP, J20, NEPxJ20 and WT mice. Brain sections stained for GFAP (**A**) and IBA-I (**B**), antibodies recognizing activated astrocytes and microglia, respectively, showed similar pattern of expression in all four groups tested.

6.5 Unchanged levels of substance P, met-enkephalin and somatostatin

To investigate the effect of neprilysin and APP overexpressions on the level of other known substrates of neprilysin, substance P, met-enkephalin and somatostatin levels were first analyzed in the frontal cortex (9 WT, 8 NEP, 8 J20 and 8 NEPxJ20) and the hippocampus (8 WT, 7 NEP, 7 J20 and 7 NEPxJ20). Their levels were further investigated in the bigger frontal brain area (9 WT, 13 NEP, 22 J20 and 15 NEPxJ20).

Genotype did not significantly affect the levels of substance P in the frontal cortex ($p=0.130$), hippocampus ($p=0.521$) and frontal brain areas ($p=0.546$) (Fig. 32A, B and C). Met-enkephalin levels were also not affected by genotype in the three areas tested (frontal brain: $p=0.375$, hippocampus: $p=0.524$, frontal brain: $p=0.069$) (Fig. 32A, B and C). Similarly, levels of somatostatin were not significantly changed in the frontal cortex ($p=0.614$), hippocampus ($p=0.429$) and frontal brain areas ($p=0.374$) (Fig. 32A, B and C).

To assess the role of neprilysin on the levels of these three substrates in other organs, kidney and heart from NEP (n=10 and 8, respectively) and WT littermates (n=8 and 10, respectively) were also analyzed. Neprilysin levels were increased in these two organs (Fig. 27E). Substance P levels were undetectable in both organs and therefore not quantifiable. In the kidney, levels of met-enkephalin and somatostatin were not affected by the overexpression of neprilysin (met-enkephalin: $p=0.657$ and somatostatin: $p=0.374$) (Fig. 32D). In the heart, a

similar absence of effect due to neprilysin overexpression was present (met-enkephalin: p=0.534 and somatostatin: p=0.248) (Fig.32E). No significant differences in the levels of substance P, met-enkephalin and somatostatin were found between the 4 groups in all three brain areas and two peripherical organs analyzed, suggesting that Aβ is a better brain substrate for neprilysin *in vivo* and that overexpression of neprilysin is unlikely to interfere with the physiological functions of these other neuropeptides.

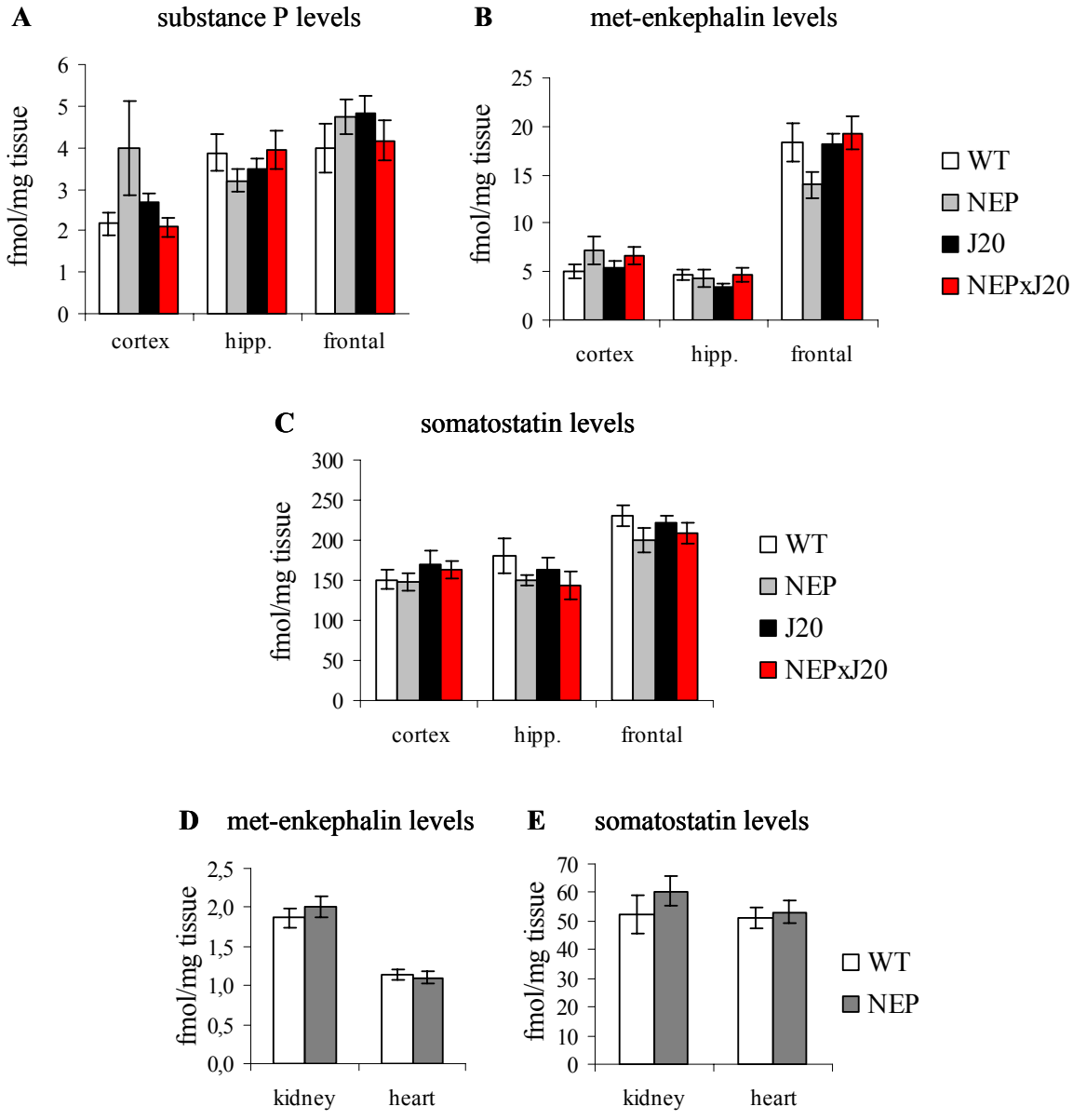

Figure 32. Substance P, met-enkephalin and somatostatin quantification in WT, NEP, J20 and NEPxJ20 mice. In the frontal cortex (cortex), hippocampus (hipp.) and frontal brain area (frontal), genotype did not affect the levels of substance P (**A**), met-enkephalin (**B**) and somatostatin (**C**). In the peripherical organs, kidney and

heart, levels of met-enkephalin (**D**) and somatostatin (**E**) were similar in NEP mice and WT littermates. In all graphs, mean ± SEM are shown.

7) Behavioral analysis of NEPxJ20 mice

7.1 Body weight, motor and sensory function

7.1.1 Transgene affected body weight

NEP and J20 mice of the 7 months and the 15 months cohorts exhibited a decrease of body weight which was constantly significant in double transgenic NEPxJ20 mice. At 4.5 months of age, the first group of mice composed only of the male progeny (17 WT, 16 NEP, 17 J20 and 13 NEPxJ20) was weighted on the conditioning day of the CTA. Body weight of the mice varied significantly between groups (genotype x body weight $p<0.0001$; Fig. 33A). WT mice (27.8 ± 0.7 g) were significantly heavier than NEP (23.8 ± 0.5 g) and NEPxJ20 mice (23.2 ± 0.8 g) ($p<0.001$ for each) while body weight of the J20 mice (25.6 ± 0.5 g) did not significantly differ from control littermates (mean ± SEM) (Fig. 33A).

The females of the second cohort (n=11 for each, age: 15.0 months) were also weighted prior to behavioral testing. Genotype also affected body weight ($p<0.008$) with the WT mice (29.6 ± 0.86 g) being significantly heavier than the J20 (25.5 ± 0.59 g) ($p<0.004$) and the NEPxJ20 mice (25.4 ± 0.77 g) ($p<0.003$). The body weight of the NEP mice (27.5 ± 1.34 g) did not significantly differ from any of the groups (Fig. 33B).

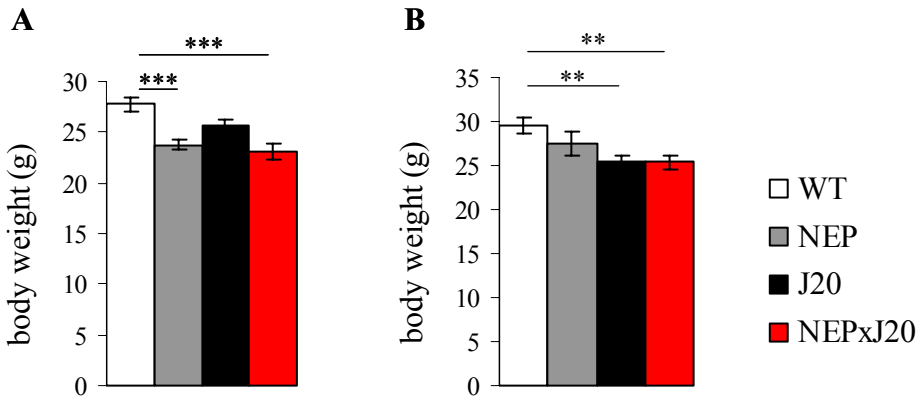

Figure 33. Weight reduction linked to the transgenes. (**A**) Body weight of the NEP and NEPxJ20 mice of the first analyzed group was significantly smaller at 4.5 months of age. (**B**) Alteration of body weight was also observed in the second group at 15 months of age with significant decrease of the J20 and NEPxJ20 mice body weight compared to WT littermates. The values represent the mean ± SEM. **: p<0.01, ***: p<0.001.

7.1.2 Normal motor functions in NEP mice

To test whether neprilysin expression and the observed decrease of body weight affected locomotor coordination, the rotarod paradigm was performed on the male NEP and WT mice of the first group (WT: n=14, NEP: n=13, age: 47.0 ± 0.2 weeks). This test did not provide any evidence of motor impairment in any of the two groups since average performance and learning rates of the two groups were similar (repeated ANOVA: genotype ns, time p<0.0001, interaction ns) (Fig. 34A).

7.1.3 No difference in pain sensitivity of NEP mice

We determined the average latency of the NEP (n=13) and WT (n=14) mice which had also performed the fear conditioning test, to react on a 55°C hotplate (age: 47.0 ± 0.2 weeks). We did not find any significant difference in the latency of the two groups to lick their paws as the sign of discomfort (factorial ANOVA: genotype ns) (Fig. 34B). Similar results were obtained when analyzing the 15 months old cohort (16 WT, 15 NEP, 16 J20 and 14 NEPxJ20, age: 16.5 months ± 0.2 weeks). The latency of the mice to lick their paws was not affected by genotype.

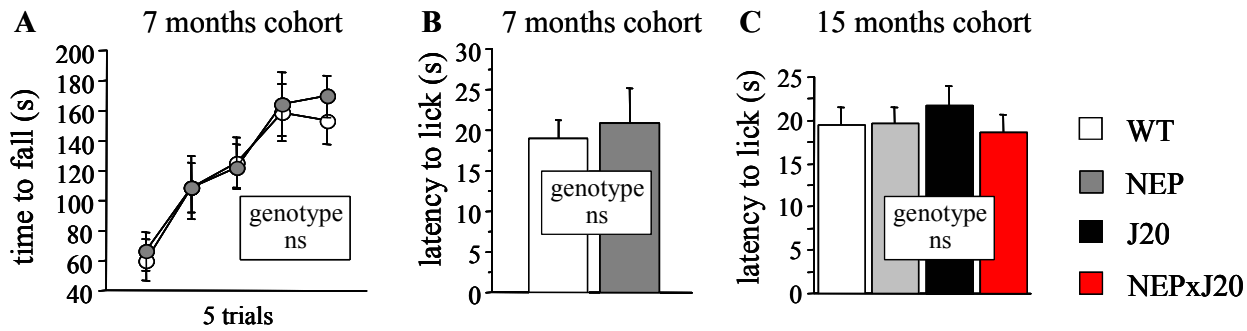

Figure 34. NEP mice were indistinguishable from controls with respect to motor coordination and pain sensitivity. (**A**). Average performance and learning rates of the NEP and WT mice from the 7 months old cohort on the accelerating Rotarod were indistinguishable. (**B**) NEP and WT mice showed the same average latency to lick their paws when placed on a 55°C hotplate. (**C**) Similar absence of genotype effect is observed on the

latency to lick their paws in the 15 months old cohort. Values represent the mean ± SEM. ns (not significant) is mentioned when p>0.1.

7.2 Exploratory behavior and anxiety

7.2.1 Additive effects on locomotion in open field test

Levels of spontaneous locomotor activity, anxiety-like behavior and exploration were assessed in the open field. Genotype strongly affected the locomotion of the 7 months (17 WT, 15 NEP, 17 J20, 12 NEPxJ20, age: 7.0 months) and the 15 months cohorts (16 WT, 16 NEP, 16 J20, 16 NEPxJ20, age: 15.6 months). While J20 mice were clearly hyperactive in both cohorts, NEP mice exhibited a lack of habituation associated with increased number of lingering and progression states only in the 7 months cohort. Neprilysin overexpression did not prevent the deficit of the J20 mice and NEPxJ20 mice presented the impairments present in both NEP and J20 mice.

At 7 months of age, genotype affected both amount and time course of locomotor activity (repeated ANOVA: genotype $p<0.0001$, time $p<0.0001$, interaction $p<0.0010$) (Fig. 35A). While WT mice showed clear habituation over time (partial ANOVA WT: time $p<0.0001$), NEP mice exhibited an abnormal temporal organization of locomotion with a locomotor activity similar to the control littermates during the first day but absence of the normal decrease of activity usually observed during the second day of the test (repeated ANOVA: genotype ns, time $p<0.0001$, interaction, $p<0.0009$; partial ANOVA time: WT $p<0.0001$, NEP ns) (Fig. 35A), indicating a lack of habituation from the NEP mice. Independently of the presence of the NEP transgene, the J20 transgene increased overall activity without affecting time course (partial repeated ANOVA J20 versus WT: genotype $p<0.0011$, time $p<0.0001$ interaction ns; NEPxJ20 versus NEP: genotype $p<0.0014$, time $p<0.0001$ interaction ns). The NEP transgene also abolished habituation in presence of the J20 transgene and slightly increased overall activity (partial repeated ANOVA NEP versus WT: genotype ns, time $p<0.0001$ interaction $p<0.0006$; NEPxJ20 versus J20: genotype $p<0.0206$, time $p<0.0013$, interaction $p<0.0141$) (Fig. 35A).

Analysis of the acceleration and velocity progression confirmed the presence of an abnormal locomotion for both transgenes (acceleration: genotype $p<0.0001$, J20 versus WT $p<0.0182$, NEP versus WT $p<0.0001$, NEPxJ20 versus NEP ns and NEPxJ20 versus J20 $p<0.0189$;

velocity progression: genotype $p<0.0001$, J20 versus WT $p<0.0002$, NEP versus WT $p<0.0041$, NEPxJ20 versus NEP $p<0.0089$ and NEPxJ20 versus J20 $p<0.0269$) (not shown).
In addition, differential analysis of motion states revealed that the frequency of lingering and progression but not resting episodes was significantly increased in the NEP mice compared to WT controls (repeated ANOVA: genotype $p<0.0002$, state $p<0.0001$, interaction $p<0.0002$; partial ANOVA genotype: rest ns, linger $p<0.0004$, progress $p<0.0011$) (Fig. 35B). However, the time spent in these different states was similar in NEP and WT groups (repeated ANOVA: state $p<0.0001$, interaction ns) (Fig. 35C) indicating that the increased frequency of lingering and progression episodes was compensated by their shorter duration. Therefore, both transgenes led to specific alteration of the locomotor pattern in this task with NEP and J20 transgenes associated with a lack of habituation and hyperlocomotion, respectively. Both related impairments were found in the NEPxJ20 mice. The parameters related to anxiety-like behavior were not affected by genotype. A similar preference for the wall zone over the center field with values clearly below chance level, confirmed that the open field center was aversive (1-sample t-test: 7 months $p<0.0001$, 15 months $p<0.0001$) (Fig. 35E). Despite a graphical trend suggesting that the J20 transgene slightly increased center time, there was only a borderline but non significant effect of genotype (repeated ANOVA: genotype ns, zone $p<0.0001$, interaction ns; time in center field genotype $p<0.0692$) (Fig. 35E).

Analysis of the 15 months cohort showed changes reminiscent of those seen in the 7 months cohort (Fig. 35D). However, many effects were weaker. Genotype affected overall level of activity without significantly changing its time course (repeated ANOVA: genotype $p<0.0001$, time $p<0.0001$, interaction ns). As in the younger cohort, WT mice showed significant habituation over time (partial ANOVA WT: time $p<0.0008$). The J20 transgene increased overall activity independently of the presence of the NEP transgene (partial repeated ANOVA J20 versus WT: $p<0.0013$, time $p<0.0002$ interaction ns; NEPxJ20 versus NEP: genotype $p<0.0005$, time $p<0.0166$, interaction ns) (Fig. 35D). In contrast to younger animals, the NEP transgene had no significant effect anymore (partial repeated ANOVA NEP versus WT: ns, time $p<0.0001$ interaction $p<0.0657$; NEPxJ20 versus J20: genotype ns, time $p<0.0917$ interaction ns). Genotype did not alter the preference for the wall zone versus the center field (1-sample t-test: $p<0.0001$) and the percentage of time spent in the center field (repeated ANOVA: genotype ns, zone $p<0.0001$, interaction ns; time in center field genotype ns) (Fig. 35F).

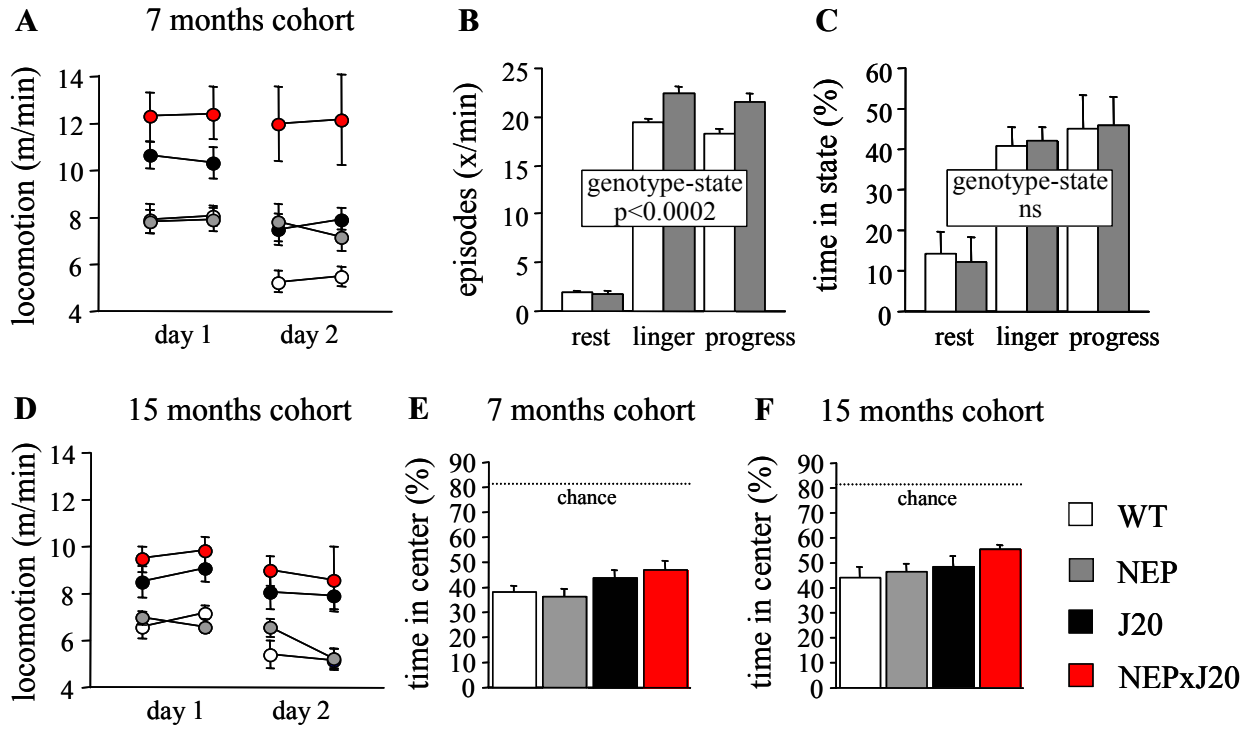

Figure 35. Additive effects of both transgenes in the open field. (**A**) In the 7 months cohort, J20 mice showed a clear overall hyperactivity and the NEP mice a significant lack of habituation during the second day of testing. Both impairments were found in the NEPxJ20 mice. (**B**) The frequency of lingering and progression but not resting episodes was increased in NEP mice compared to WT littermates. (**C**) NEP and WT mice were indistinguishable with respect to time spent in each of the three motion states. (**D**) The 15 months cohort showed changes reminiscent of those seen in the 7 months cohort with significant habituation overtime in the WT mice and significant hyperlocomotion associated with the J20 transgene. However, effects previously observed in NEP mice were not significant anymore. (**E**, **F**) The amount of time spent in the center field was below chance level and not affected by genotype in both cohorts. . ns (not significant) is mentioned when p>0.1.

7.2.2 Hyperlocomotion in the emergence test and novel object exploration in 7 months NEP mice

The emergence test is a free exploration paradigm designed to assess approach or exploratory behavior of rodents in an environment that provides a safe refuge.

Once the J20 and NEPxJ20 mice removed for biochemical analysis, NEP (n=13) and WT (n=14) mice of the 7 months cohort were tested in the emergence test at 42.6 ± 0.2 weeks of age. NEP mice showed clear signs of hyperlocomotion and a decreased habituation with time (repeated ANOVA: genotype $p<0.0001$, time $p<0.0001$, interaction $p<0.0338$; partial ANOVA time: WT $p<0.0001$, NEP $p<0.0001$) (Fig. 36A). The NEP mice also presented an increased frequency of lingering and progression and a decreased number of resting episodes

reminiscent of the open field test (repeated ANOVA: genotype p<0.0001, state p<0.0001, interaction p<0.0001; partial ANOVA genotype: rest p<0.0006, linger p<0.0001, progress p<0.0001) (Fig. 36B). The time spent during these periods was also significantly changed with increased duration of the lingering and progression periods and a decreased of the resting periods (repeated ANOVA: state p<0.0001, interaction genotype-state p<0.0001; partial ANOVA genotype: rest p<0.0001, linger p<0.0359, progress p<0.0001) (Fig. 36C).
Time in the home box, usually considered a measure of anxiety, was similar in NEP and WT mice (Fig. 36D). However, NEP mice spent significantly more time in the center field (p<0.0353), visited a larger percentage of the arena (p<0.0334) and showed a non significant reduced center field avoidance (repeated ANOVA: genotype ns, zone p<0.0001, interaction p<0.0935) (Fig. 36E) compared to their control littermates.

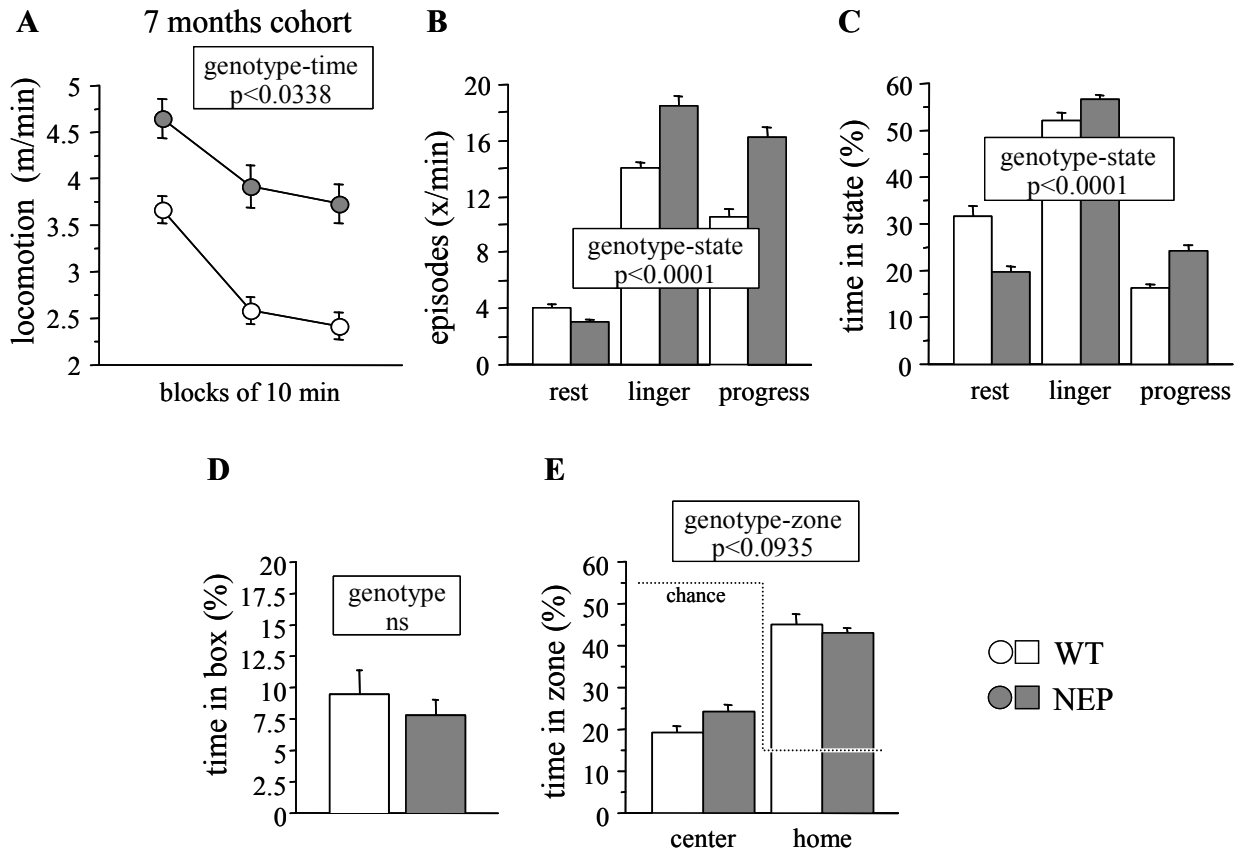

Figure 36. NEP mice were overall clearly hyperactive in the emergence test. (**A**) NEP mice were more active and habituated less during the 30 min session. (**B**). The frequency of lingering and progression episodes was increased in NEP mice, whereas resting episodes were less numerous. (**C**) Time spent with progressive locomotion and to a lesser degree time spent lingering was increased in NEP mice, at the expense of resting time which was strongly diminished. (**D**) Both groups spent a similar small amount of time inside the home box. (**E**)

Both groups strongly preferred the zone around the home box over the center field. The strength of center field avoidance tended to be slightly reduced in NEP mice. Chance levels depended on relative zone area and are indicated by a dotted line. Values represent the mean ± SEM. ns (not significant) is mentioned when p>0.1.

The novel object test is another free exploration paradigm that exposes the animals to a novel stimulus in a familiar arena and inflicts an approach avoidance conflict. Before and after introduction of the novel object into the arena NEP mice showed hyperlocomotion (repeated ANOVA: genotype p<0.0001, time p<0.0001, interaction p<0.0179) (Fig. 37A) reminiscent of the emergence test with similar temporal disorganization of the locomotion. The frequency of resting episodes was unchanged but lingering and progression episodes were significantly increased in the NEP mice (repeated ANOVA: genotype p<0.0005, state p<0.0001, interaction p<0.0001; partial ANOVA genotype: rest ns, linger p<0.0004, progress p<0.0001) (not shown). The percent of time in motion state was also modified: they spent less time resting and increased amount of time lingering and progressing (repeated ANOVA: state p<0.0001, interaction genotype-state p<0.0001; partial ANOVA genotype: rest p<0.0005, linger p<0.0026, progress p<0.0002) (not shown). The NEP mice responded to the introduction of the novel object by an increase of general activity (Fig. 37A). However, despite the marked group differences in general locomotion, interest in the new object was indistinguishable between the NEP and WT mice, which presented a similar horizontal (repeated ANOVA: genotype ns, time p<0.0001, interaction ns) (Fig. 37B) and vertical (repeated ANOVA: genotype ns, time p<0.0002, interaction ns) (Fig. 37C) activity toward the new object.

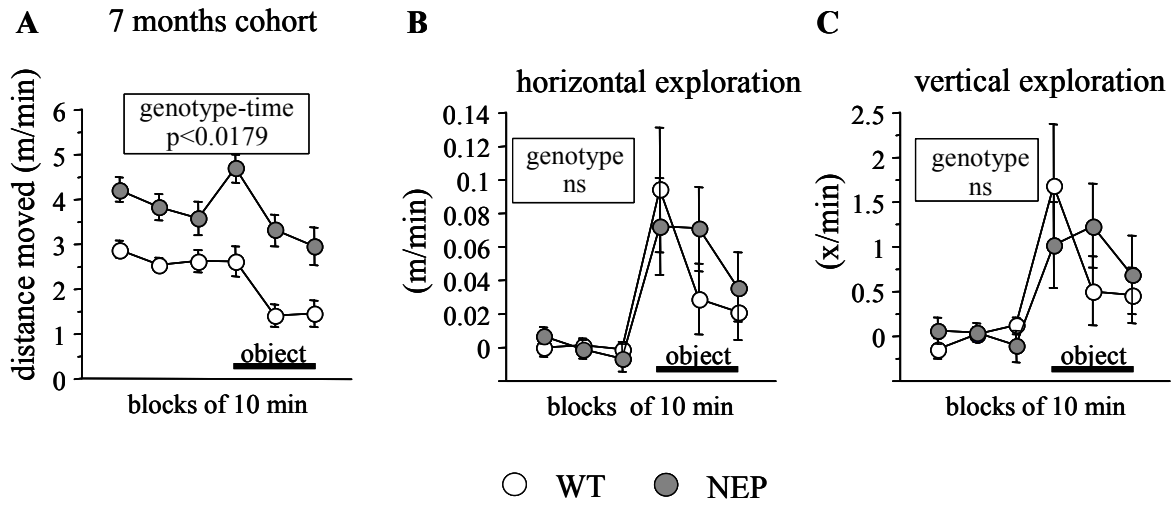

Figure 37. NEP mice are hyperactive but present a normal exploratory activity toward the novel object. (**A**) NEP mice were hyperactive and unlike WT mice, responded to the introduction of the novel object by an increase of general activity. (**B**) Horizontal exploratory activity toward the novel object was significant and indistinguishable between groups despite the marked group differences in general locomotion. (**C**) Similarly, NEP and WT mice did not differ with respect to estimated vertical activity toward the object. Values represent the mean ± SEM. ns (not significant) is mentioned when $p>0.1$.

7.2.3 NEP did not prevent J20-related hyperlocomotion in emergence test and novel object exploration at 15 months of age.

To assess the effect of age on this NEP-related hyperlocomotion, the 15 months cohort (16 WT, 15 NEP, 16 J20, 14 NEPxJ20) was also tested in the emergence paradigm (age 16.1 months). NEP mice exhibited a normal locomotion at 15 months of age in the emergence and object exploration paradigm but showed a lack of interest when the novel object was presented. J20 mice exhibited again, during both paradigms, a clear hyperlocomotion, which was not prevented by neprilysin overexpression. Exploration of the novel object was not affected in mice with the J20 transgene.

Genotype affected overall level of activity without influencing habituation over time (repeated ANOVA genotype $p<0.0001$, time $p<0.0001$, interaction ns) (Fig. 38A). The J20 transgene increased locomotor activity independently of the presence of the NEP transgene (partial ANOVA J20 versus WT: genotype $p<0.0107$; NEPxJ20 versus NEP: genotype $p<0.0062$). The NEP transgene, by contrast, had no effect on locomotor activity and did not prevent the J20-related hyperlocomotion (partial ANOVA NEP versus WT: genotype ns; NEPxJ20 versus J20: genotype ns) (Fig. 38A). Effects on measures of anxiety were only borderline with small, non cumulative attenuating effects of both transgenes on center avoidance (genotype $p<0.0443$, NEP versus WT $p<0.0175$, J20 versus WT $p<0.0394$) and no effect of genotype on percentage of time spent in the box (not shown). These data support that NEP transgene does not affect locomotion but also does not prevent the hyperlocomotion associated with the J20 transgene.

In the object exploration test, genotype affected both overall level and time course of activity (repeated ANOVA genotype $p<0.0001$, time $p<0.0001$, interaction $p<0.0242$) (Fig. 38B). As in the emergence test, the J20 transgene was associated with a general increase of locomotor activity independently of the presence of the NEP transgene (partial ANOVA J20 versus WT: genotype $p<0.001$, time $p<0.0001$, interaction ns; NEPxJ20 versus NEP: genotype $p<0.0001$, time $p<0.0749$, interaction ns) (Fig. 38B). The NEP transgene affected the time course of

activity in absence of the J20 transgene but not in its presence (partial ANOVA NEP versus WT: genotype ns, time $p<0.0001$, interaction $p<0.0155$; NEPxJ20 versus J20: genotype ns, time $p<0.0012$, interaction ns) (Fig. 38B). NEP mice were the only group responding to the introduction of the object with an increase of general locomotor activity. Genotype affected exploration parameters such as the horizontal exploratory activity (repeated ANOVA genotype $p<0.0107$, time $p<0.0001$, interaction $p<0.0035$) (Fig. 38C) and vertical movements toward the object (repeated ANOVA genotype $p<0.0103$, time $p<0.0001$, interaction $p<0.0006$) (Fig. 38D). All groups except NEP mice showed a significant exploratory response toward the object (partial ANOVA WT: time $p<0.0001$; J20: time $p<0.0001$; NEPxJ20: time $p<0.0094$; NEP: time ns). The NEP transgene reduced object exploration significantly in absence of the J20 transgene, but not in its presence (partial ANOVA NEP versus WT: genotype $p<0.0038$, time $p<0.0019$, interaction $p<0.0002$; NEPxJ20 versus J20: genotype ns, time $p<0.0001$, interaction ns). The J20 transgene had no effect on object exploration in absence of the NEP transgene but significantly improved object exploration in NEP transgenic animals (partial ANOVA J20 versus WT: genotype ns, time $p<0.0001$, interaction ns; NEPxJ20 versus NEP genotype $p<0.0247$, time $p<0.0333$, interaction $p<0.0277$). Analysis of estimated vertical movements toward the object confirmed the results obtained by analyzing horizontal exploratory activity (repeated ANOVA genotype $p<0.0103$, time $p<0.0001$, interaction $p<0.0006$). The four groups showed locomotion similar to the emergence test but NEP mice spent less time toward the object.

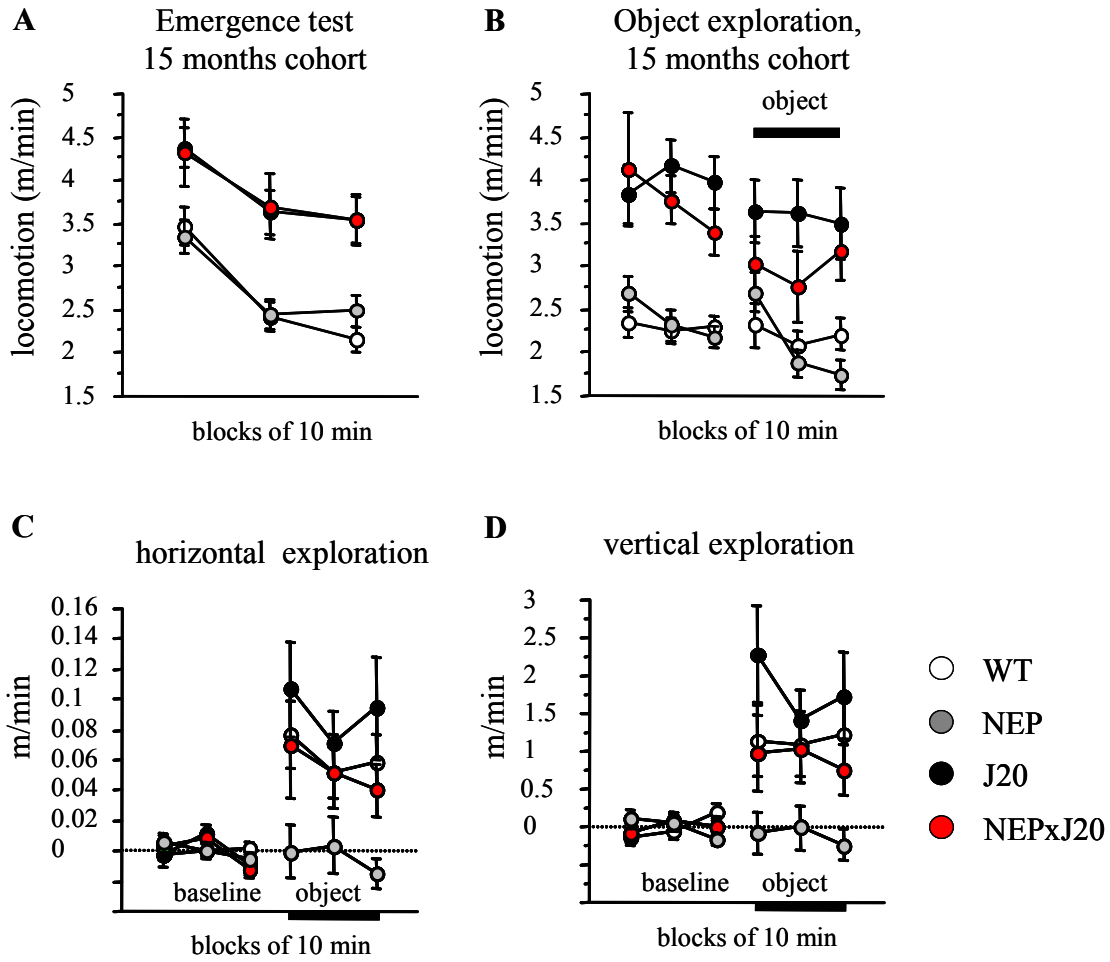

Figure 38. Emergence test and object exploration in the 15 months cohort. (**A**) Emergence test showed a clear hyperlocomotion associated with the J20 transgene, while habituation was not affected by genotype. The distance moved by NEP and WT mice was similar, but neprilysin overexpression did not prevent the J20-related hyperlocomotion. (**B**) Novel object exploration paradigm presented prior to insertion of the object a similar locomotion effect of the different transgene reminiscent of the emergence test. Insertion of the novel object induced increase of locomotion only in the NEP mice. (**C**) All groups except NEP mice showed a significant exploratory response toward the object. This lack of exploration was prevented by the presence of the J20 transgene. (**D**) Vertical movements toward the object confirmed the lack of object exploration from the NEP mice. Values represent the mean ± SEM.

7.2.4 Both transgenes are associated with decreased anxiety-like measures in elevated zero Maze

The elevated zero maze is a standard test to analyze anxiety-related behavior by measuring the avoidance of the unsheltered open sectors. The 7 months cohort (16 WT, 15 NEP; 17 J20, 12 NEPxJ20, age 7.0 months) showed no genotype effect on the total distance moved, suggesting that locomotion was not affected. Percentage entries to the open sectors were

clearly below chance for all groups, confirming their aversive nature (1-sample t-tests: WT $p<0.0001$, NEP $p<0.0001$, J20 $p<0.0001$, NEPxJ20 $p<0.0001$) (Fig. 39A). The avoidance of open sectors was significantly affected by genotype with both transgenes increasing the time spent in the open sectors (genotype: $p<0.0122$, NEP versus WT $p<0.0034$, J20 versus WT $p<0.0067$) without showing an additive effect in NEPxJ20 mice (Fig. 39A).

The number of protected and unprotected head dips were affected by genotype with J20 transgene leading to a significant increase of head dips (genotype $p<0.0009$, J20 versus WT $p<0.0016$, NEP versus WT ns, NEPxJ20 versus NEP $p<0.0181$, NEPxJ20 versus J20 ns) ((Fig. 39C). At 7 months, J20 mice were less reluctant to enter the open sectors and showed more head dips than WT mice. The NEP transgene was associated with similar significant changes, but the effects of the two transgenes were not additive. Therefore, both transgenes induced decreased anxiety in the elevated zero maze paradigm.

In the 15 months cohort (16 WT, 16 NEP; 16 J20, 15 NEPxJ20, age 15.8 months), open sectors were clearly avoided by all groups (1-sample t-tests: WT $p<0.0001$, NEP $p<0.0001$, J20 $p<0.0001$, NEPxJ20 $p<0.0001$) (Fig. 39B). Genotype effects showed a trend in the same direction as in the 7 months cohort but were much weaker and statistically only borderline: despite a graphical trend suggesting reduced open sector avoidance in NEPxJ20 mice, there was no significant effect of genotype on open sector avoidance (ANOVA genotype ns) (Fig. 39B). Genotype still significantly affected the number of head dips (genotype $p<0.0300$) with NEPxJ20 mice making more head dips compared to the NEP mice (Fig. 39D).

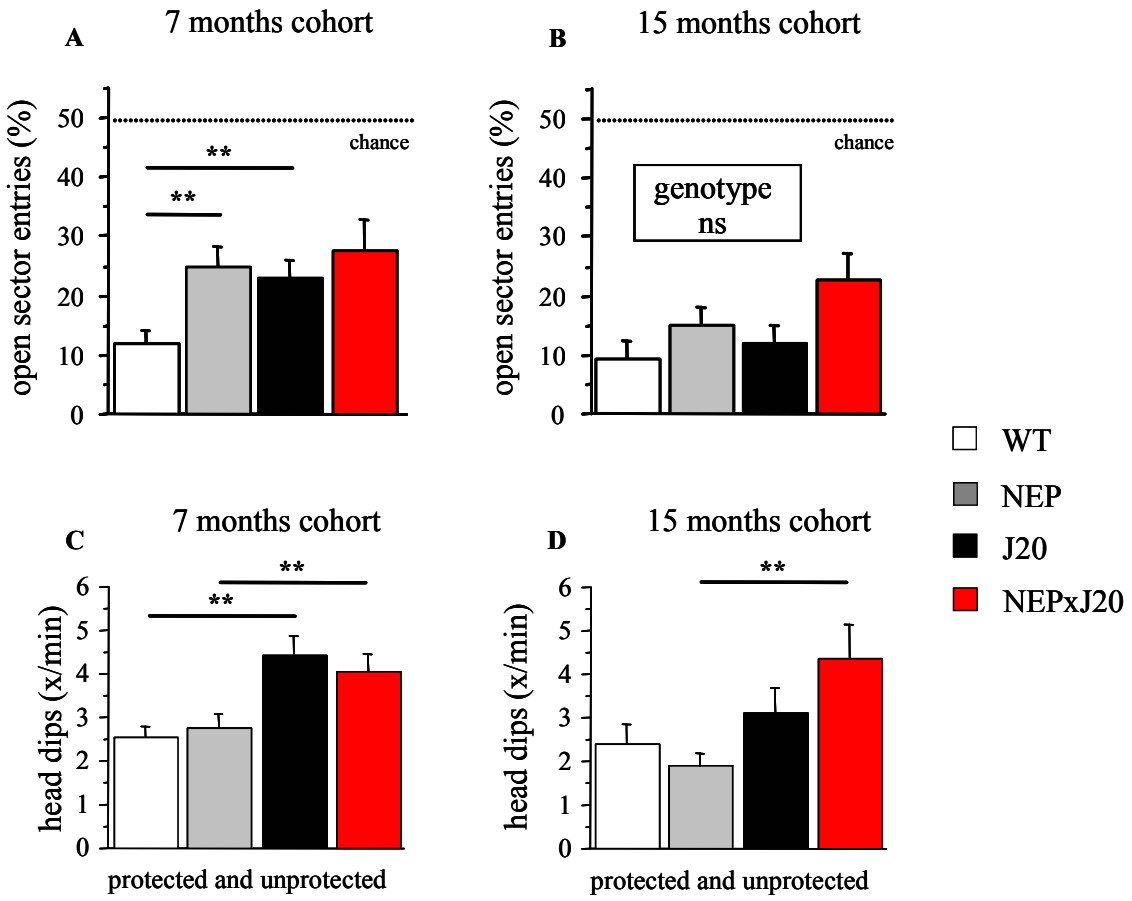

Figure 39. Both transgenes decrease anxiety parameters in the O-maze. (**A**) In the 7 months cohort, both transgenes significantly increased the percentage (%) of open sector entries compared to WT littermates. (**B**) In the 15 months cohort, genotype did not affect the percentage of open sector entries , in spite of a trend. (**C**) total number of head dips was significantly increased by J20 transgene, while NEP transgene did not have any effect by itself and did not prevent the effect of the J20 transgene. (**D**) Only NEPxJ20 mice presented a significant increase of head dips when compared to NEP mice. Values represent the mean ± SEM. **: $p<0.01$.

7.2.5 NEP and J20 transgenes decreased anxiety-related measures in the light-dark (L/D) test only when both present

Similar to the elevated zero maze, this test allows the assessment of unconditioned anxiety related parameters such as the time spent in a protected area. 10 months old mice mixed for gender (31 WT, 28 NEP, 31 J20 and 26 NEPxJ20) were tested in this paradigm.

NEP and J20 mice did not show significant decrease of anxiety-like parameters when compared to WT mice. However, NEPxJ20 mice, which entered less quickly and spent less time in the dark area than the other groups, exhibited a clear decrease of anxiety-like parameters.

A separate 2-way ANOVA with factors genotype and gender revealed no significant genotype-gender interactions. Genotype significantly affected the measures of anxiety such as the latency to enter in the dark area ($p<0.0217$) (Fig. 40A) and the time spent in the dark area ($p<0.0001$) (Fig. 40B). NEPxJ20 mice took significantly more time to enter for the first time in the dark compartment than the other groups which did not differ in this respect (NEPxJ20 versus NEP $p<0.0365$, NEPxJ20 versus J20 $p<0.0136$, NEP and J20 versus WT ns) (Fig. 40A). In agreement with the preference of the mice for dark protected area, WT mice spent more time in the dark area than the opened area. In contrast, both single transgenic groups were not significantly different from controls, but neither preferred nor avoided the dark compartment and only NEPxJ20 mice significantly avoided the dark area (one sample t-test against 50%: WT $p<0.0158$, NEP ns, J20 ns, NEPxJ20 $p<0.0001$) (Fig. 40B). In spite of a graphical trend, NEP and J20 mice did not spent significantly less time in the dark area and only the presence of both transgenes led to a significant decrease (genotype $p<0.0001$, NEP versus WT ns, J20 versus WT $p<0.0838$, NEPxJ20 versus NEP $p<0.0002$, NEPxJ20 versus J20 $p<0.0009$) (Fig. 40B). Moreover, locomotion and count of stereotypic movement like circular running and edge jumping were also modified by genotype ($p<0.0025$ and $p<0.0001$, respectively). While the NEPxJ20 mice presented a borderline non significant increase of locomotion compared to J20 littermates ($p<0.0708$) and a significant increase compared to NEP littermates ($p<0.0002$) (Fig. 40C), they also presented a significant increase of stereotypic movements compared to NEP ($p<0.0001$) and J20 littermates ($p<0.0001$) (not shown).

These data suggest that both transgenes lead in the L/D paradigm to a non significant decreased anxiety, which becomes significant in the NEPxJ20 mice and therefore present boosting effects. This decreased anxiety was associated with hyperlocomotion.

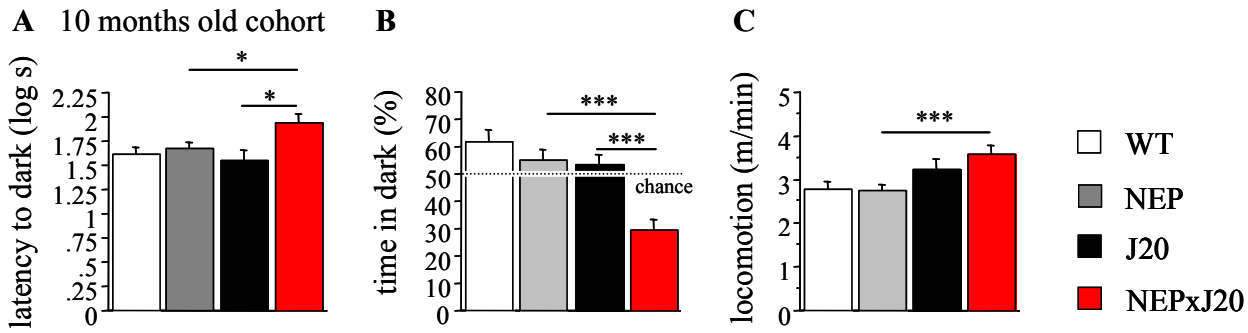

Figure 40. Presence of both transgenes led to decrease of anxiety-like measures and abnormal locomotion in the L/D test. (**A**) NEPxJ20 mice took significantly longer to enter the dark compartment for the first time than the other groups which did not differ in this respect. (**B**) While WT mice spent significantly more time in the dark compartment than chance level, NEP and J20 mice spent less amount of time in the dark box but the effect was only significant when both transgenes were present. (**C**) The J20 transgene increased locomotion in the lit compartment, but this was only significant in presence of the NEP transgene. Values represent the mean ± SEM. *: $p<0.05$; *: $p<0.001$.

7.3 Learning and memory behavior

7.3.1 Neprilysin overexpression did not prevent the memory deficit of the J20 mice in the CTA test

To investigate the potential effect of neprilysin overexpression on hipocampally-independent associative learning and memory, the mice of the 7 months cohort were tested in the CTA (17 WT, 16 NEP, 17 J20 and 13 NEPxJ20, age: 4.5 ± 0.2 months). While NEP mice learned and remembered the association like WT mice, J20 mice exhibited an impaired memory of the association. This deficit was not prevented by neprilysin overexpression.

All groups drank comparable amounts of water during the adaptation and conditioning but genotype affected the amount of saccharin drunk during the conditioning (genotype $p<0.021$; Fig. 41A). While all groups drank a similar amount of saccharin when compared to WT mice, NEP mice drank significantly less saccharin than J20 (genotype $p<0.007$) and NEPxJ20 mice (genotype $p<0.038$). 48 hours after conditioning, genotype strongly affected the strength of the conditioned aversion ($p<0.0002$) and the speed of its extinction (genotype x days $p<0.0006$; Fig. 41C). Whereas WT and NEP mice displayed an equally strong aversion against saccharin, J20 as well as NEPxJ20 mice showed a weaker conditioned aversion in the following choice tests with no difference between the two latter groups. When the avoidance of an intrinsically aversive bitter quinine solution was measured, no difference between the

four mice groups could be detected ($p<0.31$) (Fig. 41B), confirming that taste sensitivity was not altered.

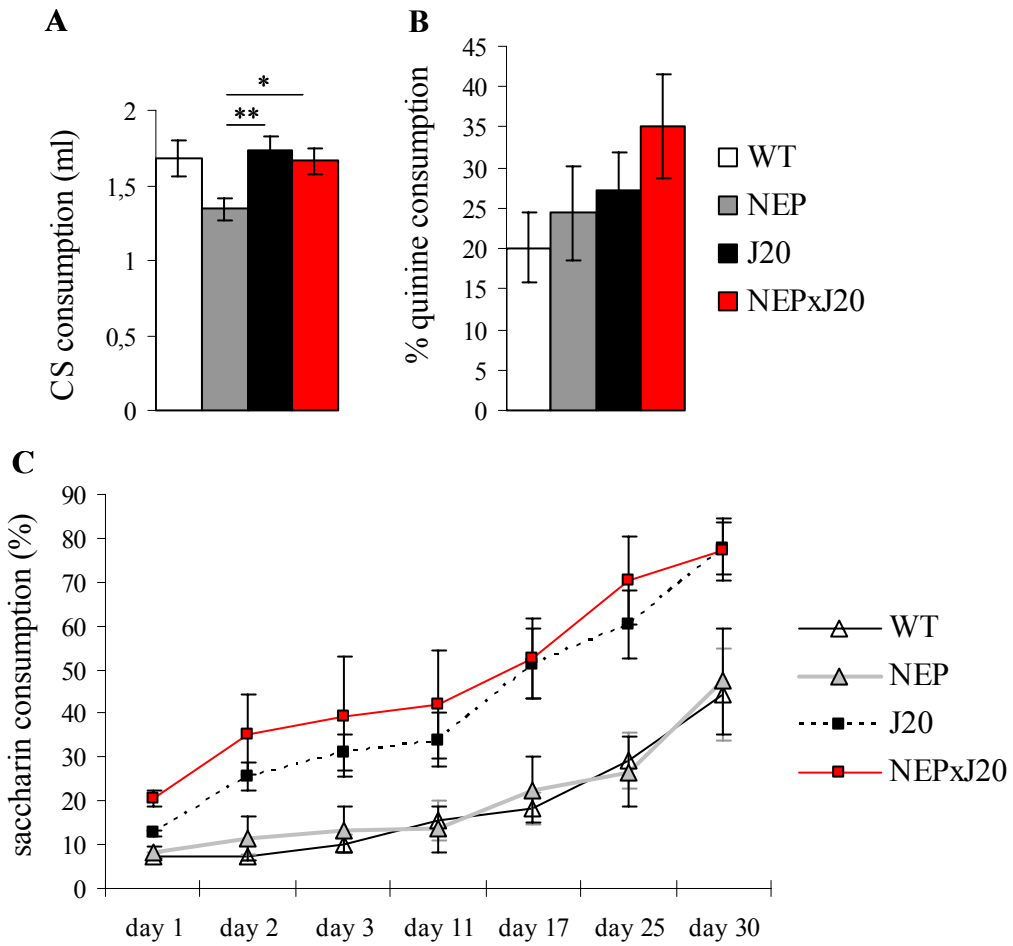

Figure 41. Neprilysin overexpression did not prevent J20 memory deficit in the conditioned taste aversion test. (**A**) NEP mice drank significantly less of the saccharin solution (CS) than J20 and NEPxJ20 but did not differ from WT mice during conditioning. (**B**) In spite a graphic trend, consumption of a bitter quinine solution was not affected by genotype. (**C**) The aversion coefficient, defined as the percentage of saccharin consumption divided by the total fluid intake, is depicted over 7 choice tests for the WT, NEP, J20 and NEPxJ20 mice. Both, J20 as well as NEPxJ20 mice displayed a similar diminished conditioned aversion against saccharin compared to NEP and WT mice. Performance of NEP mice was indifferent from their WT littermates. (*: $p<0.05$; **: $p<0.01$). Values represent the mean ± SEM

7.3.2 Neprilysin overexpression prevented the spatial memory deficit of the J20 mice in the Morris water maze test

To assess the effects of neprilysin overexpression in spatial learning and memory and its ability to prevent the Aβ-related cognitive deficits, the 7 months cohort (16 WT, 17 J20, 10 NEPxJ20, 15 NEP, age: 7.0 months) was tested in the Morris water maze paradigm. Whereas NEP mice behaved similarly to WT mice, J20 mice exhibited impairments in spatial measures while looking for the hidden platform and showed significant memory deficit. This deficit was prevented by neprilysin overexpression.

During the visible and hidden platform learning trials, mice of all groups learned to find the platform (Fig. 42A). Learning rate and overall performance during localization of the visible platform, as measured by the escape latency, was not significantly affected by genotype (repeated ANOVA visible platform: genotype ns, time $p<0.0001$, interaction ns). In the place navigation task, there was a non significant trend contributed by J20 and NEPxJ20 mice which performed similarly and took slightly longer time than the other groups when localizing the hidden platform (repeated ANOVA hidden platform: genotype $p<0.0571$, time $p<0.0001$, interaction ns) (Fig. 42A). By contrast, the genotype effect on spatial measures that are more directly related to memory and cognition was significant and demonstrated a clear beneficial effect of the NEP transgene: during the hidden platform trials, genotype affected the percentage of time spent in the goal quadrant when compared to adjacent quadrants (genotype $p<0.0008$) and goal proximity (genotype $p<0.0130$) (Table 1). This effect was specifically attributable to the J20 mice which spent significantly less time in the goal quadrant ($p<0.0003$) and swam further from the target ($p<0.0087$) as compared to WT littermates. These effects were not observed in the NEPxJ20 mice that performed normally as compared to the WT or NEP single transgenic littermates, suggesting a behaviorally-relevant therapeutic effect of overexpressing the NEP transgene.

During the probe trial, all groups showed a significant preference for the target quadrant compared to adjacent quadrants (repeated ANOVA place: WT $p<0.0001$, NEP $p<0.0001$, J20 $p<0.0084$, NEPxJ20 $p<0.0023$) but the strength of the preference for the target quadrant was significantly affected by genotype (repeated ANOVA: place $p<0.0001$, interaction place-genotype $p<0.0257$) (Table 1, Fig. 42B)). Specifically, the J20 transgene was associated with reduced preference for the target quadrant only in absence of the NEP transgene but not in its presence (partial repeated ANOVA interaction place - genotype: J20 versus WT $p<0.0231$, NEPxJ20 versus NEP ns) (Table 1, Fig. 42B). The NEP transgene had no effect in absence of the J20 transgene but improved target preference of J20 transgenic mice (partial repeated

ANOVA interaction place - genotype: NEP versus WT ns, NEPxJ20 versus J20 p<0.0458) (Table 1, Fig. 42B). The proximity measure (average distance to target) confirmed the results of quadrant time analysis. There was a significant overall genotype effect (factorial ANOVA genotype p<0.0131) with partial comparisons indicating that the J20 transgene was associated with poor proximity scores only in absence of the NEP transgene but not in its presence (J20 versus WT p<0.0163, NEPxJ20 versus NEP ns) (Table 1, Fig. 42C). The NEP transgene had no effect in absence of the J20 transgene but significantly improved proximity scores of J20 transgenic mice (NEP versus WT ns, NEPxJ20 versus J20 p<0.0369) (Table 1, Fig. 42C). Together, these data provide evidence that the transgenic expression of neuronal neprilysin alone had no effect on performance in this spatial memory task but could prevent the memory deficit of the J20 mice.

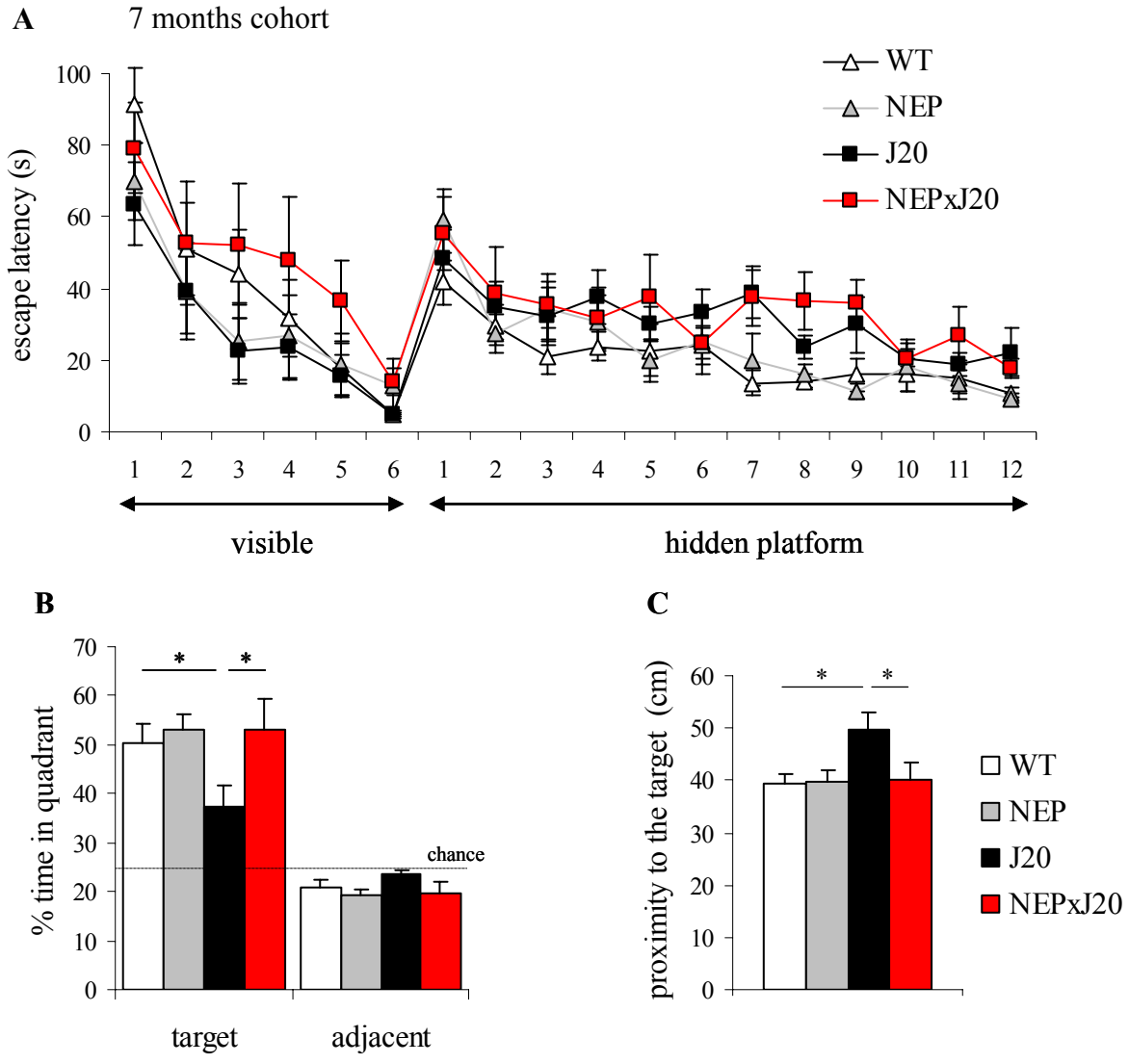

Figure 42. Neprilysin overexpression prevented spatial memory deficits of the J20 mice in the Morris water maze. (**A**) Mean escape latency of WT, NEP, J20 and NEPxJ20 mice to find a visible and a hidden platform. All groups learned to locate the visible and the hidden platform position through the trials and genotype did not significantly affect the learning rate or the overall performance. (**B**) Mean percent time spent in target and adjacent quadrants during the probe trial. All groups showed a significant preference for the target quadrant compared to adjacent quadrants. Genotype significantly affected the preference for the target quadrant. J20 mice spent significantly less time in the goal quadrant compared to WT littermates. There was no difference observed between NEP and WT mice and neprilysin transgene prevented the spatial deficit of J20 transgenic mice. (**C**) Mean distance to the platform localization during the probe trial. Genotype significantly affected the proximity to the target during the probe trial. The J20 mice swam further to the platform localization when compared to WT littermates. In contrast NEPxJ20 swam at the same average distance to the target as NEP and WT mice and performed significantly better than the J20 mice. (*: $p<0.05$). Values represent the mean ± SEM.

Table 1

	Genotype effect	J20 compare to WT	NEP compare to WT	NEPxJ20 compare to NEP	NEPxJ20 compare to J20
Hidden platform trials					
escape latency	p<0.0571	p<0.0659 ↑	ns	p<0.0317↑	ns
% time in goal quadrant	p<0.0008	p<0.0003 ↓	ns	ns	ns
goal proximity	p<0.0130	p<0.0087 ↑	ns	ns	ns
% time near wall	ns				
Probe trial					
swim speed	ns				
% time in goal quadrant	p<0.0257	p<0.0227 ↓	ns	ns	p<0.0456 ↑
goal proximity	p<0.0131	p<0.0163 ↑	ns	ns	p<0.0369 ↓
polar error	p<0.0159	p<0.0180 ↑	ns	ns	p<0.0248 ↓

Table 1. Spatial selectivity during the Morris water maze paradigm. Main effects of genotype are shown first, followed by partial genotype comparisons. For partial comparisons, vertical arrows indicate the direction of the effect. The J20 mice were impaired in spatial selectivity during the place navigation and the probe trial. In the presence of NEP transgene, this effect became non-significant during the place navigation and was significantly rescued during the probe trial. P values are only shown if <0.1 or mentioned ns (not significant).

The 15 months old cohort (15 WT, 16 NEP, 15 J20, and 14 NEPxJ20) showed better performance during cue navigation than the 7 months cohort and performed similarly in the place navigation task, again showing significant learning in both protocols. Neither learning rate nor overall performance measured by escape latency were affected by genotype (repeated ANOVA cued: genotype ns, time $p<0.0001$, interaction ns; place navigation: genotype ns, time $p<0.0001$, interaction ns) (Fig. 43A). In contrast to the 7 months cohort, the genotype

had no effect on spatial measures such as the percentage of time in goal quadrant ($p<0.0959$) or proximity to the platform (ns, not shown).

During the probe trial, preference for the target quadrant was strong overall and highly significant but no longer affected by genotype (repeated ANOVA place $p<0.0001$, interaction place-genotype ns) (Fig. 43B). In spite of a graphic tendency, neither the percentage of time spent in the goal quadrant (Fig. 43B) nor the proximity to the platform was affected by genotype (ns for both). Spatial selectivity of WT animals in this cohort was virtually identical to the younger animals. These data suggest that the impairment observed in the J20 mice of the 7 months cohort was weak and disappeared with age.

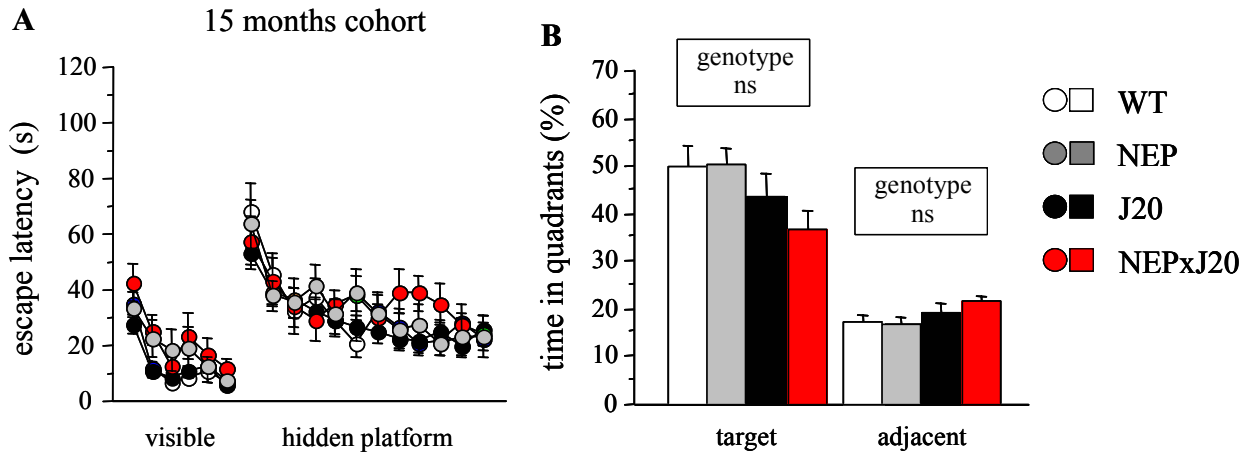

Figure 43. The 15 months cohort was not impaired in the Morris water maze paradigm. (**A**) Mean escape latency of WT, NEP, J20 and NEPxJ20 mice to find a visible and a hidden platform. All groups learned to locate the visible and the hidden platform position through the trials and genotype did not significantly affect the learning rate or the overall performance. (**B**) Mean percent time spent in target and adjacent quadrants during the probe trial. All groups showed a significant preference for the target quadrant compared to adjacent quadrants. Genotype did not significantly affect the preference for the target quadrant.

7.3.3 Similar performance in the Y maze paradigm

To assess the effects of neprilysin overexpression in spatial working memory and its ability to prevent the potential Aβ-related cognitive deficits, the 15 months cohort (16 WT, 14 NEP, 15 J20 and 13 NEPxJ20, age: 17.5 months) was tested in the Y maze paradigm. The percentage of spontaneous alternation did not differ between genotypes (Fig. 44) and was above the 22% chance level [485]. Neither neprilysin nor mutated APP overexpression affected the working memory of the mice.

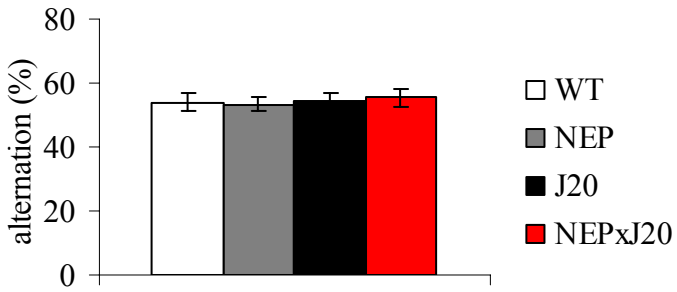

Figure 44. Spatial working memory is not affected by genotype in the Y maze paradigm. Percentage of spontaneous alternation was similar in all groups tested.

7.3.4 NEP mice showed intact cognitive abilities in the puzzle box paradigm

To further analyze the effect of neprilysin overexpression on general cognitive abilities, we tested the NEP (n=15) and WT (n=17) mice from the 7 months cohort (age 40.9 ± 0.4 weeks = 9.6 months) in the motivational driven puzzle box task. During training with an open door as well as in the burrowing and plug puzzles, the two groups showed a highly significant decrease of escape latencies with no significant effect of genotype on overall performance or learning rate (repeated ANOVA training: genotype ns, trial $p<0.0001$, interaction ns; burrowing puzzle: genotype ns, trial $p<0.0001$; plug puzzle: genotype ns, trial $p<0.0001$) (Fig. 45).

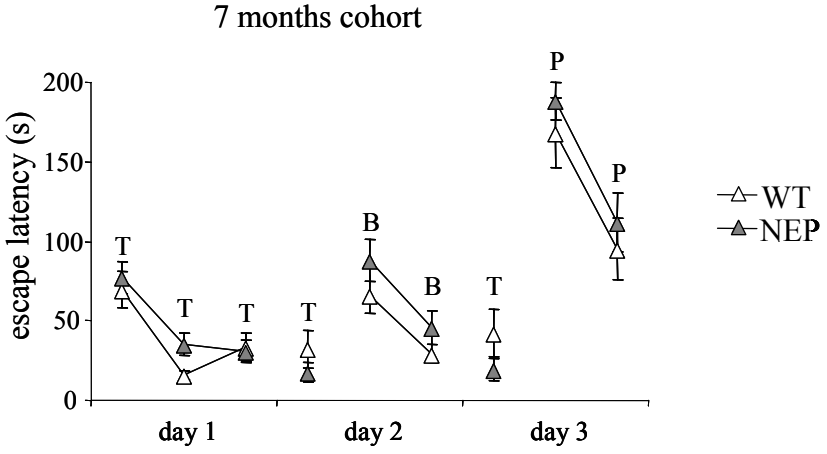

Figure 44. NEP mice show intact cognitive abilities in the puzzle box paradigm. Performance of NEP and WT mice was indistinguishable during escape training (T) with an open underpass, when the underpass was buried (B) in sawdust, and when a plug (P) had to be removed to free the underpass. Both groups learned similarly the tasks and spent less time during the second trial of the cognitive tasks. Values represent the mean ± SEM.

7.3.5 Borderline working memory deficit in NEP mice in 8-arm radial maze

NEP mice (n=12) were slightly impaired in a working memory procedure on the 8-arm radial maze when compared to WT littermates (n=10) (age 44.6 ± 0.2 weeks) but presented strong hyperactivity. The total of reentry errors declined over the 10 days of training with a significant learning and similar rates for both groups, but NEP mice tended to make more errors than control littermates (repeated ANOVA: genotype $p<0.0575$, time $p<0.0001$, interaction ns) (Fig. 46A). NEP mice also differed from WT mice in the number of correct arm choices before the occurrence of the first error and show that despite slightly reduced average performance (repeated ANOVA: genotype $p<0.0494$, time $p<0.0001$, interaction ns) (Fig. 46B), NEP mice learned at similar rate as WT and reached a performance level well above chance (22%). NEP mice also presented a strong locomotor hyperactivity. The NEP mice spent less time to remove all the pellets than WT mice ($p<0.0005$) (Fig. 46C) and traveled a longer distance ($p<0.0309$) while completing the task at an higher speed ($p<0.0066$) when compared to WT controls (not shown). Therefore, the borderline effect on working memory may be in part due to the NEP mice hyperlocomotion.

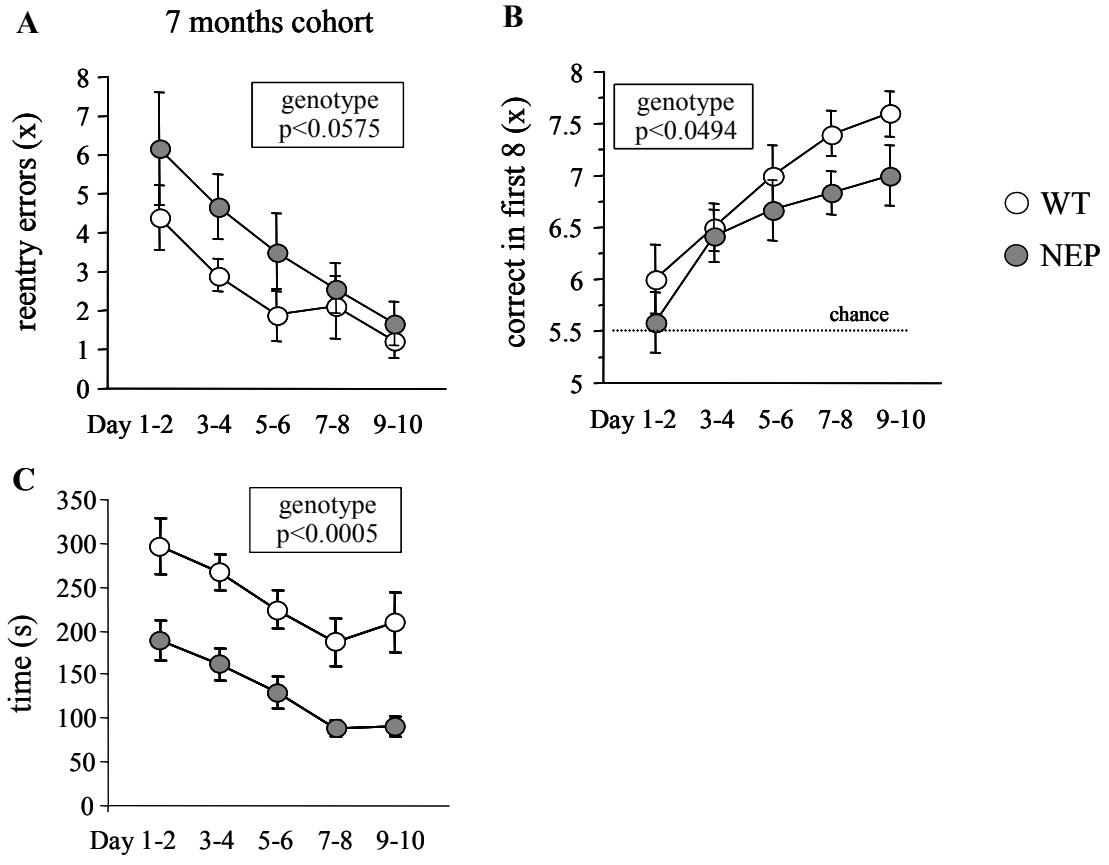

Figure 46. Slight impairment of the NEP mice in the eight-arm radial maze. (**A**) According to number of reentry errors, NEP and WT learned significantly and at indistinguishable rates, but mutants showed a borderline reduction of overall performance. (**B**) Correct choices in first 8 plotted against time show that despite slightly reduced average performance, NEP mice learn at similar rate as WT mice and reach a performance level well above chance. (**C**) NEP mice were hyperactive and needed less time to remove all the pellets when compared to WT mice. Values represent the mean ± SEM.

7.3.6 Altered fear conditioning in NEP mice

To assess associative learning, NEP (n=13) and WT (n=14) mice of the 7 months cohort (age 44.6 ± 0.2 weeks), were used in the auditory fear conditioning test and showed that NEP mice were impaired in contextual fear conditioning. The percentage of freezing during the conditioning session as well as the retrieval sessions for conditioning to context or tone was recorded. During the conditioning session, WT mice showed a high level of freezing compared to pre-training freezing percentage (Fig. 47A). However, NEP mice exhibited a higher percentage of freezing during the pre-training session (Fig. 47A), which may be due to a decreased distance moved (factorial ANOVA: genotype $p<0.0017$) (Fig. 47B), and a lack of training effect with no significant increase of percentage of freezing time (repeated ANOVA: genotype ns, training $p<0.0002$, interaction $p<0.0099$; partial ANOVA training: WT $p<0.0005$, NEP ns) (Fig. 47A). To further investigate the impairment of the NEP mice in fear conditioning, a context and a tone conditioning analysis were performed 24 hours after the training. During the retrieval test for context conditioning, similar results persisted (repeated ANOVA: genotype ns, training $p<0.0001$, interaction $p<0.0267$; partial ANOVA training: WT $p<0.0005$, NEP $p<0.0925$) (Fig. 47C). However, in spite of a weak effect, both groups reacted significantly to the tone (repeated ANOVA: genotype ns, training $p<0.0006$, interaction ns) (Fig. 47D). These data suggest that NEP mice were impaired in contextual fear conditioning.

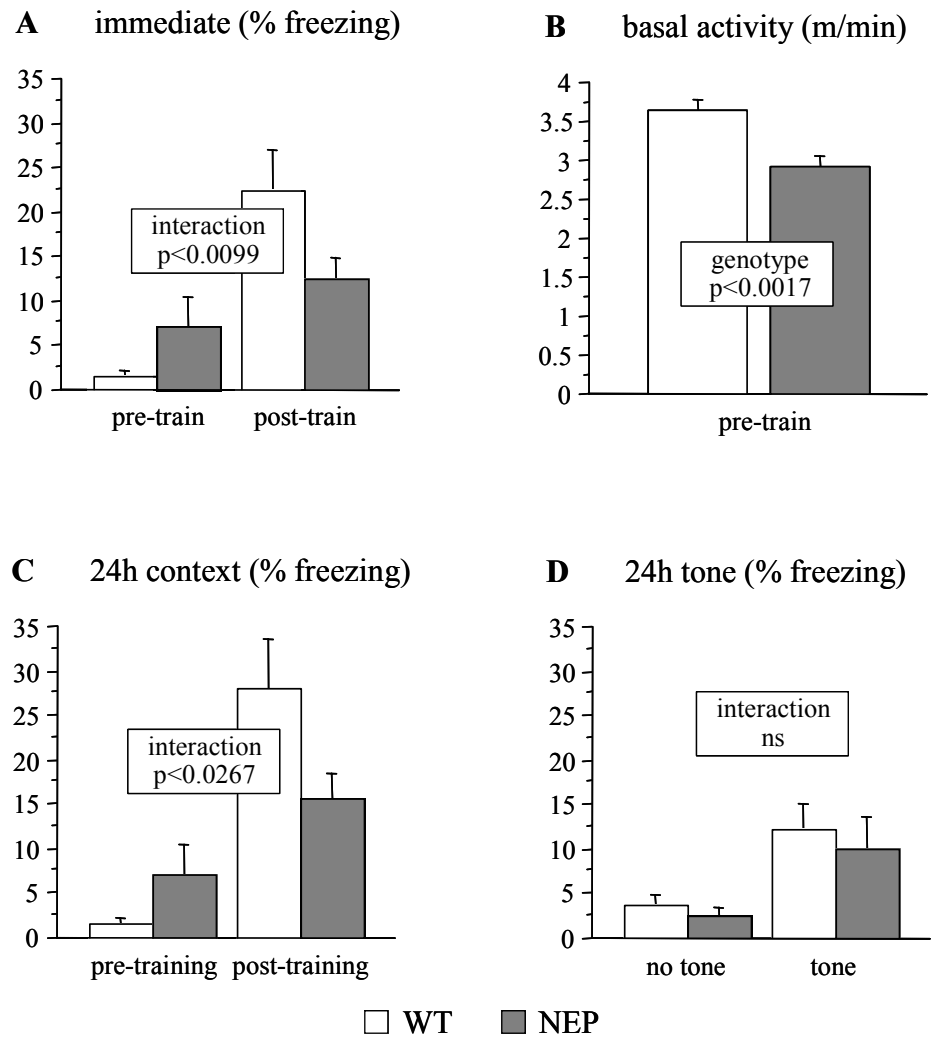

Figure 47. NEP mice were impaired in contextual fear conditioning. (**A**) WT mice showed little pre-training freezing and a clear training response when observed in the conditioning chamber immediately after training. NEP mice froze more before training and lacked a significant training effect. (**B**) NEP mice moved a significantly shorter distance during pre-training baseline recording. (**C**) Both training effect in WT and impairment of NEP mice persisted during a retest 24 h after training. (**D**) Freezing responses to the tone after 24 h were similarly weak in both groups despite a clearly observable reaction to the tone in most animals. Values represent the mean ± SEM. ns (not significant) is mentioned when $p>0.1$.

IV) DISCUSSION

1) *In vivo* effect of neprilysin deficiency

The analysis of NEP KO mice showed that neprilysin deficiency led to elevated Aβ levels and deposition of amyloid-like deposits in the brain accompanied by neurodegeneration and behavioral deficits. Western blotting with anti-APP antibodies revealed no changes in the amount of full length APP in neprilysin deleted mice. This data is confirmed by previous findings that neprilysin hydrolyzes Aβ without affecting APP metabolism [303] and that newborn and adult NEP-/- mice are normal, suggesting that the enzyme is not necessary for embryonic development, presumably due to the redundancy of the enzyme activity [314]. Taken together these results suggest that neprilysin upregulation as a therapeutic intervention would not affect APP processing and would probably not interfere with any yet unknown physiological functions of APP.

Total brain Aβ concentrations of NEP KO mice were twofold higher than the corresponding levels of WT littermates. A 1.5-fold increase in brain Aβ content of mice carrying a familial AD-causing presenilin 1 gene mutation leads to AD-like pathology in mice [486-488]. Thus, the increase in Aβ caused by neprilysin deficiency in our study was comparable to that caused by presenilin mutations. Interestingly, neprilysin deficiency seemed not to affect the levels of other NEP substrates; the enkephalin levels in brains NEP KO mice were reported to be normal [489], indicating that neprilysin paucity is compensated by other mechanisms in the case of enkephalin metabolism [488]. Similarly, neprilysin deficiency did not seem to alter the levels of somatostatin, cholecystokinin and substance P in the hippocampal formation and cerebral cortex (Iwata and Saido, unpublished observations). The fact that NEP KO and NEP+/- mice exhibited similar brain Aβ concentrations strengths the hypothesis that a partial reduction of NEP activity, which could be caused by aging [396, 397], will promote Aβ deposition in the brain [488]. These data are in concert with a report describing the selective reduction of neprilysin expression in brains with sporadic AD, particularly in high plaque regions such as hippocampus and temporal gyrus [490]. Moreover, we found that neprilysin depletion compromised the neuronal integrity as we found signs of neurodegenerartion in hippocampi of aged NEP KO mice. These findings are supported by the report of an impairment of hippocampal long-term potentiation (LTP) in NEP KO APP transgenic mice

(Haung, S.M. et al. Ann. Meeting of Soc. for Neurosci. San Diego, CA. Program no. 220.5 (2004)) and that soluble Aβ impairs hippocampal LTP in rats *in vivo* [133, 491]. Similarly, accumulation of Aβ in brains of transgenic mice expressing AD-related APP and presenilin mutations caused massive neuronal loss in the hippocampus [492-494], reconfirming that high Aβ levels are toxic to neurons *in vivo*.

Most current transgenic models of amyloid pathology that exhibit high brain Aβ levels and behavioral deficits, overexpress AD-causing human APP [495-497]. Therefore, the observed pathology and behavioral impairments in those models can, at least partially, be attributed to high levels of APP transgene and its processing products. In contrast to those studies, utilizing mice with unphysiologically high transgenic expression of AD-causing mutated forms of human APP, we employed mice with normal APP levels. The 4G8 positive amyloid deposits found in neprilysin deficient brains differed from the amyloid plaques exhibited by most AD mouse models overexpressing human AD, probably because in the neprilysin deficient mouse brains the murine Aβ, which is accumulated, is much less amyloidogenic than the human Aβ. Taken together, our results show that neurodegeneration and behavioral deficiencies can be caused by sole accumulation of Aβ in the brains. The presence of stained murine Aβ plaques and the association with intraneuronal fibrillar structure strongly suggest that neprilysin deletion leads to murine Aβ fibrillization and plaque formation. We can not exclude the theorical possibility that neprilysin deletion could lead to the fibrillization of another another substrate of neprilysin which will be immunolocalized with Aβ in these brains. Nevertheless, none of the other substrate of neprilysin is known to fibrillize *in vivo*. The confirmation of Aβ as the main component of these fibrillar structures will have to be confirmed by immunoelectron microscopy.

To test the hypothesis whether high brain Aβ levels are detrimental to neuronal function *in vivo*, the effects of Aβ accumulation in the brains were tested by subjecting the mice to CTA, an associative learning paradigm. Neprilysin deficient mice exhibited a significant two fold increase in brain Aβ levels and were significantly impaired in CTA, a measure for cognitive performance [498]. These data are in accord with a report showing that aged TgCRND8 mice, overexpressing the KM670/671 and the V717F mutations of human APP in neurons, are impaired in CTA learning and memory performance [499]. In addition, AD patients exhibit impairments at all levels of gustatory information processing. Significant losses in the ability to detect the taste of glutamic acid and to recognize olfactory stimuli were found in demented AD patients when compared with age-matched controls [500-502].

The impairment of CTA in NEP KO and NEP+/- mice, exhibiting high levels of brain Aβ, stresses the specificity of the observed effects. These differences could not be caused by a reduction in neophobia, increased inborn preference for the sweet saccharin solution or reduced inborn aversion for an aversively (bitter) tasting solution, because no genotype differences could be found with respect to all these three traits. Lesions of the basolateral nuclei of the amygdala (BLA) have a general effect on the response to novel stimuli by decreasing neophobia [503]. A large body of literature supports among other areas [504], an important involvement of the amygdala in CTA [504-507] . More specifically, the central and basolateral nuclei of the amygdala are respectively involved in the acquisition and extinction of the CTA [508]. The BLA were also proposed to modulate memory consolidation via projections to brain regions involved in consolidating lasting memory, including the hippocampus, caudate nucleus, nucleus basalis and cortex [509]. Accumulation of Aβ in the amygdala and the subsequent disruption of the pathways involved in CTA could be responsible for the decreased learning and memory observed in NEP KO and NEP+/- mice during CTA. Because Aβ is increased in various areas of NEP deficient brains including amygdala and hippocampus [488], it is conceivable that Aβ accumulation may be responsible for the observed behavioral changes in these mice. It is possible that other substrates of neprilysin, whose levels may be modified, can act on the brain areas implicated in learning and memory of the CTA, or decrease the LiCl-induced nausea. Among them, substance P, whose level was increased in the colon of NEP KO mice [351], is a nociceptor [510-512] which is also thought to play a key role in emetic responses [513, 514]. While substance P is localized within both the vagal afferent nerve fibres and brainstem emetic circuitry [515-517] its intravenous injection induces nausea and vomiting [518]. Therefore, antagonists of the substance P/neurokinin 1 receptor are now used to prevent and delay chemotherapy-induced nausea and vomiting [513]. The potential increase of substance P levels in mice due to decreased neprilysin activity would be expected to increase LiCl-induced nausea and strength the CTA. On the contrary, a decreased CTA is observed in NEP KO and NEP+/- mice. These data suggest that alteration of substance P levels was not involved in learning and memory of the CTA and that the impairment of neprilysin deficient mice observed in CTA is a sensitive measure of altered neuronal function in brain areas involved in CTA [504] in response to accumulation of endogenous murine Aβ in these brains.

It is well known that Aβ production is intracellular [519, 520] and its intraneuronal accumulation may precede plaque formation in AD brains as well as in a transgenic mouse model of AD [519, 521, 522], suggesting that sole accumulation of Aβ in brains impairs

neuronal function. Because we did not find any amyloid-like deposits in the amygdala of these mice, we hypothesize that Aβ accumulation in brain nuclei without the obvious induction of amyloid deposits may influence their functioning and induce cognitive deficits associated with AD. Indeed, soluble oligomers of Aβ were shown to induce cognitive deficits and were proposed to be one of the major toxic Aβ species *in vivo* [134, 226, 491].

This is, to our knowledge, the first study identifying murine Aβ plaque-like structures in mouse brains. In addition, our study shows that insufficient removal of Aβ from the brain, even without increasing physiological levels of APP, led to chronic accumulation of Aβ, to signs of neurodegeneration and to behavioral abnormalities. Our data support the idea that decrease of neprilysin level observed with aging [396, 397] and in vulnerable brain areas of AD patients [391, 392] may contribute to the AD pathology and strenght that brain specific elevation of neprilysin levels may prove to be useful in anti-Aβ therapies.

2) Aβ-related increase of neprilysin level

It was found in our laboratory that injection of synthetic fibrillar $A\beta_{1-42}$ into mouse brains, but not PBS or synthetic fibrillar $A\beta_{42-1}$, caused sustained increases in brain levels of neprilysin from 3 to at least of 20 weeks after injection [406]. These increases were associated with a dramatic reduction in brain tissue levels of Aβ, as well as prevention of amyloid plaque formation and reduced astrogliosos in a mouse model of amyloidosis 20 weeks after injection [406]. The mechanism that linked $A\beta_{1-42}$ to increased NEP level is unknown. The data favored the possibility of a transcriptional activation of NEP gene expression in response to injections, and a sustained stimulation of this mechanism by highly insoluble $A\beta_{1-42}$ aggregates, ensuring a long-term elevation of NEP protein levels in the brain. This scenario is supported by the fact that the synthetic Aβ aggregates injected into mouse brains were remarkably stable over 20 weeks following the injection and seem to be resistant to the clearing mechanism triggered, constantly causing the induction of the unknown signal for the NEP upregulation. This is consistent with other studies showing that aggregated Aβ is still detected at the injection site months after the injection [523-527] and may constitute local reservoirs of smaller and biologically active polymers and oligomers of Aβ which may be released and associate with brain cells, including vessels [527]. In contrast, intracranial injected soluble Aβ species are quickly cleared from the brain within minutes [317, 528], possibly via degradation [317] and receptor-mediated transport through ventricle and choroid

plexus cells [529, 530]. Furthermore, neprilysin mRNA was significantly increased by $A\beta_{1-42}$ injection but not PBS or $A\beta_{42-1}$, 20 weeks after injection [406]. Neprilysin is the major rate limiting Aβ-degrading enzyme (reviewed in [230]). While lots of evidences, including our own data, show that decrease of neprilysin mRNA and protein may contribute to AD pathology by promoting Aβ accumulation [229, 317, 391, 392, 396], neprilysin overexpression was shown by others and by us to prevent Aβ accumulation, its associated cytopathology and Aβ-related memory deficits [403, 405, 531].

Substance P and somatostatin, two substrates of neprilysin, were found to regulate neprilysin activity *in vitro* [532-534]. Based on their mode of action, it was hypothesized that this feed back loop regulation involved activation of G-protein-coupled receptors [387, 532]. Lack of somatostatin in the brain of somatostatin deficient mice was further associated with a decrease of neprilysin activity *in vivo* [532]. As a major substrate of neprilysin, the observed $A\beta_{1-42}$-related increase of neprilysin protein may involve a similar feedback loop via one of the numerous potential Aβ receptors and activated mechanisms (reviewed in [119, 535]). Determination of the pathway responsible for the Aβ-related upregulation of neprilysin mRNA and protein level could be of major interest for AD therapy and may involve few side effects since this pathway would be naturally activated by Aβ accumulation *in vivo*.

To investigate the transcriptional regulation of neprilysin and the $A\beta_{1-42}$-related upregulation of neprilysin expression observed *in vivo*, we attempted to establish an *in vitro* model, which would allow the biochemical analysis of the pathways and transcription factors involved. Because of high neprilysin expression in the kidney [240], the effect of aggregated Aβ on neprilysin transcription was first analyzed in a human embryonic kidney cell line (293T cells). Since immunohistochemical detection of neprilysin protein illustrated a neuronal localization *in vivo*, the human neuroblastoma SH-SY5Y cells, which can be differentiated into neurons, were also tested.

We took advantage of the high sensitivity of the luciferase assay system to measure the effect of Aβ on the activity of the three neprilysin promoters. The cells were transfected with a plasmid expressing firefly luciferase under the control of one of the three promoters of neprilysin (pN1, pN2 or pN3) and the effects of aggregated synthetic $A\beta_{1-42}$ or $A\beta_{42-1}$ incubation on the luciferase activity which corresponds to the neprilysin promoter activity was analyzed. The luciferase activity was initially normalized by the protein concentration of the sample analyzed and non consistent results were obtained. We postulated that small variability caused by differences in transfection efficiencies between wells could have caused

or hidden the Aβ-related effects observed. Therefore, we used a new protocol which involved simultaneous transfection of a control plasmid expressing renilla luciferase under the control of the constitutively active pRLTK promoter, with the plasmid expressing firefly luciferase under the control of the neprilysin promoters. Normalization of the firefly luciferase activity with the renilla luciferase activity took the transfection efficiency of each well into account. Stable transfection of the cell lines was not performed due to an observed increase stability of the luciferase protein over time, which could have hidden the potential small Aβ-related increase of neprilysin promoter activation.

To find out whether addition of aggregated $A\beta_{1-42}$ activates neprilysin promoters *in vitro* and determine the optimal parameters, different concentrations of aggregated $A\beta_{1-42}$ and $A\beta_{42-1}$ and different time points, which did not compromise the viability of the cells, were tested. In spite of initial small irreproducible Aβ-related increase of neprilysin promoter activities which could have been due to variability of the normalization that did not take into account transfection efficiency, $A\beta_{1-42}$ incubation did not affect neprilysin promoter activity in 293T and undifferentiated SH-SY5Y cells when compared to $A\beta_{42-1}$ and PBS treated cultures. Therefore, these cellular systems did not allow further investigation of the potential transcription factors involved. Analysis of $A\beta_{1-42}$ effect on neprilysin transcription activity in differentiated SH-SY5Y cells was also discarded due to the many fold increases of all three neprilysin promoters' activities after RA incubation , the first agent used to differentiate SH-SY5Y cells. Our data, therefore, suggest that these two cell lines are not good models for studying the Aβ-related increased neprilysin transcription observed *in vivo*.

Based on the *in vivo* data showing that biochemically induced upregulation of neprilysin by intracranial injection of aggregated $A\beta_{1-42}$ was not only found in the vicinity of the injection site but also in the contralateral hemisphere, we hypothesized that the $A\beta_{1-42}$-related increase of neprilysin mRNA and protein levels could involve a diffusible factor activated by the injection of Aβ. Aβ is known to trigger inflammation by activation of microglia and astrocytes cells leading to secretion of various diffusible factors, including cytokines such as IL-1β, IL-6 or TNFα [119, 536, 537] mainly involving the microglia cells. Intracranial injection of aggregated Aβ and its long term deposit around the injection site was shown by several other groups to have similar effects *in vivo* [523-525, 538]. One week after intracranial injection of $A\beta_{1-42}$, $A\beta_{42-1}$ and PBS, a four fold increase of neprilysin mRNA associated with an increase of protein levels was observed when compared to non-injected control mice [406]. Damage of the brain tissue, disruption of the blood brain barrier and consequences which followed including microglia and astrocytes activation may have

activated neprilysin transcription and increased its protein levels. Among the diffusible factors released by activated microglia, cytokines such as IL-1α, IL-1β, IL-6 or TNFα were already shown to increase neprilysin transcription and protein levels in different cell culture models via pathways involving cAMP signaling pathway [245, 256] in addition to increasing glucocorticoid-induced transcriptional activity [539, 540].

We first investigated the potential involvement of a microglia diffusible factor *in vitro.* We measured the activity of the neprilysin promoters in 293T cells after incubation with conditioned medium of a microglia cell line previously cultured in presence or absence of $A\beta_{1-42}$, or conditioned medium from 293T cells cultured in absence of $A\beta_{1-42}$. No effect on neprilysin transcription was observed, suggesting that the cytokines secreted by the microglia cell line, during normal conditions and under Aβ stress, did not affect neprilysin transcription in a kidney cell line. We could not, however, study whether 293T cell line express the necessary receptors and pathways to mediate the effect of the microglia-derived factors. To confirm the absence of role from these cytokines, we further analyzed their levels *in vivo*, 20 weeks after injection in the brain of WT mice, when $A\beta_{1-42}$ specifically induced an increase of neprilysin mRNA and protein levels. No difference in a cytokine array including IL-1α, IL-1β, IL-6 and TNFα were observed when comparing $A\beta_{1-42}$ and $A\beta_{42-1}$ injected mice. This does not exclude the potential role of these factors in the non-specific Aβ increase of neprilysin level one week after injection but suggests that they are not involved in the $A\beta_{1-42}$ specific effects observed after longer post-injection time.

To focus our search of an *in vitro* model we decided to determine the promoter(s) involved in the upregulation of neprilysin observed after $A\beta_{1-42}$ injection *in vivo*. New groups of mice were injected with $A\beta_{1-42}$, $A\beta_{42-1}$ or PBS and brain neprilysin mRNA and protein levels were analyzed 20 weeks after injection. A specific $A\beta_{1-42}$-related increase of neprilysin protein level was observed. However, total neprilysin mRNA levels were not changed in the brain of $A\beta_{1-42}$ injected mice when compared to PBS and $A\beta_{42-1}$ injected groups.

Since each one of the three neprilysin promoters lead to the transcription of a specific but non-coding exon, the activity of the three promoters was investigated by RT-PCR using specific primers recognizing each of the three non-coding exons. Similar to the total neprilysin mRNA level, we did not find any variation of mRNA levels specific for the activity of the three promoters of neprilysin when comparing the $A\beta_{1-42}$ and $A\beta_{42-1}$ injected group in spite of a clear $A\beta_{1-42}$-related upregulation of the neprilysin protein level. These data suggest that the upregulation of neprilysin protein level associated with intracranial injection

of fibrillar $A\beta_{1-42}$ does not require an increase of neprilysin transcription. Furthermore, careful analysis of the 20 weeks post injection groups, which previously illustrated the $A\beta_{1-42}$ specific increase of neprilysin mRNA, suggests that the increase of mRNA does not correlate with the increase of protein level. Indeed, while similar increase of mRNA levels were observed in the 4 mice of the original $A\beta_{1-42}$ treated group, only 2 showed a clear increase of neprilysin protein level [406]. Considering the precedent results, we extrapolated that two pathways may be responsible for the $A\beta_{1-42}$-related increase of neprilysin protein level: The first one implicates increased activation of neprilysin promoters, leading to an increase of mRNA and protein levels. Specific parameters such as incubation time, macromolecular identity of the injected aggregates and unknown diffusible factors are involved. The second pathway appears to be independent of neprilysin promoter activation and may be due to an increased stability of the neprilysin protein.

3) All trans retinoic acid and neprilysin transcription

In this work, RA incubation was used to differentiate the SH-SY5Y cells into neurons. Unexpectively, this treatment enhanced the activity of all three neprilysin promoters.

RA treatment of SH-SY5Y cells was previously shown to increase transcription of important proteins involved in APP processing including APP [153, 541-544], presenilin [545] and ADAM10 [546]. A recent study reported that such a treatment also increased APP and APLPs protein levels with increased release of sAPPα, no effect on C99 levels and increased levels of AICD [543]. They suggested that RA shifted the APP processing in favor of the α-secretase pathway and therefore could be beneficial in AD therapy. Interestingly, AICD from APP-like proteins (APP, APLP1, and APLP2), whose protein levels are increased after RA incubation of SH-SY5Y cells, were shown to transactivate neprilysin promoters leading to an increase of protein and activity levels *in vitro* and *in vivo* [547]. The use of APLP KO SH-SY5Y cells or incubation with presenilin inhibitors could confirm the potential role of AICDs in the observed increase of neprilysin transcription.

All three neprilysin promoters were highly activated by RA. While promoter 3 of neprilysin present three potential binding sites for retinoic acid receptors, neprilysin promoters 1 and 2 do not contain such potential binding sites for transcription factors related to retinoic acid like retinoic acid receptors or retinoid X receptors. Therefore, we could not speculate that the

increase of neprilysin transcription was due to direct effect of RA or activation of other transcriptional pathways activated by RA rather than the differentiation process.

The effect of RA incubation was confirmed in 293T cells which are not known to be differentiated by RA and presented no variation in cell proliferation rate and cell morphology during RA incubation. Again, all three neprilysin promoters were activated by RA incubation. Moreover, RA incubation also led to an increase of endogenous neprilysin protein level, providing the evidence for the specific activation of neprilysin promoters by RA in these culture systems.

Retinoic acid isomers were also shown to protect hippocampal neurons from oxidative damage [548] and Aβ-induced neurodegeneration [549], inhibiting the Aβ aggregation and destabilizing preformed Aβ fibrils [550]. From our *in vitro* data showing that RA increases neprilysin transcription and protein levels, we extrapolate that the neuroprotective effect of RA observed against Aβ toxicity may also be in part due to increased neprilysin protein levels which would lead to Aβ degradation [401, 551].

Previous studies have shown the importance of retinoid signalling in the adult brain and it has been hypothesized, based on genetic and dietary data, that defective retinoid transport and function may contribute to LOAD [552]. Dietary deficiency of vitamin A in rodents affected LTP, synaptic plasticity [553, 554] and induced reversible learning and memory impairments [555-557], all reversed by addition of retinoids in the diet.

The role of vitamin A in the pathology of AD, however, remains unclear. Retinoids levels appeared similar in normal and AD brain in spite of increased synthesis in the hippocampus [558]. Conversely, plasma levels were depleted in AD patients and subjects with mild cognitive impairment [559-561]. Vitamin A deficiency also caused deposition of Aβ in the brain of WT rats [562].

To determine if RA could also increase neprilysin protein level *in vivo* and therefore be a potential therapeutic approach for AD, we chronically treated the mice with RA during 5 days. However, the brain level of neprilysin protein was not affected by this treatment.

The concentration of RA is actively regulated at the blood brain barrier *in vivo* [563] and injection of similar RA concentrations were shown to restore decreased retinoid receptor levels in the brain of aging mice and to alleviate their memory deficit [555]. Possible explanations for the lack of effects on neprilysin protein level *in vivo* include the permeability of the blood brain barrier to RA and reequilibration of its brain level limiting its action.

We have also implanted subcutaneously RA tablettes releasing a constant RA level every day during 3 weeks in WT and transgenic mouse models of amyloidosis. Effect of RA on

neprilysin level and APP processing including Aβ production is currently under investigation. Due to its general function as a gene regulator, RA was found to regulate directly and indirectly hundreds of genes [564, 565] and therefore, its overexpression may lead to various side effects. However, RA and analogs have been used systemically in therapies against cancers [566-568] and acne [569, 570] and low and high consumption of vitamin A reached via specific diet, allow to apprehend the potential side effects [571-573]. Due to the involvement of the retinoid signalling pathways in regulating synaptic plasticity and associated learning and memory behaviors, increase of retinoid levels easily reachable via a proper diet, may be a promissing approach against the pathophysiology of AD.

4) Aβ activated the plasminogen system *in vitro* and *in vivo*

Since intracranial injection of synthetic fibrillar $A\beta_{1-42}$ caused a sustained increase of the major Aβ degrading enzyme, neprilysin [230], we hypothesized that this effect could have been a part of a general feedback loop and that this injection could have also triggered the activation of other pathways known to degrade Aβ. We further speculated that these pathways could also contribute to Aβ removal from the brain and the observed prevention of amyloid plaque and the associated cytopathology.

Brain tissue levels of IDE, ACE and the metalloprotease 3.4.24.15, which were all shown to be involved in Aβ degradation, were previously found unchanged in response to $A\beta_{1-42}$ injections [406]. However, when the activity of plasmin, another Aβ degrading enzyme [422, 447], was analyzed, a 5 fold increased activity was found 20 weeks post-injection in the brain of mice which received the $A\beta_{1-42}$ injection when compared to PBS and $A\beta_{42-1}$ injected mice. Plasmin deficiency led to increased time necessary for removal of intracranial injected $A\beta_{1-42}$ and pathological consequences [422]. The increase of plasmin activity can therefore be responsible, in part, for the observed Aβ degradation. To investigate the pathway involved in the activation of plasmin, the activity of its two known activators, uPA and tPA was determined. While tPA activity remained unchanged, uPA activity was highly increased in the brain of mice 12 and 20 weeks after $A\beta_{1-42}$ injection but almost absent in the brain of mice which received other treatments. These data strongly suggest that uPA was responsible for the observed $A\beta_{1-42}$-related increase of plasmin activity.

After $A\beta_{1-42}$ injection, uPA activity was mainly localized in the cell layers of the meninges but also detectable in neurons of the hippocampal CA1 region and dentate gyrus. Our *in vivo*

data are in agreement with previous studies showing that Aβ can stimulate the expression of uPA and its receptor with increase of uPA activity in human cerebrovascular smooth muscle cells [449]. Increase of uPA activity and the following activation of plasminogen further inhibited Aβ neurotoxicity and fibrillogenesis *in vitro* [450]. While the Aβ activated pathway leading to increase of uPA activity is unknown, cytokines including IL-1α, IL-1β, TNFα and other factors such as bFGF, IFNγ, IGF-I and IGF-II were shown to modulate uPA expression and protein level of uPA and uPAR in different *in vitro* systems [574-580]. Aβ is known to increase transcription and protein levels of some of these factors including IL-1, TNFα [537, 581, 582]. However, no variation in the levels of bFGF, IFNγ, IL-1α, TNFα or IGF-II were observed in the brain homogenates of the mice which received $A\beta_{1-42}$ and $A\beta_{42-1}$ injections and therefore, the role of these factors should be excluded. In coherence with this, the mRNA levels of uPA, uPAR and tPA were not affected in treated brains. Taken together these data suggest that the observed increase of uPA activity was not due to an increased transcription of uPA and may involve an increased stability of the protein and/or decreased levels of uPA inhibitors. However, since plasminogen activator inhibitors (PAI) inhibit similarly uPA and tPA activity, the absence of variation in tPA activity suggests that decreased levels of PAI are unlikely to be involved in the observed increase of uPA activity.

In spite of contradictory studies, uPA has been associated with LOAD [454, 455] and its decreased activity could lead to the decreased plasmin activity observed in AD patients [451, 453] and therefore create an imbalance in brain Aβ levels in favor of its production.

Furthermore, uPA can lead to degradation of Aβ via activation of plasminogen [450] and can activate many intracellular pathways via binding to its receptor [442, 443]. We decided to investigate uPA as a potential candidate promoting Aβ degradation. Published uPA transgenic mice [583, 584] unfortunately lost their brain uPA overexpression due to unknown factors with increasing generation, hampering the evaluation of uPA overexpression effect on Aβ level *in vivo*. On the other hand, we found that in uPA KO mice, the brain levels of murine Aβ were unchanged compared to brain from mice with a similar background as confirmed by a recent study [454]. It suggests that uPA is not by itself an important Aβ-degrading enzyme *in vivo*.

Interestingly, uPA activity closely correlated with neprilysin protein levels after $A\beta_{1-42}$ injection. No direct link between these two proteins was ever published. However, these proteins play an opposite role in cancer development and cell migration and their transcription is activated by similar cytokines *in vitro* [245, 256, 576, 577]. 20 weeks after

injection, $A\beta_{1-42}$ did not affect the levels of these cytokines and the transcription of uPA, uPAR and neprilysin in the brain of the mice when compared to $A\beta_{42-1}$ injected mice, suggesting that the increase of uPA activity and neprilysin level were not due to increased transcription and did not involve the factors analyzed. We then hypothesized that uPA activity and neprilysin protein level may be directly linked via increased protein stability.

Since the lack of mice overexpressing uPA in the brain did not allow us to investigate if upregulation of neprilysin protein level could be due to the increased uPA activity, we first tried to reproduce the results *in vitro*. $A\beta_{1-42}$ strongly increased uPA activities in SH-SY5Y cells, MIC cells and primary neuronal cultures. However, tPA activity was also increased suggesting that incubation with aggregated $A\beta_{1-42}$ resulted in a general activation of the plasminogen system *in vitro*. Interestingly, $A\beta_{1-42}$ incubation increased plasminogen activators activity in all *in vitro* models tested suggesting that the pathway involved was broadly present.

Since tPA can be activated by direct contact with aggregated Aβ, we also analyzed the effect of $A\beta_{42-1}$,which is a non physiological protein and aggregates less easily than $A\beta_{1-42}$. $A\beta_{42-1}$ incubation also increased with less extend uPA and tPA activity. This suggests that the $A\beta_{1-42}$-related increase of plasminogen activators activity may be due, in part, to the aggregation state of aggregated Aβ. Indeed, it is possible that binding of Aβ, or $A\beta_{1-42}$, to tPA leads to plasminogen activation and plasmin generation which is known to cleave and activate among others uPA [585]. $A\beta_{1-42}$-related increase of uPA activity in absence of tPA activity in MIC cultures suggests that increased uPA activity is not a consequence of unspecific tPA-plasminogen pathway activation. However, whether or not a sub-threshold activation of tPA takes place in these cells and would lead to increase uPA activity should be confirmed using tPA KO cell lines.

To determine if the increase of neprilysin protein level *in vivo* could be due to the Aβ-related increase of uPA activity, neprilysin protein levels were quantified after Aβ treatment in MIC cells which lacked detectable tPA activity and primary neuronal cultures since Aβ-related increase of neprilysin protein level was observed in neurons. Levels of neprilysin were unchanged by the treatment and therefore did not correlate with the $A\beta_{1-42}$-related increase of uPA activity. We concluded that increase of uPA activity observed was not responsible for the increased levels of neprilysin *in vitro*. A direct link between uPA activity and neprilysin protein level could be confirmed by investigation of brain uPA activity and neprilysin protein level after intracranial $A\beta_{1-42}$ injection in uPA KO mice and NEP KO mice compared to WT

littermates. The brain localization of the uPA activity and the potential neuronal colocalization with neprilysin could be investigated in the $A\beta_{1-42}$ injected WT mice.

To assess if increased uPA activity could be due to the increased neprilysin protein level and activity, plasminogen activators' activities were analyzed in the brain of NEP mice overexpressing neprilysin in brain neurons and presenting an increase of brain neprilysin activity. Both uPA and tPA activities were increased in frontal cortex and hippocampus of the NEP mice when compared to WT littermates. Therefore, transgenic overexpression of neprilysin in neurons induces increase of plasminogen activators activity. These data suggest in two unrelated *in vivo* systems that an elevation of neprilysin protein and activity increases uPA activity. Plasmin activity has to be determined in the brain of NEP mice and WT controls to establish a link between neprilysin and the activation of the plasminogen system *in vivo*. Indeed, the increase of tPA activity observed in the brain of NEP mice can also be explained by the the neprilysin induced increase of uPA activity and subsequent plasmin activation. Differences in adaptation mechanisms may also explain the difference observed in tPA activity between our two *in vivo* systems exhibiting a neuronal neprilysin upregulation after $A\beta_{1-42}$ injection or lifelong transgenic overexpression.

Neprilysin and uPA/uPAR complex are known to have opposite effects on cell migration and proliferation. While neprilysin prevent them by inhibiting the Akt and FAK pathways [373, 586, 587], uPA/uPAR complexes activate them [443, 588-590]. Neprilysin can act on cell migration via different pathways (reviewed in [586]): Neprilysin degrades neuropeptides such as bombesin endothelin-1 or bradykinins, which can activate, after binding to their receptors, Src phosphorylation leading to direct association and activation of FAK [372, 373], normaly resulting in cell migration. Binding to their receptors can also stimulate the phosphorylation and activation of growth factor receptors such as EGFR and IGFR [591-593] which bind and activate the PI3 kinase resulting in Akt and FAK signalling activation. Neprilysin also indirectly associates with the regulatory subunit p85 of the PI3 kinase through lyn kinase, thus inhibiting the interaction of the PI3 kinase with integrin and FAK. Neprilysin was finally shown to bind to ezrin/radixin/moesin (ERM) proteins limiting the interaction of this complex with CD44 and the subsequent cell mobility activation. On the contrary, the uPA/uPAR complex also contains the lyn kinase [594, 595] and activates the PI3 kinase which induce Akt and FAK activation leading to cell proliferation and migration. The intracellular signalling pathway induced by the uPA/uPAR complex can also be modulated by binding and activation of EGFR, IGFR, integrin or CD44 [443, 595-598].

The neuronal overexpression of neprilysin in the NEP mice may result in PI3 kinase inhibition. It was shown in endothelial cells that inhibition of PI3 kinase could lead to an increased FGF-2-mediated uPA production [599]. It is conceivable that, if in the brain, PI3 kinase activation level is regulated, its inhibition via high levels of neprilysin could lead to activation of pathways such as the uPA/uPAR complex which may counteract neprilysin effects. Decreased availability of proteins such as lyn kinase may also prolong the life of the uPA/uPAR complex prior to internalization and degradation with decreased activation of the intracellular signalling pathways but increased uPA activity.

Transgenic overexpression of neprilysin may also result in decreased levels of other enzymes competing for similar substrates. For example, the protein levels of IDE, another Aβ degrading enzyme, were decreased in the brain of a transgenic mouse overexpressing neprilysin in neurons [405]. IDE also degrades insulin and TGFα [600-603], two activators of uPA or uPA/uPAR signalling *in vitro* [604, 605]. Inhibition of ACE by a similar regulation or by increased level of neprilysin cleavage products, such as substance P (1-6) [606] or angiotensin (1-7) [607], can also lead to increased levels of bradykinin [608, 609] which was shown to decrease expression and protein levels of PAI with subsequent increase of plasminogen activators activity [610]. However, brain levels of substance P, enkephalin and somatostatin are unchanged in our NEP mice and in NEP KO brains (Iwata and Saido, unpublished data). All together, these data suggest that either these neuropeptides are not good neprilysin substrates or that the levels of these neuropeptides are tightly regulated with neprilysin dependant degradation being prevented or compensated by increased synthesis *in vivo*. Tachykinin levels are regulated in part by the kallikrein-kinin System which can release tachykinins by cleavage of precursors (reviewed in [611]). Interestingly, kallikreins were also shown to cleave pro-uPA [439, 441] and to inhibit PAI functions [612]. Activation of such a pathway may also explain the increase of uPA and tPA activity in NEP mice. It will be interesting to investigate the physiological relevance of these different pathways in the neprilysin-related increase of plasminogen activators activities observed *in vivo*.

5) Neprilysin as a potential therapeutical approach in AD

5.1 Biochemical analysis of the mice

During this thesis, transgenic mice with neuronal expression of neprilysin (NEP mice) were generated and analyzed. We found that the transgenic neprilysin overexpression in mouse brains was associated with increased neprilysin activity and reduced levels of total Aβ and both $A\beta_{1-40}$ and $A\beta_{1-42}$ when our NEP mice were bred with J20 mice, a mouse model for amyloidosis which overexpressed mutated AD-causing APP in neurons. Furthermore, no alteration of APP levels or its CTF was found in the NEPxJ20 double transgenic as compared to J20 mice, emphasizing that removal of Aβ by a NEP-dependent mechanism would not interfere with processing and physiological function of APP. These data strengths similar observations including ours using genetic deletion [229], viral [403, 531] and transgenic neprilysin overexpression [405] which confirmed neprilysin as a major rate limiting Aβ-degrading enzyme [230] and showed that its overexpression could decrease Aβ levels, prevent plaque formation and its associated glial activation without modification of APP level [303, 405].

Degree of astrocytes or microglia activation was not affected by neprilysin or mutated APP overexpression, confirming our previous data that glial activation depends mostly on amyloid plaque pathology in AD mouse models [613, 614].

Sequential extraction of Aβ and use of specific ELISA systems recognizing $A\beta_{40}$ and $A\beta_{42}$ showed that neprilysin acted differentially on Aβ species depending on their aggregation state: While triton soluble Aβ species presented a similar 70% decrease for $A\beta_{42}$ and $A\beta_{40}$ levels, SDS soluble Aβ species levels were differently affected by neprilysin overexpression. Neprilysin overexpression prevented more efficiently the aggregation of $A\beta_{42}$ species rather than $A\beta_{40}$ species in the SDS fraction with 70% and 50% decrease, respectively.

Our finding that neprilysin overexpression prevented the formation of $A\beta_{42}$ in a similar manner in the triton and the SDS fraction is consistent with the concept of equilibrium between the different aggregation states of Aβ. Consistent with our data suggesting a decreased efficiency of $A\beta_{40}$ hydrolysis by neprilysin compared to $A\beta_{42}$ species, levels of $A\beta_{40}$ species were less decreased than $A\beta_{42}$ species in another neprilysin overexpressing mouse model [405]. Infusion of the neprilysin inhibitor, thiorphan, similarly increased brain $A\beta_{42}$ levels without affecting $A\beta_{40}$ levels [317] and somatostatin deficient mice which present a reduced neprilysin activity also had a 50% increase of $A\beta_{42}$ levels without variation of $A\beta_{40}$

levels [532]. However, since the triton soluble $A\beta_{40}$ and $A\beta_{42}$ species were similarly decreased by neprilysin overexpression and only the formation of aggregated SDS soluble Aβ40 was less efficiently prevented compared to $A\beta_{42}$ species, we speculate that neprilysin degrade similarly soluble $A\beta_{40}$ and $A\beta_{42}$ species but that aggregation of Aβ present in the SDS fraction protected better $A\beta_{40}$ than $A\beta_{42}$ from neprilysin degradation.

Different studies suggested that oligomers of Aβ, rather than monomers, may be the real culprit in the pathology of AD [134, 226, 615]. The fact that neprilysin degrades mostly Aβ monomers and dimers [405] raised the question about the efficiency of neprilysin overexpression in AD therapy. However, Marr and colleagues [402] showed, using a lentivirus overexpressing neprilysin, that neprilysin overexpression in the brain could induce the degradation of aggregated Aβ including amyloid plaques, confirming *in vitro* data where neprilysin degraded both monomers and oligomers of $A\beta_{1-40}$ and $A\beta_{1-42}$ [331, 388]. Our data suggest that equilibrium exists between the different aggregation state of Aβ and that neprilysin can decrease the level of Aβ species independently on their aggregation state.

Neprilysin overexpression was shown to prevent Aβ accumulation and to degrade high levels of Aβ. Moreover, murine Aβ levels were also found decreased in neprilysin overexpressing mice suggesting that neprilysin has a physiological role in degrading Aβ and may decrease Aβ levels also in non pathological conditions [405].

The levels of substance P, enkephalin and somatostatin are reported to be generally decreased in the brain of AD patients [616-619] but also present an increased immunoreactivity associated with amyloid plaques in the brain of AD patients and mouse model of amyloidosis [620-625]. Neprilysin was shown to exhibit similar affinity for Aβ and for some of its other known substrates present in the brain such as substance P or enkephalin [294, 331]. Therefore, we determined the effect of neprilysin overexpression on substance P, enkephalin and somatostatin levels, three important brain neuropeptides shown to be degraded by neprilysin *in vitro* [279, 293, 300, 302] in our mouse models. The levels of substance P, enkephalin and somatostatin were not affected by overexpression of neprilysin and mutated APP. The absence of variation in our J20 mice can be explained by the weak pathology observed in our mice with absence of plaque formation, associated glia activation and neurodegeneration which are usually present in AD brains. Since murine Aβ levels were also found decreased in neprilysin overexpressing mice [405], our data suggest that Aβ is a better brain substrate for neprilysin than substance P, enkephalin or somatostatin *in vivo* and that overexpression of neprilysin would not interfere with the physiological functions of these neuropeptides. This is also coherent with data obtained in neprilysin deficient mice, which

present increased levels of Aβ ([229] and our data) without alteration of enkephalin [344] substance P or somatostatin levels (Iwata and Saido, unpublished data) in the brain. It is nevertheless possible that neprilysin overexpression led to non detectable decreased levels of these neuropeptides and microdialysis analysis will allow a better determination of neprilysin effect on these substrates and their functions.

Furthermore, Aβ levels in AD brains are 10^3-10^4 fold higher than those in normal brains without Aβ plaque pathology [626, 627] and neprilysin is able to degrade large amount of Aβ *in vivo* [317, 531]. Our data suggest that neprilysin preferentially degrades Aβ without altering the level of its other substrates and therefore put forward the hypothesis that neprilysin overexpression present a valid therapeutic approach against Aβ with little impact, if any, on APP procesing and the functions of its other substrates in the brain.

5.2 Behavioral consequences of neuronal neprilysin overexpression and potential prevention of Aβ-related behavioral deficits

Progressive cognitive impairment is one of the first and major symptoms in AD [6]. Multiple transgenic mice mainly overexpressing mutated APP were generated that reproduced both the amyloid deposition and progressive memory loss (reviewed in [628, 629]). Among them, the J20 mice, which neuronaly overexpress human APP with the Swedish and Indiana mutations, were previously published to present high brain levels of Aβ [70] with learning deficit in the Morris water maze paradigm at 7 months of age [69].

To determine the potential therapeutic effect of neuronal neprilysin overexpression in AD and confirm Aβ as the culprit of memory deficits in mouse models of amyloidosis, NEP mice overexpressing neprilysin in neurons were crossed with J20 mice and their progeny were analyzed in cognitive and non-cognitive tasks. Since AD patients also present behavioral impairments unrelated to cognition such as anxiety and depression [7-9, 630], we also investigated the behavioral phenotype caused by human mutated APP overexpression, and the therapeutic effect of neprilysin overexpression on non-cognitive parameters by using a comprehensive test battery covering not only cognitive skills but also exploration, anxiety and locomotor activities. A more complete analysis of the NEP mice and WT littermates was further performed to evaluate the potential side effects of neprilysin overexpression.

Genetic background can affect brain APP processing, Aβ deposition in mice [631] and behavior performances in WT [632] and APP transgenic mice [633]. Since both transgenes

were initially expressed in mice with different backgrounds, NEP males were bred with J20 females and only the male progeny was initially tested in the 7 months cohort. This approach allowed us to decrease the variability induced by sexual dimorphism [634, 635] and aleatory transmission of the 2.5% known imprinted genes [632, 636]. The strong transgene effects observed through the different behavioral tasks and the high similarity in Aβ levels quantified biochemically in J20 and NEPxJ20 mice suggest that variabilities due to background were negligeable. A second group of mice balanced with both genders was also analyzed at 15 months to determine the effects of aging in these mice.

5.2.1 Behavioral analysis of the NEP mice

Neuronal overexpression of neprilysin was triggered by the Prp promoter which was shown to induce high levels of transgene expression in brains and hearts of transgenic mice [637]. This promoter led to similar high levels of neprilysin protein in the different brain areas analyzed including the hippocampus, cortex, amygdala, cerebellum and subcortical areas. It also led to neprilysin expression in the liver, heart and kidney. Since mice devoid of prion protein exhibit deficits in exploratory behavior and cognition [638-640], we verified that the presence of an extra prion promoter did not affect the levels of the endogenous prion protein. A recent study also showed that prion protein could promote Aβ aggregation *in vivo* [641]. Furthermore, since neprilysin has a broad substrate specificity and aggregation of PrP^{sc} shares similarities with that of Aβ, endogenous level of prion protein and its potential degradation by neprilysin were investigated [642]. The brain level of Prion protein were found similar in NEP mice and WT littermates [642], suggesting that behavior changes observed in mice carrying the NEP transgene was not due to variation of the prion protein expression.

Neuronal neprilysin overexpression did not affect the well being of the transgenic mice. Despite a decreased body weight observed in the 7 months cohort, longevity (up to 27 months) and fertility were not altered by neprilysin overexpression.

Among the different brain system regulating body weight (reviewed in [643]), the hypothalamus and the amygdala are two major areas. It is noteworthy that the neuropeptide Y (NPY), a sustrate of neprilysin [644, 645], is an established potent stimulator of food intake [646-648]. In spite of lack of hyperphagy in NPY KO and NPY1 receptor KO mice, ablation in adult mice of hypothalamic neurons that express NPY and agouti-related protein was shown to cause rapid starvation [649]. Therefore, potential degradation of NPY by overexpression of neprilysin may result in decrease of body weight.

NEP transgenic mice of the 7 months cohort behaved abnormally in all exploration tests with pattern of changes which strongly depended on the test condition. They were strongly hyperactive both in the emergence and object exploration test. In the open field, they were more active only on the second day, indicating impaired habituation, which was also evident in the emergence test in addition to the general increase of activity. Independently of hyperactivity, an altered pattern of locomotion was also observed whenever the arena provided enough space for its expression: NEP mice presented shortened more frequent locomotor episodes characterized by stronger acceleration, during the open field, emergence and object exploration paradigms. Since NEP mice performed similarly to their WT littermates on the rotarod, decreased body weight and defect in locomotor coordination were not responsible for the abnormal locomotion of the NEP mice. By contrast, no evidence for increased activity was found in the light-dark box or the O-maze. Similar defects of habituation associated with enhanced locomotor activity have been frequently reported in rodents with hippocampal damage (reviewed in [650]). While the presence of an hippocampal disruption in the NEP mice is unprobable based on the normal behavior of these mice in the hippocampal-dependent Morris water maze, puzzle box or Y maze paradigms, it can not be excluded since the NEP mice also presented a contextual learning impairment during fear conditioning.

In addition to locomotor activity, anxiety-related parameters were also changed in NEP mice. Open sector avoidance on the O-maze was significantly decreased and dark time in the light-dark box was reduced, while center field time in the emergence test was slightly increased. In the open-field, NEP mice did not spend more time in the center but were significantly less attached to their home base. These changes may be interpreted as evidence for reduced anxiety.

Regarding learning and memory, NEP mice performed normally across multiple tasks. In the hippocampal-dependent Morris water-maze place navigation task, the learning rate and the overall performance as measured by the escape latency was similar in NEP and WT mice. Locomotion and ability to use visual and spatial information to find the visible and hidden platform were not affected by neprilysin overexpression.

During the CTA, a hipocampally-independent associative learning and memory task, both groups developed a comparable strong taste aversion for saccharin and similar sensitivity to a quinine solution, confirming that taste sensitivity was not altered. Neprilysin overexpression did not alter the long term memory for taste aversion. It can be concluded that neprilysin overxpression did not affect the structures and pathways involved in CTA such as the

gustatory neural pathways and among others, the nucleus of the solitary tract, the parabrachial nucleus of the pons, the hypothalamus and the amygdala (reviewed in [504]).

NEP mice behaved indistinguishably from their WT littermates in the puzzle box paradigm, which was shown to be sensitive to damage in 41 brain areas in rats [484, 651] and involves quick problem-solving tasks [652]. The motivation of both groups to reach the dark protected area was similar as shown by the escape latency during the training sessions. When the entrance was plugged by sawdust or a T-shaped cardboard, all mice adapted similarly by spending more time during the first trial and significantly less time during the second trial.

Similarly, no impairment was found in spatial working memory as assessed by spontaneous alternation behavior in the Y-maze. In the 8 arm radial maze, another working memory paradigm, NEP mice showed a borderline reduction of overall performance. However, this could be explained by strong locomotor hyperactivity: despite spending on average less time on the maze than WT mice, NEP mice traveled a longer distance while completing the task, a fact that reflect their hyperactivity in the radial maze. Therefore the observed borderline impairment was not due to cognitive deficits but rather involved hyperactivity.

Finally, NEP mice were impaired in fear conditioning and showed less contextual freezing, both immediately following training and after a 24h interval. Because they were less active than WT mice during baseline recording this is unlikely to represent a freezing deficit possibly present in hyperactive mice. Nociceptive threshold of NEP KO mice was shown to be significantly increased compared to control mice in the hotplate paradigm [344]. However, our own data contradict this finding showing no difference in pain sensitivity between NEP KO and WT mice in the hotplate task. Similarly, the pain sensitivity of the NEP mice tested in the hot plate was also unchanged and therefore, is not responsible for the observed deficit in fear conditioning. Rather, it may be taken as evidence for a reduced ability to form or retrieve an association between context and shock. Freezing to tone after 24h was significant and similarly modest in NEP and WT mice confirming the normal ability of the NEP mice to perform single association already observed in the CTA test. Since the lack of freezing was already observed during training, we could conclude that NEP mice presented a deficit in learning the context association in this specific paradigm.

While conditioning to an auditory stimulus involves projection from the auditory system to the lateral nucleus of the amygdala followed by transfert to central nucleus of the amygdala, [653], conditioning to the context is more complex and depends on intact hippocampus and projection to the basal and accessory basal nuclei of the amygdala which project to the central nucleus of the amygdala [653]. Neprilysin was overexpressed in the amygdala but we did not

specifically investigate the neprilysin overexpression in the different nuclei of the amygdala. Lesion approach and local blockade of protein synthesis showed that the central and basolateral nuclei of the amygdala are respectively involved in the acquisition and extinction of the CTA [508, 654]. Since NEP mice presented normal learning and memory during CTA, the fear conditioning impairment observed in the NEP mice can not be explained by disruption of pathways involving these nuclei. Normal learning and memory behavior of the NEP mice in the hippocampal-dependent paradigms, such as Morris water maze and the puzzle box, also suggest that the pathways involving the hippocampus are not altered. However, among the corticohippocampal circuitry taking part in mnemonic functions, neurotoxic lesions of perirhinal or postrhinal cortex that were previously shown to impair contextual fear conditioning [655, 656] or contextual discrimination [657], caused little or no impairment in place learning in the Morris water maze paradigm [658]. Therefore, the disturbance of specific cortical areas associated with the hippocampus may be responsible for the lack of contextual fear conditioning observed in the NEP mice.

Brain and peripherical levels of substance P, enkephalin and somatostatin were similar in NEP mice and WT control littermates. Therefore, their involvement in the behavior changes of the NEP mice should be excluded. It is still possible that small variations localized at the synaptic level could not have been detected and further analysis using microdialysis or quantification following injection of the radiolabeled neuropeptides could confirm our data. Other unidentified substrates of neprilysin may also play a role in the behavioral impairment of the NEP mice. Among them, only Aβ levels were found to be decreased *in vivo* by neprilysin overexpression [405]. The behavioral effects due to decrease of murine Aβ level is difficult to evaluate because of lack of proper mouse models. Indeed, no behavioral analysis of mice overexpressing Aβ-degrading enzyme has yet been published and behavioral consequences of Aβ levels decrease by deletion of APP are not dissociable from behavioral effects related to the lack of APP itself or its other proteolytic fragments. Interestingly, mice with APP deletion exhibited weight loss [62] and decreased activity in the open field [62, 659] associated with decreased muscular strength [62]. Our data show opposite effects in NEP mice and no locomotor impairments as assessed by the rotarod could be found, suggesting that decrease of Aβ levels is not responsible for the abnormal locomotion of the NEP mice. Because neprilysin was shown to be involved in intracellular signalling pathways [373, 586, 587], a potential effect of neprilysin via internal signalling should also be considered. Overexpression of an inactive neprilysin mutated in its active site [586, 660] could dissociate the behavioral effects of neprilysin overexpression due to its enzymatic

activity from intracellular signalling pathway activation. To achieve this aim, similar expression pattern and protein levels should be reached to efficiently compare both pathways in the transgenic mice.

We also found an increase in plasminogen activators activity in 18 months old NEP mice. Prior to confirmation of such an increase of uPA and tPA activity in the brain of NEP mice at a younger age, we can only speculate about the role played by these plasminogen activators in the behavioral phenotype of the NEP mice. For example, uPA transgenic mice expressing uPA in the hypothalamus, a region implicated in feeding behavior, exhibited reduced food consumption and body weight [583]. Therefore, a higher uPA activity could be responsible for the decreased body weight observed in the NEP mice. However, the same mice, which also presented increased uPA activity in cortical and hippocampal areas, exhibited impaired performance in Morris water maze and failed to normally acquire CTA [584]. The normal performance of the NEP mice from the 7 months cohort observed in these two paradigms and the lack of deficit of the 15 months old cohort in the Morris water maze suggest that the endogenous uPA upregulation observed in the NEP mice does not contribute to the behavioral changes observed in the NEP mice. A role of uPA in locomotion was proposed in a model involving chronic cocaine administration. Using regulatable virus, gene delivery of wild type uPA in the nucleus accumbens, the ventral tegmental area or the ventral subiculum increased cocaine associated hyperlocomotion. In contrast, delivery of mutated inactive uPA decreased it. However, expression of uPA did not affect the basal activity in the absence of drug [661], suggesting that increased uPA activity does not affect locomotion in normal conditions.

Similarly, tPA upregulation could be responsibe for some of the behavior effects observed in NEP mice. TPA has been shown to be involved in synaptic plasticity and LTP. Whereas genetic or pharmacological inhibition of tPA affects the late phase of LTP [430], treatment with tPA facilitates LTP [662]. The effect of tPA deletion on locomotion, habituation of object exploration or spatial memory is controversial and led to poor rearing activity, absence of habituation, poor contextual fear conditioning but enhanced cue fear conditioning in one study [663] and had no effect in a second one [662]. The potential role of tPA in contextual fear conditioning was further suggested by Ammassari-Teule *et al.* confirming that tPA KO mice spent less time freezing in the context test but more time freezing during the cue test [664]. tPA also plays an important role in amygdala-related processing including fear and anxiety [665, 666], both inducing synaptic plasticity in the amygdala [665, 667]. While tPA activity was increased in the amygdala by acute restraint stress, disruption of tPA led to lack of anxiety in the O-maze paradigm after up to three weeks of daily restraint [668]. Taken

together, these data suggest that tPA is involved in many behavioral processes including locomotion, anxiety and cognition. However, most of these data were obtained by inhibition or deletion of tPA. Since tPA deletion present similar phenotype as in the NEP mice which present an upregulation of tPA, we speculate that these impairments are not related to tPA upregulation. To our knowledge, tPA overexpressing mice were only investigated in Morris water maze paradigm where they improved learning performances [419]. We can not exclude that increase and decrease activity of the plasminogen activators may both lead to similar behavioral changes but suggest that like for uPA, if tPA deficiency leads to decreased anxiety, lack of habituation and impaired contextual fear conditioning it is unlikely that its upregulation in NEP mice would lead to similar impairments.

The behavioral analysis of the 15 months old cohort, balanced for both genders, showed that the abnormal locomotion and decreased anxiety observed in the 7 months old cohort disappeared with aging. Indeed, NEP mice did not differ anymore from their WT littermates. Body weight, locomotion in the open field, emergence and novel object exploration tests did not differ between NEP and WT mice. Interestingly, for unknown reasons, NEP mice showed lack of interest for the new object inserted during the novel object exploration task. However, no other results confirmed this finding. Anxiety-related parameters such as the preference for the open sectors and the percentage of open sector entries in the O maze were also comparable in NEP and WT mice. Like in the 7 months cohort, aged NEP mice performed similarly to WT littermates in the Morris water maze. Interestingly, the 15 months old cohort showed better performance to find the visible platform and performed similarly when the platform was hidden. We do not have a clear explanation for the age-related improvement in finding the visible platform and can only speculate that environmental conditions and age-related decreased locomotion may play a role. Furthermore, in spite of absence of sex effect, the presence of both genders in the 15 months cohort may also increase the variability of the performances.

Transgenic overexpression of neprilysin induced abnormal locomotion and decrease of anxiety-like behavior in the 7 months cohort. While the pathways responsible for these impairments are still unclear, they disappeared with age, suggesting that these effects were small and may be considered negligeable for using neprilysin overexpression therapeuticaly in AD. More importantly, neprilysin overexpression did not affect learning and memory in a battery of different cognitive tasks at two different ages. Neprilysin overexpression does not seem to present strong side effects in mice and can be considered as a potential therapeutic approach in AD.

5.2.2) Behavioral analysis of the J20 mice

Our results show that J20 mice of the 7 months old cohort were characterized by a clear decrease of body weight, hyperlocomotion, decreased anxiety and memory deficits.

The absence of similar behavioral effects observed in transgenic mice, whose transgene is driven by the PDGF promoter [128, 669] and the other studies showing similar results in transgenic mice overexpressing human mutated APP under the control of other neuronal promoters [629, 670-672] strongly suggest that the effects observed in the J20 mice are not due to impairement of the endogenous PDGF protein but involve APP overexpression.

The initial concept that brain accumulation of Aβ causes the cognitive dysfunction *in vivo* has been controversially discussed, mostly due to the lack of correlation between β-amyloid plaque load and cognitive deficits [37, 130-132]. Furthermore, studies on transgenic mice showed that neuronal dysfunctions, including memory deficits, appeared before β-amyloid plaque formation [68, 128, 129] and passive antibody transfer could reverse memory deficits without reducing β-amyloid plaque in an APP transgenic mouse model [673], suggesting Aβ fibril intermediates rather than amyloid plaques as the major cause of neuronal dysfunction and cognitive abnormalities. To circumvent the effects exerted by β-amyloid plaques and their associated cytopathology on cognition, we have tested the mice at an age prior to β-amyloid plaque formation. The immunohistochemistry data showed no β-amyloid plaque staining along with the absence of insoluble Aβ aggregates in FA extracts. Moreover, the degree of astrocytes or microglia activation did not differ between the four groups, confirming our previous data that glial activation depends mostly on amyloid plaque pathology in AD mouse models [613, 614]. Therefore, the impairments of the J20 mice observed in the different paradigms were not related to the β-amyloid plaque formation or to an associated inflammatory response.

We found that body weight of the J20 mice was smaller than their WT littermates as early as 4.5 months and 15 months of age. This is consistent with studies showing similar findings in adults with Down syndrome and in AD patients [674, 675] and may involve dysfunction in the hypothalamus which was shown by lesion studies to regulate food intake and body weight [643].

J20 mice also showed a strong hyperlocomotion across multiple tasks in both ages studied. This was particularly evident in the open field where J20 mice exhibited hyperlocomotion at

7 months and 15 months of age. Similar effect was present in the emergence test and novel object exploration paradigms performed by the 15 months old cohort.

Tested for anxiety-related parameters, J20 mice exhibited a decrease of anxiety-like behavior with a significant higher percentage of opened arm entries and higher number of head dips in elevated O-maze corroborated by non significant decrease of time spent in the dark area of the light/dark test. At 15 months of age, J20 mice showed a trend toward decrease anxiety-like responses in the O-maze task but did not reach significancy.

In addition to amnesia, AD patients exhibit neuropsychiatric symptoms such as apathy, associated with depression, dysphoria and social withdrawal [676, 677]. However, agitation, restlessness, disinhibition and euphoria are also frequently reported [678]. Our data are consistent with the uninhibited nature often observed in late AD patients [679, 680].

Disinhibition of exploratory behaviors including decrease of anxiety-like behavior was present in rodents with deficits in hippocampal function [681, 682]. Rodents with hippocampal lesions also exhibited a significant increase in locomotor activity in a novel environment [683], which may be due to a disruption in the ability to gather the spatial information necessary to establish an internal representation of the environment [684]. Since APP and Aβ were expressed in the hippocampus of the J20 mice, it is possible that the hyperlocomotion and decreased anxiety may be due to disruption of the neural pathways of the hippocampus. This assumption was further strenghted by the memory impairment observed in the Morris water maze paradigm at 7 months of age. Whereas the ability to find a visible platform was not affected, J20 mice spent significantly less time in the goal quadrant during the place navigation tasks and the probe trial indicating impairment in spatial reference memory compared to controls.

The J20 mice were previously published to present high levels of Aβ with learning deficit in the Morris water maze paradigm at 7 months of age [69], detectable amyloid deposits at 8 months of age [70] associated with glial activation at 14 months of age [405]. Differences in behavioral results between laboratories can be caused by many factors including genetic background, environmental parameters or experimental procedures [685]. However, the lack of plaque detection by immunohistochemical approach at 11 and 18 months of age in our J20 strongly suggest that the pathology of the J20 mice analyzed in our lab varied from the one previously published and therefore may explain the weaker learning deficit of the J20 mice observed in the Morris water maze paradigm.

Interestingly, other brain areas such as perirhinal cortex and amygdala act on the stress factors associated with the Morris water maze. Rats with perirhinal cortex and amygdala lesions

performed normally on the Morris water task, but showed reduced searching behavior in the correct quadrant on the probe trial [686]. Lesion studies [687] and pharmacological inhibition of the amygdala [688] were shown to further prevent, certainly via its hippocampal projections [689, 690], LTP in the hippocampus and spatial memory in Morris water maze [687, 688, 691, 692].

The potential disruption of pathways involving amygdala is further strenghted by the increased extinction of the CTA observed in the J20 mice already at 4.5 months of age. During the CTA paradigm, the J20 mice drank similar amount of saccharin during the conditioning day and avoided the bitter kinin solution similarly to the WT littermates showing normal taste function. During the first choice test, the amount of saccharin drank did not differ from WT littermates suggesting that the mice associated correctly the saccharin taste with the LiCl induced nausea. However, the J20 mice drank significantly more saccharin during the following choice tests indicating an increased extinction of taste aversion in these mice. Reduced neophobia or taste sensitivity can not explain the CTA memory deficit observed in the J20 mice. The BLA were shown to be important for extinction but not acquisition of CTA [508]. Therefore, it is possible that human APP overexpression and the subsequent accumulation of Aβ, present in the amygdala of the J20 mice, specifically disrupted the BLA without acting on the other nuclei involved in learning in the CTA such as the central nucleus [508]. A similar accelerated extinction of the CTA memory was already found in another transgenic model of amyloidosis, which also presented a learning deficit [499]. These data are in agreement with the with implicit memory deficits observed in AD patients [693, 694].

Analysis of J20 mice of the 15 months old cohort showed behavioral changes reminiscent of those seen in the 7 months cohort. However, many effects were weaker. Despite decreased locomotion, the J20 mice still presented a strong hyperlocomotion in the open field paradigm when compared to the 7 months old cohort. However, J20 mice did not show anymore signs of decreased anxiety-like behavior as assessed by the percentage of open sector entries in the elevated O-maze paradigm or memory deficit in the Morris water maze. This weakening of the effects previously observed in the 7 months cohort is similar to the ones observed for the NEP mice and therefore, may imply factors independent of the transgene expressed such as aging, housing conditions, presence of both genders etc. In the case of J20 mice, there is absence of amyloid plaque formation in both cohorts. It is also possible that oligomerization of Aβ in the 15 months old cohort involved formation of less toxic Aβ intermediates compared to the 7 months cohort where higher levels of oligomers, which were shown to

induce cognitive deficits [134, 226, 615], is expected. Interestingly, similar decrease of pathology with aging was also observed in other mouse models of amyloidosis [695] and transgenic mice overexpressing Swedish mutated APP were shown not to be impaired at 26 months of age despite the presence of high levels of Aβ [696].

5.2.3 Prevention of Aβ-related behavioral deficits by neuronal neprilysin overexpression

Our data show that overexpression of neprilysin in neurons did not prevent the non-cognitive impairments associated with neuronal expression of AD-causing human APP. The lack of effect is in part due to similar impairments present in NEP and J20 mice. Indeed, both transgenes induced a decrease in body weight and decrease of anxiety-related parameters in the O maze and L/D test. Determination of beneficial neprilysin effects on Aβ-related behavioral deficits is futher complicated by the numerous pathways activated by both transgenes which do not involve Aβ. For example, the behavioral deficits observed in the NEP mice can involve the degradation of other substrates [230] and/or activation of intracellular signaling pathways [373, 586, 587] which still need to be confirmed *in vivo*. Similarly, the non-cognitive impairments observed in J20 mice may include the involvement of APP or its other proteolytic fragments, whose levels were not modified by neprilysin overexpression. Furthermore, an additive effect of both transgenes was observed in the L/D test where decreased anxiety, determined by the decreased percentage of time spent in the dark, became significant only in NEPxJ20 mice further suggesting that the transgenes even bosted each other.

Neprilysin overexpression did not prevent the hyperlocomotion induced by the J20 transgene in the open field at 7 months of age and during the emergence and novel object exploration paradigms. These data do not allow us to confirm the role of Aβ in the decrease body weight, hyperlocomotion and decreased anxiety exhibited by the J20 mice and would rather suggest that increased levels of APP or its other proteolytic fragments are responsible for these effects. This conclusion is supported by decreased locomotor activity observed in APP deficient mice [62, 659].

On the cognitive level, our data showed that overexpression of neprilysin in neurons prevented the impairment of spatial memory associated with neuronal expression of AD-causing human APP in the highly used Morris water waze paradigm. While NEP mice behaved similarly to WT littermates, J20 and NEPxJ20 mice spent non-significantly more

time finding the hidden platform. However, NEPxJ20 mice also needed more time to find the visible platform suggesting that other parameters than cognition may have been involved. Furthermore, J20 mice also exhibited spatial memory impairments and spent less time in the goal quadrant during learning and memory tasks, the later being prevented by neprilysin overexpression. Together with a neprilysin-dependent decrease in brain levels of $A\beta_{1-40}$ and $A\beta_{1-42}$, these data provide the evidence for the therapeutic potential of neprilysin overexpression for AD therapy. Because overexpression of neprilysin did not change levels of full length APP or its other proteolytic fragments, these data strongly support a role of Aβ, as the pathogenic agent responsible for the cognitive deficits of the J20 mice in the Morris water maze.

Previous studies comparing APP transgenic mice to WT littermates demonstrated cognitive deficits linked to the APP transgene but none could provide direct evidence that the observed impairments were solely due to high brain levels of Aβ rather than high levels of APP itself or its other proteolytic fragments. Several Aβ-lowering therapeutic approaches including BACE deficiency or removal of Aβ by immunotherapy rescued cognitive impairments in mouse models [697-700] as well as in AD patients [701]. However, inhibition of BACE or γ-secretase complex also interacts with APP processing. Moreover, immunization against Aβ acts through mechanisms that include among others microglia-mediated phagocytosis [702], depletion of Aβ peripheric pool of [703] and inhibition of fibrillogenesis and cytotoxic Aβ species [704] but also involves inflammatory reactions [705, 706].

In J20 mice and other transgenic APP mouse models, hippocampal synaptophysin immunoreactivity correlated inversely with Aβ levels but not APP levels, suggesting that Aβ rather than APP is involved in synaptotoxicity [70]. However, a similar disruption or decrease of synaptophysin immunoreactivity, impaired synaptic plasticity with decreased LTP and deficits in cognitive functions were also present in mice lacking APP [707, 708] and mice ovexpressing wild type APP also exhibited memory deficits [68], rendering a definite conclusion about the role of Aβ in mice overexpressing APP difficult. Using transgenic overexpression of an Aβ-degrading enzyme such as neprilysin, we could circumvent that problem by specifically targeting Aβ without modification of the APP processing as confirmed by Western blot analysis in this study and by others [303, 405]. APP and CTF levels were similar in J20 and NEPxJ20 mice but Aβ level was highly reduced in the double transgenic mice. These results were confirmed by specific ELISA showing an approximate 70% decrease of $A\beta_{1-42}$ and $A\beta_{1-40}$ levels. Transgenic mice with neuronal overexpression of neprilysin behaved similarly to their control littermates in all cognitive tasks performed.

Therefore, it is likely that the beneficial effect of neprilysin overexpression seen in the NEPxJ20 mice in the Morris water maze was due to the ability of neprilysin to degrade the APP-transgene derived Aβ. Taken together, these data stress the specificity of the observed effects showing that in contrast to deficient performance of the J20 mice, the improved memory performance of the NEPxJ20 mice in the Morris water maze was caused by removal of Aβ from the brain.

Our data also suggest that, in J20 mice, CTA, a learning and memory paradigm involving the amygdala [504], could be a sensitive paradigm to measure early cognitive deficits in transgenic APP mouse models [499]. However, in spite of a high level of neprilysin and decreased Aβ level in the amygdala of the NEPxJ20 compared to J20 mice, neprilysin overexpression did not prevent the memory deficit of the J20 mice in the CTA test. This result can be explained by the possibility that areas and pathways involved in CTA retention [504, 709] are more sensitive to Aβ insult and that the decrease of Aβ levels observed in the amygdala of the NEPxJ20 mice was not sufficient to prevent the memory deficit. Another explanation may include the involvement of APP or its other proteolytic fragments, whose levels are not modified by neprilysin overexpression. Indeed, APP is involved in multiple functions, including learning and memory [67 for review] and cognitive impairments are present in mice overexpressing [68] or lacking APP [707, 708].

Furthermore, sAPP was shown to be neurotrophic [95] and neuroprotective [74, 99]. Intracerebroventricular injection of sAPPα further enhanced memory and blocked induced learning deficits in mice [102]. In addition, a chronic overexpression of sAPP could also affect the pathways involved in CTA. For example, sAPPα selectively suppress N-methyl-D-aspartate receptor (NMDAR) current without affecting currents induced by α-amino-3-hydroxy-5-methylisoxazole-4-propionate (AMPA) or kainate receptors in hippocampal neurons [106] and modulates the properties required for LTD and LTP on hippocampal slices [107], suggesting important roles for sAPPα in the various physiological and pathophysiological processes in which NMDAR participates, including taste memory consolidation [710, 711].

Moreover, the memory deficit observed in the CTA in J20 and NEPxJ20 mice could also be linked to the overexpression of the CTF of APP. The CTFα and CTFβ fragments, are shown to be neurotoxic *in vitro* [115, 712, 713] and their transgenic overexpression in mice induced impaired LTP [136, 714], neurodegeneration [137, 138] and cognitive impairments [137, 714]. Similarly, CTFγ was also shown to induce cytotoxicity *in vitro* [156, 157], to bind

different adaptor proteins (reviewed in [145]) which can lead to transcription of multiple known and yet unidentified genes [146, 150, 715]. By competing for adaptor proteins, CTFγ overexpression can also influence other transcription pathways [150, 159, 160] potentially leading to decreased retention in the CTA paradigm.
Different studies suggested that oligomers of Aβ, rather than monomers, may be involved in the pathology of AD [134, 226, 615]. The fact that neprilysin degrades mostly Aβ monomers [405] raised the question about the efficiency of neprilysin overexpression in AD therapy. Our data show that, independently of the aggregation state of Aβ species responsible for the memory deficit of the J20 mice in the Morris water maze, neuronal neprilysin overexpression could prevent their adverse effects. Our data confirm previous studies using APP overexpressing mice, including J20, suggesting that Aβ rather than APP is responsible for hippocampal related memory deficit [69, 130].

We could not confirm the role of Aβ and the therapeutic effect of neprilysin overexpression in the non-cognitive impairments and in the CTA memory deficit observed in the J20 mice. However, we found that elevated brain neprilysin levels rescued the spatial cognitive deficits caused by abnormal high concentrations of Aβ in the brain of a mouse model of AD, without changing APP processing or having other side effects on cognition. Our data support Aβ, but not transgenic APP expression, as the pathologically relevant culprit responsible for the memory deficit of J20 mice and strength the importance of Aβ-lowering strategies and more particularly neuronal neprilysin overexpression for AD therapy.

V) CONCLUSION

High brain concentrations of Aβ, a peptide released by the processing of the amyloid precursor protein, is associated to the pathology of AD and to cognitive deficits in transgenic mouse models. During my Ph.D. thesis, the role and regulation of neprilysin, the major enzyme known to degrade amyloid-β *in vivo*, was investigated in the concept of AD pathophysiology using cellular and animal models. While decreased levels of brain neprilysin led to increased Aβ levels in the brain of mice and for the first time presence of murine amyloid-β plaque-like, its neuronal overexpression prevented Aβ accumulation and the memory deficit of mice overexpressing the AD-causing mutated human APP without altering the endogenous levels of APP or other substrates of neprilysin in the brain. These data emphasize a major role of neprilysin in AD pathology and suggest that upregulation of neuronal neprilysin activity represents a valid Aβ-lowering therapeutic approach for AD.

ABREVIATIONS

A	Adenosine
ACE	Angiotensin-converting enzyme
AD	Alzheimer's disease
Aβ	β-amyloid
AMPA	α-amino-3-hydroxy-5-methylisoxazole-4-propionate
ANOVA	Analysis of variance
ApoE	Apolipoprotein E
APP	Amyloid precursor protein
APLP	Amyloid precursor like proteins
α-2M	α-2 macroglobulin
BACE	β-site APP cleaving enzyme (β-secretase)
BDNF	Brain-derived neurotrophic factor
BLA	Basolateral nuclei of the amygdala
bp	Base pairs
BSA	Bovine serum albumin
C	Cytosine
CALLA	Common acute lymphoblastic leukemia antigen
cDNA	Complementary desoxyribonucleic acid
CNS	Central nervous system
CS	Conditioned stimulus
CSF	Cerebrospinal fluid
Ct	Cycle threshold
CTA	Conditioned taste aversion
CTFα	C-terminal fragment of APP generated by a α-secretase
CTFβ	C-terminal fragment of APP generated by a β-secretase
CTFγ	C-terminal fragment of APP generated by a γ-secretase
CMV	Cytomegalovirus
ddH_2O	Double deionised water
DEPC	Diethylpyrocarbonate
DINE	Damage induced neuronal endopeptidase
DMEM	Dulbecco's modified Eagle medium
DMEM/F12	DMEM/Nutrient Mixture F-12
DMSO	Dimethylsulfoxid
DNA	Deoxyribonucleic acid
Dnase	Deoxyribonuclease
dNTP	Deoxynucleoside triphosphate
DTT	Dithiothreitol
E. coli	Escherichia coli
ECE	Endothelin converting enzyme
EGFP	Enhanced green fluorescent protein
ECL	Enhanced chemiluminescence
ECM	Extracellular matrix
EDTA	Ethylen-diamin-tetraacetic acid
EGTA	Ethylene-glycol-bis(2-aminoethyl)-tetraacetic acid
ELISA	Enzyme-linked immunosorbent assay
EOFAD	Early onset familial AD
FA	Formic acid

FAD	Familial form of Alzheimer's disease
FAK	Focal adhesion kinase
FCS	Fetal calf serum
FTD	Frontotemporal dementia
G	Guanosine
GAPDH	Glyceraldehyde-3-phosphate dehydrogenase
GFAP	Glial fibrillary acidic protein
GSK-3β	Glycogen synthase kinase 3β
HA	Haemagglutinin
HEK 293	A human embryonic kidney cells
HEPES	N-[2-Hydroxyethyl]piperazine-N'-[2-ethanesulfonic acid]
HPLC	High performance liquid chromatography
HRP	Horseradish peroxidase
HS	Horse serum
ICV	Intracerebroventricular
IL-1α	Interleukin-1α
IL-1β	Interleukin-1β
IL-6	Interleukin-6
ip	Intraperitonealy
J20	Transgenic mice overexpressing the Swedish and Indiana mutated human APP
kb	Kilobase
kd	Kilodalton
L/D	Light-dark test
PFA	Paraformaldehyde
KO	Knockout
LB	Luria Bertani
LC-PCR	Light Cycler quantitative real time PCR
LF2000	Lipofectamine 2000
LiCl	Lithium chlorid
LOAD	Late onset alzheimer disease
LRP	Low density lipoprotein receptor related protein
LTP	Long term potentiation
MEAP	Met-enkephalin-Arg-Phe
MIC	A human microglia cell line
mRNA	Messenger ribonucleic acid
MWM	Morris water maze
NEP	Transgenic mice overexpressing neprilysin
NEP KO	Mice with deletion of both neprilysin gene alleles
NEP-/-	similar to NEP KO
NEP+/-	Mice with deletion of one neprilysin gene allele
NFT	Neurofibrillary tangles
NMDA	*N*-methyl-D-aspartate
NPY	Neuropeptide Y
OD	Optical density
ORF	Open reading frame
PAI	Plasminogen activator inhibitors
PBS	Phosphate buffered saline containing 0.154 M NaCl, 0.0027 M KCl, 0.01 M $Na_2HPO_4.2H_20$, 0.0018 M KH_2PO_4 adjusted to pH=7.4
PC	Prostate cancer

PCR	Polymerase chain reaction
PDGF	Platelet-derived growth factor
PFA	Paraformaldehyde
Plg KO	Plasminogen deficient mice
POLR2F	Polymerase (RNA) II (DNA directed) polypeptide F
poly-dT	Desoxy thymidine polymer
prp	Prion protein
P/S	Penicillin 50 (U/ml) and streptomycin (50 µg/ml)
PSEN1	Gene encoding Presenilin 1
PSEN2	Gene encoding Presenilin 2
qRT-PCR	Quantitative real-time PCR
rAAV	Recombinant adeno-associated virus
RA	All trans retinoic acid
RIA	Radioimmunoassay
RNA	Ribonucleic acid
Rnase	Ribonuclease
Rpm	Rotations per minute
RT	Room temperature
SAP	Shrimp alkaline phosphatase
sAPP	sAPPα and sAPPβ
sAPPα	Soluble extracellular fragment of APP generated by α-cleavage
sAPPβ	Soluble extracellular fragment of APP generated by β-cleavage
sCCa	Small cell carcinomas
SDS	Sodium dodecyl sulfate
SDS-PAGE	Sodium dodecyl sulfate polyacrylamid gel electrophoresis
SEM	Standard error of the mean
SEP	Secreted endopeptidase
SH-SY5Y	A human neuroblastoma cell line
SP	Substance P
SwAPP	Transgenic mice overexpressing human APP with the Swedish double mutation
T	Thymidine
TAE	Tris acetate EDTA buffer
TBS	Tris buffered saline
TEA	Triethanolamine
TGF	Transforming growth factor
TNFα	Tumor necrosis factor α
tPA	Tissue-type plasminogen activator
uPA	Urokinase plasminogen activator
US	Unconditioned stimulus
UTR	Untranslated region
UV	Ultra-violet
v/v	Volume per volume
v/w	Volume per original weight
WB	Western blotting
WT	Wild-type
w/v	Weight per volume

REFERENCES

1. Evans, D.A., et al., *Prevalence of Alzheimer's disease in a community population of older persons. Higher than previously reported.* Jama, 1989. **262**(18): p. 2551-6.
2. Lobo, A., et al., *Prevalence of dementia and major subtypes in Europe: A collaborative study of population-based cohorts. Neurologic Diseases in the Elderly Research Group.* Neurology, 2000. **54**(11 Suppl 5): p. S4-9.
3. Bird, T.D., et al., *Phenotypic heterogeneity in familial Alzheimer's disease: a study of 24 kindreds.* Ann Neurol, 1989. **25**(1): p. 12-25.
4. Finch, C.E. and R.E. Tanzi, *Genetics of aging.* Science, 1997. **278**(5337): p. 407-11.
5. Ewbank, D.C., *Deaths attributable to Alzheimer's disease in the United States.* Am J Public Health, 1999. **89**(1): p. 90-2.
6. Petersen, R.C., et al., *Mild cognitive impairment: clinical characterization and outcome.* Arch Neurol, 1999. **56**(3): p. 303-8.
7. Mayeux, R. and M. Sano, *Treatment of Alzheimer's disease.* N Engl J Med, 1999. **341**(22): p. 1670-9.
8. Forstl, H. and A. Kurz, *Clinical features of Alzheimer's disease.* Eur Arch Psychiatry Clin Neurosci, 1999. **249**(6): p. 288-90.
9. McKhann, G., et al., *Clinical diagnosis of Alzheimer's disease: report of the NINCDS-ADRDA Work Group under the auspices of Department of Health and Human Services Task Force on Alzheimer's Disease.* Neurology, 1984. **34**(7): p. 939-44.
10. Association, A.P., *Diagnostic and Statistical Manual of Mental Disorders, Fourth Edition - Text Revision (DSMIV-TR)*. 1994.
11. Higuchi, M., et al., *19F and 1H MRI detection of amyloid beta plaques in vivo.* Nat Neurosci, 2005. **8**(4): p. 527-33.
12. Hintersteiner, M., et al., *In vivo detection of amyloid-beta deposits by near-infrared imaging using an oxazine-derivative probe.* Nat Biotechnol, 2005. **23**(5): p. 577-83.
13. Blennow, K. and H. Hampel, *CSF markers for incipient Alzheimer's disease.* Lancet Neurol, 2003. **2**(10): p. 605-13.
14. Gomez-Isla, T., et al., *Profound loss of layer II entorhinal cortex neurons occurs in very mild Alzheimer's disease.* J Neurosci, 1996. **16**(14): p. 4491-500.
15. West, M.J., et al., *Differences in the pattern of hippocampal neuronal loss in normal ageing and Alzheimer's disease.* Lancet, 1994. **344**(8925): p. 769-72.
16. Braak, H. and E. Braak, *Staging of Alzheimer-related cortical destruction.* Int Psychogeriatr, 1997. **9 Suppl 1**: p. 257-61; discussion 269-72.
17. Ball, M.J., *Neuronal loss, neurofibrillary tangles and granulovacuolar degeneration in the hippocampus with ageing and dementia. A quantitative study.* Acta Neuropathol (Berl), 1977. **37**(2): p. 111-8.
18. Grignon, Y., et al., *Cytoarchitectonic alterations in the supramarginal gyrus of late onset Alzheimer's disease.* Acta Neuropathol (Berl), 1998. **95**(4): p. 395-406.
19. Mann, D.M., *Pyramidal nerve cell loss in Alzheimer's disease.* Neurodegeneration, 1996. **5**(4): p. 423-7.
20. Herzog, A.G. and T.L. Kemper, *Amygdaloid changes in aging and dementia.* Arch Neurol, 1980. **37**(10): p. 625-9.
21. Joachim, C.L., J.H. Morris, and D.J. Selkoe, *Diffuse senile plaques occur commonly in the cerebellum in Alzheimer's disease.* Am J Pathol, 1989. **135**(2): p. 309-19.
22. Whitehouse, P.J., et al., *Alzheimer's disease and senile dementia: loss of neurons in the basal forebrain.* Science, 1982. **215**(4537): p. 1237-9.

23. Moller, H.J., *Reappraising neurotransmitter-based strategies.* Eur Neuropsychopharmacol, 1999. **9 Suppl 2**: p. S53-9.
24. Davies, P., et al., *First one in, last one out: the role of gabaergic transmission in generation and degeneration.* Prog Neurobiol, 1998. **55**(6): p. 651-8.
25. Brion, J.P., G. Tremp, and J.N. Octave, *Transgenic expression of the shortest human tau affects its compartmentalization and its phosphorylation as in the pretangle stage of Alzheimer's disease.* Am J Pathol, 1999. **154**(1): p. 255-70.
26. Ferrer, I., et al., *Current advances on different kinases involved in tau phosphorylation, and implications in Alzheimer's disease and tauopathies.* Curr Alzheimer Res, 2005. **2**(1): p. 3-18.
27. Trojanowski, J.Q. and V.M. Lee, *Phosphorylation of paired helical filament tau in Alzheimer's disease neurofibrillary lesions: focusing on phosphatases.* Faseb J, 1995. **9**(15): p. 1570-6.
28. David, D.C., et al., *Proteomic and Functional Analyses Reveal a Mitochondrial Dysfunction in P301L Tau Transgenic Mice.* J Biol Chem, 2005. **280**(25): p. 23802-23814.
29. Feany, M.B. and D.W. Dickson, *Neurodegenerative disorders with extensive tau pathology: a comparative study and review.* Ann Neurol, 1996. **40**(2): p. 139-48.
30. Iqbal, K., et al., *Mechanism of neurofibrillary degeneration in Alzheimer's disease.* Mol Neurobiol, 1994. **9**(1-3): p. 119-23.
31. Gotz, J., *Tau and transgenic animal models.* Brain Res Brain Res Rev, 2001. **35**(3): p. 266-86.
32. Dickson, D.W., *The pathogenesis of senile plaques.* J Neuropathol Exp Neurol, 1997. **56**(4): p. 321-39.
33. Selkoe, D.J., *Alzheimer's disease: a central role for amyloid.* J Neuropathol Exp Neurol, 1994. **53**(5): p. 438-47.
34. Iwatsubo, T., et al., *Amyloid beta protein (A beta) deposition: A beta 42(43) precedes A beta 40 in Down syndrome.* Ann Neurol, 1995. **37**(3): p. 294-9.
35. Iwatsubo, T., et al., *Visualization of A beta 42(43) and A beta 40 in senile plaques with end-specific A beta monoclonals: evidence that an initially deposited species is A beta 42(43).* Neuron, 1994. **13**(1): p. 45-53.
36. Braak, E., et al., *Neuropathology of Alzheimer's disease: what is new since A. Alzheimer?* Eur Arch Psychiatry Clin Neurosci, 1999. **249 Suppl 3**: p. 14-22.
37. Dickson, D.W., et al., *Correlations of synaptic and pathological markers with cognition of the elderly.* Neurobiol Aging, 1995. **16**(3): p. 285-98; discussion 298-304.
38. Morris, J.C., et al., *Cerebral amyloid deposition and diffuse plaques in "normal" aging: Evidence for presymptomatic and very mild Alzheimer's disease.* Neurology, 1996. **46**(3): p. 707-19.
39. Arriagada, P.V., et al., *Neurofibrillary tangles but not senile plaques parallel duration and severity of Alzheimer's disease.* Neurology, 1992. **42**(3 Pt 1): p. 631-9.
40. Braak, H. and E. Braak, *Neuropathological stageing of Alzheimer-related changes.* Acta Neuropathol (Berl), 1991. **82**(4): p. 239-59.
41. Gotz, J., et al., *Formation of neurofibrillary tangles in P301l tau transgenic mice induced by Abeta 42 fibrils.* Science, 2001. **293**(5534): p. 1491-5.
42. Lewis, J., et al., *Enhanced neurofibrillary degeneration in transgenic mice expressing mutant tau and APP.* Science, 2001. **293**(5534): p. 1487-91.
43. Oddo, S., et al., *Abeta immunotherapy leads to clearance of early, but not late, hyperphosphorylated tau aggregates via the proteasome.* Neuron, 2004. **43**(3): p. 321-32.

44. Kang, J., et al., *The precursor of Alzheimer's disease amyloid A4 protein resembles a cell-surface receptor.* Nature, 1987. **325**(6106): p. 733-6.
45. Goldgaber, D., et al., *Characterization and chromosomal localization of a cDNA encoding brain amyloid of Alzheimer's disease.* Science, 1987. **235**(4791): p. 877-80.
46. Johnstone, E.M., et al., *Conservation of the sequence of the Alzheimer's disease amyloid peptide in dog, polar bear and five other mammals by cross-species polymerase chain reaction analysis.* Brain Res Mol Brain Res, 1991. **10**(4): p. 299-305.
47. Haass, C., et al., *Amyloid beta-peptide is produced by cultured cells during normal metabolism.* Nature, 1992. **359**(6393): p. 322-5.
48. Panegyres, P.K., *The functions of the amyloid precursor protein gene.* Rev Neurosci, 2001. **12**(1): p. 1-39.
49. Koo, E.H., et al., *Precursor of amyloid protein in Alzheimer disease undergoes fast anterograde axonal transport.* Proc Natl Acad Sci U S A, 1990. **87**(4): p. 1561-5.
50. Rockenstein, E.M., et al., *Levels and alternative splicing of amyloid beta protein precursor (APP) transcripts in brains of APP transgenic mice and humans with Alzheimer's disease.* J Biol Chem, 1995. **270**(47): p. 28257-67.
51. Hesse, L., et al., *The beta A4 amyloid precursor protein binding to copper.* FEBS Lett, 1994. **349**(1): p. 109-16.
52. Bush, A.I., et al., *Modulation of A beta adhesiveness and secretase site cleavage by zinc.* J Biol Chem, 1994. **269**(16): p. 12152-8.
53. Multhaup, G., H. Mechler, and C.L. Masters, *Characterization of the high affinity heparin binding site of the Alzheimer's disease beta A4 amyloid precursor protein (APP) and its enhancement by zinc(II).* J Mol Recognit, 1995. **8**(4): p. 247-57.
54. Beher, D., et al., *Regulation of amyloid protein precursor (APP) binding to collagen and mapping of the binding sites on APP and collagen type I.* J Biol Chem, 1996. **271**(3): p. 1613-20.
55. Kibbey, M.C., et al., *beta-Amyloid precursor protein binds to the neurite-promoting IKVAV site of laminin.* Proc Natl Acad Sci U S A, 1993. **90**(21): p. 10150-3.
56. Smith, R.P., D.A. Higuchi, and G.J. Broze, Jr., *Platelet coagulation factor XIa-inhibitor, a form of Alzheimer amyloid precursor protein.* Science, 1990. **248**(4959): p. 1126-8.
57. Neve, R.L., E.A. Finch, and L.R. Dawes, *Expression of the Alzheimer amyloid precursor gene transcripts in the human brain.* Neuron, 1988. **1**(8): p. 669-77.
58. Weidemann, A., et al., *Identification, biogenesis, and localization of precursors of Alzheimer's disease A4 amyloid protein.* Cell, 1989. **57**(1): p. 115-26.
59. Walter, J., et al., *Ectodomain phosphorylation of beta-amyloid precursor protein at two distinct cellular locations.* J Biol Chem, 1997. **272**(3): p. 1896-903.
60. Wasco, W., et al., *Isolation and characterization of APLP2 encoding a homologue of the Alzheimer's associated amyloid beta protein precursor.* Nat Genet, 1993. **5**(1): p. 95-100.
61. Heber, S., et al., *Mice with combined gene knock-outs reveal essential and partially redundant functions of amyloid precursor protein family members.* J Neurosci, 2000. **20**(21): p. 7951-63.
62. Zheng, H., et al., *beta-Amyloid precursor protein-deficient mice show reactive gliosis and decreased locomotor activity.* Cell, 1995. **81**(4): p. 525-31.
63. Muller, U., et al., *Mice homozygous for a modified beta-amyloid precursor protein (beta APP) gene show impaired behavior and high incidence of agenesis of the corpus callosum.* Ann N Y Acad Sci, 1996. **777**: p. 65-73.

64. Muller, U., et al., *Behavioral and anatomical deficits in mice homozygous for a modified beta-amyloid precursor protein gene.* Cell, 1994. **79**(5): p. 755-65.
65. von Koch, C.S., et al., *Generation of APLP2 KO mice and early postnatal lethality in APLP2/APP double KO mice.* Neurobiol Aging, 1997. **18**(6): p. 661-9.
66. Yang, G., et al., *Reduced synaptic vesicle density and active zone size in mice lacking amyloid precursor protein (APP) and APP-like protein 2.* Neurosci Lett, 2005. **384**(1-2): p. 66-71.
67. Turner, P.R., et al., *Roles of amyloid precursor protein and its fragments in regulating neural activity, plasticity and memory.* Prog Neurobiol, 2003. **70**(1): p. 1-32.
68. Moechars, D., et al., *Early phenotypic changes in transgenic mice that overexpress different mutants of amyloid precursor protein in brain.* J Biol Chem, 1999. **274**(10): p. 6483-92.
69. Palop, J.J., et al., *Neuronal depletion of calcium-dependent proteins in the dentate gyrus is tightly linked to Alzheimer's disease-related cognitive deficits.* Proc Natl Acad Sci U S A, 2003. **100**(16): p. 9572-7.
70. Mucke, L., et al., *High-level neuronal expression of abeta 1-42 in wild-type human amyloid protein precursor transgenic mice: synaptotoxicity without plaque formation.* J Neurosci, 2000. **20**(11): p. 4050-8.
71. Rice, D.S. and T. Curran, *Mutant mice with scrambled brains: understanding the signaling pathways that control cell positioning in the CNS.* Genes Dev, 1999. **13**(21): p. 2758-73.
72. Xu, X., et al., *Wild-type but not Alzheimer-mutant amyloid precursor protein confers resistance against p53-mediated apoptosis.* Proc Natl Acad Sci U S A, 1999. **96**(13): p. 7547-52.
73. Perez, R.G., et al., *The beta-amyloid precursor protein of Alzheimer's disease enhances neuron viability and modulates neuronal polarity.* J Neurosci, 1997. **17**(24): p. 9407-14.
74. Mattson, M.P., et al., *Evidence for excitoprotective and intraneuronal calcium-regulating roles for secreted forms of the beta-amyloid precursor protein.* Neuron, 1993. **10**(2): p. 243-54.
75. Kamal, A., et al., *Axonal transport of amyloid precursor protein is mediated by direct binding to the kinesin light chain subunit of kinesin-I.* Neuron, 2000. **28**(2): p. 449-59.
76. Lazarov, O., et al., *Axonal transport, amyloid precursor protein, kinesin-1, and the processing apparatus: revisited.* J Neurosci, 2005. **25**(9): p. 2386-95.
77. Esch, F.S., et al., *Cleavage of amyloid beta peptide during constitutive processing of its precursor.* Science, 1990. **248**(4959): p. 1122-4.
78. Sisodia, S.S., et al., *Evidence that beta-amyloid protein in Alzheimer's disease is not derived by normal processing.* Science, 1990. **248**(4954): p. 492-5.
79. Marcinkiewicz, M. and N.G. Seidah, *Coordinated expression of beta-amyloid precursor protein and the putative beta-secretase BACE and alpha-secretase ADAM10 in mouse and human brain.* J Neurochem, 2000. **75**(5): p. 2133-43.
80. Lammich, S., et al., *Constitutive and regulated alpha-secretase cleavage of Alzheimer's amyloid precursor protein by a disintegrin metalloprotease.* Proc Natl Acad Sci U S A, 1999. **96**(7): p. 3922-7.
81. Buxbaum, J.D., et al., *Evidence that tumor necrosis factor alpha converting enzyme is involved in regulated alpha-secretase cleavage of the Alzheimer amyloid protein precursor.* J Biol Chem, 1998. **273**(43): p. 27765-7.
82. Vassar, R., et al., *Beta-secretase cleavage of Alzheimer's amyloid precursor protein by the transmembrane aspartic protease BACE.* Science, 1999. **286**(5440): p. 735-41.

83. Farzan, M., et al., *BACE2, a beta -secretase homolog, cleaves at the beta site and within the amyloid-beta region of the amyloid-beta precursor protein.* Proc Natl Acad Sci U S A, 2000. **97**(17): p. 9712-7.
84. Luo, Y., et al., *Mice deficient in BACE1, the Alzheimer's beta-secretase, have normal phenotype and abolished beta-amyloid generation.* Nat Neurosci, 2001. **4**(3): p. 231-2.
85. Naslund, J., et al., *The metabolic pathway generating p3, an A beta-peptide fragment, is probably non-amyloidogenic.* Biochem Biophys Res Commun, 1994. **204**(2): p. 780-7.
86. Takasugi, N., et al., *The role of presenilin cofactors in the gamma-secretase complex.* Nature, 2003. **422**(6930): p. 438-41.
87. Edbauer, D., et al., *Reconstitution of gamma-secretase activity.* Nat Cell Biol, 2003. **5**(5): p. 486-8.
88. De Strooper, B., *Aph-1, Pen-2, and Nicastrin with Presenilin generate an active gamma-Secretase complex.* Neuron, 2003. **38**(1): p. 9-12.
89. Wilson, C.A., et al., *Presenilins are not required for A beta 42 production in the early secretory pathway.* Nat Neurosci, 2002. **5**(9): p. 849-55.
90. Palmert, M.R., et al., *The beta-amyloid protein precursor of Alzheimer disease has soluble derivatives found in human brain and cerebrospinal fluid.* Proc Natl Acad Sci U S A, 1989. **86**(16): p. 6338-42.
91. Nitsch, R.M., et al., *Release of Alzheimer amyloid precursor derivatives stimulated by activation of muscarinic acetylcholine receptors.* Science, 1992. **258**(5080): p. 304-7.
92. Nitsch, R.M., et al., *Release of amyloid beta-protein precursor derivatives by electrical depolarization of rat hippocampal slices.* Proc Natl Acad Sci U S A, 1993. **90**(11): p. 5191-3.
93. Fazeli, M.S., et al., *Increase in extracellular NCAM and amyloid precursor protein following induction of long-term potentiation in the dentate gyrus of anaesthetized rats.* Neurosci Lett, 1994. **169**(1-2): p. 77-80.
94. Jin, L.W., et al., *Peptides containing the RERMS sequence of amyloid beta/A4 protein precursor bind cell surface and promote neurite extension.* J Neurosci, 1994. **14**(9): p. 5461-70.
95. Ohsawa, I., C. Takamura, and S. Kohsaka, *The amino-terminal region of amyloid precursor protein is responsible for neurite outgrowth in rat neocortical explant culture.* Biochem Biophys Res Commun, 1997. **236**(1): p. 59-65.
96. Roch, J.M., et al., *Increase of synaptic density and memory retention by a peptide representing the trophic domain of the amyloid beta/A4 protein precursor.* Proc Natl Acad Sci U S A, 1994. **91**(16): p. 7450-4.
97. Furukawa, K., et al., *Increased activity-regulating and neuroprotective efficacy of alpha-secretase-derived secreted amyloid precursor protein conferred by a C-terminal heparin-binding domain.* J Neurochem, 1996. **67**(5): p. 1882-96.
98. Goodman, Y. and M.P. Mattson, *Secreted forms of beta-amyloid precursor protein protect hippocampal neurons against amyloid beta-peptide-induced oxidative injury.* Exp Neurol, 1994. **128**(1): p. 1-12.
99. Smith-Swintosky, V.L., et al., *Secreted forms of beta-amyloid precursor protein protect against ischemic brain injury.* J Neurochem, 1994. **63**(2): p. 781-4.
100. Moechars, D., et al., *Expression in brain of amyloid precursor protein mutated in the alpha-secretase site causes disturbed behavior, neuronal degeneration and premature death in transgenic mice.* Embo J, 1996. **15**(6): p. 1265-74.
101. Rossjohn, J., et al., *Crystal structure of the N-terminal, growth factor-like domain of Alzheimer amyloid precursor protein.* Nat Struct Biol, 1999. **6**(4): p. 327-31.

102. Meziane, H., et al., *Memory-enhancing effects of secreted forms of the beta-amyloid precursor protein in normal and amnestic mice.* Proc Natl Acad Sci U S A, 1998. **95**(21): p. 12683-8.
103. Anderson, J.J., et al., *Reduced cerebrospinal fluid levels of alpha-secretase-cleaved amyloid precursor protein in aged rats: correlation with spatial memory deficits.* Neuroscience, 1999. **93**(4): p. 1409-20.
104. Lannfelt, L., et al., *Decreased alpha-secretase-cleaved amyloid precursor protein as a diagnostic marker for Alzheimer's disease.* Nat Med, 1995. **1**(8): p. 829-32.
105. Van Nostrand, W.E., et al., *Decreased levels of soluble amyloid beta-protein precursor in cerebrospinal fluid of live Alzheimer disease patients.* Proc Natl Acad Sci U S A, 1992. **89**(7): p. 2551-5.
106. Furukawa, K. and M.P. Mattson, *Secreted amyloid precursor protein alpha selectively suppresses N-methyl-D-aspartate currents in hippocampal neurons: involvement of cyclic GMP.* Neuroscience, 1998. **83**(2): p. 429-38.
107. Ishida, A., et al., *Secreted form of beta-amyloid precursor protein shifts the frequency dependency for induction of LTD, and enhances LTP in hippocampal slices.* Neuroreport, 1997. **8**(9-10): p. 2133-7.
108. Seubert, P., et al., *Secretion of beta-amyloid precursor protein cleaved at the amino terminus of the beta-amyloid peptide.* Nature, 1993. **361**(6409): p. 260-3.
109. Jarrett, J.T., E.P. Berger, and P.T. Lansbury, Jr., *The carboxy terminus of the beta amyloid protein is critical for the seeding of amyloid formation: implications for the pathogenesis of Alzheimer's disease.* Biochemistry, 1993. **32**(18): p. 4693-7.
110. Burdick, D., et al., *Assembly and aggregation properties of synthetic Alzheimer's A4/beta amyloid peptide analogs.* J Biol Chem, 1992. **267**(1): p. 546-54.
111. Younkin, S.G., *Evidence that A beta 42 is the real culprit in Alzheimer's disease.* Ann Neurol, 1995. **37**(3): p. 287-8.
112. Kamenetz, F., et al., *APP processing and synaptic function.* Neuron, 2003. **37**(6): p. 925-37.
113. Yan, S.D., et al., *An intracellular protein that binds amyloid-beta peptide and mediates neurotoxicity in Alzheimer's disease.* Nature, 1997. **389**(6652): p. 689-95.
114. Walsh, D.M., et al., *Amyloid-beta oligomers: their production, toxicity and therapeutic inhibition.* Biochem Soc Trans, 2002. **30**(4): p. 552-7.
115. Yankner, B.A., et al., *Neurotoxicity of a fragment of the amyloid precursor associated with Alzheimer's disease.* Science, 1989. **245**(4916): p. 417-20.
116. Yankner, B.A., L.K. Duffy, and D.A. Kirschner, *Neurotrophic and neurotoxic effects of amyloid beta protein: reversal by tachykinin neuropeptides.* Science, 1990. **250**(4978): p. 279-82.
117. Kim, H.J., et al., *Selective neuronal degeneration induced by soluble oligomeric amyloid beta protein.* Faseb J, 2003. **17**(1): p. 118-20.
118. Lambert, M.P., et al., *Diffusible, nonfibrillar ligands derived from Abeta1-42 are potent central nervous system neurotoxins.* Proc Natl Acad Sci U S A, 1998. **95**(11): p. 6448-53.
119. Small, D.H., S.S. Mok, and J.C. Bornstein, *Alzheimer's disease and Abeta toxicity: from top to bottom.* Nat Rev Neurosci, 2001. **2**(8): p. 595-8.
120. Combs, C.K., et al., *Identification of microglial signal transduction pathways mediating a neurotoxic response to amyloidogenic fragments of beta-amyloid and prion proteins.* J Neurosci, 1999. **19**(3): p. 928-39.
121. Behl, C., et al., *Hydrogen peroxide mediates amyloid beta protein toxicity.* Cell, 1994. **77**(6): p. 817-27.

122. Hensley, K., et al., *A model for beta-amyloid aggregation and neurotoxicity based on free radical generation by the peptide: relevance to Alzheimer disease.* Proc Natl Acad Sci U S A, 1994. **91**(8): p. 3270-4.
123. Mattson, M.P., K.J. Tomaselli, and R.E. Rydel, *Calcium-destabilizing and neurodegenerative effects of aggregated beta-amyloid peptide are attenuated by basic FGF.* Brain Res, 1993. **621**(1): p. 35-49.
124. Mattson, M.P., et al., *beta-Amyloid peptides destabilize calcium homeostasis and render human cortical neurons vulnerable to excitotoxicity.* J Neurosci, 1992. **12**(2): p. 376-89.
125. Lin, H., R. Bhatia, and R. Lal, *Amyloid beta protein forms ion channels: implications for Alzheimer's disease pathophysiology.* Faseb J, 2001. **15**(13): p. 2433-44.
126. Lashuel, H.A., et al., *Neurodegenerative disease: amyloid pores from pathogenic mutations.* Nature, 2002. **418**(6895): p. 291.
127. Yan, S.D., et al., *RAGE and amyloid-beta peptide neurotoxicity in Alzheimer's disease.* Nature, 1996. **382**(6593): p. 685-91.
128. Lee, K.W., et al., *Progressive cognitive impairment and anxiety induction in the absence of plaque deposition in C57BL/6 inbred mice expressing transgenic amyloid precursor protein.* J Neurosci Res, 2004. **76**(4): p. 572-80.
129. Buttini, M., et al., *Modulation of Alzheimer-like synaptic and cholinergic deficits in transgenic mice by human apolipoprotein E depends on isoform, aging, and overexpression of amyloid beta peptides but not on plaque formation.* J Neurosci, 2002. **22**(24): p. 10539-48.
130. Westerman, M.A., et al., *The relationship between Abeta and memory in the Tg2576 mouse model of Alzheimer's disease.* J Neurosci, 2002. **22**(5): p. 1858-67.
131. Terry, R.D., et al., *Physical basis of cognitive alterations in Alzheimer's disease: synapse loss is the major correlate of cognitive impairment.* Ann Neurol, 1991. **30**(4): p. 572-80.
132. Giannakopoulos, P., et al., *Cerebral cortex pathology in aging and Alzheimer's disease: a quantitative survey of large hospital-based geriatric and psychiatric cohorts.* Brain Res Brain Res Rev, 1997. **25**(2): p. 217-45.
133. Walsh, D.M., et al., *Naturally secreted oligomers of amyloid beta protein potently inhibit hippocampal long-term potentiation in vivo.* Nature, 2002. **416**(6880): p. 535-9.
134. Cleary, J.P., et al., *Natural oligomers of the amyloid-beta protein specifically disrupt cognitive function.* Nat Neurosci, 2005. **8**(1): p. 79-84.
135. Kammesheidt, A., et al., *Deposition of beta/A4 immunoreactivity and neuronal pathology in transgenic mice expressing the carboxyl-terminal fragment of the Alzheimer amyloid precursor in the brain.* Proc Natl Acad Sci U S A, 1992. **89**(22): p. 10857-61.
136. Cullen, W.K., et al., *Block of LTP in rat hippocampus in vivo by beta-amyloid precursor protein fragments.* Neuroreport, 1997. **8**(15): p. 3213-7.
137. Berger-Sweeney, J., et al., *Impairments in learning and memory accompanied by neurodegeneration in mice transgenic for the carboxyl-terminus of the amyloid precursor protein.* Brain Res Mol Brain Res, 1999. **66**(1-2): p. 150-62.
138. Oster-Granite, M.L., et al., *Age-dependent neuronal and synaptic degeneration in mice transgenic for the C terminus of the amyloid precursor protein.* J Neurosci, 1996. **16**(21): p. 6732-41.
139. Choi, S.H., et al., *Memory impairment and cholinergic dysfunction by centrally administered Abeta and carboxyl-terminal fragment of Alzheimer's APP in mice.* Faseb J, 2001. **15**(10): p. 1816-8.

140. Hecimovic, S., et al., *Mutations in APP have independent effects on Abeta and CTFgamma generation.* Neurobiol Dis, 2004. **17**(2): p. 205-18.
141. Bergman, A., et al., *APP intracellular domain formation and unaltered signaling in the presence of familial Alzheimer's disease mutations.* Exp Cell Res, 2003. **287**(1): p. 1-9.
142. Farris, W., et al., *Insulin-degrading enzyme regulates the levels of insulin, amyloid beta-protein, and the beta-amyloid precursor protein intracellular domain in vivo.* Proc Natl Acad Sci U S A, 2003. **100**(7): p. 4162-7.
143. Edbauer, D., et al., *Insulin-degrading enzyme rapidly removes the beta-amyloid precursor protein intracellular domain (AICD).* J Biol Chem, 2002. **277**(16): p. 13389-93.
144. Nunan, J., et al., *The C-terminal fragment of the Alzheimer's disease amyloid protein precursor is degraded by a proteasome-dependent mechanism distinct from gamma-secretase.* Eur J Biochem, 2001. **268**(20): p. 5329-36.
145. Kawasumi, M., et al., *Cytoplasmic tail adaptors of Alzheimer's amyloid-beta protein precursor.* Mol Neurobiol, 2004. **30**(2): p. 185-200.
146. von Rotz, R.C., et al., *The APP intracellular domain forms nuclear multiprotein complexes and regulates the transcription of its own precursor.* J Cell Sci, 2004. **117**(Pt 19): p. 4435-48.
147. Kinoshita, A., et al., *Direct visualization of the gamma secretase-generated carboxyl-terminal domain of the amyloid precursor protein: association with Fe65 and translocation to the nucleus.* J Neurochem, 2002. **82**(4): p. 839-47.
148. Gao, Y. and S.W. Pimplikar, *The gamma -secretase-cleaved C-terminal fragment of amyloid precursor protein mediates signaling to the nucleus.* Proc Natl Acad Sci U S A, 2001. **98**(26): p. 14979-84.
149. Cao, X. and T.C. Sudhof, *A transcriptionally [correction of transcriptively] active complex of APP with Fe65 and histone acetyltransferase Tip60.* Science, 2001. **293**(5527): p. 115-20.
150. Baek, S.H., et al., *Exchange of N-CoR corepressor and Tip60 coactivator complexes links gene expression by NF-kappaB and beta-amyloid precursor protein.* Cell, 2002. **110**(1): p. 55-67.
151. Honda, S., et al., *Changes in morphology of neuroblastoma cells treated with all-trans retinoic acid combined with transfer of the C-terminal region of the amyloid precursor protein.* J Clin Lab Anal, 1998. **12**(3): p. 172-8.
152. Lahiri, D.K. and C. Nall, *Promoter activity of the gene encoding the beta-amyloid precursor protein is up-regulated by growth factors, phorbol ester, retinoic acid and interleukin-1.* Brain Res Mol Brain Res, 1995. **32**(2): p. 233-40.
153. Beckman, M. and K. Iverfeldt, *Increased gene expression of beta-amyloid precursor protein and its homologues APLP1 and APLP2 in human neuroblastoma cells in response to retinoic acid.* Neurosci Lett, 1997. **221**(2-3): p. 73-6.
154. Satoh, J. and Y. Kuroda, *Amyloid precursor protein beta-secretase (BACE) mRNA expression in human neural cell lines following induction of neuronal differentiation and exposure to cytokines and growth factors.* Neuropathology, 2000. **20**(4): p. 289-96.
155. Leissring, M.A., et al., *A physiologic signaling role for the gamma -secretase-derived intracellular fragment of APP.* Proc Natl Acad Sci U S A, 2002. **99**(7): p. 4697-702.
156. Kinoshita, A., et al., *The gamma secretase-generated carboxyl-terminal domain of the amyloid precursor protein induces apoptosis via Tip60 in H4 cells.* J Biol Chem, 2002. **277**(32): p. 28530-6.

157. Kim, H.S., et al., *C-terminal fragments of amyloid precursor protein exert neurotoxicity by inducing glycogen synthase kinase-3beta expression.* Faseb J, 2003. **17**(13): p. 1951-3.
158. Lau, K.F., et al., *Fe65 and X11beta co-localize with and compete for binding to the amyloid precursor protein.* Neuroreport, 2000. **11**(16): p. 3607-10.
159. Roncarati, R., et al., *The gamma-secretase-generated intracellular domain of beta-amyloid precursor protein binds Numb and inhibits Notch signaling.* Proc Natl Acad Sci U S A, 2002. **99**(10): p. 7102-7.
160. Kinoshita, A., et al., *The intracellular domain of the low density lipoprotein receptor-related protein modulates transactivation mediated by amyloid precursor protein and Fe65.* J Biol Chem, 2003. **278**(42): p. 41182-8.
161. Pedersen, N.L., et al., *How heritable is Alzheimer's disease late in life? Findings from Swedish twins.* Ann Neurol, 2004. **55**(2): p. 180-5.
162. Gatz, M., et al., *Heritability for Alzheimer's disease: the study of dementia in Swedish twins.* J Gerontol A Biol Sci Med Sci, 1997. **52**(2): p. M117-25.
163. Gatz, M., et al., *Complete ascertainment of dementia in the Swedish Twin Registry: the HARMONY study.* Neurobiol Aging, 2005. **26**(4): p. 439-47.
164. Mayeux, R., et al., *Risk of dementia in first-degree relatives of patients with Alzheimer's disease and related disorders.* Arch Neurol, 1991. **48**(3): p. 269-73.
165. Tanzi, R.E., *A genetic dichotomy model for the inheritance of Alzheimer's disease and common age-related disorders.* J Clin Invest, 1999. **104**(9): p. 1175-9.
166. Goate, A., et al., *Segregation of a missense mutation in the amyloid precursor protein gene with familial Alzheimer's disease.* Nature, 1991. **349**(6311): p. 704-6.
167. Sherrington, R., et al., *Cloning of a gene bearing missense mutations in early-onset familial Alzheimer's disease.* Nature, 1995. **375**(6534): p. 754-60.
168. Rogaev, E.I., et al., *Familial Alzheimer's disease in kindreds with missense mutations in a gene on chromosome 1 related to the Alzheimer's disease type 3 gene.* Nature, 1995. **376**(6543): p. 775-8.
169. Levy-Lahad, E., et al., *Candidate gene for the chromosome 1 familial Alzheimer's disease locus.* Science, 1995. **269**(5226): p. 973-7.
170. Hutton, M., et al., *Complete analysis of the presenilin 1 gene in early onset Alzheimer's disease.* Neuroreport, 1996. **7**(3): p. 801-5.
171. Campion, D., et al., *Early-onset autosomal dominant Alzheimer disease: prevalence, genetic heterogeneity, and mutation spectrum.* Am J Hum Genet, 1999. **65**(3): p. 664-70.
172. Mann, D.M. and M.M. Esiri, *The pattern of acquisition of plaques and tangles in the brains of patients under 50 years of age with Down's syndrome.* J Neurol Sci, 1989. **89**(2-3): p. 169-79.
173. Kehoe, P., et al., *A full genome scan for late onset Alzheimer's disease.* Hum Mol Genet, 1999. **8**(2): p. 237-45.
174. Holmans, P., et al., *Genome screen for loci influencing age at onset and rate of decline in late onset Alzheimer's disease.* Am J Med Genet B Neuropsychiatr Genet, 2005. **135**(1): p. 24-32.
175. Farrer, L.A., et al., *Effects of age, sex, and ethnicity on the association between apolipoprotein E genotype and Alzheimer disease. A meta-analysis. APOE and Alzheimer Disease Meta Analysis Consortium.* Jama, 1997. **278**(16): p. 1349-56.
176. Strittmatter, W.J., et al., *Apolipoprotein E: high-avidity binding to beta-amyloid and increased frequency of type 4 allele in late-onset familial Alzheimer disease.* Proc Natl Acad Sci U S A, 1993. **90**(5): p. 1977-81.

177. Schmechel, D.E., et al., *Increased amyloid beta-peptide deposition in cerebral cortex as a consequence of apolipoprotein E genotype in late-onset Alzheimer disease.* Proc Natl Acad Sci U S A, 1993. **90**(20): p. 9649-53.
178. Corder, E.H., et al., *Gene dose of apolipoprotein E type 4 allele and the risk of Alzheimer's disease in late onset families.* Science, 1993. **261**(5123): p. 921-3.
179. Breitner, J.C., et al., *APOE-epsilon4 count predicts age when prevalence of AD increases, then declines: the Cache County Study.* Neurology, 1999. **53**(2): p. 321-31.
180. Blacker, D., et al., *ApoE-4 and age at onset of Alzheimer's disease: the NIMH genetics initiative.* Neurology, 1997. **48**(1): p. 139-47.
181. Boyles, J.K., et al., *A role for apolipoprotein E, apolipoprotein A-I, and low density lipoprotein receptors in cholesterol transport during regeneration and remyelination of the rat sciatic nerve.* J Clin Invest, 1989. **83**(3): p. 1015-31.
182. Boyles, J.K., et al., *Apolipoprotein E associated with astrocytic glia of the central nervous system and with nonmyelinating glia of the peripheral nervous system.* J Clin Invest, 1985. **76**(4): p. 1501-13.
183. Mauch, D.H., et al., *CNS synaptogenesis promoted by glia-derived cholesterol.* Science, 2001. **294**(5545): p. 1354-7.
184. Nathan, B.P., et al., *The inhibitory effect of apolipoprotein E4 on neurite outgrowth is associated with microtubule depolymerization.* J Biol Chem, 1995. **270**(34): p. 19791-9.
185. Nathan, B.P., et al., *Differential effects of apolipoproteins E3 and E4 on neuronal growth in vitro.* Science, 1994. **264**(5160): p. 850-2.
186. Holtzman, D.M., et al., *Low density lipoprotein receptor-related protein mediates apolipoprotein E-dependent neurite outgrowth in a central nervous system-derived neuronal cell line.* Proc Natl Acad Sci U S A, 1995. **92**(21): p. 9480-4.
187. Puttfarcken, P.S., et al., *Effect of apolipoprotein E on neurite outgrowth and beta-amyloid-induced toxicity in developing rat primary hippocampal cultures.* J Neurochem, 1997. **68**(2): p. 760-9.
188. Beffert, U., et al., *Apolipoprotein E and beta-amyloid levels in the hippocampus and frontal cortex of Alzheimer's disease subjects are disease-related and apolipoprotein E genotype dependent.* Brain Res, 1999. **843**(1-2): p. 87-94.
189. Holtzman, D.M., et al., *Apolipoprotein E isoform-dependent amyloid deposition and neuritic degeneration in a mouse model of Alzheimer's disease.* Proc Natl Acad Sci U S A, 2000. **97**(6): p. 2892-7.
190. Ma, J., et al., *Amyloid-associated proteins alpha 1-antichymotrypsin and apolipoprotein E promote assembly of Alzheimer beta-protein into filaments.* Nature, 1994. **372**(6501): p. 92-4.
191. Evans, K.C., et al., *Apolipoprotein E is a kinetic but not a thermodynamic inhibitor of amyloid formation: implications for the pathogenesis and treatment of Alzheimer disease.* Proc Natl Acad Sci U S A, 1995. **92**(3): p. 763-7.
192. Lambert, J.C., et al., *Association at LRP gene locus with sporadic late-onset Alzheimer's disease.* Lancet, 1998. **351**(9118): p. 1787-8.
193. Blacker, D., et al., *Alpha-2 macroglobulin is genetically associated with Alzheimer disease.* Nat Genet, 1998. **19**(4): p. 357-60.
194. Narita, M., et al., *Alpha2-macroglobulin complexes with and mediates the endocytosis of beta-amyloid peptide via cell surface low-density lipoprotein receptor-related protein.* J Neurochem, 1997. **69**(5): p. 1904-11.
195. Du, Y., et al., *alpha2-Macroglobulin as a beta-amyloid peptide-binding plasma protein.* J Neurochem, 1997. **69**(1): p. 299-305.

196. Van Gool, D., et al., *alpha 2-Macroglobulin expression in neuritic-type plaques in patients with Alzheimer's disease.* Neurobiol Aging, 1993. **14**(3): p. 233-7.
197. Herz, J. and D.K. Strickland, *LRP: a multifunctional scavenger and signaling receptor.* J Clin Invest, 2001. **108**(6): p. 779-84.
198. Bu, G., et al., *Expression and function of the low density lipoprotein receptor-related protein (LRP) in mammalian central neurons.* J Biol Chem, 1994. **269**(28): p. 18521-8.
199. Tanzi, R.E., R.D. Moir, and S.L. Wagner, *Clearance of Alzheimer's Abeta peptide: the many roads to perdition.* Neuron, 2004. **43**(5): p. 605-8.
200. Zlokovic, B.V., *Clearing amyloid through the blood-brain barrier.* J Neurochem, 2004. **89**(4): p. 807-11.
201. Shibata, M., et al., *Clearance of Alzheimer's amyloid-ss(1-40) peptide from brain by LDL receptor-related protein-1 at the blood-brain barrier.* J Clin Invest, 2000. **106**(12): p. 1489-99.
202. Deane, R., et al., *LRP/amyloid beta-peptide interaction mediates differential brain efflux of Abeta isoforms.* Neuron, 2004. **43**(3): p. 333-44.
203. Kang, D.E., et al., *Modulation of amyloid beta-protein clearance and Alzheimer's disease susceptibility by the LDL receptor-related protein pathway.* J Clin Invest, 2000. **106**(9): p. 1159-66.
204. Ertekin-Taner, N., et al., *Genetic variants in a haplotype block spanning IDE are significantly associated with plasma Abeta42 levels and risk for Alzheimer disease.* Hum Mutat, 2004. **23**(4): p. 334-42.
205. Bian, L., et al., *Insulin-degrading enzyme and Alzheimer disease: a genetic association study in the Han Chinese.* Neurology, 2004. **63**(2): p. 241-5.
206. Shi, J., et al., *Mutation screening and association study of the neprilysin gene in sporadic Alzheimer's disease in Chinese persons.* J Gerontol A Biol Sci Med Sci, 2005. **60**(3): p. 301-6.
207. Sakai, A., et al., *Association of the Neprilysin gene with susceptibility to late-onset Alzheimer's disease.* Dement Geriatr Cogn Disord, 2004. **17**(3): p. 164-9.
208. Helisalmi, S., et al., *Polymorphisms in neprilysin gene affect the risk of Alzheimer's disease in Finnish patients.* J Neurol Neurosurg Psychiatry, 2004. **75**(12): p. 1746-8.
209. Kehoe, P.G., et al., *Common variants of ACE contribute to variable age-at-onset of Alzheimer's disease.* Hum Genet, 2004. **114**(5): p. 478-83.
210. Elkins, J.S., V.C. Douglas, and S.C. Johnston, *Alzheimer disease risk and genetic variation in ACE: a meta-analysis.* Neurology, 2004. **62**(3): p. 363-8.
211. Boussaha, M., et al., *Polymorphisms of insulin degrading enzyme gene are not associated with Alzheimer's disease.* Neurosci Lett, 2002. **329**(1): p. 121-3.
212. Lilius, L., et al., *No association between polymorphisms in the neprilysin promoter region and Swedish Alzheimer's disease patients.* Neurosci Lett, 2003. **337**(2): p. 111-3.
213. Monastero, R., et al., *Lack of association between angiotensin converting enzyme polymorphism and sporadic Alzheimer's disease.* Neurosci Lett, 2002. **335**(2): p. 147-9.
214. Glenner, G.G. and C.W. Wong, *Alzheimer's disease and Down's syndrome: sharing of a unique cerebrovascular amyloid fibril protein.* Biochem Biophys Res Commun, 1984. **122**(3): p. 1131-5.
215. Dodart, J.C., et al., *Gene delivery of human apolipoprotein E alters brain Abeta burden in a mouse model of Alzheimer's disease.* Proc Natl Acad Sci U S A, 2005. **102**(4): p. 1211-6.

216. Janus, C. and D. Westaway, *Transgenic mouse models of Alzheimer's disease.* Physiol Behav, 2001. **73**(5): p. 873-86.
217. Higgins, G.A. and H. Jacobsen, *Transgenic mouse models of Alzheimer's disease: phenotype and application.* Behav Pharmacol, 2003. **14**(5-6): p. 419-38.
218. Hsiao, K., et al., *Correlative memory deficits, Abeta elevation, and amyloid plaques in transgenic mice.* Science, 1996. **274**(5284): p. 99-102.
219. Polvikoski, T., et al., *Apolipoprotein E, dementia, and cortical deposition of beta-amyloid protein.* N Engl J Med, 1995. **333**(19): p. 1242-7.
220. Lemere, C.A., et al., *Sequence of deposition of heterogeneous amyloid beta-peptides and APO E in Down syndrome: implications for initial events in amyloid plaque formation.* Neurobiol Dis, 1996. **3**(1): p. 16-32.
221. Irizarry, M.C., et al., *APPSw transgenic mice develop age-related A beta deposits and neuropil abnormalities, but no neuronal loss in CA1.* J Neuropathol Exp Neurol, 1997. **56**(9): p. 965-73.
222. Games, D., et al., *Alzheimer-type neuropathology in transgenic mice overexpressing V717F beta-amyloid precursor protein.* Nature, 1995. **373**(6514): p. 523-7.
223. Stein, T.D. and J.A. Johnson, *Lack of neurodegeneration in transgenic mice overexpressing mutant amyloid precursor protein is associated with increased levels of transthyretin and the activation of cell survival pathways.* J Neurosci, 2002. **22**(17): p. 7380-8.
224. Stein, T.D., et al., *Neutralization of transthyretin reverses the neuroprotective effects of secreted amyloid precursor protein (APP) in APPSW mice resulting in tau phosphorylation and loss of hippocampal neurons: support for the amyloid hypothesis.* J Neurosci, 2004. **24**(35): p. 7707-17.
225. Carro, E., et al., *Serum insulin-like growth factor I regulates brain amyloid-beta levels.* Nat Med, 2002. **8**(12): p. 1390-7.
226. De Felice, F.G., et al., *Targeting the neurotoxic species in Alzheimer's disease: inhibitors of Abeta oligomerization.* Faseb J, 2004. **18**(12): p. 1366-72.
227. Wang, H.W., et al., *Soluble oligomers of beta amyloid (1-42) inhibit long-term potentiation but not long-term depression in rat dentate gyrus.* Brain Res, 2002. **924**(2): p. 133-40.
228. Dahlgren, K.N., et al., *Oligomeric and fibrillar species of amyloid-beta peptides differentially affect neuronal viability.* J Biol Chem, 2002. **277**(35): p. 32046-53.
229. Iwata, N., et al., *Metabolic regulation of brain Abeta by neprilysin.* Science, 2001. **292**(5521): p. 1550-2.
230. Iwata, N., M. Higuchi, and T.C. Saido, *Metabolism of amyloid-beta peptide and Alzheimer's disease.* Pharmacol Ther, 2005.
231. Tanzi, R.E., et al., *The gene defects responsible for familial Alzheimer's disease.* Neurobiol Dis, 1996. **3**(3): p. 159-68.
232. Poduslo, S.E., et al., *A familial case of Alzheimer's disease without tau pathology may be linked with chromosome 3 markers.* Hum Genet, 1999. **105**(1-2): p. 32-7.
233. Shipp, M.A., et al., *Molecular cloning of the common acute lymphoblastic leukemia antigen (CALLA) identifies a type II integral membrane protein.* Proc Natl Acad Sci U S A, 1988. **85**(13): p. 4819-23.
234. D'Adamio, L., et al., *Organization of the gene encoding common acute lymphoblastic leukemia antigen (neutral endopeptidase 24.11): multiple miniexons and separate 5' untranslated regions.* Proc Natl Acad Sci U S A, 1989. **86**(18): p. 7103-7.
235. Haouas, H., et al., *Characterization of the 5' region of the CD10/neutral endopeptidase 24.11 gene.* Biochem Biophys Res Commun, 1995. **207**(3): p. 933-42.

236. Li, C., et al., *Comparison of the structure and expression of the human and rat neprilysin (endopeptidase 24.11)-encoding genes.* Gene, 1995. **164**(2): p. 363-6.
237. Chen, C.Y., et al., *Murine common acute lymphoblastic leukemia antigen (CD10 neutral endopeptidase 24.11). Molecular characterization, chromosomal localization, and modeling of the active site.* J Immunol, 1992. **148**(9): p. 2817-25.
238. Shipp, M.A., et al., *Common acute lymphoblastic leukemia antigen (CALLA) is active neutral endopeptidase 24.11 ("enkephalinase"): direct evidence by cDNA transfection analysis.* Proc Natl Acad Sci U S A, 1989. **86**(1): p. 297-301.
239. Letarte, M., et al., *Common acute lymphocytic leukemia antigen is identical to neutral endopeptidase.* J Exp Med, 1988. **168**(4): p. 1247-53.
240. Li, C., R.M. Booze, and L.B. Hersh, *Tissue-specific expression of rat neutral endopeptidase (neprilysin) mRNAs.* J Biol Chem, 1995. **270**(11): p. 5723-8.
241. Ishimaru, F. and M.A. Shipp, *Analysis of the human CD10/neutral endopeptidase 24.11 promoter region: two separate regulatory elements.* Blood, 1995. **85**(11): p. 3199-207.
242. Ishimaru, F., B. Mari, and M.A. Shipp, *The type 2 CD10/neutral endopeptidase 24.11 promoter: functional characterization and tissue-specific regulation by CBF/NF-Y isoforms.* Blood, 1997. **89**(11): p. 4136-45.
243. Shen, R., et al., *Identification and characterization of two androgen response regions in the human neutral endopeptidase gene.* Mol Cell Endocrinol, 2000. **170**(1-2): p. 131-42.
244. Casey, M.L., et al., *Progesterone-regulated cyclic modulation of membrane metalloendopeptidase (enkephalinase) in human endometrium.* J Biol Chem, 1991. **266**(34): p. 23041-7.
245. van der Velden, V.H., et al., *Cytokines and glucocorticoids modulate human bronchial epithelial cell peptidases.* Cytokine, 1998. **10**(1): p. 55-65.
246. Graf, K., et al., *Glucocorticoids and protein kinase C regulate neutral endopeptidase 24.11 in human vascular smooth muscle cells.* Basic Res Cardiol, 1998. **93**(1): p. 11-7.
247. Borson, D.B. and D.C. Gruenert, *Glucocorticoids induce neutral endopeptidase in transformed human tracheal epithelial cells.* Am J Physiol, 1991. **260**(2 Pt 1): p. L83-9.
248. Sezaki, N., et al., *The type 1 CD10/neutral endopeptidase 24.11 promoter: functional characterization of the 5'-untranslated region.* Br J Haematol, 2003. **123**(1): p. 177-83.
249. Pugh, B.F. and R. Tjian, *Transcription from a TATA-less promoter requires a multisubunit TFIID complex.* Genes Dev, 1991. **5**(11): p. 1935-45.
250. Gardiner-Garden, M. and M. Frommer, *CpG islands in vertebrate genomes.* J Mol Biol, 1987. **196**(2): p. 261-82.
251. Brandeis, M., et al., *Sp1 elements protect a CpG island from de novo methylation.* Nature, 1994. **371**(6496): p. 435-8.
252. Li, L., et al., *Gene regulation by Sp1 and Sp3.* Biochem Cell Biol, 2004. **82**(4): p. 460-71.
253. Usmani, B.A., et al., *Methylation of the neutral endopeptidase gene promoter in human prostate cancers.* Clin Cancer Res, 2000. **6**(5): p. 1664-70.
254. Osman, I., et al., *Neutral endopeptidase protein expression and prognosis in localized prostate cancer.* Clin Cancer Res, 2004. **10**(12 Pt 1): p. 4096-100.
255. Papandreou, C.N., et al., *Neutral endopeptidase 24.11 loss in metastatic human prostate cancer contributes to androgen-independent progression.* Nat Med, 1998. **4**(1): p. 50-7.

256. Kondepudi, A. and A. Johnson, *Cytokines increase neutral endopeptidase activity in lung fibroblasts.* Am J Respir Cell Mol Biol, 1993. **8**(1): p. 43-9.
257. Uehara, C., et al., *Upregulation of neutral endopeptidase expression and enzymatic activity during the differentiation of human choriocarcinoma cells.* Placenta, 2001. **22**(6): p. 540-9.
258. Wice, B., et al., *Modulators of cyclic AMP metabolism induce syncytiotrophoblast formation in vitro.* Exp Cell Res, 1990. **186**(2): p. 306-16.
259. Strauss, J.F., 3rd, et al., *The cAMP signalling system and human trophoblast function.* Placenta, 1992. **13**(5): p. 389-403.
260. Suzuki, T., et al., *Neutral endopeptidase/CD10 expression during phorbol ester-induced differentiation of choriocarcinoma cells through the protein kinase C- and extracellular signal-regulated kinase-dependent signalling pathway.* Placenta, 2002. **23**(6): p. 475-82.
261. Malfroy, B., et al., *Molecular cloning and amino acid sequence of human enkephalinase (neutral endopeptidase).* FEBS Lett, 1988. **229**(1): p. 206-10.
262. Malfroy, B., et al., *Molecular cloning and amino acid sequence of rat enkephalinase.* Biochem Biophys Res Commun, 1987. **144**(1): p. 59-66.
263. Oefner, C., et al., *Structure of human neutral endopeptidase (Neprilysin) complexed with phosphoramidon.* J Mol Biol, 2000. **296**(2): p. 341-9.
264. Tam, L.T., et al., *The importance of disulfide bridges in human endopeptidase (enkephalinase) after proteolytic cleavage.* Biochem Biophys Res Commun, 1985. **133**(3): p. 1187-92.
265. Oefner, C., et al., *Structural analysis of neprilysin with various specific and potent inhibitors.* Acta Crystallogr D Biol Crystallogr, 2004. **60**(Pt 2): p. 392-6.
266. Shimada, K., M. Takahashi, and K. Tanzawa, *Cloning and functional expression of endothelin-converting enzyme from rat endothelial cells.* J Biol Chem, 1994. **269**(28): p. 18275-8.
267. Shimada, K., et al., *Identification and characterization of two isoforms of an endothelin-converting enzyme-1.* FEBS Lett, 1995. **371**(2): p. 140-4.
268. Emoto, N. and M. Yanagisawa, *Endothelin-converting enzyme-2 is a membrane-bound, phosphoramidon-sensitive metalloprotease with acidic pH optimum.* J Biol Chem, 1995. **270**(25): p. 15262-8.
269. Lee, S., et al., *Molecular cloning and primary structure of Kell blood group protein.* Proc Natl Acad Sci U S A, 1991. **88**(14): p. 6353-7.
270. Kiryu-Seo, S., et al., *Damage-induced neuronal endopeptidase (DINE) is a unique metallopeptidase expressed in response to neuronal damage and activates superoxide scavengers.* Proc Natl Acad Sci U S A, 2000. **97**(8): p. 4345-50.
271. Valdenaire, O., et al., *XCE, a new member of the endothelin-converting enzyme and neutral endopeptidase family, is preferentially expressed in the CNS.* Brain Res Mol Brain Res, 1999. **64**(2): p. 211-21.
272. Ouimet, T., et al., *Neprilysin II: A putative novel metalloprotease and its isoforms in CNS and testis.* Biochem Biophys Res Commun, 2000. **271**(3): p. 565-70.
273. Ikeda, K., et al., *Molecular identification and characterization of novel membrane-bound metalloprotease, the soluble secreted form of which hydrolyzes a variety of vasoactive peptides.* J Biol Chem, 1999. **274**(45): p. 32469-77.
274. Ghaddar, G., et al., *Molecular cloning and biochemical characterization of a new mouse testis soluble-zinc-metallopeptidase of the neprilysin family.* Biochem J, 2000. **347**(Pt 2): p. 419-29.
275. Turner, A.J., R.E. Isaac, and D. Coates, *The neprilysin (NEP) family of zinc metalloendopeptidases: genomics and function.* Bioessays, 2001. **23**(3): p. 261-9.

276. Turner, A.J., et al., *Endopeptidase-24.11 (neprilysin) and relatives: twenty years on.* Adv Exp Med Biol, 1996. **389**: p. 141-8.
277. Kerr, M.A. and A.J. Kenny, *The purification and specificity of a neutral endopeptidase from rabbit kidney brush border.* Biochem J, 1974. **137**(3): p. 477-88.
278. Matsas, R., A.J. Kenny, and A.J. Turner, *An immunohistochemical study of endopeptidase-24.11 ("enkephalinase") in the pig nervous system.* Neuroscience, 1986. **18**(4): p. 991-1012.
279. Matsas, R., et al., *Substance P and [Leu]enkephalin are hydrolyzed by an enzyme in pig caudate synaptic membranes that is identical with the endopeptidase of kidney microvilli.* Proc Natl Acad Sci U S A, 1983. **80**(10): p. 3111-5.
280. Erdos, E.G., et al., *Neutral metalloendopeptidase in human male genital tract. Comparison to angiotensin I-converting enzyme.* Lab Invest, 1985. **52**(4): p. 437-47.
281. Johnson, A.R., et al., *Neutral metalloendopeptidase in human lung tissue and cultured cells.* Am Rev Respir Dis, 1985. **132**(3): p. 564-8.
282. Gee, N.S., R. Matsas, and A.J. Kenny, *A monoclonal antibody to kidney endopeptidase-24.11. Its application in immunoadsorbent purification of the enzyme and immunofluorescent microscopy of kidney and intestine.* Biochem J, 1983. **214**(2): p. 377-86.
283. Painter, R.G., et al., *Function of neutral endopeptidase on the cell membrane of human neutrophils.* J Biol Chem, 1988. **263**(19): p. 9456-61.
284. Cutrona, G., et al., *CD10 is a marker for cycling cells with propensity to apoptosis in childhood ALL.* Br J Cancer, 2002. **86**(11): p. 1776-85.
285. Bene, M.C. and G.C. Faure, *CD10 in acute leukemias. GEIL (Groupe d'Etude Immunologique des Leucemies).* Haematologica, 1997. **82**(2): p. 205-10.
286. Facchinetti, P., et al., *Ontogeny, regional and cellular distribution of the novel metalloprotease neprilysin 2 in the rat: a comparison with neprilysin and endothelin-converting enzyme-1.* Neuroscience, 2003. **118**(3): p. 627-39.
287. De La Baume, S., G. Patey, and J.C. Schwartz, *Subcellular distribution of enkephalin-dipeptidyl carboxypeptidase (enkephalinase) in rat brain.* Neuroscience, 1981. **6**(3): p. 315-21.
288. Fukami, S., et al., *Abeta-degrading endopeptidase, neprilysin, in mouse brain: synaptic and axonal localization inversely correlating with Abeta pathology.* Neurosci Res, 2002. **43**(1): p. 39-56.
289. Waksman, G., et al., *Neuronal localization of the neutral endopeptidase 'enkephalinase' in rat brain revealed by lesions and autoradiography.* Embo J, 1986. **5**(12): p. 3163-6.
290. Pollard, H., et al., *Detailed immunoautoradiographic mapping of enkephalinase (EC 3.4.24.11) in rat central nervous system: comparison with enkephalins and substance P.* Neuroscience, 1989. **30**(2): p. 339-76.
291. Turner, *Handbook of Proteolytic Enzymes*. 1998. 1080-1085.
292. Erdos, E.G. and R.A. Skidgel, *Neutral endopeptidase 24.11 (enkephalinase) and related regulators of peptide hormones.* Faseb J, 1989. **3**(2): p. 145-51.
293. Bunnett, N.W., et al., *Isolation of endopeptidase-24.11 (EC 3.4.24.11, "enkephalinase") from the pig stomach. Hydrolysis of substance P, gastrin-releasing peptide 10, [Leu5] enkephalin, and [Met5] enkephalin.* Gastroenterology, 1988. **95**(4): p. 952-7.
294. Matsas, R., A.J. Kenny, and A.J. Turner, *The metabolism of neuropeptides. The hydrolysis of peptides, including enkephalins, tachykinins and their analogues, by endopeptidase-24.11.* Biochem J, 1984. **223**(2): p. 433-40.

295. Malfroy, B., et al., *High-affinity enkephalin-degrading peptidase in brain is increased after morphine.* Nature, 1978. **276**(5687): p. 523-6.
296. Stephenson, S.L. and A.J. Kenny, *The hydrolysis of alpha-human atrial natriuretic peptide by pig kidney microvillar membranes is initiated by endopeptidase-24.11.* Biochem J, 1987. **243**(1): p. 183-7.
297. Shipp, M.A., et al., *CD10/neutral endopeptidase 24.11 hydrolyzes bombesin-like peptides and regulates the growth of small cell carcinomas of the lung.* Proc Natl Acad Sci U S A, 1991. **88**(23): p. 10662-6.
298. Vijayaraghavan, J., et al., *The hydrolysis of endothelins by neutral endopeptidase 24.11 (enkephalinase).* J Biol Chem, 1990. **265**(24): p. 14150-5.
299. Gafford, J.T., et al., *Human kidney "enkephalinase", a neutral metalloendopeptidase that cleaves active peptides.* Biochemistry, 1983. **22**(13): p. 3265-71.
300. Sakurada, C., H. Yokosawa, and S. Ishii, *The degradation of somatostatin by synaptic membrane of rat hippocampus is initiated by endopeptidase-24.11.* Peptides, 1990. **11**(2): p. 287-92.
301. Gu, Z.F., et al., *Neutral endopeptidase (EC 3.4.24.11) modulates the contractile effects of neuropeptides on muscle cells from the guinea-pig stomach.* Exp Physiol, 1993. **78**(1): p. 35-48.
302. Barnes, K., S. Doherty, and A.J. Turner, *Endopeptidase-24.11 is the integral membrane peptidase initiating degradation of somatostatin in the hippocampus.* J Neurochem, 1995. **64**(4): p. 1826-32.
303. Howell, S., J. Nalbantoglu, and P. Crine, *Neutral endopeptidase can hydrolyze beta-amyloid(1-40) but shows no effect on beta-amyloid precursor protein metabolism.* Peptides, 1995. **16**(4): p. 647-52.
304. Defendini, R., et al., *Angiotensin-converting enzyme in epithelial and neuroepithelial cells.* Neuroendocrinology, 1983. **37**(1): p. 32-40.
305. Barnes, K. and A.J. Turner, *The endothelin system and endothelin-converting enzyme in the brain: molecular and cellular studies.* Neurochem Res, 1997. **22**(8): p. 1033-40.
306. Rose, C., et al., *Cell-specific activity of neprilysin 2 isoforms and enzymic specificity compared with neprilysin.* Biochem J, 2002. **363**(Pt 3): p. 697-705.
307. Rupreht, J., et al., *Effect of phosphoramidon - a selective enkephalinase inhibitor - on nociception and behaviour.* Neurosci Lett, 1983. **41**(3): p. 331-5.
308. Fulcher, I.S., et al., *Kidney neutral endopeptidase and the hydrolysis of enkephalin by synaptic membranes show similar sensitivity to inhibitors.* Biochem J, 1982. **203**(2): p. 519-22.
309. Roques, B.P., et al., *The enkephalinase inhibitor thiorphan shows antinociceptive activity in mice.* Nature, 1980. **288**(5788): p. 286-8.
310. Elsner, D., et al., *Effectiveness of endopeptidase inhibition (candoxatril) in congestive heart failure.* Am J Cardiol, 1992. **70**(4): p. 494-8.
311. Cruden, N.L., et al., *Neutral endopeptidase inhibition augments vascular actions of bradykinin in patients treated with angiotensin-converting enzyme inhibition.* Hypertension, 2004. **44**(6): p. 913-8.
312. Blais, C., Jr., et al., *Contribution of angiotensin-converting enzyme to the cardiac metabolism of bradykinin: an interspecies study.* Am J Physiol, 1997. **273**(5 Pt 2): p. H2263-71.
313. Skidgel, R.A., H.L. Jackman, and E.G. Erdos, *Metabolism of substance P and bradykinin by human neutrophils.* Biochem Pharmacol, 1991. **41**(9): p. 1335-44.
314. Lu, B., et al., *Neutral endopeptidase modulation of septic shock.* J Exp Med, 1995. **181**(6): p. 2271-5.

315. Martins, M.A., et al., *Peptidase modulation of the pulmonary effects of tachykinins in tracheal superfused guinea pig lungs.* J Clin Invest, 1990. **85**(1): p. 170-6.
316. Webb, R.L., et al., *Degradation of atrial natriuretic peptide: pharmacologic effects of protease EC 24.11 inhibition.* J Cardiovasc Pharmacol, 1989. **14**(2): p. 285-93.
317. Iwata, N., et al., *Identification of the major Abeta1-42-degrading catabolic pathway in brain parenchyma: suppression leads to biochemical and pathological deposition.* Nat Med, 2000. **6**(2): p. 143-50.
318. Miyamoto, A., S. Murata, and A. Nishio, *Role of ACE and NEP in bradykinin-induced relaxation and contraction response of isolated porcine basilar artery.* Naunyn Schmiedebergs Arch Pharmacol, 2002. **365**(5): p. 365-70.
319. Fossiez, F., et al., *Secretion of a functional soluble form of neutral endopeptidase-24.11 from a baculovirus-infected insect cell line.* Biochem J, 1992. **284 (Pt 1)**: p. 53-9.
320. Skidgel, R.A. and E.G. Erdos, *Angiotensin converting enzyme (ACE) and neprilysin hydrolyze neuropeptides: a brief history, the beginning and follow-ups to early studies.* Peptides, 2004. **25**(3): p. 521-5.
321. Yang, H.Y., E.G. Erdos, and Y. Levin, *A dipeptidyl carboxypeptidase that converts angiotensin I and inactivates bradykinin.* Biochim Biophys Acta, 1970. **214**(2): p. 374-6.
322. Savage, P., et al., *Differential inhibition of wild-type endothelin-converting enzyme-1 and its mutants.* J Cardiovasc Pharmacol, 1998. **31 Suppl 1**: p. S16-8.
323. Kukkola, P.J., et al., *Differential structure-activity relationships of phosphoramidon analogues for inhibition of three metalloproteases: endothelin-converting enzyme, neutral endopeptidase, and angiotensin-converting enzyme.* J Cardiovasc Pharmacol, 1995. **26 Suppl 3**: p. S65-8.
324. Takahashi, M., et al., *Localization of rat endothelin-converting enzyme to vascular endothelial cells and some secretory cells.* Biochem J, 1995. **311 (Pt 2)**: p. 657-65.
325. Barnes, K. and A.J. Turner, *Endothelin converting enzyme is located on alpha-actin filaments in smooth muscle cells.* Cardiovasc Res, 1999. **42**(3): p. 814-22.
326. Barnes, K., et al., *Expression of endothelin-converting enzyme in both neuroblastoma and glial cell lines and its localization in rat hippocampus.* J Neurochem, 1997. **68**(2): p. 570-7.
327. Turner, A.J. and L.J. Murphy, *Molecular pharmacology of endothelin converting enzymes.* Biochem Pharmacol, 1996. **51**(2): p. 91-102.
328. Loffler, B.M., *Endothelin-converting enzyme inhibitors: current status and perspectives.* J Cardiovasc Pharmacol, 2000. **35**(4 Suppl 2): p. S79-82.
329. Janas, J., et al., *Endothelin-1 inactivating peptidase in the human kidney and urine.* J Hypertens, 2000. **18**(4): p. 475-83.
330. Janas, J., et al., *Characterization of a novel, high-molecular weight, acidic, endothelin-1 inactivating metalloendopeptidase from the rat kidney.* J Hypertens, 1994. **12**(10): p. 1155-62.
331. Shirotani, K., et al., *Neprilysin degrades both amyloid beta peptides 1-40 and 1-42 most rapidly and efficiently among thiorphan- and phosphoramidon-sensitive endopeptidases.* J Biol Chem, 2001. **276**(24): p. 21895-901.
332. Mierau, I., et al., *Cloning and sequencing of the gene for a lactococcal endopeptidase, an enzyme with sequence similarity to mammalian enkephalinase.* J Bacteriol, 1993. **175**(7): p. 2087-96.
333. Awano, S., et al., *Sequencing, expression and biochemical characterization of the Porphyromonas gingivalis pepO gene encoding a protein homologous to human endothelin-converting enzyme.* FEBS Lett, 1999. **460**(1): p. 139-44.

334. Coates, D., R. Siviter, and R.E. Isaac, *Exploring the Caenorhabditis elegans and Drosophila melanogaster genomes to understand neuropeptide and peptidase function.* Biochem Soc Trans, 2000. **28**(4): p. 464-9.
335. Zhang, A.Z., H.Y. Yang, and E. Costa, *Nociception, enkephalin content and dipeptidyl carboxypeptidase activity in brain of mice treated with exopeptidase inhibitors.* Neuropharmacology, 1982. **21**(7): p. 625-30.
336. Mendelsohn, L.G., et al., *Thiorphan and analogs: lack of correlation between potency to inhibit "enkephalinase A" in vitro and analgesic potency in vivo.* J Pharmacol Exp Ther, 1985. **234**(2): p. 386-90.
337. Chipkin, R.E., et al., *Pharmacology of SCH 34826, an orally active enkephalinase inhibitor analgesic.* J Pharmacol Exp Ther, 1988. **245**(3): p. 829-38.
338. Patey, G., et al., *Selective protection of methionine enkephalin released from brain slices by enkephalinase inhibition.* Science, 1981. **212**(4499): p. 1153-5.
339. Altstein, M., et al., *Protection of enkephalins from enzymatic degradation utilizing selective metal-chelating inhibitors.* Eur J Pharmacol, 1983. **91**(4): p. 353-61.
340. Chaillet, P., et al., *Inhibition of enkephalin metabolism by, and antinociceptive activity of, bestatin, an aminopeptidase inhibitor.* Eur J Pharmacol, 1983. **86**(3-4): p. 329-36.
341. Parsons, C.G. and A. Herz, *Peripheral opioid receptors mediating antinociception in inflammation. Evidence for activation by enkephalin-like opioid peptides after cold water swim stress.* J Pharmacol Exp Ther, 1990. **255**(2): p. 795-802.
342. Costentin, J., et al., *Dissociated effects of inhibitors of enkephalin-metabolising peptidases or naloxone on various nociceptive responses.* Eur J Pharmacol, 1986. **123**(1): p. 37-44.
343. Murthy, L.R., et al., *Inhibitors of an enkephalin degrading membrane-bound metalloendopeptidase: analgesic properties and effects on striatal enkephalin levels.* Eur J Pharmacol, 1984. **102**(2): p. 305-13.
344. Saria, A., et al., *Opioid-related changes in nociceptive threshold and in tissue levels of enkephalins after target disruption of the gene for neutral endopeptidase (EC 3.4.24.11) in mice.* Neurosci Lett, 1997. **234**(1): p. 27-30.
345. Fischer, H.S., et al., *Neutral endopeptidase knockout induces hyperalgesia in a model of visceral pain, an effect related to bradykinin and nitric oxide.* J Mol Neurosci, 2002. **18**(1-2): p. 129-34.
346. O'Connor, T.M., et al., *The role of substance P in inflammatory disease.* J Cell Physiol, 2004. **201**(2): p. 167-80.
347. Liddle, R.A. and J.D. Nathan, *Neurogenic inflammation and pancreatitis.* Pancreatology, 2004. **4**(6): p. 551-9; discussion 559-60.
348. Groneberg, D.A., et al., *Neurogenic mechanisms in bronchial inflammatory diseases.* Allergy, 2004. **59**(11): p. 1139-52.
349. Di Maria, G.U., S. Bellofiore, and P. Geppetti, *Regulation of airway neurogenic inflammation by neutral endopeptidase.* Eur Respir J, 1998. **12**(6): p. 1454-62.
350. Okamoto, A., et al., *Interactions between neutral endopeptidase (EC 3.4.24.11) and the substance P (NK1) receptor expressed in mammalian cells.* Biochem J, 1994. **299 (Pt 3)**: p. 683-93.
351. Sturiale, S., et al., *Neutral endopeptidase (EC 3.4.24.11) terminates colitis by degrading substance P.* Proc Natl Acad Sci U S A, 1999. **96**(20): p. 11653-8.
352. Barbara, G., et al., *Neutral endopeptidase (EC 3.4.24.11) downregulates the onset of intestinal inflammation in the nematode infected mouse.* Gut, 2003. **52**(10): p. 1457-64.
353. Lu, B., et al., *The control of microvascular permeability and blood pressure by neutral endopeptidase.* Nat Med, 1997. **3**(8): p. 904-7.

354. Kirkwood, K.S., et al., *Deletion of neutral endopeptidase exacerbates intestinal inflammation induced by Clostridium difficile toxin A.* Am J Physiol Gastrointest Liver Physiol, 2001. **281**(2): p. G544-51.
355. Scholzen, T.E., et al., *Neutral endopeptidase terminates substance P-induced inflammation in allergic contact dermatitis.* J Immunol, 2001. **166**(2): p. 1285-91.
356. Nadel, J.A. and D.B. Borson, *Modulation of neurogenic inflammation by neutral endopeptidase.* Am Rev Respir Dis, 1991. **143**(3 Pt 2): p. S33-6.
357. Nadel, J.A., *Mechanisms of inflammation and potential role in the pathogenesis of asthma.* Allergy Proc, 1991. **12**(2): p. 85-8.
358. Nadel, J.A., *Neutral endopeptidase modulation of neurogenic inflammation in airways.* Eur Respir J Suppl, 1990. **12**: p. 645s-651s.
359. Kohrogi, H., et al., *Recombinant human enkephalinase (neutral endopeptidase) prevents cough induced by tachykinins in awake guinea pigs.* J Clin Invest, 1989. **84**(3): p. 781-6.
360. Rubinstein, I., et al., *Recombinant neutral endopeptidase attenuates substance P-induced plasma extravasation in the guinea pig skin.* Int Arch Allergy Appl Immunol, 1990. **91**(3): p. 232-8.
361. Parkin, D.M., et al., *Global cancer statistics, 2002.* CA Cancer J Clin, 2005. **55**(2): p. 74-108.
362. Parkin, D.M., *Global cancer statistics in the year 2000.* Lancet Oncol, 2001. **2**(9): p. 533-43.
363. Dusser, D.J., et al., *Cigarette smoke induces bronchoconstrictor hyperresponsiveness to substance P and inactivates airway neutral endopeptidase in the guinea pig. Possible role of free radicals.* J Clin Invest, 1989. **84**(3): p. 900-6.
364. Aguayo, S.M., et al., *Increased levels of bombesin-like peptides in the lower respiratory tract of asymptomatic cigarette smokers.* J Clin Invest, 1989. **84**(4): p. 1105-13.
365. Willey, J.C., J.F. Lechner, and C.C. Harris, *Bombesin and the C-terminal tetradecapeptide of gastrin-releasing peptide are growth factors for normal human bronchial epithelial cells.* Exp Cell Res, 1984. **153**(1): p. 245-8.
366. Aguayo, S.M., et al., *Increased pulmonary neuroendocrine cells with bombesin-like immunoreactivity in adult patients with eosinophilic granuloma.* J Clin Invest, 1990. **86**(3): p. 838-44.
367. Cuttitta, F., et al., *Bombesin-like peptides can function as autocrine growth factors in human small-cell lung cancer.* Nature, 1985. **316**(6031): p. 823-6.
368. Bunn, P.A., Jr., et al., *Effects of recombinant neutral endopeptidase (EC 3.4.24.11) on the growth of lung cancer cell lines in vitro and in vivo.* Clin Cancer Res, 1998. **4**(11): p. 2849-58.
369. Aprikian, A.G., et al., *Bombesin stimulates the motility of human prostate-carcinoma cells through tyrosine phosphorylation of focal adhesion kinase and of integrin-associated proteins.* Int J Cancer, 1997. **72**(3): p. 498-504.
370. Nelson, J.B. and M.A. Carducci, *Small bioactive peptides and cell surface peptidases in androgen-independent prostate cancer.* Cancer Invest, 2000. **18**(1): p. 87-96.
371. Freedland, S.J., et al., *Loss of CD10 (neutral endopeptidase) is a frequent and early event in human prostate cancer.* Prostate, 2003. **55**(1): p. 71-80.
372. Zachary, I. and E. Rozengurt, *Focal adhesion kinase (p125FAK): a point of convergence in the action of neuropeptides, integrins, and oncogenes.* Cell, 1992. **71**(6): p. 891-4.
373. Sumitomo, M., et al., *Neutral endopeptidase inhibits prostate cancer cell migration by blocking focal adhesion kinase signaling.* J Clin Invest, 2000. **106**(11): p. 1399-407.

374. Dai, J., et al., *Tumor-suppressive effects of neutral endopeptidase in androgen-independent prostate cancer cells.* Clin Cancer Res, 2001. **7**(5): p. 1370-7.
375. Shen, R., et al., *Androgen-induced growth inhibition of androgen receptor expressing androgen-independent prostate cancer cells is mediated by increased levels of neutral endopeptidase.* Endocrinology, 2000. **141**(5): p. 1699-704.
376. Kajiyama, H., et al., *Neutral endopeptidase 24.11/CD10 suppresses progressive potential in ovarian carcinoma in vitro and in vivo.* Clin Cancer Res, 2005. **11**(5): p. 1798-808.
377. Burns, D.M., et al., *Breast cancer cell-associated endopeptidase EC 24.11 modulates proliferative response to bombesin.* Br J Cancer, 1999. **79**(2): p. 214-20.
378. Bagnato, A., et al., *Autocrine actions of endothelin-1 as a growth factor in human ovarian carcinoma cells.* Clin Cancer Res, 1995. **1**(9): p. 1059-66.
379. Bagnato, A., et al., *Activation of mitogenic signaling by endothelin 1 in ovarian carcinoma cells.* Cancer Res, 1997. **57**(7): p. 1306-11.
380. Suzuki, T., et al., *Imbalance between neutral endopeptidase 24.11 and endothelin-1 expression in human endometrial carcinoma.* Oncology, 2001. **60**(3): p. 258-67.
381. Khin, E.E., et al., *Neutral endopeptidase/CD10 expression in the stroma of epithelial ovarian carcinoma.* Int J Gynecol Pathol, 2003. **22**(2): p. 175-80.
382. Tse, G.M., et al., *Stromal CD10 expression in mammary fibroadenomas and phyllodes tumours.* J Clin Pathol, 2005. **58**(2): p. 185-9.
383. Iwaya, K., et al., *Stromal expression of CD10 in invasive breast carcinoma: a new predictor of clinical outcome.* Virchows Arch, 2002. **440**(6): p. 589-93.
384. Savage, M.J., et al., *Turnover of amyloid beta-protein in mouse brain and acute reduction of its level by phorbol ester.* J Neurosci, 1998. **18**(5): p. 1743-52.
385. Saido, T.C., *Alzheimer's disease as proteolytic disorders: anabolism and catabolism of beta-amyloid.* Neurobiol Aging, 1998. **19**(1 Suppl): p. S69-75.
386. Turner, A.J., L. Fisk, and N.N. Nalivaeva, *Targeting amyloid-degrading enzymes as therapeutic strategies in neurodegeneration.* Ann N Y Acad Sci, 2004. **1035**: p. 1-20.
387. Saito, T., et al., *Alzheimer's disease, neuropeptides, neuropeptidase, and amyloid-beta peptide metabolism.* Sci Aging Knowledge Environ, 2003. **2003**(3): p. PE1.
388. Kanemitsu, H., T. Tomiyama, and H. Mori, *Human neprilysin is capable of degrading amyloid beta peptide not only in the monomeric form but also the pathological oligomeric form.* Neurosci Lett, 2003. **350**(2): p. 113-6.
389. Newell, A.J., et al., *Thiorphan-induced neprilysin inhibition raises amyloid beta levels in rabbit cortex and cerebrospinal fluid.* Neurosci Lett, 2003. **350**(3): p. 178-80.
390. Marr, R.A., et al., *Neprilysin regulates amyloid Beta peptide levels.* J Mol Neurosci, 2004. **22**(1-2): p. 5-11.
391. Akiyama, H., et al., *Immunohistochemical localization of neprilysin in the human cerebral cortex: inverse association with vulnerability to amyloid beta-protein (Abeta) deposition.* Brain Res, 2001. **902**(2): p. 277-81.
392. Yasojima, K., et al., *Reduced neprilysin in high plaque areas of Alzheimer brain: a possible relationship to deficient degradation of beta-amyloid peptide.* Neurosci Lett, 2001. **297**(2): p. 97-100.
393. Carpentier, M., et al., *Declining expression of neprilysin in Alzheimer disease vasculature: possible involvement in cerebral amyloid angiopathy.* J Neuropathol Exp Neurol, 2002. **61**(10): p. 849-56.
394. Tsubuki, S., Y. Takaki, and T.C. Saido, *Dutch, Flemish, Italian, and Arctic mutations of APP and resistance of Abeta to physiologically relevant proteolytic degradation.* Lancet, 2003. **361**(9373): p. 1957-8.

395. Yamada, M., *Cerebral amyloid angiopathy and gene polymorphisms.* J Neurol Sci, 2004. **226**(1-2): p. 41-4.
396. Iwata, N., et al., *Region-specific reduction of A beta-degrading endopeptidase, neprilysin, in mouse hippocampus upon aging.* J Neurosci Res, 2002. **70**(3): p. 493-500.
397. Caccamo, A., et al., *Age- and region-dependent alterations in Abeta-degrading enzymes: implications for Abeta-induced disorders.* Neurobiol Aging, 2005. **26**(5): p. 645-54.
398. Sodeyama, N., et al., *Lack of association of neprilysin polymorphism with Alzheimer's disease and Alzheimer's disease-type neuropathological changes.* J Neurol Neurosurg Psychiatry, 2001. **71**(6): p. 817-8.
399. Oda, M., et al., *Dinucleotide repeat polymorphisms in the neprilysin gene are not associated with sporadic Alzheimer's disease.* Neurosci Lett, 2002. **320**(1-2): p. 105-7.
400. Clarimon, J., et al., *Possible increased risk for Alzheimer's disease associated with neprilysin gene.* J Neural Transm, 2003. **110**(6): p. 651-7.
401. Hama, E., et al., *Clearance of extracellular and cell-associated amyloid beta peptide through viral expression of neprilysin in primary neurons.* J Biochem (Tokyo), 2001. **130**(6): p. 721-6.
402. Marr, R.A., et al., *Neprilysin gene transfer reduces human amyloid pathology in transgenic mice.* J Neurosci, 2003. **23**(6): p. 1992-6.
403. Iwata, N., et al., *Presynaptic localization of neprilysin contributes to efficient clearance of amyloid-beta peptide in mouse brain.* J Neurosci, 2004. **24**(4): p. 991-8.
404. Mohajeri, M.H., et al., *Anti-amyloid activity of neprilysin in plaque-bearing mouse models of Alzheimer's disease.* FEBS Lett, 2004. **562**(1-3): p. 16-21.
405. Leissring, M.A., et al., *Enhanced proteolysis of beta-amyloid in APP transgenic mice prevents plaque formation, secondary pathology, and premature death.* Neuron, 2003. **40**(6): p. 1087-93.
406. Mohajeri, M.H., M.A. Wollmer, and R.M. Nitsch, *Abeta 42-induced increase in neprilysin is associated with prevention of amyloid plaque formation in vivo.* J Biol Chem, 2002. **277**(38): p. 35460-5.
407. Raum, D., et al., *Synthesis of human plasminogen by the liver.* Science, 1980. **208**(4447): p. 1036-7.
408. Mayer, M., *Biochemical and biological aspects of the plasminogen activation system.* Clin Biochem, 1990. **23**(3): p. 197-211.
409. Andreasen, P.A., et al., *Plasminogen activator inhibitor from human fibrosarcoma cells binds urokinase-type plasminogen activator, but not its proenzyme.* J Biol Chem, 1986. **261**(17): p. 7644-51.
410. Steiner, J.P., M. Migliorini, and D.K. Strickland, *Characterization of the reaction of plasmin with alpha 2-macroglobulin: effect of antifibrinolytic agents.* Biochemistry, 1987. **26**(25): p. 8487-95.
411. Vassalli, J.D., A.P. Sappino, and D. Belin, *The plasminogen activator/plasmin system.* J Clin Invest, 1991. **88**(4): p. 1067-72.
412. Bugge, T.H., et al., *Loss of fibrinogen rescues mice from the pleiotropic effects of plasminogen deficiency.* Cell, 1996. **87**(4): p. 709-19.
413. Alexander, C.M. and Z. Werb, *Proteinases and extracellular matrix remodeling.* Curr Opin Cell Biol, 1989. **1**(5): p. 974-82.
414. Werb, Z., *ECM and cell surface proteolysis: regulating cellular ecology.* Cell, 1997. **91**(4): p. 439-42.
415. Chen, Z.L. and S. Strickland, *Neuronal death in the hippocampus is promoted by plasmin-catalyzed degradation of laminin.* Cell, 1997. **91**(7): p. 917-25.

416. Strickland, S., *Tissue plasminogen activator in nervous system function and dysfunction.* Thromb Haemost, 2001. **86**(1): p. 138-43.
417. Nakagami, Y., et al., *Laminin degradation by plasmin regulates long-term potentiation.* J Neurosci, 2000. **20**(5): p. 2003-10.
418. Pang, P.T., et al., *Cleavage of proBDNF by tPA/plasmin is essential for long-term hippocampal plasticity.* Science, 2004. **306**(5695): p. 487-91.
419. Madani, R., et al., *Enhanced hippocampal long-term potentiation and learning by increased neuronal expression of tissue-type plasminogen activator in transgenic mice.* Embo J, 1999. **18**(11): p. 3007-12.
420. Pawlak, R., et al., *Rapid, specific and active site-catalyzed effect of tissue-plasminogen activator on hippocampus-dependent learning in mice.* Neuroscience, 2002. **113**(4): p. 995-1001.
421. Tucker, H.M., et al., *The plasmin system is induced by and degrades amyloid-beta aggregates.* J Neurosci, 2000. **20**(11): p. 3937-46.
422. Melchor, J.P., R. Pawlak, and S. Strickland, *The tissue plasminogen activator-plasminogen proteolytic cascade accelerates amyloid-beta (Abeta) degradation and inhibits Abeta-induced neurodegeneration.* J Neurosci, 2003. **23**(26): p. 8867-71.
423. Salonen, E.M., A. Zitting, and A. Vaheri, *Laminin interacts with plasminogen and its tissue-type activator.* FEBS Lett, 1984. **172**(1): p. 29-32.
424. Salonen, E.M., et al., *Plasminogen and tissue-type plasminogen activator bind to immobilized fibronectin.* J Biol Chem, 1985. **260**(22): p. 12302-7.
425. Kranenburg, O., et al., *Tissue-type plasminogen activator is a multiligand cross-beta structure receptor.* Curr Biol, 2002. **12**(21): p. 1833-9.
426. Wnendt, S., I. Wetzels, and W.A. Gunzler, *Amyloid beta peptides stimulate tissue-type plasminogen activator but not recombinant prourokinase.* Thromb Res, 1997. **85**(3): p. 217-24.
427. Kingston, I.B., M.J. Castro, and S. Anderson, *In vitro stimulation of tissue-type plasminogen activator by Alzheimer amyloid beta-peptide analogues.* Nat Med, 1995. **1**(2): p. 138-42.
428. Salles, F.J. and S. Strickland, *Localization and regulation of the tissue plasminogen activator-plasmin system in the hippocampus.* J Neurosci, 2002. **22**(6): p. 2125-34.
429. Sappino, A.P., et al., *Extracellular proteolysis in the adult murine brain.* J Clin Invest, 1993. **92**(2): p. 679-85.
430. Baranes, D., et al., *Tissue plasminogen activator contributes to the late phase of LTP and to synaptic growth in the hippocampal mossy fiber pathway.* Neuron, 1998. **21**(4): p. 813-25.
431. Yepes, M., et al., *Tissue-type plasminogen activator induces opening of the blood-brain barrier via the LDL receptor-related protein.* J Clin Invest, 2003. **112**(10): p. 1533-40.
432. Medina, M.G., et al., *Tissue plasminogen activator mediates amyloid-induced neurotoxicity via Erk1/2 activation.* Embo J, 2005. **24**(9): p. 1706-16.
433. Liu, D., et al., *Tissue plasminogen activator neurovascular toxicity is controlled by activated protein C.* Nat Med, 2004. **10**(12): p. 1379-83.
434. Petersen, L.C., et al., *One-chain urokinase-type plasminogen activator from human sarcoma cells is a proenzyme with little or no intrinsic activity.* J Biol Chem, 1988. **263**(23): p. 11189-95.
435. Bugge, T.H., et al., *Plasminogen deficiency causes severe thrombosis but is compatible with development and reproduction.* Genes Dev, 1995. **9**(7): p. 794-807.

436. Nauland, U. and D.C. Rijken, *Activation of thrombin-inactivated single-chain urokinase-type plasminogen activator by dipeptidyl peptidase I (cathepsin C).* Eur J Biochem, 1994. **223**(2): p. 497-501.
437. Kobayashi, H., et al., *Cathepsin B efficiently activates the soluble and the tumor cell receptor-bound form of the proenzyme urokinase-type plasminogen activator (Pro-uPA).* J Biol Chem, 1991. **266**(8): p. 5147-52.
438. Goretzki, L., et al., *Effective activation of the proenzyme form of the urokinase-type plasminogen activator (pro-uPA) by the cysteine protease cathepsin L.* FEBS Lett, 1992. **297**(1-2): p. 112-8.
439. List, K., et al., *Plasminogen-independent initiation of the pro-urokinase activation cascade in vivo. Activation of pro-urokinase by glandular kallikrein (mGK-6) in plasminogen-deficient mice.* Biochemistry, 2000. **39**(3): p. 508-15.
440. Ichinose, A., K. Fujikawa, and T. Suyama, *The activation of pro-urokinase by plasma kallikrein and its inactivation by thrombin.* J Biol Chem, 1986. **261**(8): p. 3486-9.
441. Frenette, G., et al., *Prostatic kallikrein hK2, but not prostate-specific antigen (hK3), activates single-chain urokinase-type plasminogen activator.* Int J Cancer, 1997. **71**(5): p. 897-9.
442. Stefansson, S. and D.A. Lawrence, *Old dogs and new tricks: proteases, inhibitors, and cell migration.* Sci STKE, 2003. **2003**(189): p. pe24.
443. Blasi, F. and P. Carmeliet, *uPAR: a versatile signalling orchestrator.* Nat Rev Mol Cell Biol, 2002. **3**(12): p. 932-43.
444. Andreasen, P.A., R. Egelund, and H.H. Petersen, *The plasminogen activation system in tumor growth, invasion, and metastasis.* Cell Mol Life Sci, 2000. **57**(1): p. 25-40.
445. Powell, E.M., W.M. Mars, and P. Levitt, *Hepatocyte growth factor/scatter factor is a motogen for interneurons migrating from the ventral to dorsal telencephalon.* Neuron, 2001. **30**(1): p. 79-89.
446. Exley, C. and O.V. Korchazhkina, *Plasmin cleaves Abeta42 in vitro and prevents its aggregation into beta-pleated sheet structures.* Neuroreport, 2001. **12**(13): p. 2967-70.
447. Van Nostrand, W.E. and M. Porter, *Plasmin cleavage of the amyloid beta-protein: alteration of secondary structure and stimulation of tissue plasminogen activator activity.* Biochemistry, 1999. **38**(35): p. 11570-6.
448. Tucker, H.M., et al., *Tissue plasminogen activator requires plasminogen to modulate amyloid-beta neurotoxicity and deposition.* J Neurochem, 2000. **75**(5): p. 2172-7.
449. Davis, J., et al., *Amyloid beta-protein stimulates the expression of urokinase-type plasminogen activator (uPA) and its receptor (uPAR) in human cerebrovascular smooth muscle cells.* J Biol Chem, 2003. **278**(21): p. 19054-61.
450. Tucker, H.M., M. Kihiko-Ehmann, and S. Estus, *Urokinase-type plasminogen activator inhibits amyloid-beta neurotoxicity and fibrillogenesis via plasminogen.* J Neurosci Res, 2002. **70**(2): p. 249-55.
451. Ledesma, M.D., et al., *Brain plasmin enhances APP alpha-cleavage and Abeta degradation and is reduced in Alzheimer's disease brains.* EMBO Rep, 2000. **1**(6): p. 530-5.
452. Tucker, H.M., et al., *Plasmin deficiency does not alter endogenous murine amyloid beta levels in mice.* Neurosci Lett, 2004. **368**(3): p. 285-9.
453. Ledesma, M.D., et al., *Raft disorganization leads to reduced plasmin activity in Alzheimer's disease brains.* EMBO Rep, 2003. **4**(12): p. 1190-6.
454. Ertekin-Taner, N., et al., *Elevated amyloid beta protein (Abeta42) and late onset Alzheimer's disease are associated with single nucleotide polymorphisms in the urokinase-type plasminogen activator gene.* Hum Mol Genet, 2005. **14**(3): p. 447-60.

455. Finckh, U., et al., *Association of late-onset Alzheimer disease with a genotype of PLAU, the gene encoding urokinase-type plasminogen activator on chromosome 10q22.2.* Neurogenetics, 2003. **4**(4): p. 213-7.
456. Myers, A.J., et al., *Variation in the urokinase-plasminogen activator gene does not explain the chromosome 10 linkage signal for late onset AD.* Am J Med Genet B Neuropsychiatr Genet, 2004. **124**(1): p. 29-37.
457. Papassotiropoulos, A., et al., *No association of a non-synonymous PLAU polymorphism with Alzheimer's disease and disease-related traits.* Am J Med Genet B Neuropsychiatr Genet, 2005. **132**(1): p. 21-3.
458. Bagnoli, S., et al., *The urokinase-plasminogen activator (PLAU) gene is not associated with late onset Alzheimer's disease.* Neurogenetics, 2005. **6**(1): p. 53-4.
459. Mullis, K.B., *Target amplification for DNA analysis by the polymerase chain reaction.* Ann Biol Clin (Paris), 1990. **48**(8): p. 579-82.
460. Mullis, K.B., *The unusual origin of the polymerase chain reaction.* Sci Am, 1990. **262**(4): p. 56-61, 64-5.
461. Sanger, F., S. Nicklen, and A.R. Coulson, *DNA sequencing with chain-terminating inhibitors.* Proc Natl Acad Sci U S A, 1977. **74**(12): p. 5463-7.
462. Paterna, J.C., et al., *Influence of promoter and WHV post-transcriptional regulatory element on AAV-mediated transgene expression in the rat brain.* Gene Ther, 2000. **7**(15): p. 1304-11.
463. Lee, Y.B., et al., *Increased utility in the CNS of a powerful neuron-specific tetracycline-regulatable adenoviral system developed using a post-transcriptional enhancer.* J Gene Med, 2005. **7**(5): p. 576-83.
464. Auricchio, A., et al., *Isolation of highly infectious and pure adeno-associated virus type 2 vectors with a single-step gravity-flow column.* Hum Gene Ther, 2001. **12**(1): p. 71-6.
465. Southern, E.M., *Detection of specific sequences among DNA fragments separated by gel electrophoresis.* J Mol Biol, 1975. **98**(3): p. 503-17.
466. Chomczynski, P., *A reagent for the single-step simultaneous isolation of RNA, DNA and proteins from cell and tissue samples.* Biotechniques, 1993. **15**(3): p. 532-4, 536-7.
467. Vassalli, J.D., J. Hamilton, and E. Reich, *Macrophage plasminogen activator: induction by concanavalin A and phorbol myristate acetate.* Cell, 1977. **11**(3): p. 695-705.
468. Vassalli, J.D. and D. Belin, *Amiloride selectively inhibits the urokinase-type plasminogen activator.* FEBS Lett, 1987. **214**(1): p. 187-91.
469. Belin, D., F. Godeau, and J.D. Vassalli, *Tumor promoter PMA stimulates the synthesis and secretion of mouse pro-urokinase in MSV-transformed 3T3 cells: this is mediated by an increase in urokinase mRNA content.* Embo J, 1984. **3**(8): p. 1901-6.
470. Pype, S., et al., *Characterization of amyloid beta peptides from brain extracts of transgenic mice overexpressing the London mutant of human amyloid precursor protein.* J Neurochem, 2003. **84**(3): p. 602-9.
471. Vandermeeren, M., et al., *The functional gamma-secretase inhibitor prevents production of amyloid beta 1-34 in human and murine cell lines.* Neurosci Lett, 2001. **315**(3): p. 145-8.
472. Zhou, Q., et al., *Alteration in the brain content of substance P (1-7) during withdrawal in morphine-dependent rats.* Neuropharmacology, 1998. **37**(12): p. 1545-52.

473. Persson, S., et al., *Decreased neuropeptide-converting enzyme activities in cerebrospinal fluid during acute but not chronic phases of collagen induced arthritis in rats.* Brain Res, 1992. **581**(2): p. 273-82.
474. Johansson, P., et al., *The effect on opioid peptides in the rat brain, after chronic treatment with the anabolic androgenic steroid, nandrolone decanoate.* Brain Res Bull, 2000. **51**(5): p. 413-8.
475. Hallberg, M., et al., *Anabolic-androgenic steroids affect the content of substance P and substance P(1-7) in the rat brain.* Peptides, 2000. **21**(6): p. 845-52.
476. Janabi, N., et al., *Establishment of human microglial cell lines after transfection of primary cultures of embryonic microglial cells with the SV40 large T antigen.* Neurosci Lett, 1995. **195**(2): p. 105-8.
477. Encinas, M., et al., *Sequential treatment of SH-SY5Y cells with retinoic acid and brain-derived neurotrophic factor gives rise to fully differentiated, neurotrophic factor-dependent, human neuron-like cells.* J Neurochem, 2000. **75**(3): p. 991-1003.
478. Borchelt DR, D.J., Fischer M, Lee MK, Slunt HH, Ratovitsky T, Regard J, Copeland NG, Jenkins NA, Sisodia SS, Price DL., *A vector for expressing foreign genes in the brains and hearts of transgenic mice.* Genet Anal., 1996. **13**(6): p. 159-163.
479. Franklin, K.B.J., and Paxinos, G., *The Mouse Brain in Stereotaxic Coordinates.* Academic Press, San Diego, CA, 1996.
480. Imai, Y., et al., *A novel gene iba1 in the major histocompatibility complex class III region encoding an EF hand protein expressed in a monocytic lineage.* Biochem Biophys Res Commun, 1996. **224**(3): p. 855-62.
481. Ohsawa, K., et al., *Involvement of Iba1 in membrane ruffling and phagocytosis of macrophages/microglia.* J Cell Sci, 2000. **113 (Pt 17)**: p. 3073-84.
482. Morris, R., *Spatial localization does not depend on the presence of local cues.* Learn Motiv, 1981: p. 239-260.
483. Wolfer, D.P., et al., *Extended analysis of path data from mutant mice using the public domain software Wintrack.* Physiol Behav, 2001. **73**(5): p. 745-53.
484. Thompson, R., et al., *Brain structures important for solving a sawdust-digging problem in the rat.* Physiol Behav, 1990. **48**(1): p. 107-11.
485. Holcomb, L.A., et al., *Behavioral changes in transgenic mice expressing both amyloid precursor protein and presenilin-1 mutations: lack of association with amyloid deposits.* Behav Genet, 1999. **29**(3): p. 177-85.
486. Holcomb, L., et al., *Accelerated Alzheimer-type phenotype in transgenic mice carrying both mutant amyloid precursor protein and presenilin 1 transgenes.* Nat Med, 1998. **4**(1): p. 97-100.
487. Duff, K., et al., *Increased amyloid-beta42(43) in brains of mice expressing mutant presenilin 1.* Nature, 1996. **383**(6602): p. 710-3.
488. Iwata, N., et al., *Metabolic regulation of brain Abeta by neprilysin.* Science, 2001. **292**(5521): p. 1550-2.
489. Saria, A., et al., *Opioid-related changes in nociceptive threshold and in tissue levels of enkephalins after target disruption of the gene for neutral endopeptidase (EC 3.4.24.11) in mice.* Neurosci Lett, 1997. **234**(1): p. 27-30.
490. Yasojima, K., et al., *Reduced neprilysin in high plaque areas of Alzheimer brain: a possible relationship to deficient degradation of beta-amyloid peptide.* Neurosci Lett, 2001a. **297**(2): p. 97-100.
491. Klyubin, I., et al., *Soluble Arctic amyloid beta protein inhibits hippocampal long-term potentiation in vivo.* Eur J Neurosci, 2004. **19**(10): p. 2839-46.
492. Dickson, D.W., *Building a more perfect beast: APP transgenic mice with neuronal loss.* Am J Pathol, 2004. **164**(4): p. 1143-6.

493. Casas, C., et al., *Massive CA1/2 neuronal loss with intraneuronal and N-terminal truncated Abeta42 accumulation in a novel Alzheimer transgenic model.* Am J Pathol, 2004. **165**(4): p. 1289-300.
494. Schmitz, C., et al., *Hippocampal neuron loss exceeds amyloid plaque load in a transgenic mouse model of Alzheimer's disease.* Am J Pathol, 2004. **164**(4): p. 1495-502.
495. Hsiao, K., et al., *Correlative memory deficits, Abeta elevation, and amyloid plaques in transgenic mice [see comments].* Science, 1996. **274**(5284): p. 99-102.
496. Chen, G., et al., *A learning deficit related to age and beta-amyloid plaques in a mouse model of Alzheimer's disease.* Nature, 2000. **408**(6815): p. 975-9.
497. Janus, C., et al., *A beta peptide immunization reduces behavioural impairment and plaques in a model of Alzheimer's disease.* Nature, 2000. **408**(6815): p. 979-82.
498. Desmedt, A., S. Hazvi, and Y. Dudai, *Differential pattern of cAMP response element-binding protein activation in the rat brain after conditioned aversion as a function of the associative process engaged: taste versus context association.* J Neurosci, 2003. **23**(14): p. 6102-10.
499. Janus, C., et al., *Impaired conditioned taste aversion learning in APP transgenic mice.* Neurobiol Aging, 2004. **25**(9): p. 1213-9.
500. Schiffman, S.S., C.M. Clark, and Z.S. Warwick, *Gustatory and olfactory dysfunction in dementia: not specific to Alzheimer's disease.* Neurobiol Aging, 1990. **11**(6): p. 597-600.
501. Polani, P.E., *Olfactory dysfunction in Alzheimer's disease.* Lancet, 2000. **355**(9208): p. 1015.
502. Broggio, E., et al., *[Taste impairment in Alzheimer's disease].* Rev Neurol (Paris), 2001. **157**(4): p. 409-13.
503. Dunn, L.T. and B.J. Everitt, *Double dissociations of the effects of amygdala and insular cortex lesions on conditioned taste aversion, passive avoidance, and neophobia in the rat using the excitotoxin ibotenic acid.* Behav Neurosci, 1988. **102**(1): p. 3-23.
504. Welzl, H., P. D'Adamo, and H.P. Lipp, *Conditioned taste aversion as a learning and memory paradigm.* Behav Brain Res, 2001. **125**(1-2): p. 205-13.
505. Yasoshima, Y., T. Shimura, and T. Yamamoto, *Single unit responses of the amygdala after conditioned taste aversion in conscious rats.* Neuroreport, 1995. **6**(17): p. 2424-8.
506. Lamprecht, R., S. Hazvi, and Y. Dudai, *cAMP response element-binding protein in the amygdala is required for long- but not short-term conditioned taste aversion memory.* J Neurosci, 1997. **17**(21): p. 8443-50.
507. Aja, S., et al., *Basolateral and central amygdaloid lesions leave aversion to dietary amino acid imbalance intact.* Physiol Behav, 2000. **71**(5): p. 533-41.
508. Bahar, A., et al., *The amygdalar circuit that acquires taste aversion memory differs from the circuit that extinguishes it.* Eur J Neurosci, 2003. **17**(7): p. 1527-30.
509. McGaugh, J.L., *Memory consolidation and the amygdala: a systems perspective.* Trends Neurosci, 2002. **25**(9): p. 456.
510. Zylka, M.J., *Nonpeptidergic circuits feel your pain.* Neuron, 2005. **47**(6): p. 771-2.
511. Zubrzycka, M. and A. Janecka, *Substance P: transmitter of nociception (Minireview).* Endocr Regul, 2000. **34**(4): p. 195-201.
512. Suzuki, H., *[Tachykininergic neurotransmission in the central nervous system].* J Nippon Med Sch, 2002. **69**(4): p. 322-7.
513. Prommer, E., *Aprepitant (EMEND)The Role of Substance P in Nausea and Vomiting.* J Pain Palliat Care Pharmacother, 2005. **19**(3): p. 31-9.

514. Hesketh, P.J., *New treatment options for chemotherapy-induced nausea and vomiting.* Support Care Cancer, 2004. **12**(8): p. 550-4.
515. Katz, D.M. and H.J. Karten, *Substance P in the vagal sensory ganglia: localization in cell bodies and pericellular arborizations.* J Comp Neurol, 1980. **193**(2): p. 549-64.
516. Andrews, P.L. and G.J. Sanger, *Abdominal vagal afferent neurones: an important target for the treatment of gastrointestinal dysfunction.* Curr Opin Pharmacol, 2002. **2**(6): p. 650-6.
517. Saria, A., *The tachykinin NK1 receptor in the brain: pharmacology and putative functions.* Eur J Pharmacol, 1999. **375**(1-3): p. 51-60.
518. Diemunsch, P. and L. Grelot, *Potential of substance P antagonists as antiemetics.* Drugs, 2000. **60**(3): p. 533-46.
519. Mohajeri, M.H., K.D. Saini, and R.M. Nitsch, *Transgenic BACE expression in mouse neurons accelerates amyloid plaque pathology.* J Neural Transm, 2004. **111**(3): p. 413-25.
520. Cook, D.G., et al., *Alzheimer's A beta(1-42) is generated in the endoplasmic reticulum/intermediate compartment of NT2N cells.* Nat Med, 1997. **3**(9): p. 1021-3.
521. Gouras, G.K., et al., *Intraneuronal Abeta42 accumulation in human brain.* Am J Pathol, 2000. **156**(1): p. 15-20.
522. Wirths, O., et al., *Intraneuronal Abeta accumulation precedes plaque formation in beta- amyloid precursor protein and presenilin-1 double-transgenic mice.* Neurosci Lett, 2001. **306**(1-2): p. 116-20.
523. Weldon, D.T., et al., *Fibrillar beta-amyloid induces microglial phagocytosis, expression of inducible nitric oxide synthase, and loss of a select population of neurons in the rat CNS in vivo.* J Neurosci, 1998. **18**(6): p. 2161-73.
524. Stephan, A., S. Laroche, and S. Davis, *Learning deficits and dysfunctional synaptic plasticity induced by aggregated amyloid deposits in the dentate gyrus are rescued by chronic treatment with indomethacin.* Eur J Neurosci, 2003. **17**(9): p. 1921-7.
525. Stephan, A., S. Laroche, and S. Davis, *Generation of aggregated beta-amyloid in the rat hippocampus impairs synaptic transmission and plasticity and causes memory deficits.* J Neurosci, 2001. **21**(15): p. 5703-14.
526. Giovannelli, L., et al., *Long-term changes in the aggregation state and toxic effects of beta-amyloid injected into the rat brain.* Neuroscience, 1998. **87**(2): p. 349-57.
527. Frautschy, S.A., G.M. Cole, and A. Baird, *Phagocytosis and deposition of vascular beta-amyloid in rat brains injected with Alzheimer beta-amyloid.* Am J Pathol, 1992. **140**(6): p. 1389-99.
528. Ghersi-Egea, J.F., et al., *Fate of cerebrospinal fluid-borne amyloid beta-peptide: rapid clearance into blood and appreciable accumulation by cerebral arteries.* J Neurochem, 1996. **67**(2): p. 880-3.
529. Zlokovic, B.V., et al., *Glycoprotein 330/megalin: probable role in receptor-mediated transport of apolipoprotein J alone and in a complex with Alzheimer disease amyloid beta at the blood-brain and blood-cerebrospinal fluid barriers.* Proc Natl Acad Sci U S A, 1996. **93**(9): p. 4229-34.
530. Mackic, J.B., et al., *Human blood-brain barrier receptors for Alzheimer's amyloid-beta 1- 40. Asymmetrical binding, endocytosis, and transcytosis at the apical side of brain microvascular endothelial cell monolayer.* J Clin Invest, 1998. **102**(4): p. 734-43.
531. Marr, R.A., et al., *Neprilysin gene transfer reduces human amyloid pathology in transgenic mice.* J Neurosci, 2003. **23**(6): p. 1992-6.
532. Saito, T., et al., *Somatostatin regulates brain amyloid beta peptide Abeta42 through modulation of proteolytic degradation.* Nat Med, 2005. **11**(4): p. 434-9.

533. Joshi, D.D., et al., *Negative feedback on the effects of stem cell factor on hematopoiesis is partly mediated through neutral endopeptidase activity on substance P: a combined functional and proteomic study.* Blood, 2001. **98**(9): p. 2697-706.
534. Bae, S.J., et al., *Substance P induced preprotachykinin-a mRNA, neutral endopeptidase mRNA and substance P in cultured normal fibroblasts.* Int Arch Allergy Immunol, 2002. **127**(4): p. 316-21.
535. Verdier, Y. and B. Penke, *Binding sites of amyloid beta-peptide in cell plasma membrane and implications for Alzheimer's disease.* Curr Protein Pept Sci, 2004. **5**(1): p. 19-31.
536. Fiala, M., et al., *Amyloid-beta induces chemokine secretion and monocyte migration across a human blood--brain barrier model.* Mol Med, 1998. **4**(7): p. 480-9.
537. Cacquevel, M., et al., *Cytokines in neuroinflammation and Alzheimer's disease.* Curr Drug Targets, 2004. **5**(6): p. 529-34.
538. Giovannini, M.G., et al., *Beta-amyloid-induced inflammation and cholinergic hypofunction in the rat brain in vivo: involvement of the p38MAPK pathway.* Neurobiol Dis, 2002. **11**(2): p. 257-74.
539. Arzt, E., et al., *Functional cross-talk among cytokines, T-cell receptor, and glucocorticoid receptor transcriptional activity and action.* Ann N Y Acad Sci, 2000. **917**: p. 672-7.
540. Angeli, A., et al., *Modulation by cytokines of glucocorticoid action.* Ann N Y Acad Sci, 1999. **876**: p. 210-20.
541. Ruiz-Leon, Y. and A. Pascual, *Induction of tyrosine kinase receptor b by retinoic acid allows brain-derived neurotrophic factor-induced amyloid precursor protein gene expression in human SH-SY5Y neuroblastoma cells.* Neuroscience, 2003. **120**(4): p. 1019-26.
542. Konig, G., C.L. Masters, and K. Beyreuther, *Retinoic acid induced differentiated neuroblastoma cells show increased expression of the beta A4 amyloid gene of Alzheimer's disease and an altered splicing pattern.* FEBS Lett, 1990. **269**(2): p. 305-10.
543. Holback, S., L. Adlerz, and K. Iverfeldt, *Increased processing of APLP2 and APP with concomitant formation of APP intracellular domains in BDNF and retinoic acid-differentiated human neuroblastoma cells.* J Neurochem, 2005.
544. Adlerz, L., et al., *Accumulation of the amyloid precursor-like protein APLP2 and reduction of APLP1 in retinoic acid-differentiated human neuroblastoma cells upon curcumin-induced neurite retraction.* Brain Res Mol Brain Res, 2003. **119**(1): p. 62-72.
545. Flood, F., et al., *Presenilin expression during induced differentiation of the human neuroblastoma SH-SY5Y cell line.* Neurochem Int, 2004. **44**(7): p. 487-96.
546. Prinzen, C., et al., *Genomic structure and functional characterization of the human ADAM10 promoter.* Faseb J, 2005. **19**(11): p. 1522-4.
547. Pardossi-Piquard, R., et al., *Presenilin-dependent transcriptional control of the Abeta-degrading enzyme neprilysin by intracellular domains of betaAPP and APLP.* Neuron, 2005. **46**(4): p. 541-54.
548. Ahlemeyer, B. and J. Krieglstein, *Inhibition of glutathione depletion by retinoic acid and tocopherol protects cultured neurons from staurosporine-induced oxidative stress and apoptosis.* Neurochem Int, 2000. **36**(1): p. 1-5.
549. Sahin, M., et al., *Retinoic acid isomers protect hippocampal neurons from amyloid-beta induced neurodegeneration.* Neurotox Res, 2005. **7**(3): p. 243-50.
550. Ono, K., et al., *Vitamin A exhibits potent antiamyloidogenic and fibril-destabilizing effects in vitro.* Exp Neurol, 2004. **189**(2): p. 380-92.

551. Hama, E., et al., *Effects of neprilysin chimeric proteins targeted to subcellular compartments on amyloid beta peptide clearance in primary neurons.* J Biol Chem, 2004. **279**(29): p. 30259-64.
552. Goodman, A.B. and A.B. Pardee, *Evidence for defective retinoid transport and function in late onset Alzheimer's disease.* Proc Natl Acad Sci U S A, 2003. **100**(5): p. 2901-5.
553. Misner, D.L., et al., *Vitamin A deprivation results in reversible loss of hippocampal long-term synaptic plasticity.* Proc Natl Acad Sci U S A, 2001. **98**(20): p. 11714-9.
554. Chiang, M.Y., et al., *An essential role for retinoid receptors RARbeta and RXRgamma in long-term potentiation and depression.* Neuron, 1998. **21**(6): p. 1353-61.
555. Etchamendy, N., et al., *Alleviation of a selective age-related relational memory deficit in mice by pharmacologically induced normalization of brain retinoid signaling.* J Neurosci, 2001. **21**(16): p. 6423-9.
556. Etchamendy, N., et al., *Vitamin A deficiency and relational memory deficit in adult mice: relationships with changes in brain retinoid signalling.* Behav Brain Res, 2003. **145**(1-2): p. 37-49.
557. Cocco, S., et al., *Vitamin A deficiency produces spatial learning and memory impairment in rats.* Neuroscience, 2002. **115**(2): p. 475-82.
558. Connor, M.J. and N. Sidell, *Retinoic acid synthesis in normal and Alzheimer diseased brain and human neural cells.* Mol Chem Neuropathol, 1997. **30**(3): p. 239-52.
559. Zaman, Z., et al., *Plasma concentrations of vitamins A and E and carotenoids in Alzheimer's disease.* Age Ageing, 1992. **21**(2): p. 91-4.
560. Wien, E.M. and O.A. Ojo, *Serum vitamin A, carotene and cholesterol levels in Nigerian women using various types of contraceptives.* Nutr Rep Int, 1982. **25**(4): p. 687-96.
561. Rinaldi, P., et al., *Plasma antioxidants are similarly depleted in mild cognitive impairment and in Alzheimer's disease.* Neurobiol Aging, 2003. **24**(7): p. 915-9.
562. Corcoran, J.P., P.L. So, and M. Maden, *Disruption of the retinoid signalling pathway causes a deposition of amyloid beta in the adult rat brain.* Eur J Neurosci, 2004. **20**(4): p. 896-902.
563. Pardridge, W.M., R. Sakiyama, and W.A. Coty, *Restricted transport of vitamin D and A derivatives through the rat blood-brain barrier.* J Neurochem, 1985. **44**(4): p. 1138-41.
564. Lane, M.A. and S.J. Bailey, *Role of retinoid signalling in the adult brain.* Prog Neurobiol, 2005. **75**(4): p. 275-93.
565. Balmer, J.E. and R. Blomhoff, *Gene expression regulation by retinoic acid.* J Lipid Res, 2002. **43**(11): p. 1773-808.
566. Bertram, J.S. and A.L. Vine, *Cancer prevention by retinoids and carotenoids: independent action on a common target.* Biochim Biophys Acta, 2005. **1740**(2): p. 170-8.
567. Abu, J., et al., *Retinoic acid and retinoid receptors: potential chemopreventive and therapeutic role in cervical cancer.* Lancet Oncol, 2005. **6**(9): p. 712-20.
568. Pfahl, M., *Retinoid related molecules: new promises against lung and breast cancer.* Expert Opin Investig Drugs, 1998. **7**(4): p. 601-6.
569. Kang, S., *The mechanism of action of topical retinoids.* Cutis, 2005. **75**(2 Suppl): p. 10-3; discussion 13.
570. Chivot, M., *Retinoid therapy for acne. A comparative review.* Am J Clin Dermatol, 2005. **6**(1): p. 13-9.
571. Snodgrass, S.R., *Vitamin neurotoxicity.* Mol Neurobiol, 1992. **6**(1): p. 41-73.

572. Carrillo-Esper, R., et al., *[All-trans retinoic acid syndrome. Case report and a review of the literature]*. Gac Med Mex, 2004. **140**(5): p. 547-52.
573. Bendich, A. and L. Langseth, *Safety of vitamin A.* Am J Clin Nutr, 1989. **49**(2): p. 358-71.
574. Tran-Thang, C., et al., *Modulation of the plasminogen activation system by inflammatory cytokines in human colon carcinoma cells.* Br J Cancer, 1996. **74**(6): p. 846-52.
575. Sieuwerts, A.M., et al., *Cytokine-regulated urokinase-type-plasminogen-activator (uPA) production by human breast fibroblasts in vitro.* Breast Cancer Res Treat, 1999. **55**(1): p. 9-20.
576. Niiya, K., et al., *Modulation of urokinase-type plasminogen activator gene expression by inflammatory cytokines in human pre-B lymphoma cell line RC-K8.* Thromb Haemost, 1995. **74**(6): p. 1511-5.
577. Iwamoto, J., et al., *Expression of urokinase-type plasminogen activator and its receptor in gastric fibroblasts and effects of nonsteroidal antiinflammatory drugs and prostaglandin.* Dig Dis Sci, 2003. **48**(12): p. 2247-56.
578. Feliciani, C., et al., *Urokinase plasminogen activator mRNA is induced by IL-1alpha and TNF-alpha in in vitro acantholysis.* Exp Dermatol, 2003. **12**(4): p. 466-71.
579. Chavakis, T., et al., *Release of soluble urokinase receptor from vascular cells.* Thromb Haemost, 2001. **86**(2): p. 686-93.
580. Bechtel, M.J., et al., *Upregulation of cell-surface-associated plasminogen activation in cultured keratinocytes by interleukin-1 beta and tumor necrosis factor-alpha.* Exp Cell Res, 1996. **223**(2): p. 395-404.
581. White, J.A., et al., *Differential effects of oligomeric and fibrillar amyloid-beta 1-42 on astrocyte-mediated inflammation.* Neurobiol Dis, 2005. **18**(3): p. 459-65.
582. Meda, L., P. Baron, and G. Scarlato, *Glial activation in Alzheimer's disease: the role of Abeta and its associated proteins.* Neurobiol Aging, 2001. **22**(6): p. 885-93.
583. Miskin, R. and T. Masos, *Transgenic mice overexpressing urokinase-type plasminogen activator in the brain exhibit reduced food consumption, body weight and size, and increased longevity.* J Gerontol A Biol Sci Med Sci, 1997. **52**(2): p. B118-24.
584. Meiri, N., et al., *Overexpression of urokinase-type plasminogen activator in transgenic mice is correlated with impaired learning.* Proc Natl Acad Sci U S A, 1994. **91**(8): p. 3196-200.
585. Feldkamp, J., et al., *Soluble Fas is increased in hyperthyroidism independent of the underlying thyroid disease.* J Clin Endocrinol Metab, 2001. **86**(9): p. 4250-3.
586. Sumitomo, M., R. Shen, and D.M. Nanus, *Involvement of neutral endopeptidase in neoplastic progression.* Biochim Biophys Acta, 2005. **1751**(1): p. 52-9.
587. Sumitomo, M., et al., *Synergy in tumor suppression by direct interaction of neutral endopeptidase with PTEN.* Cancer Cell, 2004. **5**(1): p. 67-78.
588. Tang, H., et al., *The urokinase-type plasminogen activator receptor mediates tyrosine phosphorylation of focal adhesion proteins and activation of mitogen-activated protein kinase in cultured endothelial cells.* J Biol Chem, 1998. **273**(29): p. 18268-72.
589. Galaria, II, et al., *Urokinase-induced smooth muscle cell migration requires PI3-K and Akt activation.* J Surg Res, 2005. **127**(1): p. 46-52.
590. Chandrasekar, N., et al., *Downregulation of uPA inhibits migration and PI3k/Akt signaling in glioblastoma cells.* Oncogene, 2003. **22**(3): p. 392-400.
591. Foschi, M., et al., *Biphasic activation of p21ras by endothelin-1 sequentially activates the ERK cascade and phosphatidylinositol 3-kinase.* Embo J, 1997. **16**(21): p. 6439-51.

592. Du, J., et al., *G-protein and tyrosine kinase receptor cross-talk in rat aortic smooth muscle cells: thrombin- and angiotensin II-induced tyrosine phosphorylation of insulin receptor substrate-1 and insulin-like growth factor 1 receptor.* Biochem Biophys Res Commun, 1996. **218**(3): p. 934-9.
593. Vacca, F., et al., *Transactivation of the epidermal growth factor receptor in endothelin-1-induced mitogenic signaling in human ovarian carcinoma cells.* Cancer Res, 2000. **60**(18): p. 5310-7.
594. Dumler, I., et al., *The Jak/Stat pathway and urokinase receptor signaling in human aortic vascular smooth muscle cells.* J Biol Chem, 1998. **273**(1): p. 315-21.
595. Bohuslav, J., et al., *Urokinase plasminogen activator receptor, beta 2-integrins, and Src-kinases within a single receptor complex of human monocytes.* J Exp Med, 1995. **181**(4): p. 1381-90.
596. Jo, M., et al., *Dynamic assembly of the urokinase-type plasminogen activator signaling receptor complex determines the mitogenic activity of urokinase-type plasminogen activator.* J Biol Chem, 2005. **280**(17): p. 17449-57.
597. Wang, X.Q., P. Sun, and A.S. Paller, *Gangliosides inhibit urokinase-type plasminogen activator (uPA)-dependent squamous carcinoma cell migration by preventing uPA receptor/alphabeta integrin/epidermal growth factor receptor interactions.* J Invest Dermatol, 2005. **124**(4): p. 839-48.
598. Kobayashi, H., et al., *CD44 stimulation by fragmented hyaluronic acid induces upregulation of urokinase-type plasminogen activator and its receptor and subsequently facilitates invasion of human chondrosarcoma cells.* Int J Cancer, 2002. **102**(4): p. 379-89.
599. Mochizuki, Y., et al., *Negative regulation of urokinase-type plasminogen activator production through FGF-2-mediated activation of phosphoinositide 3-kinase.* Oncogene, 2002. **21**(46): p. 7027-33.
600. Shearer, J.D., et al., *Insulin is degraded extracellularly in wounds by insulin-degrading enzyme (EC 3.4.24.56).* Am J Physiol, 1997. **273**(4 Pt 1): p. E657-64.
601. Hamel, F.G., et al., *Identification of the cleavage sites of transforming growth factor alpha by insulin-degrading enzymes.* Biochim Biophys Acta, 1997. **1338**(2): p. 207-14.
602. Garcia, J.V., B.D. Gehm, and M.R. Rosner, *An evolutionarily conserved enzyme degrades transforming growth factor-alpha as well as insulin.* J Cell Biol, 1989. **109**(3): p. 1301-7.
603. Gehm, B.D. and M.R. Rosner, *Regulation of insulin, epidermal growth factor, and transforming growth factor-alpha levels by growth factor-degrading enzymes.* Endocrinology, 1991. **128**(3): p. 1603-10.
604. Jensen, P.J. and U. Rodeck, *Autocrine/paracrine regulation of keratinocyte urokinase plasminogen activator through the TGF-alpha/EGF receptor.* J Cell Physiol, 1993. **155**(2): p. 333-9.
605. Petty, H.R., R.G. Worth, and R.F. Todd, 3rd, *Interactions of integrins with their partner proteins in leukocyte membranes.* Immunol Res, 2002. **25**(1): p. 75-95.
606. Rogerson, F.M., et al., *Inhibition of angiotensin converting enzyme by N-terminal fragments of substance P.* Neuropeptides, 1989. **14**(4): p. 213-7.
607. Santos, R.A., et al., *Angiotensin-(1-7) and its receptor as a potential targets for new cardiovascular drugs.* Expert Opin Investig Drugs, 2005. **14**(8): p. 1019-31.
608. Tom, B., A. Dendorfer, and A.H. Danser, *Bradykinin, angiotensin-(1-7), and ACE inhibitors: how do they interact?* Int J Biochem Cell Biol, 2003. **35**(6): p. 792-801.
609. Tom, B., et al., *Bradykinin potentiation by angiotensin-(1-7) and ACE inhibitors correlates with ACE C- and N-domain blockade.* Hypertension, 2001. **38**(1): p. 95-9.

610. Okada, H., et al., *Bradykinin decreases plasminogen activator inhibitor-1 expression and facilitates matrix degradation in the renal tubulointerstitium under angiotensin-converting enzyme blockade.* J Am Soc Nephrol, 2004. **15**(9): p. 2404-13.
611. Moreau, M.E., et al., *The kallikrein-kinin system: current and future pharmacological targets.* J Pharmacol Sci, 2005. **99**(1): p. 6-38.
612. Mikolajczyk, S.D., et al., *Prostatic human kallikrein 2 inactivates and complexes with plasminogen activator inhibitor-1.* Int J Cancer, 1999. **81**(3): p. 438-42.
613. Mohajeri, M.H., et al., *Anti-amyloid activity of neprilysin in plaque-bearing mouse models of Alzheimer's disease.* FEBS Lett, 2004a. **562**(1-3): p. 16-21.
614. Mohajeri, M.H., K.D. Saini, and R.M. Nitsch, *Transgenic BACE expression in mouse neurons accelerates amyloid plaque pathology.* J Neural Transm, 2004b. **111**(3): p. 413-25.
615. Klyubin, I., et al., *Amyloid beta protein immunotherapy neutralizes Abeta oligomers that disrupt synaptic plasticity in vivo.* Nat Med, 2005.
616. Davies, P., R. Katzman, and R.D. Terry, *Reduced somatostatin-like immunoreactivity in cerebral cortex from cases of Alzheimer disease and Alzheimer senile dementa.* Nature, 1980. **288**(5788): p. 279-80.
617. Crystal, H.A. and P. Davies, *Cortical substance P-like immunoreactivity in cases of Alzheimer's disease and senile dementia of the Alzheimer type.* J Neurochem, 1982. **38**(6): p. 1781-4.
618. Kumar, U., *Expression of somatostatin receptor subtypes (SSTR1-5) in Alzheimer's disease brain: an immunohistochemical analysis.* Neuroscience, 2005. **134**(2): p. 525-38.
619. Beal, M.F., N.W. Kowall, and M.F. Mazurek, *Neuropeptides in Alzheimer's disease.* J Neural Transm Suppl, 1987. **24**: p. 163-74.
620. Struble, R.G., et al., *Neuropeptidergic systems in plaques of Alzheimer's disease.* J Neuropathol Exp Neurol, 1987. **46**(5): p. 567-84.
621. Diez, M., et al., *Neuropeptide alterations in the hippocampal formation and cortex of transgenic mice overexpressing beta-amyloid precursor protein (APP) with the Swedish double mutation (APP23).* Neurobiol Dis, 2003. **14**(3): p. 579-94.
622. Diez, M., et al., *Neuropeptides in hippocampus and cortex in transgenic mice overexpressing V717F beta-amyloid precursor protein--initial observations.* Neuroscience, 2000. **100**(2): p. 259-86.
623. Armstrong, D.M., et al., *Substance P and somatostatin coexist within neuritic plaques: implications for the pathogenesis of Alzheimer's disease.* Neuroscience, 1989. **31**(3): p. 663-71.
624. Armstrong, D.M. and R.D. Terry, *Substance P immunoreactivity within neuritic plaques.* Neurosci Lett, 1985. **58**(1): p. 139-44.
625. Unger, J.W., et al., *Neuropeptides and neuropathology in the amygdala in Alzheimer's disease: relationship between somatostatin, neuropeptide Y and subregional distribution of neuritic plaques.* Brain Res, 1988. **452**(1-2): p. 293-302.
626. Morishima-Kawashima, M., et al., *Effect of apolipoprotein E allele epsilon4 on the initial phase of amyloid beta-protein accumulation in the human brain.* Am J Pathol, 2000. **157**(6): p. 2093-9.
627. Funato, H., et al., *Quantitation of amyloid beta-protein (A beta) in the cortex during aging and in Alzheimer's disease.* Am J Pathol, 1998. **152**(6): p. 1633-40.
628. Price, D.L., et al., *Alzheimer's disease: genetic studies and transgenic models.* Annu Rev Genet, 1998. **32**: p. 461-93.
629. Ashe, K.H., *Learning and memory in transgenic mice modeling Alzheimer's disease.* Learn Mem, 2001. **8**(6): p. 301-8.

630. Schofield, P.W., et al., *Consistency of clinical diagnosis in a community-based longitudinal study of dementia and Alzheimer's disease.* Neurology, 1995. **45**(12): p. 2159-64.
631. Lehman, E.J., et al., *Genetic background regulates beta-amyloid precursor protein processing and beta-amyloid deposition in the mouse.* Hum Mol Genet, 2003. **12**(22): p. 2949-56.
632. Crawley, J.N., et al., *Behavioral phenotypes of inbred mouse strains: implications and recommendations for molecular studies.* Psychopharmacology (Berl), 1997. **132**(2): p. 107-24.
633. Carlson, G.A., et al., *Genetic modification of the phenotypes produced by amyloid precursor protein overexpression in transgenic mice.* Hum Mol Genet, 1997. **6**(11): p. 1951-9.
634. Parra, A., et al., *Sex differences in the effects of neuroleptics on escape-avoidance behavior in mice: a review.* Pharmacol Biochem Behav, 1999. **64**(4): p. 813-20.
635. Beatty, W.W., *Gonadal hormones and sex differences in nonreproductive behaviors in rodents: organizational and activational influences.* Horm Behav, 1979. **12**(2): p. 112-63.
636. Luedi, P.P., A.J. Hartemink, and R.L. Jirtle, *Genome-wide prediction of imprinted murine genes.* Genome Res, 2005. **15**(6): p. 875-84.
637. Borchelt, D.R., et al., *A vector for expressing foreign genes in the brains and hearts of transgenic mice.* Genet Anal, 1996. **13**(6): p. 159-63.
638. Katamine, S., et al., *Impaired motor coordination in mice lacking prion protein.* Cell Mol Neurobiol, 1998. **18**(6): p. 731-42.
639. Coitinho, A.S., et al., *Cellular prion protein ablation impairs behavior as a function of age.* Neuroreport, 2003. **14**(10): p. 1375-9.
640. Criado, J.R., et al., *Mice devoid of prion protein have cognitive deficits that are rescued by reconstitution of PrP in neurons.* Neurobiol Dis, 2005. **19**(1-2): p. 255-65.
641. Schwarze-Eicker, K., et al., *Prion protein (PrPc) promotes beta-amyloid plaque formation.* Neurobiol Aging, 2005. **26**(8): p. 1177-82.
642. Glatzel, M., et al., *No influence of amyloid-beta-degrading neprilysin activity on prion pathogenesis.* J Gen Virol, 2005. **86**(Pt 6): p. 1861-7.
643. Kishi, T. and J.K. Elmquist, *Body weight is regulated by the brain: a link between feeding and emotion.* Mol Psychiatry, 2005. **10**(2): p. 132-46.
644. van der Velden, V.H. and A.R. Hulsmann, *Peptidases: structure, function and modulation of peptide-mediated effects in the human lung.* Clin Exp Allergy, 1999. **29**(4): p. 445-56.
645. Fujiwara, H., et al., *Effect of neuropeptide Y on human bronchus and its modulation of neutral endopeptidase.* J Allergy Clin Immunol, 1993. **92**(1 Pt 1): p. 89-94.
646. Blomqvist, A.G. and H. Herzog, *Y-receptor subtypes--how many more?* Trends Neurosci, 1997. **20**(7): p. 294-8.
647. Hokfelt, T., et al., *Neuropeptide Y: some viewpoints on a multifaceted peptide in the normal and diseased nervous system.* Brain Res Brain Res Rev, 1998. **26**(2-3): p. 154-66.
648. Inui, A., *Neuropeptide Y feeding receptors: are multiple subtypes involved?* Trends Pharmacol Sci, 1999. **20**(2): p. 43-6.
649. Luquet, S., et al., *NPY/AgRP neurons are essential for feeding in adult mice but can be ablated in neonates.* Science, 2005. **310**(5748): p. 683-5.
650. Gray, J.A. and N. McNaughton, *Comparison between the behavioural effects of septal and hippocampal lesions: a review.* Neurosci Biobehav Rev, 1983. **7**(2): p. 119-88.

651. Yu, J., et al., *Learning ability in young rats with single and double lesions to the "general learning system".* Physiol Behav, 1989. **45**(1): p. 133-44.
652. Crinella, F.M. and J. Yu, *Brain mechanisms in problem solving and intelligence: A replication and extension.* 1995. **21**(2): p. 225.
653. LeDoux, J.E., *Emotion circuits in the brain.* Annu Rev Neurosci, 2000. **23**: p. 155-84.
654. Reilly, S. and M.A. Bornovalova, *Conditioned taste aversion and amygdala lesions in the rat: a critical review.* Neurosci Biobehav Rev, 2005. **29**(7): p. 1067-88.
655. Burwell, R.D., et al., *Perirhinal and postrhinal contributions to remote memory for context.* J Neurosci, 2004. **24**(49): p. 11023-8.
656. Bucci, D.J., R.G. Phillips, and R.D. Burwell, *Contributions of postrhinal and perirhinal cortex to contextual information processing.* Behav Neurosci, 2000. **114**(5): p. 882-94.
657. Bucci, D.J., M.P. Saddoris, and R.D. Burwell, *Contextual fear discrimination is impaired by damage to the postrhinal or perirhinal cortex.* Behav Neurosci, 2002. **116**(3): p. 479-88.
658. Burwell, R.D., et al., *Corticohippocampal contributions to spatial and contextual learning.* J Neurosci, 2004. **24**(15): p. 3826-36.
659. Tremml, P., et al., *Enriched early experiences of mice underexpressing the beta-amyloid precursor protein restore spatial learning capabilities but not normal openfield behavior of adult animals.* Genes Brain Behav, 2002. **1**(4): p. 230-41.
660. Marie-Claire, C., et al., *Evidence by site-directed mutagenesis that arginine 203 of thermolysin and arginine 717 of neprilysin (neutral endopeptidase) play equivalent critical roles in substrate hydrolysis and inhibitor binding.* Biochemistry, 1997. **36**(45): p. 13938-45.
661. Bahi, A., et al., *In vivo gene delivery of urokinase-type plasminogen activator with regulatable lentivirus induces behavioural changes in chronic cocaine administration.* Eur J Neurosci, 2004. **20**(12): p. 3473-88.
662. Huang, Y.Y., et al., *Mice lacking the gene encoding tissue-type plasminogen activator show a selective interference with late-phase long-term potentiation in both Schaffer collateral and mossy fiber pathways.* Proc Natl Acad Sci U S A, 1996. **93**(16): p. 8699-704.
663. Calabresi, P., et al., *Tissue plasminogen activator controls multiple forms of synaptic plasticity and memory.* Eur J Neurosci, 2000. **12**(3): p. 1002-12.
664. Ammassari-Teule, M., et al., *Learning about the context in genetically-defined mice.* Behav Brain Res, 2001. **125**(1-2): p. 195-204.
665. Rogan, M.T. and J.E. LeDoux, *Emotion: systems, cells, synaptic plasticity.* Cell, 1996. **85**(4): p. 469-75.
666. Fanselow, M.S. and J.E. LeDoux, *Why we think plasticity underlying Pavlovian fear conditioning occurs in the basolateral amygdala.* Neuron, 1999. **23**(2): p. 229-32.
667. Rogan, M.T., U.V. Staubli, and J.E. LeDoux, *Fear conditioning induces associative long-term potentiation in the amygdala.* Nature, 1997. **390**(6660): p. 604-7.
668. Pawlak, R., et al., *Tissue plasminogen activator in the amygdala is critical for stress-induced anxiety-like behavior.* Nat Neurosci, 2003. **6**(2): p. 168-74.
669. Kuteeva, E., T. Hokfelt, and S.O. Ogren, *Behavioural characterisation of young adult transgenic mice overexpressing galanin under the PDGF-B promoter.* Regul Pept, 2005. **125**(1-3): p. 67-78.
670. Dumont, M., et al., *Spatial learning and exploration of environmental stimuli in 24-month-old female APP23 transgenic mice with the Swedish mutation.* Brain Res, 2004. **1024**(1-2): p. 113-21.

671. Lalonde, R., et al., *Transgenic mice expressing the betaAPP695SWE mutation: effects on exploratory activity, anxiety, and motor coordination.* Brain Res, 2003. **977**(1): p. 38-45.
672. Jensen, M.T., et al., *Lifelong immunization with human beta-amyloid (1-42) protects Alzheimer's transgenic mice against cognitive impairment throughout aging.* Neuroscience, 2005. **130**(3): p. 667-84.
673. Dodart, J.C., et al., *Immunization reverses memory deficits without reducing brain Abeta burden in Alzheimer's disease model.* Nat Neurosci, 2002. **5**(5): p. 452-7.
674. Guerin, O., et al., *Different modes of weight loss in Alzheimer disease: a prospective study of 395 patients.* Am J Clin Nutr, 2005. **82**(2): p. 435-41.
675. Prasher, V.P., T. Metseagharun, and S. Haque, *Weight loss in adults with Down syndrome and with dementia in Alzheimer's disease.* Res Dev Disabil, 2004. **25**(1): p. 1-7.
676. Petry, S., et al., *Personality alterations in dementia of the Alzheimer type.* Arch Neurol, 1988. **45**(11): p. 1187-90.
677. Frisoni, G.B., et al., *Behavioral syndromes in Alzheimer's disease: description and correlates.* Dement Geriatr Cogn Disord, 1999. **10**(2): p. 130-8.
678. Chung, J.A. and J.L. Cummings, *Neurobehavioral and neuropsychiatric symptoms in Alzheimer's disease: characteristics and treatment.* Neurol Clin, 2000. **18**(4): p. 829-46.
679. Stout, J.C., et al., *Frontal behavioral syndromes and functional status in probable Alzheimer disease.* Am J Geriatr Psychiatry, 2003. **11**(6): p. 683-6.
680. Gauthier, S., *Update on diagnostic methods, natural history and outcome variables in Alzheimer's disease.* Dement Geriatr Cogn Disord, 1998. **9 Suppl 3**: p. 2-7.
681. McDaniel, W.F., D.M. Compton, and S.R. Smith, *Spatial learning following posterior parietal or hippocampal lesions.* Neuroreport, 1994. **5**(14): p. 1713-7.
682. Wright, J.W., et al., *Influence of hippocampectomy on habituation, exploratory behavior, and spatial memory in rats.* Brain Res, 2004. **1023**(1): p. 1-14.
683. Myhrer, T., *Exploratory behavior and reaction to novelty in rats with hippocampal perforant path systems disrupted.* Behav Neurosci, 1988. **102**(3): p. 356-62.
684. Poucet, B., *Spatial cognitive maps in animals: new hypotheses on their structure and neural mechanisms.* Psychol Rev, 1993. **100**(2): p. 163-82.
685. Chesler, E.J., et al., *Identification and ranking of genetic and laboratory environment factors influencing a behavioral trait, thermal nociception, via computational analysis of a large data archive.* Neurosci Biobehav Rev, 2002. **26**(8): p. 907-23.
686. Moses, S.N., C. Cole, and J.D. Ryan, *Relational memory for object identity and spatial location in rats with lesions of perirhinal cortex, amygdala and hippocampus.* Brain Res Bull, 2005. **65**(6): p. 501-12.
687. Kim, J.J., et al., *Amygdala is critical for stress-induced modulation of hippocampal long-term potentiation and learning.* J Neurosci, 2001. **21**(14): p. 5222-8.
688. Kim, J.J., et al., *Amygdalar inactivation blocks stress-induced impairments in hippocampal long-term potentiation and spatial memory.* J Neurosci, 2005. **25**(6): p. 1532-9.
689. Pikkarainen, M., et al., *Projections from the lateral, basal, and accessory basal nuclei of the amygdala to the hippocampal formation in rat.* J Comp Neurol, 1999. **403**(2): p. 229-60.
690. Krettek, J.E. and J.L. Price, *Projections from the amygdaloid complex and adjacent olfactory structures to the entorhinal cortex and to the subiculum in the rat and cat.* J Comp Neurol, 1977. **172**(4): p. 723-52.

691. Roozendaal, B., et al., *The hippocampus mediates glucocorticoid-induced impairment of spatial memory retrieval: dependence on the basolateral amygdala.* Proc Natl Acad Sci U S A, 2003. **100**(3): p. 1328-33.
692. McGaugh, J.L., *Memory--a century of consolidation.* Science, 2000. **287**(5451): p. 248-51.
693. Pasquier, F., et al., *Memory impairment differs in frontotemporal dementia and Alzheimer's disease.* Neurocase, 2001. **7**(2): p. 161-71.
694. Woodruff-Pak, D.S., *Eyeblink classical conditioning differentiates normal aging from Alzheimer's disease.* Integr Physiol Behav Sci, 2001. **36**(2): p. 87-108.
695. Huitron-Resendiz, S., et al., *Age-independent and age-related deficits in visuospatial learning, sleep-wake states, thermoregulation and motor activity in PDAPP mice.* Brain Res, 2002. **928**(1-2): p. 126-37.
696. Savonenko, A.V., et al., *Normal cognitive behavior in two distinct congenic lines of transgenic mice hyperexpressing mutant APP SWE.* Neurobiol Dis, 2003. **12**(3): p. 194-211.
697. Younkin, S.G., *Amyloid beta vaccination: reduced plaques and improved cognition.* Nat Med, 2001. **7**(1): p. 18-9.
698. Ohno, M., et al., *BACE1 Deficiency Rescues Memory Deficits and Cholinergic Dysfunction in a Mouse Model of Alzheimer's Disease.* Neuron, 2004. **41**(1): p. 27-33.
699. Morgan, D., et al., *A beta peptide vaccination prevents memory loss in an animal model of Alzheimer's disease.* Nature, 2000. **408**(6815): p. 982-5.
700. Janus, C., et al., *A beta peptide immunization reduces behavioural impairment and plaques in a model of Alzheimer's disease.* Nature, 2000. **408**(6815): p. 979-82.
701. Hock, C., et al., *Antibodies against beta-amyloid slow cognitive decline in Alzheimer's disease.* Neuron, 2003. **38**(4): p. 547-54.
702. Bard, F., et al., *Peripherally administered antibodies against amyloid beta-peptide enter the central nervous system and reduce pathology in a mouse model of Alzheimer disease.* Nat Med, 2000. **6**(8): p. 916-9.
703. DeMattos, R.B., et al., *Peripheral anti-A beta antibody alters CNS and plasma A beta clearance and decreases brain A beta burden in a mouse model of Alzheimer's disease.* Proc Natl Acad Sci U S A, 2001. **98**(15): p. 8850-5.
704. Solomon, B., et al., *Monoclonal antibodies inhibit in vitro fibrillar aggregation of the Alzheimer beta-amyloid peptide.* Proc Natl Acad Sci U S A, 1996. **93**(1): p. 452-5.
705. Monsonego, A. and H.L. Weiner, *Immunotherapeutic approaches to Alzheimer's disease.* Science, 2003. **302**(5646): p. 834-8.
706. Tabira, T. and H. Hara, *Treatment of Alzheimer disease: A beta vaccine.* Rinsho Shinkeigaku, 2004. **44**(11): p. 778-80.
707. Dawson, G.R., et al., *Age-related cognitive deficits, impaired long-term potentiation and reduction in synaptic marker density in mice lacking the beta-amyloid precursor protein.* Neuroscience, 1999. **90**(1): p. 1-13.
708. Seabrook, G.R., et al., *Mechanisms contributing to the deficits in hippocampal synaptic plasticity in mice lacking amyloid precursor protein.* Neuropharmacology, 1999. **38**(3): p. 349-59.
709. McGaugh, J.L., C.K. McIntyre, and A.E. Power, *Amygdala modulation of memory consolidation: interaction with other brain systems.* Neurobiol Learn Mem, 2002. **78**(3): p. 539-52.
710. Zhenzhong Cui, K.A.L., Bing Mei, Shuqing Zhang, Joe Z. Tsien, *Requirement of NMDA receptor reactivation for consolidation and storage of nondeclarative taste memory revealed by inducible NR1 knockout.* European Journal of Neuroscience, 2005. **22**(3): p. 755.

711. Ferreira, G., et al., *Differential involvement of cortical muscarinic and NMDA receptors in short- and long-term taste aversion memory.* Eur J Neurosci, 2002. **16**(6): p. 1139-45.
712. Fukuchi, K., et al., *Selective neurotoxicity of COOH-terminal fragments of the beta-amyloid precursor protein.* Neurosci Lett, 1993. **154**(1-2): p. 145-8.
713. Sopher, B.L., et al., *Cytotoxicity mediated by conditional expression of a carboxyl-terminal derivative of the beta-amyloid precursor protein.* Brain Res Mol Brain Res, 1994. **26**(1-2): p. 207-17.
714. Nalbantoglu, J., et al., *Impaired learning and LTP in mice expressing the carboxy terminus of the Alzheimer amyloid precursor protein.* Nature, 1997. **387**(6632): p. 500-5.
715. Cao, X. and T.C. Sudhof, *A transcriptionally active complex of APP with Fe65 and histone acetyltransferase Tip60.* Science, 2001. **293**(5527): p. 115-20.

ACKNOWLEDGEMENTS

First of all, I am grateful to Dr. Hasan Mohajeri, who supervised this work, for improving my self confidence and for having given me the liberty and responsibility to do the research I wanted. I particularly appreciated his respect and availability.

I am indebted to Prof. Roger Nitsch for the opportunity to do my Ph.D. in such a good environment and for his continous support during my Ph.D.

I would like to thank all the people with whom I collaborated during this thesis. Their help, knowledge and technical skills gave me the chance to answer questions which hopefully will improve the knowledge of Alzheimer's disease. Among them, I would like to especially express my gratitude to Dr. Rime Madani, Inger Drescher and Dr. David Wolfer from the Institute of Anatomy, University of Zurich, Switzerland, Dr. El Mouedden from the CNS-Pain & Alzheimer Department, Janssen Pharmaceutica, Belgium, Prof. Louis Hersh from the Department of Molecular and Cellular Biochemistry and the Center for Structural Biology, University of Kentucky, USA and Prof. Nyberg from the Department of Pharmaceutical Biosciences, Division of Biological Research on Drug Dependence, Uppsala University, Sweden.

I would like to thank my colleagues at the Division of Psychiatry Research. Many of them have been fun to work with and their dynamism helped in making my Ph.D. an unforgettable time. I especially want to thank Della David for her continous friendship and support throughout this Ph.D.. You will always stay in my heart.

Last but not least, special thanks to my family and friends who were always there for me during the hard time and the great one too.

CURRICULUM VITAE

Family name: **Poirier**
First name: **Raphael**
Date of birth: August 09, 1978
Nationality: French

Education

1995-1996 Baccalauréat Scientifique, Besançon, France

1996-1998 DEUG Life and Natural Sciences (1st and 2nd year of Biology at the University) at the University of Franche Comté, Besançon, France

1998-1999 Licence in Biochemistry (3rd year of University, equivalent to the Bachelor of Science in Biochemistry), option Neurosciences and Immunology at the University of Minnesota, Minneapolis, USA with equivalency at the University of Franche Comté, Besançon, France

1999-2000 Maitrise in Cell Biology and Physiology (4th year of University), option Neurosciences at the University Louis Pasteur, Strasbourg, France

2000-2001 D.E.A. in Neurosciences (5th year of University equivalent to a master in Neurosciences) at the University Louis Pasteur, Strasbourg, France

Title of Diploma Thesis: Effect of single or repeated cocaine injections on the regulation of gene expression in rat brain.
Supervisor Dr. Jean Zwiller, Biologie de la communication cellulaire - INSERM U338, Strasbourg, France

2001-present Ph.D. in Molecular Biology and Neurosciences

Title of Ph.D. Thesis: Upregulation of neprilysin as a potential therapeutic approach in Alzheimer's disease.
Supervisor Dr. Hasan Mohajeri, Department of Psuchiatric Research, Zürich, Switzerland

TRAINING PERIODS

June - August 1999:
Monitoring of gap junctions proteins levels in frog embryos during their early development.
Supervisor : Dr. Ross Johnson, Department. of Genetics, Cell Biology and Development, University of Minnesota, Minneapolis, USA

2000 - 2 weeks :
Supervisor : Dr. Jean-Pierre Gies, Laboratoire de pathologie des communications entre cellules nerveuses et musculaires - UPRESS 2308, Strasbourg, France

July - September 2000 :
Adaptatation of a magnetic bead procedure for the isolation of gap junction proteins from rat liver and heart.
Supervisor : Dr. Ross Johnson, Department. of Genetics, Cell Biology and Development, University of Minnesota, Minneapolis, USA

2001 - 2 weeks :
5-HT1a receptor-mediated control of hippocampal cholinergic tone in the rat: influence of age and of age-related cognitive deficits degree.
Supervisor : Dr. Fabrice Bertrand Neurosciences comportementales et cognitives - UMR 7521 CNRS, Strasbourg, France

PUBLICATIONS AND HONORS

Publications :

Lazaris A, Bertrand F, Lazarus C, Galani R, Stemmelin J, **Poirier R**, Kelche C, Cassel JC. Baseline and 8-OH-DPAT-induced release of acetylcholine in the hippocampus of aged rats with different levels of cognitive dysfunction. Brain Res. **2003** Mar 28;967 (1-2):181-90.

Mohajeri MH, **Poirier R**, Li H, Wollmer MA, Nitsch RM. Neprlysin mediated prevention of amyloid plaque formation. New trends in Alzheimer and Parkinson related disorders. AD/PD **2003**: 139-143

de Quervain DJ, **Poirier R**, Wollmer MA, Grimaldi LM, Tsolaki M, Streffer JR, Hock C, Nitsch RM, Mohajeri MH, Papassotiropoulos A. Glucocorticoid-related genetic susceptibility for Alzheimer's disease. Hum Mol Genet. **2004** Jan 1;13 (1):47-52.

Mohajeri MH, Kuehnle K, Li H, **Poirier R**, Tracy J, Nitsch RM. Anti-amyloid activity of neprilysin in plaque-bearing mouse models of Alzheimer's disease. FEBS Lett. **2004** Mar 26;562 (1-3):16-21.

Dietrich JB, **Poirier R**, Aunis D, Zwiller J. Cocaine downregulates the expression of the mitochondrial genome in rat brain. Ann N Y Acad Sci. **2004** Oct;1025:345-50.

Glatzel M, Mohajeri MH, **Poirier R**, Nitsch RM, Schwarz P, Lu B, Aguzzi A. No influence of amyloid-beta-degrading neprilysin activity on prion pathogenesis. J Gen Virol. **2005** Jun;86 (Pt 6):1861-7.

Poirier R, Wolfer DP, Tracy J, Welzl H, Galsworthy MJ, Nitsch RM, Mohajeri MH. Neuronal Neprilysin Overexpression Prevents Aβ-Related Spatial Memory Deficit. Submitted

Poirier R, Madani R, Wolfer DP, Welzl H, Groscurth P, Lipp HP, Lu B, El Mouedden M, Mercken M, Nitsch RM, Mohajeri MH. Presence of amyloid-like deposits in brain, neurodegeneration and behavioral impairment of mice with targeted depletion of *neprilysin* gene. Submitted

Honor : (1999) received the Richard C. Nelson award in Biochemistry (recognition of a successful career in science)